

NASA CR 72290  
GE R67FPD309



FACILITY FORM 602

ACCESSION NUMBER	N67-33370	(THRU)	
(PAGES)	C1-72290	(CODE)	15
(NASA CR OR TMX OR AD NUMBER)		(CATEGORY)	

# BEARING FATIGUE INVESTIGATION

by

E.N. Bamberger

prepared for

NATIONAL AERONAUTICS AND SPACE ADMINISTRATION

Contract NAS 3-7261

FLIGHT PROPULSION DIVISION

GENERAL  ELECTRIC

LYNN, MASSACHUSETTS/CINCINNATI, OHIO



# NOTICE

This report was prepared as an account of Government sponsored work. Neither the United States, nor the National Aeronautics and Space Administration (NASA), nor any person acting on behalf of NASA:

- A.) Makes any warranty or representation, expressed or implied, with respect to the accuracy, completeness, or usefulness of the information contained in this report, or that the use of any information, apparatus, method, or process disclosed in this report may not infringe privately owned rights; or
- B.) Assumes any liabilities with respect to the use of, or for damages resulting from the use of any information, apparatus, method or process disclosed in this report.

**As** used above, "person acting on behalf of NASA" includes any employee or contractor of NASA, or employee of such contractor, to the extent that such employee or contractor of NASA, or employee of such contractor prepares, disseminates, or provides access to, any information pursuant to his employment or contract with NASA, or his employment with such contractor.

Requests for copies of this report should be referred to:

National Aeronautics and Space Administration  
Office of Scientific and Technical Information  
Attention: AFSS-A  
Washington, D.C. 20546

NASA CR-72290  
GE R67FPD309

FINAL REPORT

BEARING FATIGUE INVESTIGATION

by

E. N. Bamberger

prepared for

NATIONAL AERONAUTICS AND SPACE ADMINISTRATION

September 15, 1967

CONTRACT NAS 3-7261

Technical Management  
NASA Lewis Research Center  
Cleveland, Ohio

Project Manager  
D. P. Townsend  
Air Breathing Engine Division

Research Advisor  
E. V. Zaretsky  
Fluid Systems Component Division

GENERAL ELECTRIC COMPANY  
Flight Propulsion Division  
Cincinnati, Ohio

## FOREWORD

The work reported herein was performed at the facilities of the Flight Propulsion Division, General Electric Company, Cincinnati, Ohio, under NASA Contract NAS 3-7261. The NASA Project Manager was Mr. D. Townsend and the NASA Research Advisor was Mr. E. V. Zaretsky,

The author would like to acknowledge the efforts of the following personnel who aided significantly in the performance of the program. **Mr.** C. C. Moore under whose supervision the full scale bearing tests were performed and who was instrumental in the conception and design of the bearing testers. Mr. D. Smeaton who guided the construction of the testers and supporting facilities. Messrs. C. Johnson and R. Brooks who performed the actual bearing tests. Mr. D. Kroeger who performed the RC Rig testing and Messrs. J. Fausz and P. Schneider who performed respectively the lubricant analysis and the bearing weight and dimensional measurements.

## BEARING FATIGUE INVESTIGATION

By

E. N. Bamberger

### ABSTRACT

A research program has been performed to establish the feasibility of operating large diameter rolling element bearings at 600F under conditions of load and speed approximating those experienced by main shaft bearings in jet engines. Two bearing materials (CVM M-50 and WB-49) and three advanced lubricants were investigated. The lubricants were: a) synthetic paraffinic oil, Mobil XRM-177F, b) polymeric perfluorinated fluid, DuPont PR-143, and c) inhibited, mixed isomeric 5-ring polyphenyl ether 5P4E, Monsanto MCS-354. Over 54,000 hours of bearing testing were accumulated. Additionally, a large number of bench type rolling contact fatigue tests were conducted, as well as extensive lubricant and metallurgical analysis. The data shows that the paraffinic oil will provide satisfactory hydrodynamic lubrication at 600F in an inerted atmosphere. The polyphenyl ether and the polymeric fluid are marginal in their lubricating capability at the 600F temperature. Bearing failures at 600F are similar to those observed at lower temperatures. CVM M-50 is suitable for bearing applications up to and including 600F.



## TABLE OF CONTENTS

	<u>Page</u>
List of Illustrations	
List of Tables	
1.0 Summary and Conclusions	1
2.0 Introduction	2
3.0 Lubricants and Bearing Materials	4
3.1 Lubricants	4
3.2 Bearing Materials	7
4.0 Test Facilities	22
4.1 Rolling Contact Fatigue Tester (RC Rig)	22
4.2 120 mm Bore Bearing Tester	26
5.0 Rolling Element Computer Analysis Program	49
6.0 Test Results	54
6.1 RC Rig Tests	54
6.2 Full Scale Bearing Tests	63
6.2.1 Test Series I	70
6.2.2 Test Series II	95
6.2.3 Test Series III	111
6.2.4 Test Series IV	130
6.2.5 Test Series V	145
6.2.6 Test Series VI	149
7.0 Metallurgical Analysis	156
8.0 Lubricant Analysis	166
9.0 Bearing Measurements	171
10.0 Discussion	173
11.0 Table of References	182

## LIST OF ILLUSTRATIONS

### Figure

1. Kinematic Viscosity vs. Temperature - Mobil XRM-177F.
2. 120 mm NASA Bearing (GE Dwg. #4012286-955).
3. General Electric Rolling Contact Fatigue Tester (RC Rig).
4. Close-up of RC Rig - Test Bar Geometry,
5. Failure Comparison RC Rig - Ball Bearing.
6. RC Rig Oil Miniscus.
7. Infrared Pyrometer in Use on RC Rig.
8. High Frequency Induction Coils on RC Rig.
9. Tandem Carbon Oil Seal (GE Dwg. #578C839).
10. 120 mm Bearing Tester (GE Dwg. #4012287-034).
11. Hot Oil Pump Performance Curves.
12. Schematic of 120 mm Bearing Test Stand.
13. View of Bearing Test Area.
14. Calibration Curves, Bearing Tester Springs and Bellows.
15. Schematic of Bearing Tester Load Structure.
16. Calibration Curve, Oil Tank Temp. vs. Bearing Outer Ring Temp.
17. Typical Computer Run for RECAP Analysis.
18. RC Rig Weibull Curve - XRM-177F.
19. RC Rig Weibull Curve - MCS-354.
20. RC Rig Weibull Curve - PR-143.
21. Composite Weibull Curve.
22. RC Rig Weibull Curve - Ball vs. Ring Material with XRM-177F.
23. RC Rig Weibull Curve - Ball vs. Ring Material with MCS-354.
24. RC Rig Weibull Curve - WB-49.
25. RC Rig Weibull Curve - Air vs. N<sub>2</sub> Testing.
26. Schematic of Lubricant Deaeration Apparatus.
27. Photo of Lubricant Deaeration Apparatus.
28. Weibull Curve Test Series I.
29. Overall View, Bearing S/N 15.
30. Cage Failure, Bearing SN 15.
31. Outer Ring Fatigue Failure SN 15.

LIST OF ILLUSTRATIONS, Cont.

Figure

32. Ball Fatigue Failures, Bearing S/N 15.
33. Ball Fatigue Failure, Bearing S/N 18.
34. Inner Ring Ball Path, Bearing S/N 18.
35. Retainer Ball Pockets, Bearing S/N 18.
36. Ball Fatigue Failures, Bearing S/N 17.
37. Outer Ring Fatigue Failures, Bearing S/N 17.
38. Inner Ring Fatigue Failure, Bearing S/N 33.
39. Typical Balls, Bearing S/N 10.
40. Outer Ring, Ball Path Bearing S/N 10.
41. Overall View, Bearing S/N 13.
42. Typical Balls, Bearing S/N 13.
43. Retainer Ball Pockets, Bearing S/N 13,
44. Inner Ring Ball Path, Bearing S/N 13.
45. Outer Ring Ball Path, Bearing S/N 13.
46. Wear and Micropitting on Balls, Bearing S/N 21,
47. Primary Retainer Failure, Bearing S/N 28.
48. Secondary Retainer Failure, Bearing S/N 28.
49. Typical Balls, Bearing S/N 28.
50. Inner Ring, Bearing S/N 28.
51. Shoulder Damage on Outer Ring, Bearing S/N 28.
52. Inner Ring Ball Path, Bearing S/N 24.
53. Outer Ring Ball Path, Bearing S/N 24.
54. Typical Balls, Bearing S/N 24.
55. Track Damage, Outer Ring, Bearing S/N 34.
56. Track Damage, Inner Ring, Bearing S/N 34.
57. Typical Balls, Bearing S/N 54.
58. Retainer Rail Failure and Ball Pocket Wear, Bearing S/N 54.
59. Outer Ring Bearing S/N 54.
60. Inner Ring Bearing S/N 54.
61. Outer Ring Fatigue Failure, Bearing S/N 40.

LIST OF ILLUSTRATIONS, Cont.

Figure

62. Inner Ring Fatigue Failures, Bearing S/N 40.
63. Typical Balls, Bearing S/N 40.
64. Retainer, Bearing S/N 40.
65. Weibull Curve, Test Series II.
66. Retainer Ball Pocket, Bearing S/N 45.
67. Typical Balls, Bearing S/N 45.
68. Outer Ring Ball Track, Bearing S/N 45,
69. Inner Ring Ball Track, Bearing S/N 45.
70. Ball Fatigue Failures, Bearing S/N 52.
71. Inner Ring Ball Track, Bearing S/N 52.
72. Ball Fatigue Failures, Bearing S/N 51.
73. Retainer Failure, Bearing S/N 51.
74. Inner Ring Fatigue Failure, Bearing S/N 51.
75. Outer Ring Fatigue Failure, Bearing S/N 51.
76. Inner Ring Ball Track and Balls, Bearing S/N 71.
77. Outer Ring Ball Track, Bearing S/N 71.
78. Retainer, Bearing S/N 71.
79. Weibull Curve, Test Series 111.
80. Damaged Inner Ring, Bearing S/N 78.
81. Retainer Fracture, Bearing S/N 78.
82. Damaged Balls, Bearing S/N 78.
83. Outer Ring Damage, Bearing S/N 78.
84. Inner Ring Fatigue Failure, Bearing S/N 73.
85. Outer Ring Fatigue Failure, Bearing S/N 73,
86. Inner Ring, Bearing S/N 81.
87. Outer Ring Fatigue Failure, Bearing S/N 81.
88. Typical Balls, Bearing S/N 81.
89. Inner Ring Fatigue Failure, Bearing S/N 74.
90. Outer Ring Fatigue Failure, Bearing S/N 74.
91. Corrosion on Inner Ring Shoulder, Bearing S/N 74.



LIST OF ILLUSTRATIONS, Cont .

Figure

92. Inner Ring Damage, Bearing S/N 93.
93. Retainer, Bearing S/N 93.
94. Inner Ring, Bearing S/N 88.
95. Typical Balls, Bearing S/N **88**.
96. Retainer, Bearing S/N 88.
97. Damaged Retainer, Bearing S/N 100.
98. Weibull Curve, Test Series IV.
99. Inner Ring Fatigue Failures and Balls from Bearing S/N 254.
100. Outer Ring Failure, Bearing S/N 251.
101. Inner Ring Failure, Bearing S/N 256.
102. Fatigue Failures, Outer and Inner Rings, Bearing S/N 257.
103. Outer Ring Failure, Bearing S/N 258,
104. Overall View, Bearing S/N 272.
105. Ball and Retainer Failures, Bearing S/N 272.
106. Outer Ring Fracture and Inner Ring Fatigue, Bearing S/N 272.
107. Circumferential Outer Ring Fracture, Bearing S/N 272.
108. Inner Ring Fatigue Failures, Bearing S/N 252.
109. Weibull Curve, Test Series V.
110. Weibull Curve, Test Series VI.
- 111.** Overall View, Bearing S/N 172.
112. Balls and Retainer, Bearing S/N 172.
113. Inner and Outer Rings, Bearing S/N 172.
114. Photomicrograph of Ball Fatigue, Bearing S/N 17.
115. Photomicrograph of Ball Fatigue, Bearing S/N 17.
116. Photomicrograph of Ball Fatigue, Bearing S/N 15.
117. Cross Section Through Area of Ball Wear.
118. Typical Microstructure, ~~CMM50~~ 50.
119. Cross Section Through Area of Ball Wear.
120. Photomicrograph of Inner Ring Fatigue Failure, Bearing S/N 40.
121. Photomicrograph of Inner Ring Fatigue Failure, Bearing S/N 39.

LIST OF ILLUSTRATIONS, Cont.

Figure

- 122. Typical Microstructures of WB-49.
- 123. Massive Carbide Banding in WB-49.
- 124. Photomicrograph of WB-49 Inner Ring Fatigue Failure.
- 125. Effect of Thermal Exposure and Mechanical Stress on Viscosity of XRM-177F.
- 126. Effect of Thermal Exposure and Mechanical Stress on Viscosity of MCS-354.
- 127. Effect of Thermal Exposure and Mechanical Stress on Viscosity of PR-143.
- 128. Viscosity-Temperature Relationship - 3 Test Fluids.
- 129. 600F Viscosity vs. Rolling Contact Fatigue Life.

## LIST OF TABLES

1. Physical Property Data - Mobil Oil XRM-177F.
2. Physical Property Data - DuPont PR-143.
3. Specific Heat and Thermal Conductivity - 3 Test Fluids.
4. Physical Property Data - Monsanto MCS-354.
5. Chemical Analyses of Bearing Materials.
6. Hardness Measurements - M-50 Outer Rings.
7. Hardness Measurements - M-50 Balls.
8. Hardness Measurements - M-50 Inner Rings.
9. Hardness Measurements - WB-49 Inner Rings.
10. Hardness Measurements - WB-49 Outer Rings.
11. Results of Corrosion Study with DuPont PR-143.
12. Bearing Test Results, Test Series I.
13. Bearing Test Results, Test Series II.
14. Bearing Test Results, Test Series III.
15. Bearing Test Results, Test Series IV.
16. Bearing Test Results, Test Series V.
17. Bearing Test Results, Test Series VI.

## 1.0 Summary and Conclusions

A research program has been conducted to establish the feasibility of operating large diameter rolling element bearings at **600F** under conditions of load and speed approximating those experienced by main shaft bearings in jet engines. **Two** major bearing materials and three fluids were evaluated. Over **54,000** hours of bearing testing were accumulated, 27,000 of which were at **600F**. Additionally, a considerable number of bench type (RC Rig) rolling contact fatigue tests were conducted, as well as extensive lubricant and metallurgical analyses. The major conclusions are:

- A synthetic paraffinic oil will provide satisfactory bearing operation at **600F** under a nitrogen atmosphere.
- Using the synthetic paraffinic oil there appears to be no significant effect of temperature on bearing operation in the range **400F-600F**.
- Bearing failures at **600F** are similar to those experienced at lower temperatures, i.e., sub-surface initiated spalling fatigue.
- At **600F**, with the synthetic paraffinic oil and M-50 bearings, bearing life is over 2 times computed life **or** 12 times catalog life.
- At **600F** in an air atmosphere a modified polyphenyl ether does not provide satisfactory lubrication, resulting in considerable component wear and surface distress.
- At **600F**, using M-50 bearings, a polymeric perfluorinated fluid generally provides adequate lubrication, although the adequacy of the lubricant film is not consistent.
- WB-49, an alternate high temperature bearing material, is significantly inferior to M-50 when compared at **600F** and with the synthetic paraffinic oil as a lubricant.
- S-Monel retainers are highly satisfactory for **600F** operation.



## 2.0 Introduction

The phenomenal growth of the aircraft industry in the last decade, spurred on primarily by the rapid advancement in propulsion systems, has placed unprecedented demands on materials and lubricants engineering. Traditionally, bearing operating temperatures were dictated by the thermal capability of the lubricating fluid. Bearing structural materials such as M-50, M-1, 440C, etc. had temperature capabilities exceeding available synthetic lubricants such as the diesters and polyesters. Within the last few years, however, a number of new fluids have been developed which show promise of a breakthrough in terms of increasing the usable temperature range of lubricating oils. Among these are the polyphenyl ethers, the synthetic oils and the polymeric perfluorinated fluids.

One of the critical problems foreseen in the operation of supersonic and hypersonic aircraft will be the high ambient temperature to which the engine and gearbox bearings will be exposed. These components are normally lubricated by oil which also acts as an effective heat transfer medium, passing much of the heat generated by the bearings to an available heat sink such as the fuel. With increased speeds, however, and particularly in the Mach 3+ regime, the heat transfer capacity decreases due to the inherently higher temperature of the fuel and greater demands for cooling capacity elsewhere. This, coupled with the increased heat generation by the bearings due to higher speeds and heavier loads, requires improved lubricants and to a lesser extent, better structural materials for the bearings,

The formulation of advanced thermally stable oils is, however, only the first step in this quest for bearing systems capable of higher temperatures. Design data relating the performance of these fluids and bearing materials at the elevated temperatures must be obtained. Relationships vital to bearing design and life predictions such as load/life and temperature/life need to be determined. Extrapolation of existing data simply is not good enough since totally new families of fluids are

being utilized, or the more common fluids are being operated at their maximum capacity and are thus in an area of essentially unpredictable performance .

The availability of these new lubricating fluids, along with initially encouraging basic engineering properties indicating their potential for high temperature bearing operation, prompted NASA to undertake a study of these fluids under conditions of load, speed and temperature approximating those seen in main shaft jet engine bearings.

General Electric, under contract to NASA-Lewis Research Center, has been performing a portion of these studies. The primary emphasis of the General Electric studies was the determination of bearing performance in the temperature range 400F-600F. The bearings used were 120 mm bore, split inner ring, angular contact bearings.

The program as originally conceived was designed to evaluate three new families of high temperature fluids in combination with two high temperature bearing steels. Based on the results of these studies, a load-life test series was then to be conducted with the best fluid-bearing material combination. This latter test sequence was subsequently changed to the determination of a life-temperature relationship. The reason for this modification will be explained in a later section of this report.

Supporting the full scale bearing tests were a number of complementary studies designed to aid in the analysis of the bearing test data. Included in these supporting tests were rolling contact fatigue studies (RC Rig), computer analysis of bearing kinematics and stresses, as well as lubricant and metallurgical evaluations.

### 3.0 Lubricants and Bearing Materials

The program was designed to provide an evaluation of the operating characteristics of three advanced lubricants, at elevated temperatures and under realistic operating conditions of load and speed. To provide the greatest chance of achieving this prime objective, the prime bearing material selected was CVM M-50, a Cr-Mo-V high speed tool steel, currently used by all major jet engine manufacturers in high temperature and/or critical bearing applications. In addition to this material, an alternate high temperature bearing material was included, in order to have a back-up in the event the M-50 was found to be unable to provide satisfactory operation at the proposed test temperatures of 600F. This alternate material was Crucible Steel's WB-49, a high alloy tool steel, specifically developed for high temperature bearing applications.

Specific details regarding the test fluids and bearing materials are presented in the following pages.

#### 3.1 Lubricants

The three lubricants selected for evaluation were:

- a. Synthetic paraffinic oil - Mobil XRM-177F
- b. Polymeric perfluorinated fluid - DuPont PR-143
- c. Inhibited, mixed isomeric 5-ring polyphenyl ether, 5P4E, - Monsanto MCS-354

Mobil XRM-177F is a 100% synthetic paraffinic oil having excellent high temperature viscosity characteristics. As originally planned, the oil to be used in the General Electric work was to be Mobil XRM-109F, which is the same fluid minus an EP additive. However, before the GE testing was initiated, SKF reported<sup>(1)\*</sup> that the EP additive was essential to achieve satisfactory life from this fluid. Consequently, the XRM-109F on hand was returned to Mobil Oil Company for modification into the XRM-177F. Physical property data furnished by Mobil Oil Company is presented in Table 1 and Figure 1.

\* See Table of References.

Table 1

Properties of XRM-177F-2

Kinematic Viscosity (CS)

OF - 37,497

100F - 443.3

210F - 39.72

400F - 5.83

Viscosity Index 124

Pour Point, °F -35

Flash Point, °F 515

Fire Point, °F 600

Autogeneous Ignition, °F 805

Volatility (6.5 hrs. @  
500F) 14.2%

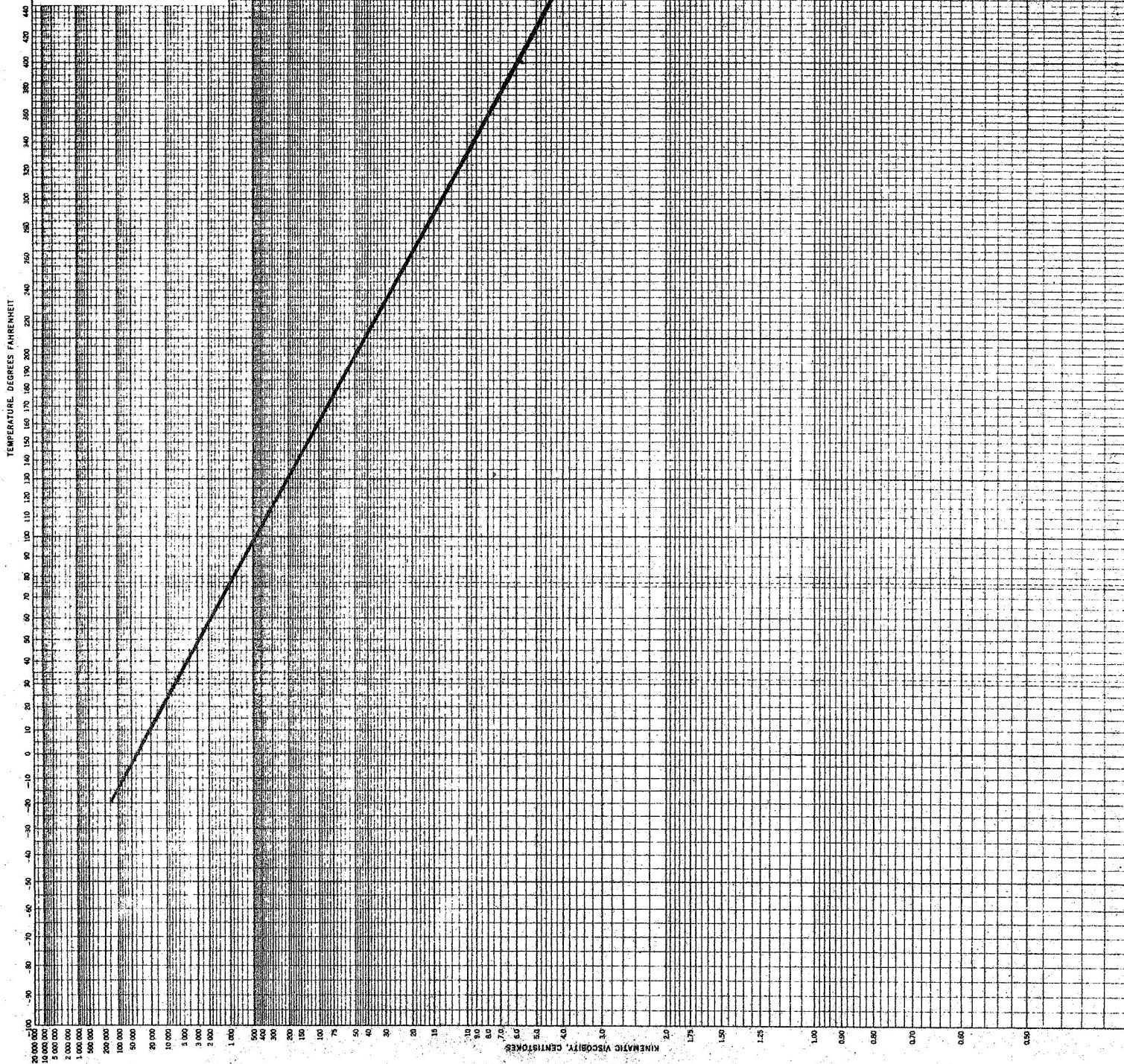
Specific Heat (See Table 3)

Thermal Conductivity (See Table 3)



ASTM STANDARD VISCOSITY-TEMPERATURE CHARTS  
FOR LIQUID PETROLEUM PRODUCTS (D 34)  
CHART G: KINEMATIC VISCOSITY, EXTENDED RANGE

FIGURE 1.  
MOBIL XRM-177F



DuPont PR-143 is a polymeric perfluorinated high temperature fluid having high oxidative and thermal stability. Shortly after its development, the material was evaluated by General Electric under rolling contact conditions and was found to be capable of providing satisfactory bearing operation up to and including 600F. <sup>(2)</sup> This fluid is extensively documented in an Air Force report <sup>(3)</sup> and pertinent physical property data of the batch used in the General Electric Program is shown in Tables 2 and 3.

Monsanto MCS-354, the third fluid is an inhibited mixed isomeric 5-ring polyphenyl ether ~~5P4E~~, developed for use in high-temperature hydraulic, heat transfer and lubricant applications. The properties of this fluid have been extensively documented. <sup>(4)</sup> The pertinent physical properties for the batch of material used in the current program are shown in Tables 3 and 4.

### 3.2 Bearings and Bearing Materials

The test bearings used in this program are shown in Figure 2 (GE Dwg. #4012286-956). A detailed stress analysis of this bearing is presented in section 5.0 of this report, and the major critical dimensions, ball diameters, contact angles, etc. are shown in Figure 2.

The initial order of bearing components for this program was as follows:

<u>Component</u>	<u>Quantity</u>	<u>Material</u>
1. Outer Ring	158	CVMM5 0
2. Outer Ring	90	WB-49
3. Inner Ring	158	CVMM5 0
4. Inner Ring	90	WB-49
5. Retainer	130	S-Mone 1
6. Retainer	120	M-1
7. Balls	2686	CVMM5 0
8. Balls	1530	M-1

Table 2

Properties PR-143AC, Lot 5

Density @ 75°F, g./ml.	1.8798
Viscosity, cs.	
@ 0°F	32,062
@ 100°F	298.3
@ 210°F	29.81
@ 400°F	4.55
Viscosity Index (ASTM D-567)	123
Viscosity Index (ASTM D-2270)	146
ASTM Slope	0.562
Pour Point, °F	-30
Volatility, wt. per cent 6 1/2 hrs. @ 500°F	18.0
Oxidation - Corrosion Data @ 650°F. 72 hrs. with 5 liters dry air/hr: Metals, mg./cm. <sup>2</sup> - day	
QQ-S-636	-3.15
301 SS	-2.74
M-50 Tool Steel	-2.67
440C SS	-3.74
Ti (8Mn)	-4.61
<u>% Fluid Loss</u>	
Cell	0
Overall	0
<u>% Viscosity Change</u>	
100°F	+8.0
210°F	+3.6

Table 3

Specific Heat and Thermal Conductivity  
Of Three Test Fluids

		<u>PR-143</u>	<u>MCS-354</u>	<u>XRM-177</u>
1. Specific Heat <sup>(1)</sup>	100F	0.241	0.35	0.475
	200F	0.260	0.39	0.530
	300F	0.279	0.44	0.585
	400F	0.279	0.48	0.640
	500F	0.316	0.53	0.695
2. Thermal Conductivity <sup>(2)</sup>	100F	52.1	84.0	79.0
	200F	52.0	81.0	77.0
	300F	51.8	79.0	75.0
	400F	51.6	78.0	72.0
	500F	51.5	78.0	70.0

(1) Specific Heat - BTU/lb/°F

(2) Thermal Conductivity - BTU/hr/(ft)<sup>2</sup> (°F/ft) × 10<sup>3</sup>

Table 4

Properties of MCS-354

Viscosity (CS)

100F - 358.0

210F - 13.0

400F - 2.1

500F - 1.2

600F - 0.85

Pour Point, °F +40F

Vapor Pressure 0.76 mm @ 500F

Specific Gravity 1.200 @ 25/25C

Refractive Index  $n_D^{25}$  1.6307

Flash Point 540F

Evaporation Loss  
6 1/2 hrs. @ 500F @ 140 mm 8.5%

Fire Point, °F 660

Autogeneous Ignition Temp., °F 1135

Specific Heat (See Table 3)

Thermal Conductivity (See Table 3)



The materials selection was made on the premise that the majority of the testipg would be performed with the **M-50/S-Monel** combination. In the event that the S-Monel cages proved marginal, a substitution to M-1 cages was to be made. Similarly, sufficient **WB-49** components were procured in the event that the **M-50** would prove unsuitable and/or marginal, **for the 600F** operation, Based on NASA experience, <sup>(5)</sup> it was also decided to outfit the **WB-49** bearings with M-1 balls, as this latter material had provided satisfactory operation, especially when exposed to the **PR-143** fluid,

The metallurgical aspect of the bearing procurement was a particularly stringent one, and was essential to insure the repeatability and credibility of the bearing test data. The most salient points of the metallurgical control were as follows:

1. All bearing components made from the same material were to be made from one heat of material.
2. Hardness requirements **for** the various components were as follows:

<b>M-50</b> Rings	Rc <b>62-64</b>
<b>WB-49</b> Rings	Rc <b>64-66</b>
M-50 Balls	Rc <b>62.5-63.5</b>
M-1 Balls	Rc <b>64.5-65.5</b>
S-Monel Retainers	Rc <b>33 ± 1</b>
M-1 Retainers	Rc <b>55 ± 1</b>

3. Raceway surface finish was not to exceed two r.m.s.

The above conditions were successfully met, with the exception of the M-50 components in Item 1 (above). In this case, insufficient material was available from a single CVM billet to produce all components.

Consequently, this requirement was relaxed to allow the M-50 balls to be made from separate CVM billets, although these were still from the same heat as the one used for the rings. (It should be noted that the interpretation of a material "heat" is a controversial subject and the author would like to clarify General Electric's position on this subject. There are essentially two "heats" as such in a consumable vacuum melting process. The first of these is the air melted master heat from which as many as six CVM electrodes can be obtained to produce individual CVM billets. The master heat can be as much as 15-20,000 lbs., whereas a CVM billet rarely exceeds 3,000 lbs. Despite very close control of the CVM process, sufficient variations can occur during the process, so that General Electric considers each CVM billet an individual heat, and thus not necessarily the same as a similar billet made from the same master material, but melted at a different time.) Table 5 presents the Chemical Analysis of the materials used in the current program. To control the hardness tolerances, specifically on the balls, two extra balls were made for each bearing specifically for hardness checks.

To illustrate the hardness control achieved, a summary of hardness measurements is presented in Tables 6 through 10,

Additionally, from each heat of material with the exception of those used for the retainers, RC Rig test bars were made and submitted to General Electric for evaluation. These tests and their results are discussed in another section of this report. To further assure the soundness of the bearing material, X-ray diffraction measurements were made to determine retained austenite contents. The following excerpt from a Marlin Rockwell Bearing Company letter describes the technique used by this company to determine retained austenite.

"MRC uses the integrated intensities method of determining retained austenite on a GE XRD 5 Diffractometer using a CA 7H X-ray tube and a #6 SPG counter tube.



Table 5

Chemical Analysis of Materials Used in  
Bearing Components for NASA 3-7.261

	<u>C</u>	<u>Mn</u>	<u>P</u>	<u>S</u>	<u>Si</u>	<u>Cr</u>	<u>Mo</u>	<u>V</u>	<u>Ni</u>	<u>W</u>	<u>Co</u>	<u>Fe</u>	<u>Cu</u>
CVM-M50 <sup>(1)</sup>													
Ring Material	.802	.24	.008	.003	.18	3.95	4.36	.93	-	-	-	Bal.	
GVM-M50 <sup>(2)</sup>													
Ball Material	.802	.24	.008	.003	.18	3.95	4.36	.93	-	-	-	Bal.	
CVM-WB-49 <sup>(3)</sup>	1.06	.44	.004	.008	.32	4.22	3.76	1.86	.08	6.82	5.29	Bal.	
M-1 <sup>(4)</sup>	.798	.28	.020	.005	.29	3.74	8.71	1.11	-	1.53	-	Bal.	
S-Mone 1 <sup>(5)</sup>	.095	.74	-	-	3.69	-	-	-	65.28	-	-	.66	28.78

(1) Allegheny Ludlum Steel Co. Heat #25431

(2) CVM Billet #A - CVM Billet #B

(3) Crucible Steel Co. Heat #07833

(4) Allegheny Ludlum Steel Co. Heat #W81154

(5) Janney Cylinder Co. Heat #AA1(6755)

Table 6

\*

Hardness MeasurementsOuter Rings (CVM-M-50)

<u>Bearing Number</u>				<u>Bearing Number</u>				<u>Bearing Number</u>			
1.	63.0	63.0	63.0	37.	63.0	63.0	63.1	73.	63.0	63.2	63.0
2.	63.1	63.0	63.0	38.	63.0	63.0	63.0	74.	63.0	63.0	63.0
3.	63.0	63.0	63.2	39.	63.3	63.0	63.0	75.	63.0	63.0	63.0
4.	63.0	63.0	63.0	40.	63.0	63.0	63.1	76.	63.0	63.0	63.0
5.	63.1	63.1	63.0	41.	62.9	63.0	63.0	77.	63.0	63.0	63.0
6.	63.0	63.0	63.0	42.	63.0	63.2	63.0	78.	63.0	63.0	63.0
7.	63.2	63.0	63.1	43.	63.0	63.4	63.0	79.	63.0	63.0	63.0
8.	63.0	63.0	63.1	44.	62.9	62.9	63.0	80.	63.0	63.2	63.1
9.	63.0	63.0	63.0	45.	63.0	63.0	63.0	81.	63.0	63.0	63.1
10.	63.0	63.1	63.1	46.	63.0	63.0	62.9	82.	63.0	63.0	63.2
11.	62.9	63.3	63.1	47.	63.0	63.0	63.0	83.	63.0	63.0	63.0
12.	63.1	63.0	63.1	48.	63.0	63.0	63.0	84.	63.2	63.0	63.3
13.	63.0	63.1	63.1	49.	63.0	63.0	63.0	85.	63.0	63.0	63.0
14.	63.0	63.1	63.0	50.	63.0	63.0	63.0	86.	63.0	63.0	63.0
15.	63.0	63.0	63.1	51.	63.0	63.0	63.0	87.	63.0	63.0	63.0
16.	63.0	63.0	63.0	52.	63.2	63.3	63.4	88.	63.0	63.0	63.0
17.	63.2	63.2	63.1	53.	63.0	63.2	63.0	89.	62.9	63.0	62.9
18.	63.0	62.7	63.0	54.	63.0	63.0	63.0	90.	63.2	63.2	63.0
19.	63.0	63.0	63.0	55.	63.0	63.0	63.1	91.	63.0	62.9	63.0
20.	63.0	63.4	63.1	56.	63.0	63.2	63.2	92.	63.0	63.1	63.1
21.	63.0	63.0	63.0	57.	63.0	63.1	63.0	93.	63.0	63.0	63.0
22.	63.0	63.0	63.0	58.	63.0	63.0	63.2	94.	62.9	63.0	63.0
23.	63.4	63.0	63.2	59.	63.0	63.0	63.0	95.	63.0	63.0	63.0
24.	63.2	63.2	63.1	60.	63.0	63.0	63.1	96.	63.0	63.0	63.0
25.	63.0	63.0	62.9	61.	63.0	63.0	63.0	97.	63.0	63.0	63.0
26.	63.4	63.2	63.2	62.	63.3	63.2	63.2	98.	62.9	63.0	63.0
27.	63.0	63.0	63.1	63.	63.0	63.0	63.0	99.	63.0	63.0	63.0
28.	63.2	63.3	63.1	64.	63.0	63.0	63.0	100.	63.0	63.0	63.0
29.	63.0	63.0	63.1	65.	63.0	63.2	63.1	101.	63.0	63.0	63.2
30.	63.0	63.0	62.9	66.	63.0	63.0	63.0	102.	63.0	63.0	63.6
31.	63.0	63.0	63.0	67.	63.0	63.0	63.0	103.	63.0	63.1	63.1
32.	63.0	63.1	63.0	68.	63.2	63.1	63.1	104.	63.0	63.0	63.0
33.	63.0	63.0	63.0	69.	63.0	63.0	63.0	105.	63.0	63.0	63.0
34.	63.0	63.0	63.0	70.	62.9	63.1	63.0	106.	63.0	63.0	63.0
35.	63.0	63.0	63.0	71.	63.0	63.0	63.0	107.	63.0	63.0	63.0
36.	63.0	63.0	63.0	72.	63.0	63.0	63.0	108.	63.0	62.9	62.9

\* All hardness measurements in Rockwell C

Table 7

Hardness\* MeasurementsBalls . 005 (CVM-M-50)Bearing  
Number

1.	63.0	63.0	63.0
2.	63.0	63.0	63.0
3.	63.0	63.0	63.2
4.	63.0	63.0	63.2
5.	63.2	63.2	63.5
6.	63.0	63.0	63.1
7.	63.5	63.4	63.0
8.	63.0	63.5	63.2
9.	63.0	63.0	63.4
10.	63.0	63.0	63.0
11.	63.0	63.2	63.1
12.	63.0	63.0	63.0
13.	63.0	63.0	63.0
14.	63.0	63.0	63.0
15.	63.0	63.5	63.2
16.	63.2	63.2	63.0
17.	63.0	63.0	63.0
18.	63.0	63.0	63.0
19.	63.0	63.0	63.5
20.	63.0	63.0	63.0
21.	63.0	63.0	63.5
22.	63.0	63.0	63.0
23.	63.0	63.Q	63.1
24.	63.0	63.0	63.0
25.	63.0	63.3	63.1
26.	63.1	63.0	63.0
27.	63.0	63.0	63.0
28.	62.9	63.0	63.3
29.	63.0	63.0	63.2
30.	63.0	63.4	63.1
31.	63.2	63.0	63.4
32.	63.0	63.0	63.0
33.	63.1	63.0	63.0
34.	63.0	63.2	63.0
35.	63.0	63.0	63.0
36.	63.0	63.0	63.0

Bearing  
Number

37.	63.0	63.2	63.0
38.	63.5	63.5	63.1
39.	63.0	63.4	63.5
40.	63.0	63.0	63.5
41.	63.0	63.0	63.0
42.	63.0	63.0	63.0
43.	63.0	63.0	63.0
44.	63.0	63.1	63.0
45.	63.0	63.0	63.3
46.	63.0	63.0	63.2
47.	63.0	63.0	63.0
48.	63.0	63.0	63.5
49.	63.5	63.0	63.0
50.	63.0	63.4	63.0
51.	63.0	63.1	63.2
52.	63.4	63.0	63.0
53.	63.0	63.0	62.9
54.	63.0	63.0	63.0
55.	63.0	63.0	63.1
56.	63.0	63.3	63.0
57.	63.0	63.1	63.5
58.	63.5	63.5	63.2
59.	63.0	63.0	63.0
60.	63.2	63.3	63.3
61.	63.2	63.0	63.4
62.	63.1	63.0	63.0
63.	63.0	63.5	63.1
64.	63.0	63.0	63.0
65.	63.0	63.0	63.0
66.	63.5	63.4	63.5
67.	63.0	63.0	63.0
68.	63.0	63.4	63.1
69.	63.2	63.0	63.0
70.	63.5	63.1	63.0
71.	63.2	63.0	63.0
72.	63.3	63.0	63.0

\* All hardness measurements in Rockwell C

Table 8

\*

Hardness MeasurementsPuller Grooved Inner Rings(CVM M-50)

<u>Bearing Number</u>				<u>Bearing Number</u>				<u>Bearing Number</u>			
1.	63.0	63.5	63.1	38.	62.9	63.0	62.9	75.	63.0	63.0	63.0
2.	63.0	63.0	63.2	39.	63.2	63.0	63.0	76.	63.0	62.9	63.0
3.	63.0	63.0	63.0	40.	63.0	63.0	63.2	77.	63.0	63.0	63.0
4.	63.0	63.0	63.0	41.	63.2	63.3	63.0	78.	63.0	63.2	63.0
5.	63.2	63.5	63.0	42.	63.0	63.0	63.0	79.	63.2	63.4	63.2
6.	63.0	63.0	63.4	43.	63.0	63.0	63.0	80.	63.0	63.0	63.1
7.	63.2	63.2	63.0	44.	63.1	63.0	63.4	81.	63.0	63.0	63.0
8.	63.0	63.2	63.0	45.	63.0	63.0	63.3	82.	63.0	63.0	62.9
9.	65.5	63.0	63.0	46.	63.0	63.0	63.0	83.	63.0	63.0	63.3
10.	63.0	63.2	63.0	47.	62.9	62.9	63.1	84.	63.0	63.0	63.0
11.	63.0	63.0	63.3	48.	63.2	63.0	63.0	85.	63.0	63.0	63.0
12.	63.0	63.0	63.0	49.	63.0	62.9	63.3	86.	63.0	63.0	63.0
13.	63.0	62.9	63.2	50.	63.0	63.1	63.0	87.	63.0	63.0	63.5
14.	63.0	63.1	63.4	51.	63.0	63.0	63.0	88.	63.0	63.0	63.0
15.	63.0	62.9	63.1	52.	63.0	63.0	62.9	89.	63.1	63.0	63.0
16.	63.0	63.0	63.0	53.	63.2	63.5	63.3	90.	63.0	63.0	63.0
17.	63.2	63.0	63.0	54.	63.0	63.0	63.0	91.	63.0	63.0	63.5
18.	63.0	63.2	63.1	55.	63.0	63.0	63.0	92.	63.0	63.0	63.4
19.	63.0	63.0	62.9	56.	63.0	63.1	63.0	93.	63.0	63.0	63.1
20.	63.0	63.5	63.2	57.	63.2	63.0	63.0	94.	63.0	63.0	63.3
21.	63.0	63.0	63.0	58.	63.0	63.0	63.2	95.	63.0	63.2	63.2
22.	63.0	63.0	63.0	59.	63.0	63.0	63.5	96.	63.0	63.0	63.0
23.	63.0	62.9	62.9	60.	63.0	63.5	63.2	97.	63.0	63.0	63.0
24.	63.0	63.0	63.0	61.	63.0	63.0	63.0	98.	62.9	63.0	63.0
25.	63.0	63.0	63.0	62.	63.0	63.0	62.9	99.	63.0	63.0	63.3
26.	63.0	62.9	62.9	63.	63.2	63.2	63.0	100.	63.0	63.0	63.0
27.	63.1	63.3	63.0	64.	63.2	63.0	63.0	101.	63.0	63.0	63.2
28.	63.0	63.0	63.0	65.	63.5	63.1	63.2	102.	63.0	63.0	62.9
29.	63.0	63.0	63.0	66.	63.0	63.0	63.2	103.	63.4	63.0	62.9
30.	63.0	63.0	63.0	67.	63.2	63.4	63.1	104.	63.4	63.0	63.3
31.	63.2	63.2	63.0	68.	63.0	63.0	63.0	105.	63.2	63.2	63.0
32.	63.0	63.0	63.0	69.	63.0	63.0	62.9	106.	62.9	63.0	62.9
33.	63.0	63.2	63.1	70.	63.0	63.0	63.0	107.	63.1	63.0	63.2
34.	63.0	63.2	63.1	71.	63.0	63.0	63.0	108.	63.3	63.0	63.0
35.	63.1	63.0	63.4	72.	62.9	62.9	63.0	109.	63.2	63.0	63.3
36.	63.0	63.0	63.0	73.	63.0	63.0	63.1	110.	63.0	63.0	63.0
37.	63.0	63.2	63.1	74.	63.0	63.1	63.2	111.	63.0	63.2	63.0

\* All hardness measurements in Rockwell C

Table 9

Hardness MeasurementsInner Rings (WB-49)Bearing  
NumberBearing  
NumberBearing  
Number

1.	64.9	65.0	64.9	33.	64.9	64.9	64.5	65.	65.0	65.0	65.0
2.	65.0	64.9	65.0	34.	64.8	64.9	64.8	66.	65.0	65.0	65.1
3.	65.0	65.0	65.0	35.	65.0	65.0	64.8	67.	65.0	65.0	65.0
4.	65.0	65.0	64.9	36.	65.0	65.0	65.0	68.	64.9	65.0	65.0
5.	65.0	65.0	65.0	37.	64.9	65.0	65.0	69.	65.0	64.9	65.0
6.	65.0	65.0	65.0	38.	65.0	64.9	65.0	70.	65.0	65.0	64.9
7.	65.0	65.0	64.9	39.	65.0	65.0	65.0	71.	64.9	64.8	64.8
8.	65.0	65.0	65.0	40.	65.0	64.8	65.0	72.	65.0	65.0	64.9
9.	65.0	65.0	65.0	41.	65.0	65.0	65.0	73.	65.0	64.8	65.0
10.	65.0	64.8	65.0	42.	64.9	64.9	64.6	74.	65.0	65.0	65.0
11.	65.0	65.0	65.0	43.	65.0	64.9	65.0	75.	65.0	64.9	65.0
12.	64.9	64.8	65.0	44.	65.0	65.0	65.0	76.	64.8	65.0	65.0
13.	65.0	64.9	65.0	45.	64.9	64.8	65.0	77.	65.0	65.0	64.9
14.	65.0	65.0	65.0	46.	64.9	64.9	64.9	78.	65.0	64.9	65.0
15.	64.8	65.0	64.8	47.	65.0	64.9	65.0	79.	65.0	64.8	65.0
16.	64.9	65.1	65.0	48.	64.9	64.9	65.0	80.	65.0	65.0	64.9
17.	65.0	64.9	64.7	49.	64.8	65.0	65.0	81.	65.0	65.0	64.8
18.	65.0	64.8	65.0	50.	65.0	65.0	65.0	82.	65.0	65.0	65.0
19.	65.0	65.0	65.0	51.	64.8	65.0	65.0	83.	64.8	65.0	65.0
20.	65.0	65.0	65.0	52.	64.9	65.0	65.0	84.	65.0	65.0	64.7
21.	65.0	65.0	64.8	53.	65.0	65.0	65.0	85.	65.0	65.0	64.9
22.	64.9	64.9	65.0	54.	64.9	65.0	65.0	86.	65.1	64.6	65.0
23.	65.0	64.9	65.0	55.	65.0	65.0	64.9	87.	65.0	64.8	65.0
24.	65.0	65.0	65.0	56.	64.9	64.9	64.8	88.	65.0	65.1	65.2
25.	65.0	65.1	65.0	57.	65.0	65.0	65.0	89.	64.7	64.9	65.0
26.	65.0	65.0	64.9	58.	64.9	65.0	64.9	90.	64.7	64.9	65.0
27.	65.0	65.0	64.9	59.	64.9	64.9	64.6	91.	64.5	64.8	64.9
28.	65.0	65.0	65.0	60.	64.9	64.9	64.9	92.	65.0	65.0	65.1
29.	65.0	65.0	65.0	61.	65.0	64.9	65.0	93.	64.9	65.0	65.2
30.	65.0	65.0	64.8	62.	64.8	64.8	65.0	94.	64.5	64.9	64.9
31.	65.0	65.0	64.9	63.	65.0	65.0	65.0	95.	65.0	65.0	65.2
32.	64.9	65.0	64.9	64.	65.0	65.0	64.8				

\* All hardnesses in Rockwell C

Table 10

\*

Hardness MeasurementsOuter Rings (WB-49)

<u>Bearing Number</u>				<u>Bearing Number</u>				<u>Bearing Number</u>			
1.	65.4	65.2	65.0	31.	65.0	65.0	65.0	61.	65.0	65.0	65.0
2.	65.0	65.0	65.0	32.	65.2	65.0	65.0	62.	65.0	65.0	65.0
3.	65.0	65.0	65.2	33.	65.0	65.1	65.0	63.	65.2	65.0	65.1
4.	65.0	65.0	65.0	34.	65.0	65.1	65.0	64.	65.1	65.1	65.0
5.	65.0	65.0	65.0	35.	65.0	65.0	65.0	65.	65.0	65.0	65.0
6.	65.0	65.0	65.0	36.	65.2	65.0	65.1	66.	65.1	65.0	65.0
7.	65.0	65.0	65.0	37.	65.1	65.2	65.2	67.	65.0	65.1	65.1
8.	65.0	65.0	65.0	38.	65.0	65.0	64.9	68.	65.1	65.1	65.0
9.	65.0	65.0	65.0	39.	65.0	65.0	65.0	69.	65.0	65.0	65.0
10.	64.8	65.0	65.0	40.	65.0	65.0	65.0	70.	64.8	64.6	64.8
11.	65.0	65.0	65.0	41.	65.1	65.0	65.3	71.	64.8	64.8	64.8
12.	65.0	65.0	65.1	42.	65.5	65.3	65.0	72.	65.0	64.8	64.9
13.	66.0	65.0	65.0	43.	65.0	65.1	65.2	73.	65.0	64.7	64.8
14.	65.0	65.0	65.0	44.	65.0	65.0	65.0	74.	64.8	64.9	64.9
15.	65.0	65.0	65.0	45.	64.5	64.5	65.0	75.	64.9	64.8	65.0
16.	65.2	65.2	65.0	46.	65.0	65.2	65.2	76.	64.8	64.8	64.8
17.	65.1	65.0	65.0	47.	65.1	65.3	65.0	77.	64.7	64.3	65.0
18.	65.0	65.0	64.8	48.	65.0	65.2	65.0	78.	64.8	64.5	65.0
19.	65.1	65.0	64.9	49.	65.0	65.0	65.0	79.	64.9	64.9	64.9
20.	65.0	65.0	65.1	50.	65.0	65.2	65.1	80.	64.7	64.7	65.0
21.	65.2	65.2	65.0	51.	65.1	65.0	65.0	81.	64.5	64.9	64.9
22.	65.0	65.1	65.1	52.	65.0	65.0	65.0	82.	64.7	64.8	64.7
23.	65.0	65.0	65.1	53.	65.0	65.1	65.0	83.	64.9	64.8	64.8
24.	65.1	65.0	65.0	54.	65.1	65.0	65.2	84.	64.8	64.8	64.8
25.	65.2	66.4	65.1	55.	65.2	65.2	65.1	85.	64.8	64.9	65.0
26.	65.0	65.0	65.0	56.	65.2	65.0	65.0	86.	65.0	64.6	64.7
27.	65.2	65.0	65.1	57.	65.0	65.1	65.0	87.	64.8	64.9	64.9
28.	65.0	65.0	65.0	58.	65.0	65.0	65.1	88.	64.8	64.9	64.7
29.	65.0	65.0	65.0	59.	65.0	65.0	65.0	89.	64.8	64.8	64.9
30.	65.0	65.0	64.9	60.	65.1	65.0	65.0				

\* All hardnesses in Rockwell C

Surface preparation is particularly important to assure that no heat treating or grinding conditions affect the measurements. MRC electro-polishes all surfaces to be tested. A minimum depth of .001" is used for ground parts, .020" for unground surfaces. Other methods of preparation are not acceptable as false readings will always be found.

Parts are tested at the following machine settings:

Chrome Radiation 50 KVP 30 MA  
 3° Medium Resolution Beam Collimator  
 Medium Resolution Detector Collimator  
 .0015" Vanadium Filter  
 500 Count Per Second on Rate Meter  
 2 Second Time Constant  
 Goniometer Speed 2° per Minute  
 Chart Speed 60" per Hour

M-50 steel is scanned for the 200 austenite line from 20 74° through 20 83°, the peak occurring at about 79.4' 20, The martensite 200 peak is scanned between 20 98' and 20 114°, the peak being found at about 106° 20. A further scan may be made for the 220 austenite line between 20 122' and 20 134°.

The chart is placed on a desk and a straight line drawn through the background radiation. The area above the line and under the peaks is measured with a planimeter and put in the formula:

$$\text{Ret, Aust.} = \frac{1.0 - .04 \text{ (Carbide Correction)}}{\left( \frac{\text{Area Martensite } 200}{\text{Area Austenite } 200} \times 1.74 \right) + 1}$$

$$\text{or } V = \frac{1}{1 + \frac{200a}{\frac{200r}{.576}}}$$

In general production, a scan for the austenite 200 line is sufficient to determine if a peak is present. No peak at this location indicates a retained austenite content of less than 5%."

Using the above technique, the retained austenite content was determined to be less than 3% in the ring and ball material.



#### 4.0 Test Facilities

To perform the testing phase of this program, two major test facilities were required. Of these, the rolling contact fatigue testers (RC Rig) were available and could be immediately utilized. The full scale bearing testers, however, had to be designed, constructed and installed and checked out. Both of these facilities will be described in the following paragraphs.

##### 4.1 Rolling Contact Fatigue Testing (RC Rig)

To determine the relative effects of the three experimental lubricants on the selected bearing materials, Rolling Contact Fatigue tests were performed prior to initiation of the full scale bearing tests. Testing was also conducted to determine the differences to be expected between the two major bearing materials (M-50, WB-49) and between the two CVM heats of M-50 used in the subject program.

The RC Rig, briefly described below, became a major tool in the pre-bearing test evaluation of the three fluids and two bearing materials. A view of the RC Rig is shown in Figure 3 and a close-up of the test bar roller geometry is shown in Figure 4. The cylindrical bar, three inches long by .375" D., which is the test specimen, drives two hemispherically ground rollers. These rollers are each 7 1/2" D. and have a contact radius of 1/4". They are mounted via double row ball bearings and are supported by a massive pendulum yoke. Load is applied by closing the rollers together against the test bar. The loading train consists of a micrometer threaded turnbuckle and a calibrated load cell. The load cell is a four strain gage bridge which feeds into a Baldwin SR4 strain analyzer. The load cells are calibrated using a tensile machine and obtaining a load versus micro-inch deflection curve. The rollers impinging upon the test bar produce a compressive stress pattern (Hertzian stress) very similar to that seen on the inner ring of a ball bearing. The resultant spalling fatigue failure is essentially identical to that observed on actual bearing races as shown in Figure 5. Lubrication is by a drip feed system, a needle valve being used to control the flow rate

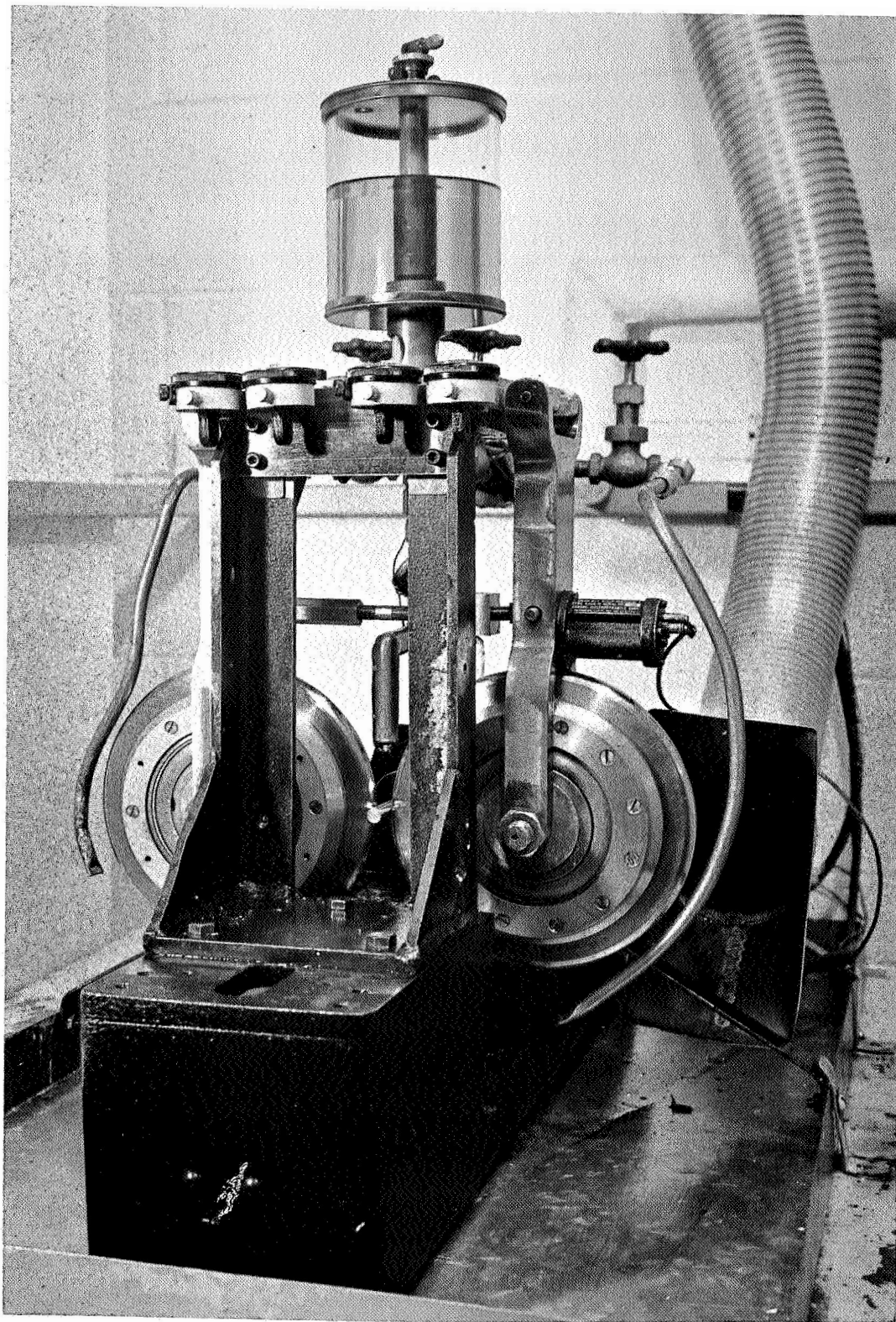


FIGURE 3. GENERAL ELECTRIC RC RIG (C65062510)

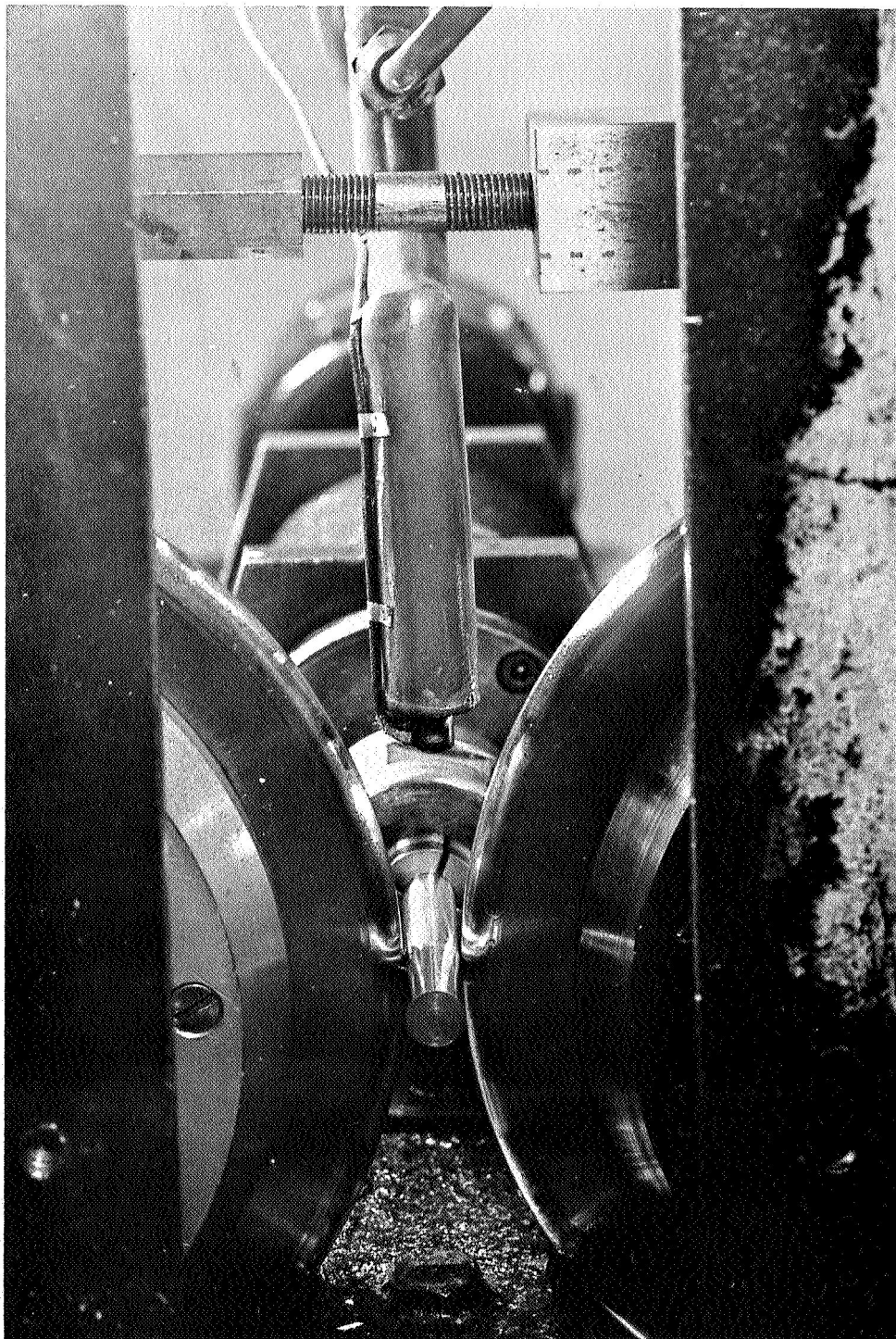


FIGURE: 4. CLOSE-UP OF RC TEST BAR - ROLLER GEOMETRY (C65062512)



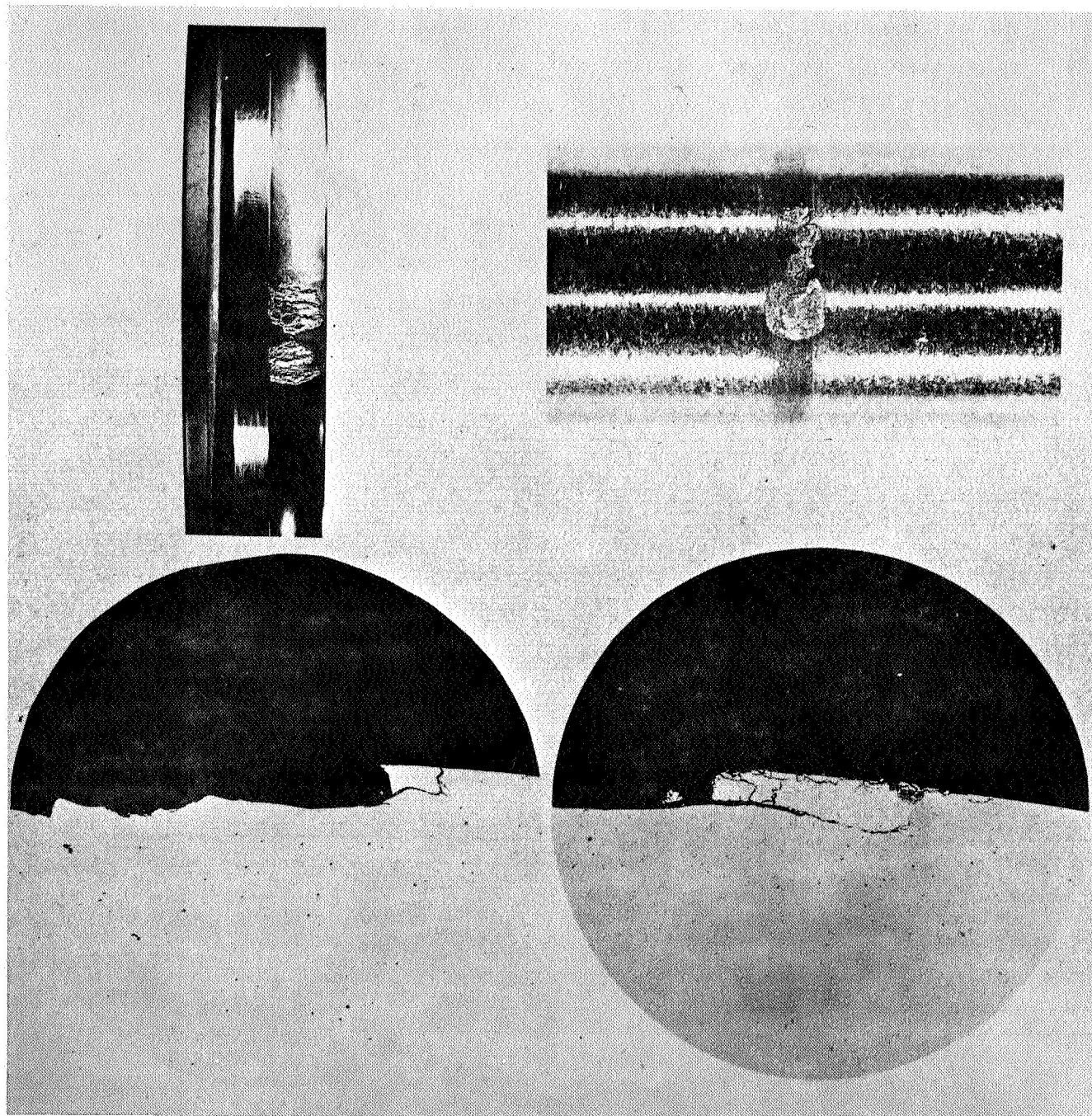


FIGURE 5. FAILURE SIMILARITY BETWEEN ACTUAL BEARING AND RC RIG SPECIMEN

TOP LEFT:	FATIGUE SPALL ON INNER RING OF BEARING.
TOP RIGHT:	FATIGUE SPALL ON RC RIG BAR.
BOTTOM LEFT:	PHOTOMICROGRAPH OF FATIGUE SPALL ON BEARING.
BOTTOM RIGHT:	PHOTOMICROGRAPH OF FATIGUE SPALL ON RC RIG BAR.

at a constant rate of 20 drops per minute. Studies have shown that this flow rate is sufficient to provide adequate lubrication as evidenced by the oil meniscus, seen in Figure 6. A velocity type vibration pick-up is mounted on one of the support yokes. This instrument acts as a failure sensor and terminates the test immediately upon occurrence of a spalling fatigue failure.

In the current program, the test bars were heated via a high frequency induction coil wrapped around the test bar both fore and aft of the contacting rollers. An "Ircon" Infra-red Pyrometer trained on the contact area measures and controls the temperature. Exact temperature control is achieved by using a pyrometer controlled saturable reactor control to cycle the induction heater, Figure 7 shows a view of the Pyrometer Control set-up and a close-up of the induction coil is shown in Figure 8,

The oil is heated by passing it through a hot air heat exchanger prior to dropping it onto the bar. A thermocouple at the outlet of the heat exchanger section measures the oil drop prior to its release. This is shown clearly in Figure 4. Lastly, the rollers are heated by a hot air manifold around a portion of the rollers. This is shown in Figure 3. Heating the rollers prevents thermal gradients and helps to achieve and maintain, close temperature control.

#### 4.2 120 mm Bearing Tester

The design of the bearing testers was dictated by the severe environmental conditions expected during the test, Among these were:

- Continued and prolonged high speed operation at 600F,
- Maintenance of N<sub>2</sub> atmosphere having less than 5 ppm of O<sub>2</sub>
- Exposure to potentially corrosive fluids,

The first of the above listed conditions required that all tester components requiring absolute dimensional integrity over the duration of the test

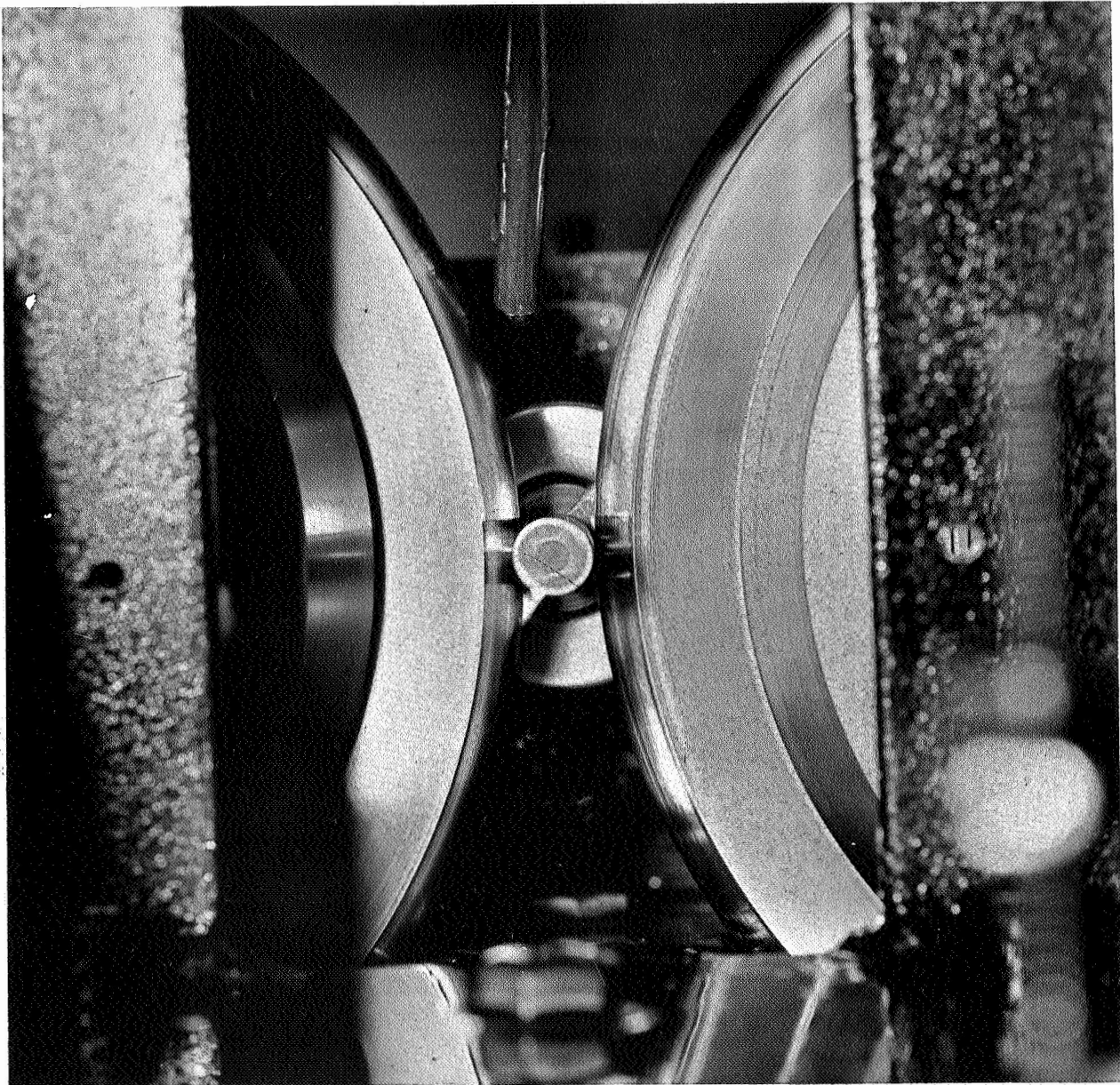


FIGURE 6. HIGH SPEED PHOTOGRAPH OF RC RIG TEST BAR AND ROLLERS. NOTE OIL MENISCUS BETWEEN BAR AND ROLLERS INDICATING PROPER LEVEL OF LUBRICATION.





FIGURE 7. INFRARED PYROMETER IN **USE** ON RC RIG



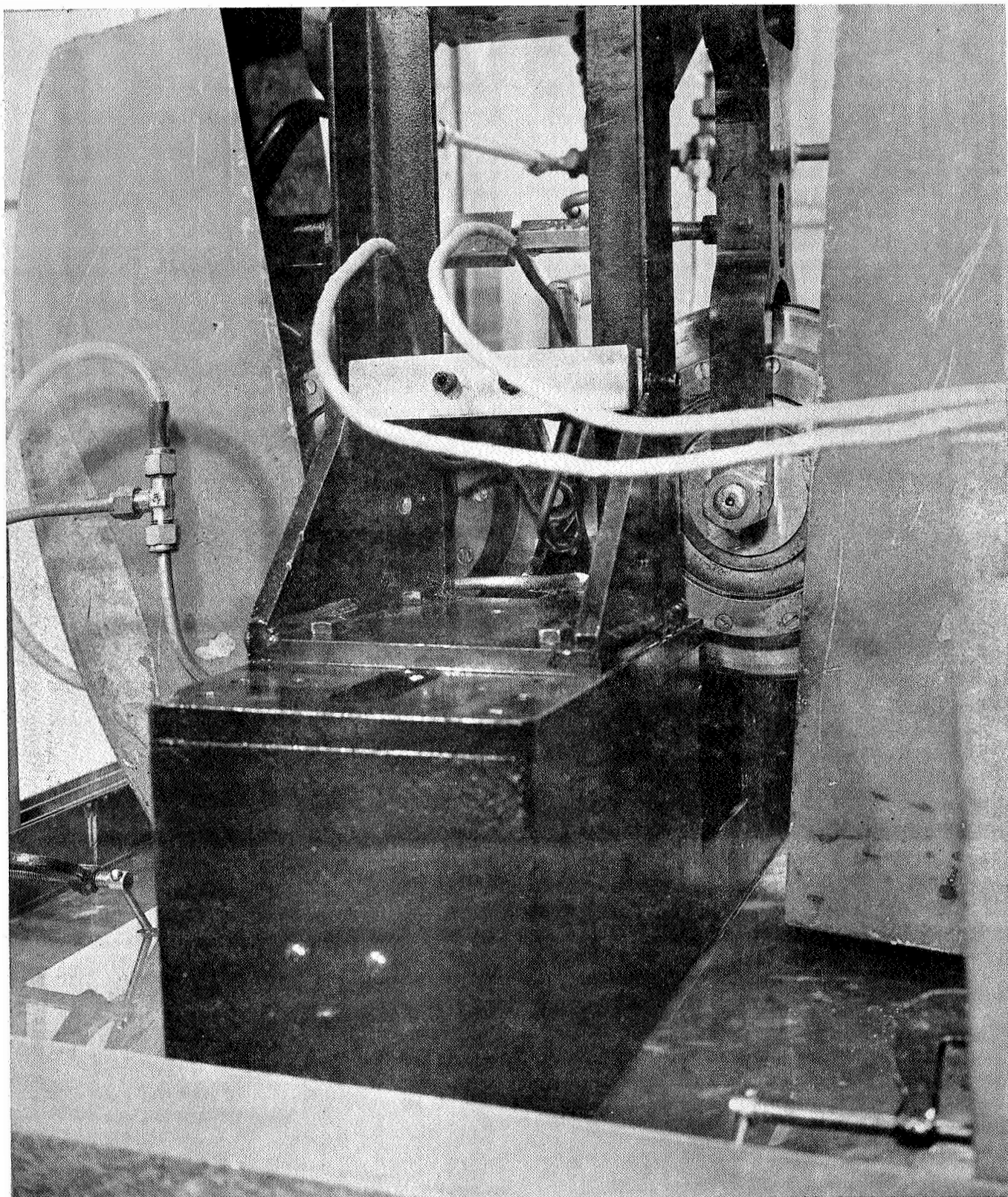


FIGURE 8. HIGH FREQUENCY INDUCTION COILS ON RC RIG.



period had to be made out of a material having good creep properties in the temperature range of interest. AISI 4340 and 4140 were selected and heat treated to assure dimensional stability to temperatures well above the expected maximum operating temperature of 600F.

The N<sub>2</sub> atmosphere was maintained by creating a 5 psi positive pressure in the test cavity. This was achieved by using the tandem carbon seal (Figure 9 ) used in the #1 seal position on the General Electric J79 turbo jet engine. The N<sub>2</sub> gas is introduced between the two seal elements and thus simultaneously pressurizes the seal as well as inerts the test cavity. Since the test cavity and the test oil sump are an integral sealed system, inertion is simultaneously maintained on the test oil reservoir. To maintain a positive flow a vent line from the oil tank allows overboarding of exhaust fumes. The inerting system described, above was totally successful as will be seen later in the section on test results.

The potential corrosiveness of the fluorinated polymer had been cited<sup>(3)</sup> and consequently steps were taken to negate any potential effects on the bearing tests caused by the reaction of this material with tester components. A metallurgical investigation was performed by the Materials Development Laboratory (MDLO) in which samples of materials under consideration for the bearing tester structural members were exposed to the PR-143 in air, at 600F for periods up to 44 hours. The results of this examination are shown in Table 11. In addition to noting the vispal appearance of the test samples, metallographic examination of the specimens were also made and showed no evidence of subsurface and/or intergranular attack on either the Mi plated materials or the Monel.

Based on these results, it was decided that all parts in the main tester body subject to contact with the test oil would be given a Nickel plating per AMS Spec. 2404. Plating thickness was .0003" min. Furthermore, all parts which either because of their unsuitability to reliable plating,

BALTIMORE, MD.		
STEIN SEAL CO. PHILADELPHIA, PA.	SSCY 1888417	578C839 P2
	A3	B
		DELETED CRITICAL SYMBOL FROM NOTE 3 CIDN 111871
	C7 B3	C
		DADDED DADDED NOTE 7
		ECN 95234

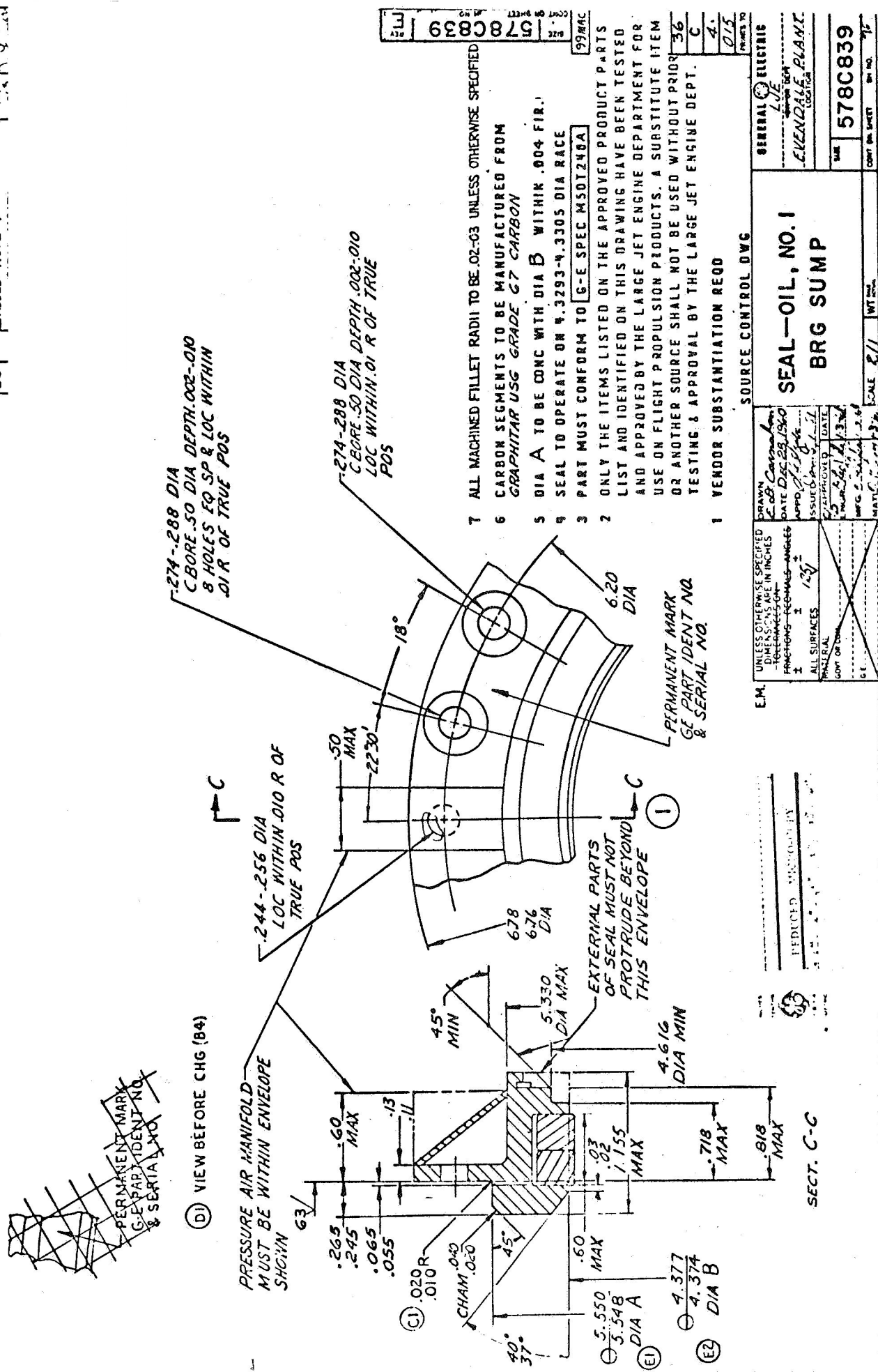


FIGURE 9. NITROGEN SEAL FOR TEST RIG

Table 11

Corrosion Test of Potential  
Bearing Test Rig Materials In  
DuPont PR-143 (Fluorinated Polymer)  
At 600°F Lubricant Temperature

<u>Test Sample Material</u>	<u>Initial Weight</u>	<u>Final Weight</u>	<u>% Changed</u>	<u>Appearance</u>
1. 302 Stainless	7.7273	7.8657 *	+ 1.8	Corroded
2. 302 Stainless	7.8975	8.0324 *	+ 1.7	Some attack
3. Monel	27.2087	27.2718 *	+ 0.2	Very good
4. Monel	27.3449	27.4459 *	+ 0.2	Very slight attack
5. M-50	5.8108	5.8271 *	+ 0.2	Discolored
6. M-50	7.0273	7.0499 *	+ 0.3	Discolored
7. Uncoated Low Carbon Steel (4340)	15.5346	15.4477 **	- 7.	Very corroded flaky rust
8. Nickel Plated <sup>(1)</sup> Low Carbon Steel (4340)	16.4636	16.4639 **	nil	Excellent
9. Nickel Plated <sup>(1)</sup> Low Carbon Steel (4140)	15.9177	15.9177 **	nil	Excellent

The stainless and M-50 samples were sanded with emery cloth to assure complete contact of all surfaces with the PR-143. All samples were then degreased with acetone and dried before weighing initially. The first six samples were started 12:00 noon, 1/4/65, removed at 8:00 a.m., 1/5/65 cleaned with acetone, dried and reweighed (interim weight not shown),

The low carbon steel samples were prepared, degreased with acetone, weighed and all nine samples were put into the 600°F furnace @ 9:15 a.m., 1/5/65.

All samples were removed from furnace @ 9:15, 1/6/65, rinsed with acetone, dried and reweighed (final weight column).

(1) .0003" min thickness, plated per AMS 2404.

\* 44 hours immersion

\*\* 24 hours immersion

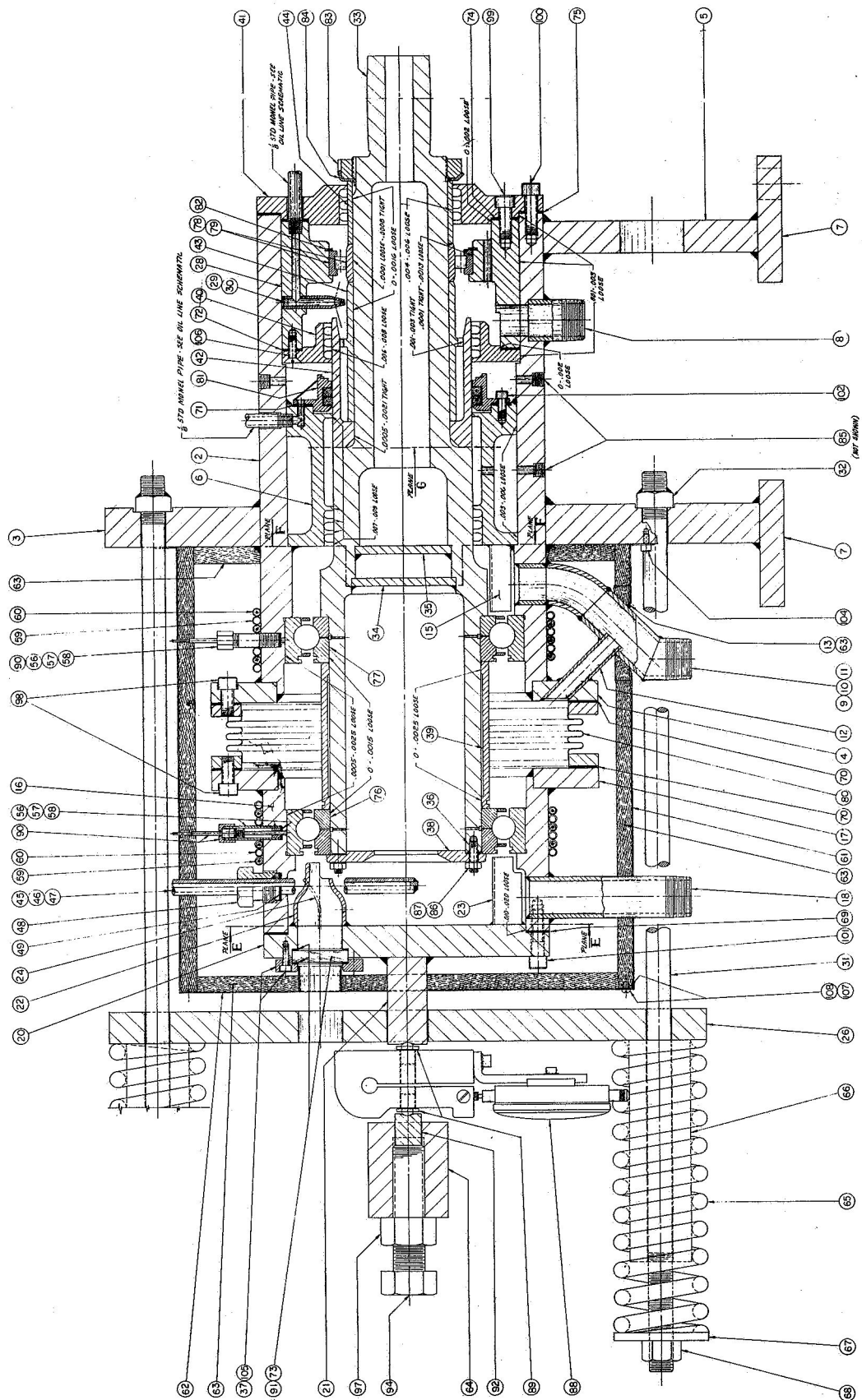
such as the ID of tubes and fittings, or those parts subject to wear, such as pumps, would be made out of Monel. Consequently, the specially designed vane lube pump, the oil tank, all oil supply and return lines were manufactured out of Monel. Also made out of Monel were parts which, because of repeated use would not retain their plating. This included studs, bolt heads and other similar fasteners.

Additionally, compatibility tests were conducted on various elastomers and gasketing materials and it was found that both Viton A and Teflon were acceptable when used with the PR-143.

The test machine assembly is shown in Figure 10. Two stationary housings connected by a bellows form the test sump. One housing is fixed and contains a slave or auxiliary roller bearing to support the test shaft at the drive end; the second housing is free floating and is loaded by a system containing ten springs of 1,000 lb. working capacity each. The test bearings in each housing are axially loaded against each other by the spring system. The load path is from the springs to a circular load plate, through studs, strongback and force-gage to the forward housing. From the forward housing the load is transmitted through the forward test bearing shaft sleeve and aft test bearing to the aft housing, thence to springs via tie rods which penetrate the load plate. The two test bearings are mounted on a test shaft, and are separated by the sleeve which conducts the axial load between inner races. The test bearings are retained on the shaft by a bolted retaining plate, the shaft is therefore located by the test bearings and has axial freedom through the slave roller bearing. Drive of the test rig is accomplished by a flat belt on a crowed spindle at the roller bearing end of shaft.

Initially, two oil systems were provided. These were:

1. Individual oil jets for each test bearing in conjunction with a single axial jet into the: hollow shaft.



SECTION A-A (COMPOSITE)

FIGURE 10 120 MM BEARING TESTER

2. A single oil jet into the hollow shaft with test bearing oil feed achieved by radial metering holes through the Shaft wall to bearing inner ring split.

In each system approximately three gpm (@ 600F) was assigned for maintaining temperatures and exited from the shaft bore, with an additional three gpm routed through the test bearings. Gravity drainage is provided by a single exit from each sump zone outboard of the test bearings with an auxiliary drain from the sump zone between bearings.


It was found that the oil jet into the hollow shaft was not required for good temperature control and did in fact, contribute to a foaming problem. Consequently, this system was eliminated during the check-out phase of the program.

Sealing between the hot oil sump and the auxiliary bearing sump was achieved by a labyrinth seal and a tandem carbon seal. The latter is nitrogen pressurized to maintain a neutral atmosphere in the test oil system. The tandem carbon seal provides radial sealing against a hollow seal race cooled by oil from the auxiliary bearing oil system.

Lubrication of the auxiliary bearing was provided by a common system for the eight test machines, which feeds two double jets in each tester, 1.0 gpm assigned to the roller bearing, 1.0 gpm for heat removal from carbon seal race.

The hollow shaft contains a double bulkhead between the hot test sump zone and the auxiliary bearing/seal zone. The auxiliary bearing end of the bore is cooled by an air tube projecting through the drive spindle. Auxiliary bearing oil seal is achieved by labyrinth seals.

Test oil circulation was accomplished by a slinger-type pump immersed in the test oil reservoir, discharged through a 100 mesh filter. Figure 11



illustrates the data obtained in evaluating the capacity of this pump at 600F and using both oil delivery methods. Eventually, the oil pressure was set and maintained at 2.7 gpm at 26 psi using only the two oil jets to lubricate the bearing. The test oil reservoir is heated through a salt-bath transfer medium by 4KW strip heaters, thermostatically controlled.

The test shaft is driven at 12,000 rpm by a flat belt from a 40 hp, 3550 rpm motor mounted beneath the test assembly. Safety circuits were provided on each machine, activated by test oil pressure and temperature, test bearing temperature, auxiliary oil pressure and temperature, test bearing fatigue failure (vibration), drive belt failure, and loss of nitrogen pressure. Figure 12 is a schematic of the test stand, drive and hot oil system. Figure 13 is an overall view of the test area.

Instrumentation consisted of:

1. Test bearing temperature achieved by:

Contact thermocouples at the test bearing outer races, continuously operative.

Correlative determination of bearing inner-race temperature by optical pyrometer through a sapphire window in the floating housing, for which a shielding tube in the sump and a calibration thermocouple (on the shield) are provided.

2. Vibration

3. Oil Temperature

4. N<sub>2</sub> Dew Point

5. N<sub>2</sub> Flow and Pressure

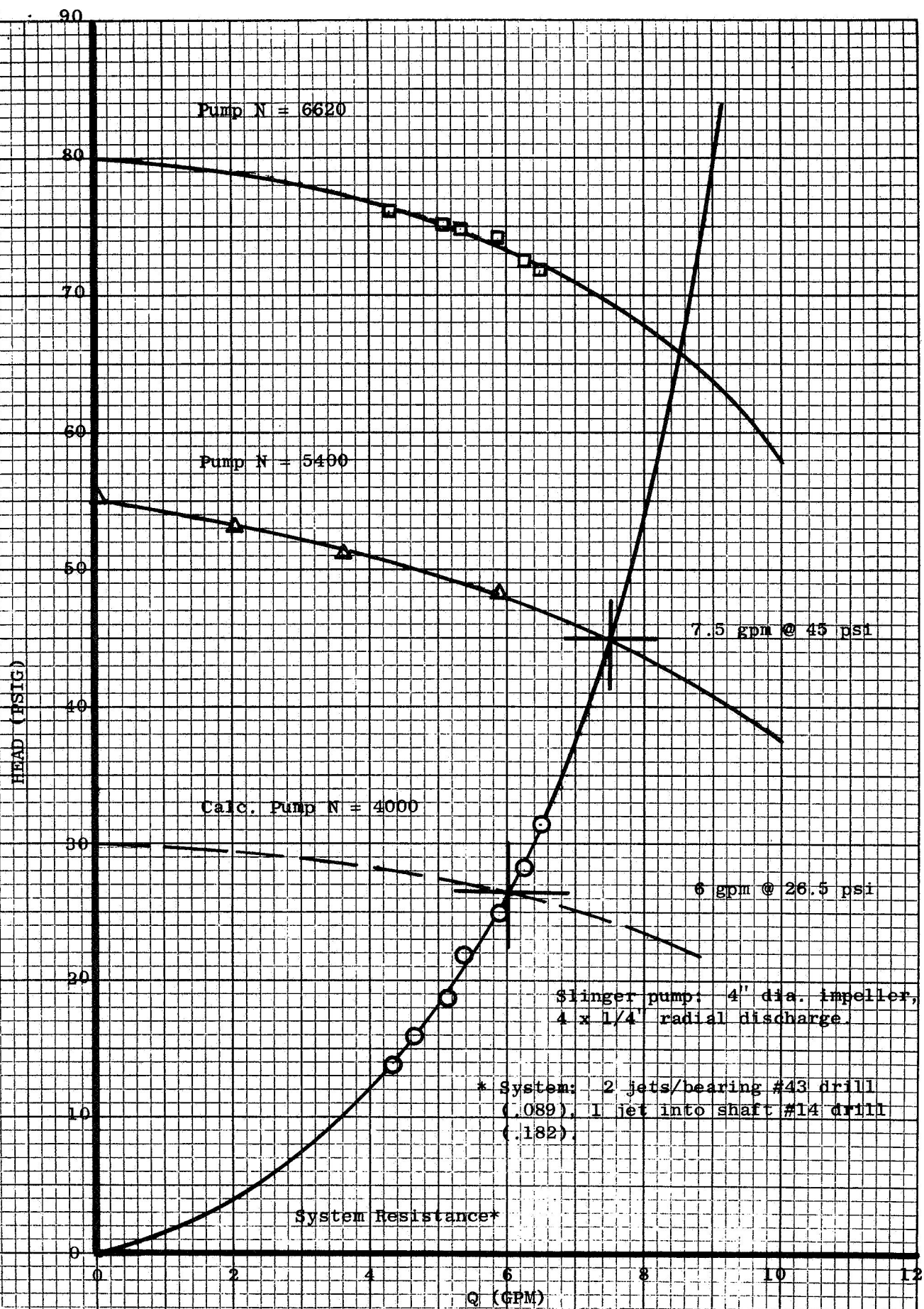


FIGURE 11, HOT OIL PUMP PERFORMANCE





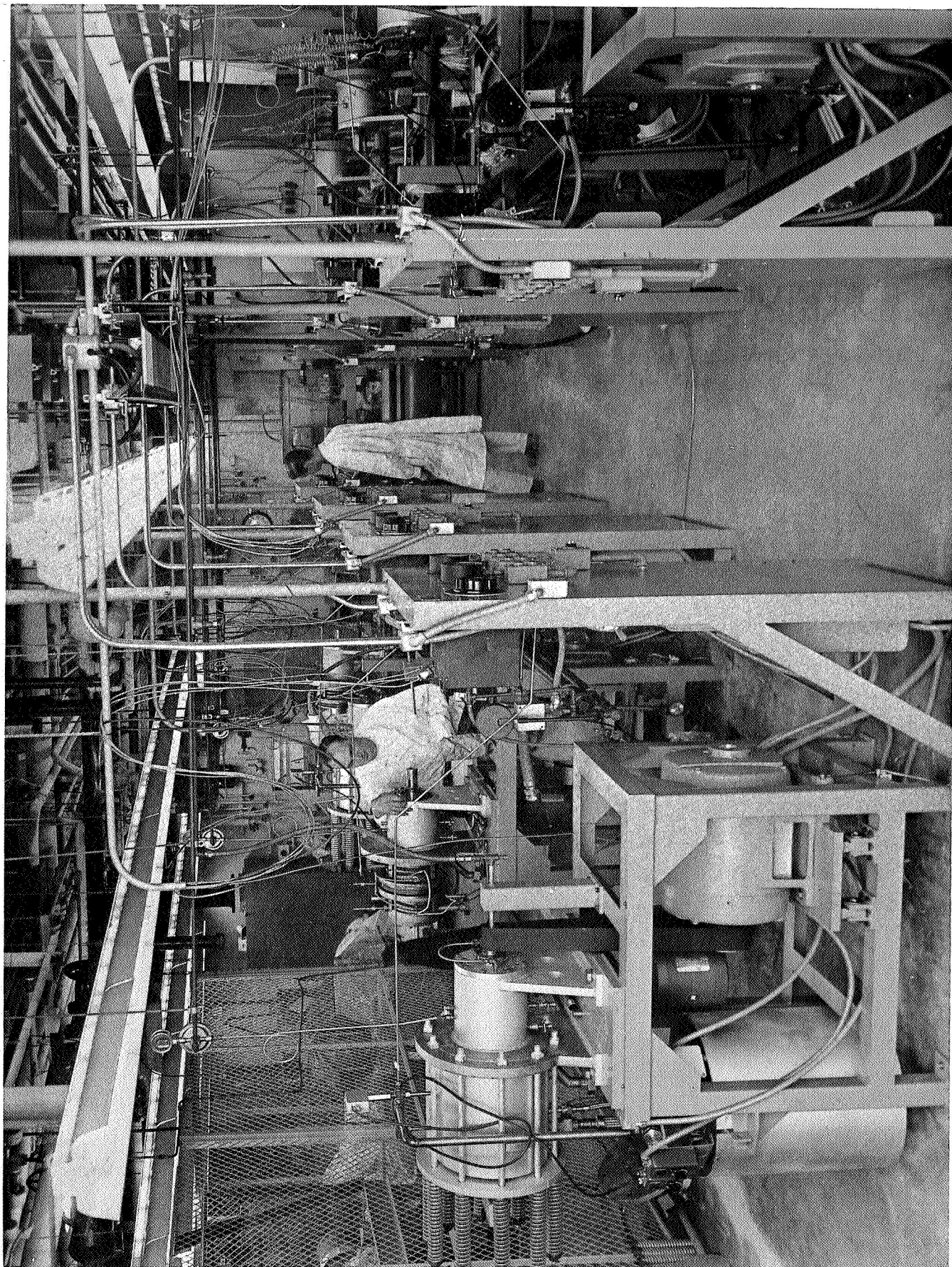


FIGURE 13 VIEW OF BEARING TEST AREA

## 6. Speed

The use of infra-red pyrometry to measure inner ring temperatures proved to be quite effective. The testers were equipped with two reference points used to calibrate the pyrometer. One of these is a target which is thermocoupled and is just inside the viewing port. The second is the bearing outer ring which is also continually temperature monitored with a thermocouple. By calibrating the pyrometer against these two reference points, and then focusing on the inner ring, a very accurate measurement of inner ring temperature could be made.

Two methods were used to provide continuous monitoring of test bearing performance. A rotary switch of 45-second cycle provides 5-second sensing of vibration pick-up output at each machine plus one 5-second spare station and simultaneously connects the appropriate trip circuits, the latter providing a means of shutting down individual machines by interruption of the common holding circuit through all load contacts. The vibration millivolt output is channeled to give a read-out of displacement and also to energize a limit meter which will trip out the appropriate machine when a manually set limit is exceeded. A fuse to ground is used in each trip circuit to identify shutdowns caused specifically by vibration. A selector switch in the temperature recorder provided trip circuit shutdown of individual machines from test bearing over-temperature, the cycle providing sensing of test bearing temperatures (two bearings per machine) on a 40-second interval.

The determination of proper bearing loading was by means of loading spring deflection and a Dillon force gage. Calibration curves for the springs and the bellows connecting the front and rear bearing housing are shown in Figure 14. Figure 15 is a schematic of the loading system and is included for reference to the assembling and loading procedure described below:



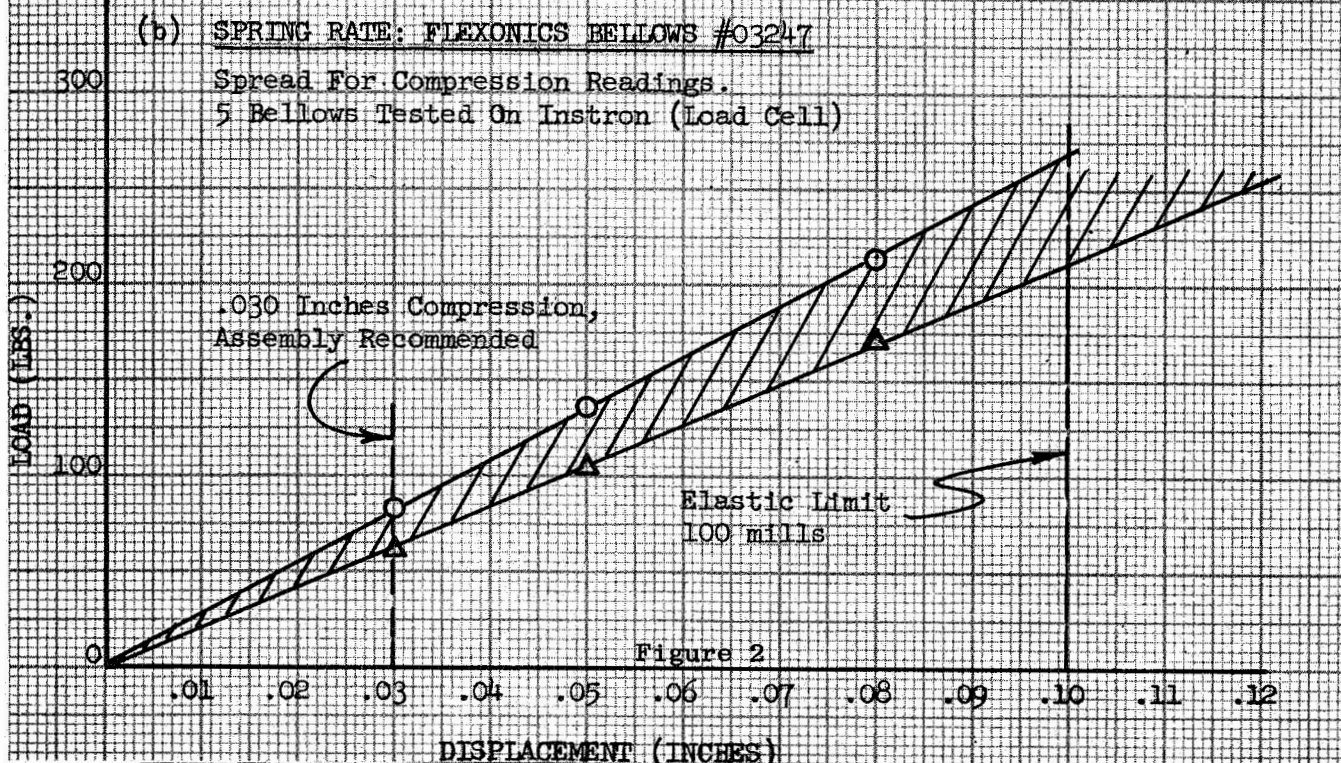
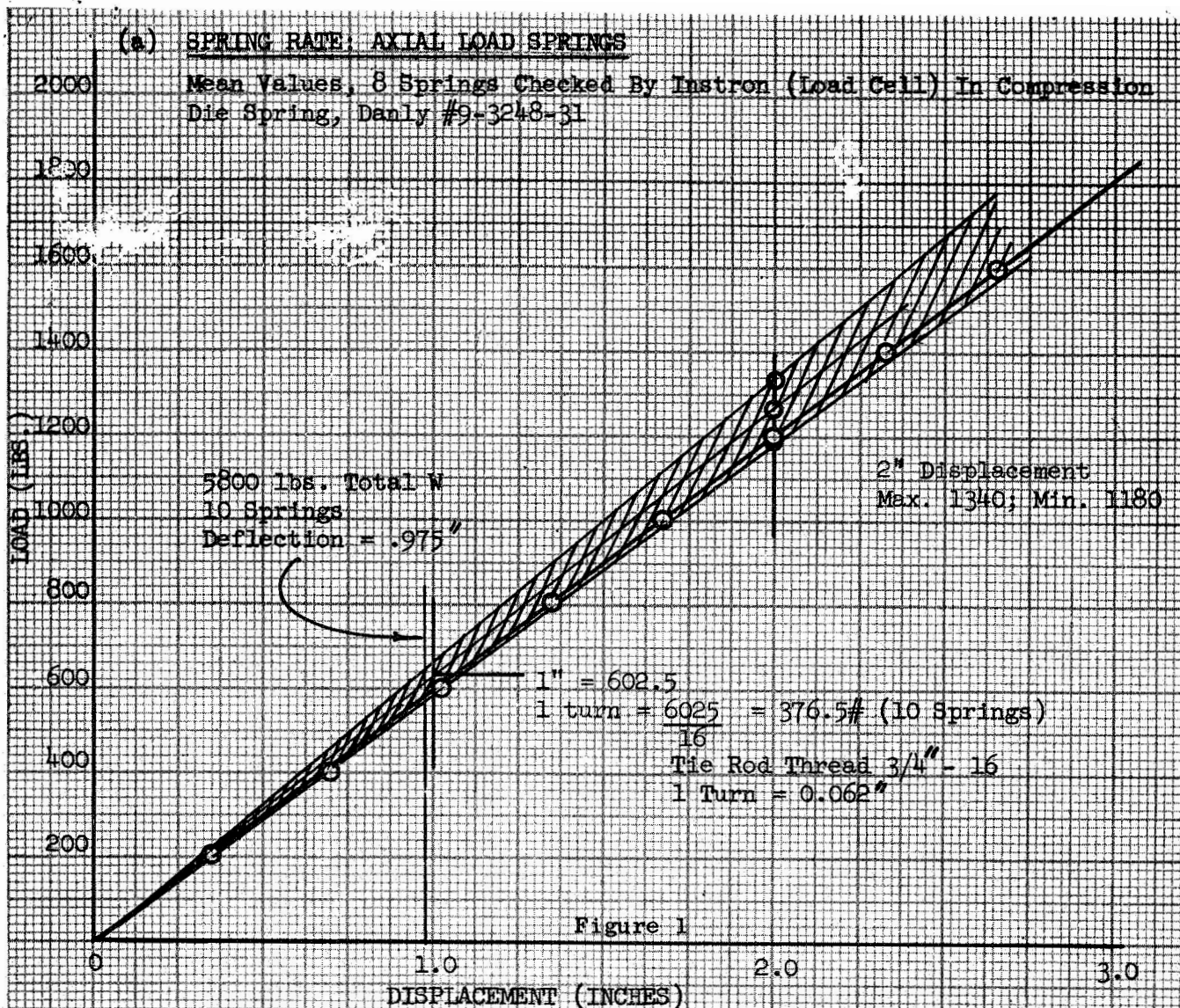


FIGURE 14. CALIBRATION CURVES, BEARING TESTER SPRINGS AND BELLOWS

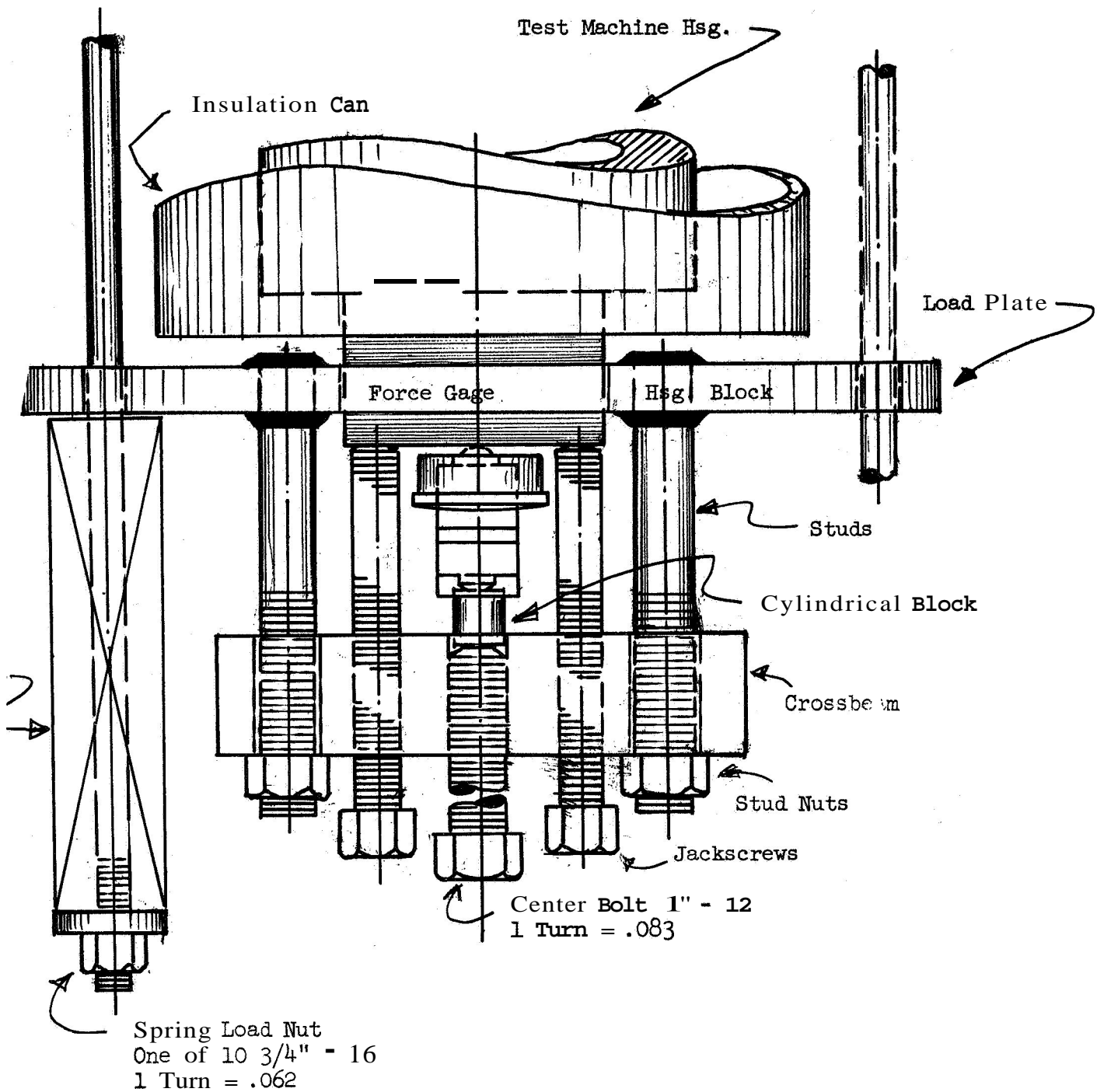


FIGURE 15. SCHEMATIC OF BEARING TESTER LOAD STRUCTURE

1. With floating-housing/bellows flange unbolted, a 10,000 lb. load is applied through the load structure and force gage to align the floating test bearing. The bellows flange bolts are tightened while this load remains applied, so that no radial load component is exerted by the bellows in the final assembly.
2. For 5800 lb. final load setting, the initial 10,000 lb. load is reduced to 725 lb. The load-plate is aligned parallel to the housing face by adjustment of diagonally opposite springs. The cross beam is then aligned parallel to the load-plate, and is shifted within stud clearance to align the force gage load-axis perpendicular to the load-block and load-plate.
3. The gage load is set at 725 lb. by adjustment of the center bolt.
4. The load is transferred to the jackscrews, the gage is removed and a steel ball and spacer block are substituted.
5. Load is transferred to the steel ball,
6. Working load is applied by torqueing the nuts on the ten spring tie-rods in diagonal sequence, a few turns at a time to a total of 14 turns/spring, to give a final load of  $725 + (14)(376.5) = 5800$  lb.
7. Upon completion of a test run, the load is checked prior to dismantling the test machine. This is done by transferring the full load from the steel ball to the force gage using the jackscrews and center bolt, i.e., by supporting the load on the jackscrews during removal of ball by backing-off center bolt, so that no displacement of the load structure occurs during transfer. Some error due to bolt friction is incurred but results check 4 100 lb. and serve to verify test loads.

The inerting nitrogen was supplied through a manifold system emanating from a vaporizer connected to a 125,000 ft.<sup>3</sup> capacity liquid N<sub>2</sub> receiver. To check the quality of the N<sub>2</sub> being supplied to the test bearings, a Beckman Model 778 Oxygen Analyzer was used to perform the O<sub>2</sub> measurements.

The Model 778, while not as sensitive as some oxygen analysis equipment, was considered to be satisfactory for this particular application. It is used to determine the combined O<sub>2</sub> content in the gas entering the tester and the gas escaping from the oil tank vent line. The O<sub>2</sub> content of the N<sub>2</sub> entering the tester is guaranteed by the supplier to be less than 5 ppm. Consequently, if the O<sub>2</sub> content of the N<sub>2</sub> at the vent line is identical to that entering the tester, it is reasonable to assume that an atmosphere containing not more than 5 ppm of O<sub>2</sub> is achieved in the tester.

The procedure used to check this was as follows. The Model 778 Range Selector is set on the most sensitive scale, which is 1-5% O<sub>2</sub> full band width. At this range, accuracy is  $\pm 1\%$  full scale at constant temperature. Linearity and repeatability are  $\pm 0.5\%$  and  $\pm 1\%$  full scale, respectively. The Analyzer probe is inserted into a small-neck reagent bottle along with a discharge line from the N<sub>2</sub> supply manifold. The bottle is capped with a top having a small hole, which reduces the possibility of an excessive pressure build-up in the bottle. The bottle is then purged for about 10 minutes, at which time the zero adjust is used to set the read-out dial on the Oxygen Analyzer at 0.5%. The reason for setting it at this level rather than 0 is merely a matter of convenience in that the .5% point is more accurately readable than the 0 point. The procedure is then repeated, using the line from the tester vent port. Since the exhaust gas contains some oil vapors, it is necessary to insert a condensator into the system. This is achieved by constructing a simple cold trap consisting of a copper coil immersed in a Dewar filled with acetone and dry ice. In the measurements made on the exhaust gas, the 0.5% level was achieved rapidly, indicating that the O<sub>2</sub> level of the escaping gas is essentially the same as that entering the tester.

The Oxygen Analyzer has also been used to obtain a measure of the absolute  $O_2$  content. In this case, the zero oxygen level is set by immersing the probe into a solution of  $Na_2SO_3$  and water. In each case, the vented gas caused the indicator to drive to the zero point indicating a low  $O_2$  content. The overall sensitivity of the instrument was not sufficient to achieve a precise quantitative measurement of the  $O_2$  level.

As with any other test equipment, some modifications were required after initial check-out tests, although in the present case these were held to a minimum and were related primarily to the oil temperature control. Initially, it was thought that external heating of both the tester body and test oil would be necessary to attain and maintain the 600F bearing temperature. However, during the check-out runs, the continual rise in temperature of the lubricating fluid indicated the need for cooling, partly due to the fact that the insulation of the lubricant tank was more effective than originally estimated. Hence, the power generated by the bearings was sufficient to maintain bearing and oil temperatures above 600F without external heating. In the check-out of the last test machine with XRM-177F, it was found that about 1/2 hour of operation would bring the oil temperature up from the 250F starting level to 600F.

Unfortunately, due to the high viscosity of all of the test oils at room temperature, it was necessary to heat them to 250F in order to achieve adequate pumpability. Consequently, in order to achieve control of the operating temperature, cooling coils were added to the salt bath,

A measurement of oil  $\Delta T$  and flow rate showed that 10.6 HP was being removed by the oil from the bearing test housing and returned to the tank. A similar heat balance on the cooling water showed a removal of 6.2 HP. Therefore, 4.4 HP is being rejected from the oil tank and piping by convection. Since the bearing power loss was calculated at 13 HP, it can be inferred that 2.4 HP is rejected by convection of the bearing housing. The table below summarizes the power levels in the system.



1. Bearing Power Loss (Calculated)	13.0 HP
2. Bearing Housing Heat Rejection (By Difference)	2.4 HP
3. Heat Removal by Oil (Measured)	10.6 HP
4. Heat Rejection from Oil Tank (By Difference)	4.4 HP
5. Heat Removal by Cooling Water (Measured)	6.2 HP

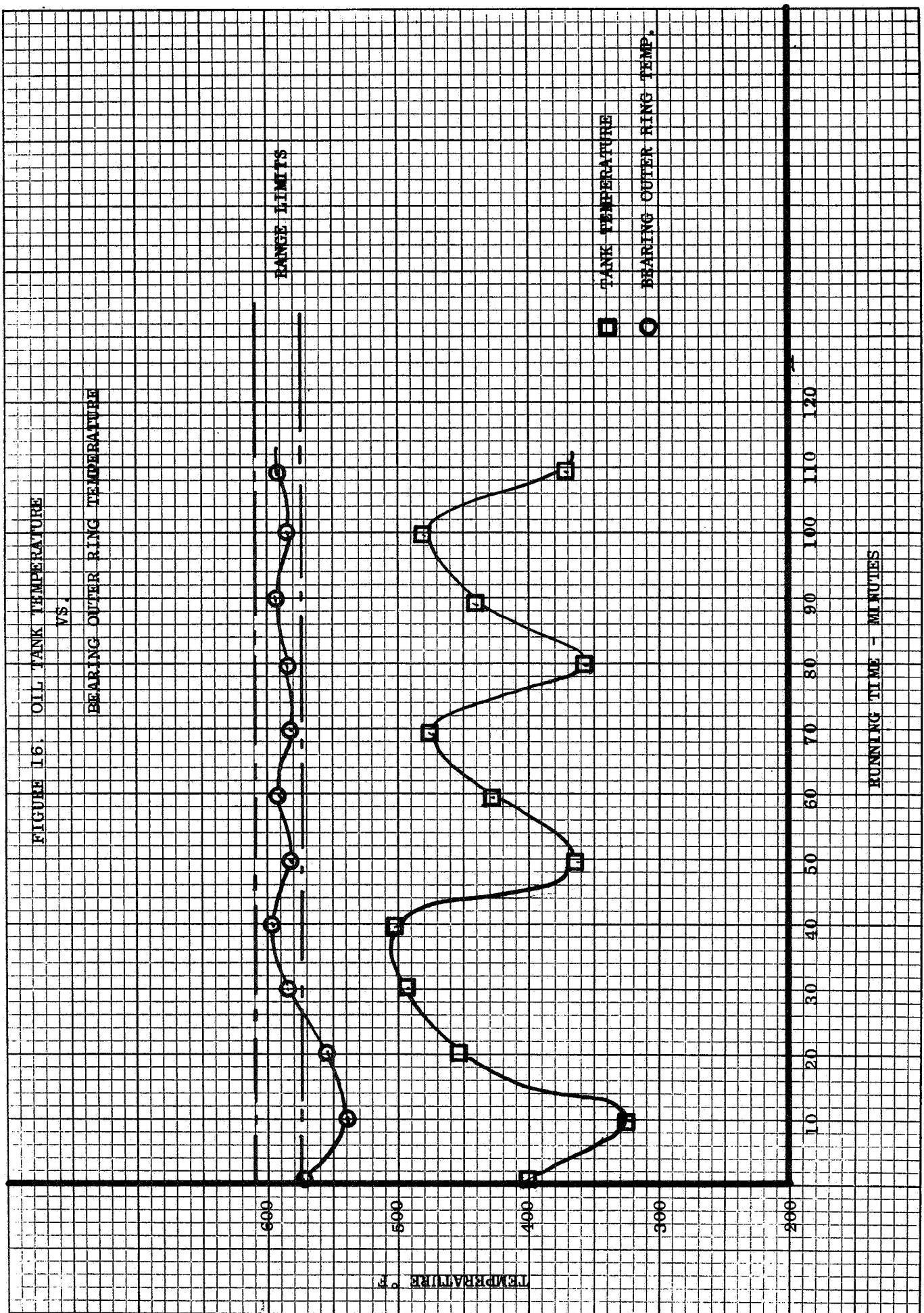
From this information it was determined that a cooling capacity between three and six HP would maintain the bearing outer race temperatures in the desired temperature range of 575F to 610F.

After experimenting with various lengths and diameters of cooling coils, it was determined that 25 feet of 3/8" bore Monel tubing would give the necessary heat transfer surface and would be short enough to prevent vaporization of the cooling water. Figure 16 shows that this system would control outer ring temperatures within the desired range. This cooling system was therefore, installed in the testers with automatic temperature sensors.

The decision made later in the program to adjust temperatures downward to 500F and 400F increased the need for additional heat exchanger capacity and consequently, required the investigation and fabrication of the proper size oil-water heat exchangers.

A second problem was that initially some foaming of both the MCS-354 and the XRM-177F was encountered. The addition of a small quantity (15 cc) of GE F-50 Silicone Fluid to the MCS-354 resulted in an almost immediate cessation of the foaming. The F-50, however, did not react similarly with the XRM-177F. In the case of this fluid, 5 ml of a standard anti-foam agent (10% DC-200, 90% toluene) served to reduce, although not completely eliminate, foaming. To further decrease the foaming, several changes

FIGURE 16. OIL TANK TEMPERATURE  
VS.  
BEARING OUTER RING TEMPERATURE



were made in the tester pump arrangement. The drain lines were shortened so that they now terminated above the level of the fluid. This eliminated the possibility of exposing the pump to a large amount of entrapped  $N_2$ , and allowed more settling time for foam. In addition, the oil flow to the center of the shaft was eliminated in order to reduce the total amount of oil in circulation. Lastly, the center drain line was closed up, forcing all of the oil to exit on the outside drains, thus assuring sufficient lubrication of the bearings.

There was some reservation regarding the last two modifications with regard to their effect on bearing temperature distribution. It was found, however, that temperature control was improved as evidenced by the fact that the outer races of the two test bearings now have the same temperature, where previously a  $2^\circ$  differential existed.

The addition of an anti-foaming agent to the mineral oil was discussed with Mobil Oil technical personnel, who expressed the opinion that the addition of this material would have no effect whatsoever on the performance of the XRM-177F. This information was reviewed with NASA personnel who had previously verbally approved the use of the anti-foam additive.

Other than the above two problems, no major difficulties were encountered with the testers. Some operational problems were encountered, however these were caused by the nature and behavior of the test fluids and will be discussed in the appropriate sections of this report.

## 5.0 Rolling Element Computer Analysis Program (RECAP)

The testing of precision bearings may appear to be a relatively simple task in that the bearings are placed in a suitable machine, a load is applied, the bearing is brought to speed and temperature and run until failure occurs. Unfortunately, this is a gross over-simplification. A rolling element bearing is a highly complex device and as such carries with it extremely complex stress patterns and variables affecting its ultimate performance.

The individual stress distributions, component kinematics and interactions must be known and controlled in order to achieve meaningful test data. The relationships of the rolling elements under actual engine operating conditions have always been a challenge to bearing designers due to a firm lack of understanding and because of the extremely tedious and relatively inaccurate hand calculations required to define these variables. Consequently, several years ago, Mr. A. B. Jones, under a consulting agreement with General Electric, developed a digital computer program to solve and clarify the above calculations.<sup>(6)</sup> This program now in general use by General Electric is known as RECAP (Rolling Element Computer Analysis Program). This program was used prior to and during the testing phase to predict inner and outer race contact angles, stresses, and lives in an effort to eliminate stress differences and thus, fatigue life differences between test bearings due to contact angle and curvature variations.

An important input to the program were the results obtained on the RC Rig materials which indicated the relative degree of improvement and/or degradation which could be expected with the various fluids and at the proposed operating temperature.

A typical RECAP data sheet is shown in Figure 17. This particular set of conditions examines the bearing used in the current program at an axial load of 5800 lbs. and a speed of 12,000 rpm. As may be seen,

the fatigue life prediction for the entire bearing is  $\sim 15.3 \times 10^6$  revolutions which is  $\sim 21$  hours. Multiplying this by five for M-50, it can be seen that the  $B_{10}$  life is close to the 100 hours  $B_{10}$  life set for this program. It should be pointed out that the AFBMA life prediction for this bearing is 18.7 hours using the race curvatures ( $f_1 = 54$ ,  $f_0 = 52$ ) used in the subject test bearings,

COLLING ELEMENT COMPUTED ANALYSIS PROGRAM  
 GENERAL ELECTRIC COMPANY  
 ADVANCE TECHNOLOGY AND DEMONSTRATOR PROGRAMS DEPARTMENT  
 ADVANCED BEARING AND SEAL TECHNOLOGY UNIT

CC #CCRE X4407  
 NASA HRG

SYSTEM PARAMETERS

BEARING NUMBER	NUMBER OF BALLS/ROLLS	BALL/ROLL DIAMETER	PITCH DIAMETER	RACE CURVATURES		CONTACT ANGLE	DIAMETRAL CLEARANCE	INITIAL PRELOAD	DISTANCE TO MOMENT CENTER
1	1.5000E 01	8.1250E-01	6.1023E 00	OUTER	INNER	5.4000E-01	-0.	-0.	1.8000E 01
2	2.8000E 01	4.3300E-01	4.6800E 00	-0.	-0.	-0.	5.0000E-03	-0.	-1.8000E 01
BEARING NUMBER	CONTROL ASSUMPTION	DENSITY	ELASTIC MODULUS	POISSON'S RATIO	BALLS/ROLLS	FRICITION COEFFICIENT	TOTAL ROLL LENGTH	1 = CALCULATED STRESSES	
1	1.0000E 00	2.8300E-01	2.9000E 07	2.5000E-01	2.5000E-01	7.5000E-02	-0.	1.0000E 00	
2	-0.	2.8300E-01	2.9000E 07	2.5000E-01	2.5000E-01	7.5000E-02	4.3000E-01	1.0000E 00	
BEARING NUMBER	EFFECTIVE ROLL LENGTH	S IN/ROLL	CONSTANT INNER R	SPIN/ROLL EXPONENT	FATIGUE CONSTANT	ROLL LAMBDA			
1	-0.	-0.	-0.	-0.	OUTER INNER	OUTER INNER			
2	3.3000E-04	-0.	-0.	-0.	7.1400E 03 4.9500E 04	-0. 0.1000E-01			
BEARING NUMBER	PHASE ANGLE	CONSTANT THRUST	1 = FLOAT RADIALY	INITIAL DISPLACEMENTS			SHIM		
1	-0.	-0.	-0.	ALONG X	ALONG Y	ALONG Z	ABOUT Z		
2	-0.	-0.	-0.	-0.	-0.	-0.	-0.		

INPUT DATA FROM LOAD CONDITION 1

EXTERNAL LOADS APPLIED AT MOMENT CENTER

ALONG X ALONG Y ALONG Z ABOUT Y ABOUT Z

-5.8000E 03 -0. 2.0000E 00 -0.

LOAD VECTOR ROTATES WITH RESPECT TO OUTER RACES

LOAD VECTOR ROTATES WITH RESPECT TO INNER RACES

6 ITERATIONS WITH 8 BALLS ELEMENTS PLUS 1 WITH COMPLETE COMPONENT

SYSTEM COMPUT DATA

BEARING NUMBER	ALONG X	ALONG Y	ALONG Z	ABOUT Y	ABOUT Z
1	5.8000E 03	-1.0001E-03	-1.9993E 00	3.6001E 01	-1.3657E-03
2	0.	0.	0.	0.	0.
BEARING NUMBER	ALONG X	ALONG Y	ALONG Z	ABOUT Y	ABOUT Z
1	4.7202E	30.71615E-10	-4.7747E-04	2.4567E-05	5.3077E-11
2	2.0642E 06	4.1225E 06	4.1226E 06	1.5551E 09	1.5551E 09

FIGURE 17

RELATIVE DISPLACEMENTS AT BEARING CENTER  
 A CNE X ALONG Y ALONG Z ABOUT Y ABOUT Z  
 4.7202E-03 -5.7498E-11 -3.5262E-05 2.4567E-05 9.0265E-11

NON-LINEAR SPRING RATES AT BEARING CENTER  
 A CNE X ALONG Y ALONG Z ABOUT Y ABOUT Z  
 2.0642E-06 4.1225E-06 4.1226E-06 9.8018E-06 9.8017E-06

FATIGUE LIFE  
 OUTER RACE INNER RACE BEARING BEARING TORQUE  
 1.2542E-02 1.6675E-01 1.5227E-01 4.2429E-01

BALL/ROLL NUMBER	ANGULAR POSITION	BALL/ROLL LOADS	OPERATING CONTACT ANGLES	CENTRIFUGAL FORCE	GYROSCOPIC MOMENT	TYPE OF CONTACT	VECTOR ATTITUDE
1	0.	1.0209E-03 8.4511E-02 2.0797E-01 2.7348E-01	1.9395E-02	-1.1191E-01	Q00000	1.8390E-01	
2	2.4000E-01	1.0209E-03 8.4506E-02 2.0790E-01 2.7339E-01	1.9395E-02	-1.1187E-01	Q00000	1.8384E-01	
3	4.8000E-01	1.0208E-03 8.4493E-02 2.0771E-01 2.7314E-01	1.9394E-02	-1.1176E-01	Q00000	1.8367E-01	
4	7.2000E-01	1.0206E-03 8.4474E-02 2.0742E-01 2.7277E-01	1.9391E-02	-1.1160E-01	Q00000	1.8341E-01	
5	9.6000E-01	1.0204E-03 8.4454E-02 2.0709E-01 2.7235E-01	1.9389E-02	-1.1142E-01	Q00000	1.8312E-01	
6	1.2000E-02	1.0203E-03 8.4436E-02 2.0677E-01 2.7194E-01	1.9387E-02	-1.1124E-01	Q00000	1.8284E-01	
7	1.4400E-02	1.0202E-03 8.4424E-02 2.0652E-01 2.7163E-01	1.9385E-02	-1.1110E-01	Q00000	1.8262E-01	
8	1.6800E-02	1.0201E-03 8.4417E-02 2.0639E-01 2.7145E-01	1.9384E-02	-1.1103E-01	Q00000	1.8250E-01	
9	1.9200E-02	1.0201E-03 8.4417E-02 2.0639E-01 2.7145E-01	1.9384E-02	-1.1103E-01	Q00000	1.8250E-01	
10	2.1600E-02	1.0202E-03 8.4424E-02 2.0652E-01 2.7163E-01	1.9385E-02	-1.1110E-01	Q00000	1.8262E-01	
11	2.4000E-02	1.0203E-03 8.4436E-02 2.0677E-01 2.7194E-01	1.9387E-02	-1.1124E-01	Q00000	1.8284E-01	
12	2.6400E-02	1.0204E-03 8.4454E-02 2.0709E-01 2.7235E-01	1.9389E-02	-1.1142E-01	Q00000	1.8312E-01	
13	2.8800E-02	1.0206E-03 8.4474E-02 2.0742E-01 2.7277E-01	1.9391E-02	-1.1160E-01	Q00000	1.8341E-01	
14	3.1200E-02	1.0208E-03 8.4493E-02 2.0771E-01 2.7314E-01	1.9394E-02	-1.1176E-01	Q00000	1.8367E-01	
15	3.3600E-02	1.0209E-03 8.4506E-02 2.0790E-01 2.7339E-01	1.9395E-02	-1.1187E-01	Q00000	1.8384E-01	

BALL/ROLL NUMBER	GYRO SLIP COEFFICIENT	ORBITAL VELOCITY	ROTATIONAL VELOCITY	SPINNING VELOCITY	ROLLING VELOCITY	SPIN/ROLL RATIO	SPINNING TORQUES
1	2.6982E-02	5.3079E-03	-4.4877E-04	1.0062E-04	-3.9875E-04	2.0014E-01	OUTER 3.4608E-00 INNER 2.1155E-00
2	2.6974E-02	5.3078E-03	-4.4877E-04	1.0059E-04	-3.9875E-04	2.0007E-01	OUTER 3.4606E-00 INNER 2.1153E-00
3	2.0950E-02	5.3077E-03	-4.4876E-04	1.0050E-04	-3.9874E-04	1.9990E-01	OUTER 3.4601E-00 INNER 2.1149E-00
4	2.0916E-02	5.3074E-03	-4.4874E-04	1.0038E-04	-3.9871E-04	1.9964E-01	OUTER 3.4594E-00 INNER 2.1142E-00
5	2.0876E-02	5.3071E-03	-4.4873E-04	1.0023E-04	-3.9869E-04	1.9934E-01	OUTER 3.4586E-00 INNER 2.1136E-00
6	2.0838E-02	5.3068E-03	-4.4871E-04	1.0009E-04	-3.9867E-04	1.9906E-01	OUTER 3.4580E-00 INNER 2.1130E-00
7	2.0808E-02	5.3065E-03	-4.4870E-04	9.9981E-05	-3.9865E-04	1.9883E-01	OUTER 3.4575E-00 INNER 2.1128E-00
8	2.0791E-02	5.3064E-03	-4.4869E-04	9.9921E-05	-3.9864E-04	1.9871E-01	OUTER 3.4573E-00 INNER 2.1123E-00
9	2.0791E-02	5.3064E-03	-4.4869E-04	9.9921E-05	-3.9864E-04	1.9871E-01	OUTER 3.4573E-00 INNER 2.1123E-00
10	2.0808E-02	5.3065E-03	-4.4870E-04	9.9981E-05	-3.9865E-04	1.9883E-01	OUTER 3.4575E-00 INNER 2.1128E-00
11	2.0838E-02	5.3068E-03	-4.4871E-04	1.0009E-04	-3.9867E-04	1.9906E-01	OUTER 3.4580E-00 INNER 2.1130E-00
12	2.0876E-02	5.3071E-03	-4.4873E-04	1.0023E-04	-3.9869E-04	1.9934E-01	OUTER 3.4586E-00 INNER 2.1136E-00
13	2.0916E-02	5.3074E-03	-4.4874E-04	1.0038E-04	-3.9871E-04	1.9964E-01	OUTER 3.4594E-00 INNER 2.1142E-00
14	2.0950E-02	5.3077E-03	-4.4876E-04	1.0050E-04	-3.9874E-04	1.9990E-01	OUTER 3.4601E-00 INNER 2.1149E-00
15	2.0982E-02	5.3079E-03	-4.4877E-04	1.0059E-04	-3.9875E-04	2.0007E-01	OUTER 3.4606E-00 INNER 2.1153E-00

BALL/ROLL NUMBER	ROLLING TORQUES	OPERATING PITCH DIA.	SEMI-MAJOR AXIS	SEMI-MINOR AXIS	MEAN COMPRESSIVE STRESS
1	2.0683E-01 8.9745E-02	6.1039E-00	1.1753E-01 8.5674E-02	1.5518E-02 1.4586E-02	OUTER 1.7817E-05 INNER 2.1527E-05
2	2.0682E-01 8.9737E-02	6.1039E-00	1.1753E-01 8.5673E-02	1.5518E-02 1.4585E-02	OUTER 1.7817E-05 INNER 2.1527E-05
3	2.0678E-01 8.9714E-02	6.1039E-00	1.1752E-01 8.5668E-02	1.5517E-02 1.4584E-02	OUTER 1.7816E-05 INNER 2.1526E-05
4	2.0673E-01 8.9681E-02	6.1039E-00	1.1752E-01 8.5662E-02	1.5517E-02 1.4583E-02	OUTER 1.7815E-05 INNER 2.1525E-05
5	2.0667E-01 8.9647E-02	6.1039E-00	1.1751E-01 8.5656E-02	1.5516E-02 1.4581E-02	OUTER 1.7814E-05 INNER 2.1524E-05
6	2.0662E-01 8.9616E-02	6.1039E-00	1.1751E-01 8.5650E-02	1.5516E-02 1.4580E-02	OUTER 1.7813E-05 INNER 2.1523E-05
7	2.0658E-01 8.9594E-02	6.1039E-00	1.1750E-01 8.5646E-02	1.5515E-02 1.4579E-02	OUTER 1.7812E-05 INNER 2.1522E-05
8	2.0657E-01 8.9583E-02	6.1039E-00	1.1750E-01 8.5644E-02	1.5515E-02 1.4578E-02	OUTER 1.7812E-05 INNER 2.1522E-05
9	2.0658E-01 8.9594E-02	6.1039E-00	1.1750E-01 8.5646E-02	1.5515E-02 1.4579E-02	OUTER 1.7812E-05 INNER 2.1522E-05
10	2.0658E-01 8.9594E-02	6.1039E-00	1.1750E-01 8.5646E-02	1.5515E-02 1.4579E-02	OUTER 1.7812E-05 INNER 2.1522E-05
11	2.0662E-01 8.9616E-02	6.1039E-00	1.1751E-01 8.5650E-02	1.5516E-02 1.4580E-02	OUTER 1.7813E-05 INNER 2.1523E-05
12	2.0667E-01 8.9647E-02	6.1039E-00	1.1751E-01 8.5656E-02	1.5516E-02 1.4581E-02	OUTER 1.7814E-05 INNER 2.1524E-05
13	2.0673E-01 8.9681E-02	6.1039E-00	1.1752E-01 8.5662E-02	1.5517E-02 1.4583E-02	OUTER 1.7815E-05 INNER 2.1525E-05
14	2.0678E-01 8.9714E-02	6.1039E-00	1.1752E-01 8.5668E-02	1.5517E-02 1.4584E-02	OUTER 1.7816E-05 INNER 2.1526E-05
15	2.0682E-01 8.9737E-02	6.1039E-00	1.1753E-01 8.5673E-02	1.5518E-02 1.4585E-02	OUTER 1.7817E-05 INNER 2.1527E-05

FIGURE 17 (CONTD)

BALL/ROLL NUMBER	UPPER EDGE OF PATH		LOWER EDGE OF PATH		H/D VALUES		SV	
	OUTER	INNER	OUTER	INNER	OUTER	INNER	VALUE	VALUE
1	3.6949E 01	3.8608E 01	4.6453E 00	1.6087E 01	1.0443E-01	1.1803E-01	1.145E 00	1.2145E 00
2	3.6942E 01	3.8599E 01	4.6386E 00	1.6079E 01	1.0439E-01	1.1797E-01	1.2141E 00	1.2130E 00
3	3.0921E 01	3.8573E 01	4.6196E 00	1.6054E 01	1.0428E-01	1.1782E-01	1.2130E 00	1.2113E 00
4	3.0892E 01	3.8536E 01	4.5917E 00	1.6018E 01	1.0412E-01	1.1760E-01	1.2094E 00	1.2076E 00
5	3.0858E 01	3.8493E 01	4.5596E 00	1.5977E 01	1.0393E-01	1.1735E-01	1.2054E 00	1.2034E 00
6	3.0825E 01	3.8452E 01	4.5288E 00	1.5937E 01	1.0376E-01	1.1711E-01	1.2028E 00	1.2008E 00
7	3.0800E 01	3.8419E 01	4.5048E 00	1.5906E 01	1.0362E-01	1.1692E-01	1.2008E 00	1.1988E 00
8	3.0786E 01	3.8402E 01	4.4917E 00	1.5889E 01	1.0355E-01	1.1682E-01	1.2008E 00	1.1988E 00
9	3.0786E 01	3.8402E 01	4.4917E 00	1.5889E 01	1.0355E-01	1.1682E-01	1.2008E 00	1.1988E 00
10	3.0800E 01	3.8419E 01	4.5048E 00	1.5906E 01	1.0362E-01	1.1692E-01	1.2008E 00	1.1988E 00
11	3.0825E 01	3.8452E 01	4.5288E 00	1.5937E 01	1.0376E-01	1.1711E-01	1.2008E 00	1.1988E 00
12	3.0858E 01	3.8493E 01	4.5596E 00	1.5977E 01	1.0393E-01	1.1735E-01	1.2008E 00	1.1988E 00
13	3.0892E 01	3.8536E 01	4.5917E 00	1.6018E 01	1.0412E-01	1.1760E-01	1.2113E 00	1.2100E 00
14	3.0921E 01	3.8573E 01	4.6196E 00	1.6054E 01	1.0428E-01	1.1782E-01	1.2130E 00	1.2113E 00
15	3.0942E 01	3.8599E 01	4.6386E 00	1.6079E 01	1.0439E-01	1.1797E-01	1.2141E 00	1.2124E 00

BALL/ROLL NUMBER	MAXIMUM ORTHOGONAL SHEAR STRESS		MAXIMUM SHEAR STRESS		INNEP DEP-H	
	OUTER PSI	OUTER DEPTH	INNER PSI	INNER DEPTH	OUTER PSI	OUTER DEPTH
1	1.2544E 02	7.6611E-03	1.0382E 02	7.1428E-03	1.1777E-02	-1.0501E 05
2	1.2543E 02	7.6610E-03	1.0382E 02	7.1427E-03	1.1777E-02	-1.0501E 05
3	1.2542E 02	7.6608E-03	1.0380E 02	7.1422E-03	1.1776E-02	-1.0500E 05
4	1.2540E 02	7.6604E-03	1.0378E 02	7.1415E-03	1.1776E-02	-1.0500E 05
5	1.2538E 02	7.6601E-03	1.0375E 02	7.1407E-03	1.1775E-02	-1.0499E 05
6	1.2536E 02	7.6599E-03	1.0373E 02	7.1401E-03	1.1775E-02	-1.0498E 05
7	1.2535E 02	7.6597E-03	1.0371E 02	7.1396E-03	1.1775E-02	-1.0498E 05
8	1.2534E 02	7.6596E-03	1.0371E 02	7.1393E-03	1.1775E-02	-1.0498E 05
9	1.2534E 02	7.6596E-03	1.0371E 02	7.1393E-03	1.1775E-02	-1.0498E 05
10	1.2535E 02	7.6597E-03	1.0371E 02	7.1396E-03	1.1775E-02	-1.0498E 05
11	1.2536E 02	7.6599E-03	1.0373E 02	7.1401E-03	1.1775E-02	-1.0498E 05
12	1.2538E 02	7.6601E-03	1.0375E 02	7.1407E-03	1.1775E-02	-1.0499E 05
13	1.2540E 02	7.6604E-03	1.0378E 02	7.1415E-03	1.1776E-02	-1.0500E 05
14	1.2542E 02	7.6608E-03	1.0380E 02	7.1422E-03	1.1776E-02	-1.0500E 05
15	1.2543E 02	7.6610E-03	1.0382E 02	7.1427E-03	1.1777E-02	-1.0501E 05

OUTPUT FOR BEA IN 3 NO Z

BEAR IN NC ZIS <COMPLETELY UNLOADED

FIGURE 17 (CONTD)



## 6.0 Test Results

### 6.1 RC Rig Tests

RC Rig testing was performed under the following conditions for all but one test series.

Temperature :	Metal 600F $\pm$ 5F Oil 500F $\pm$ 20F
Load:	700,000 psi max. hertz
Speed:	25,000 stress cycles/min, (1350 fpm surface speed)
Atmosphere:	Air

One test series was performed in an inerted atmosphere to determine whether this would have any effect on the test results. The results of this test will be discussed later,

The first series of RC Rig tests was conducted on the three base fluids and CVM M-50 material. The data from these tests are presented in Weibull distribution in Figures 18 through 20. These data as well as the composite curve (Figure 21) have been published in an NASA TN dated May, 1967. <sup>(7)</sup>

The three curves in the above figures are a composite of essentially three heats of M-50. A master heat (Latrobe 54265) used by General Electric for rig qualification and verification studies and the two CVM billet heats used respectively for the rings and rolling elements of the test bearings. The data, taken as a composite show the following trend:

<u>Lubricant</u>	<u>B<sub>10</sub> Life (Millions of Stress) Cycles</u>	<u>B<sub>50</sub> Life (Millions of Stress) Cycles</u>	<u>Weibull Slope</u>
Mobil XRM-177F	2.35	7.26	1.7
Monsanto MCS-354	.69	2.70	1.4
DuPont PR-143	1.04	6.76	1.0
AFBMA *	1.4	-	-

\* The AFBMA value is shown for the RC Rig at a maximum hertz stress of 700,000 psi and for CVM M-50.

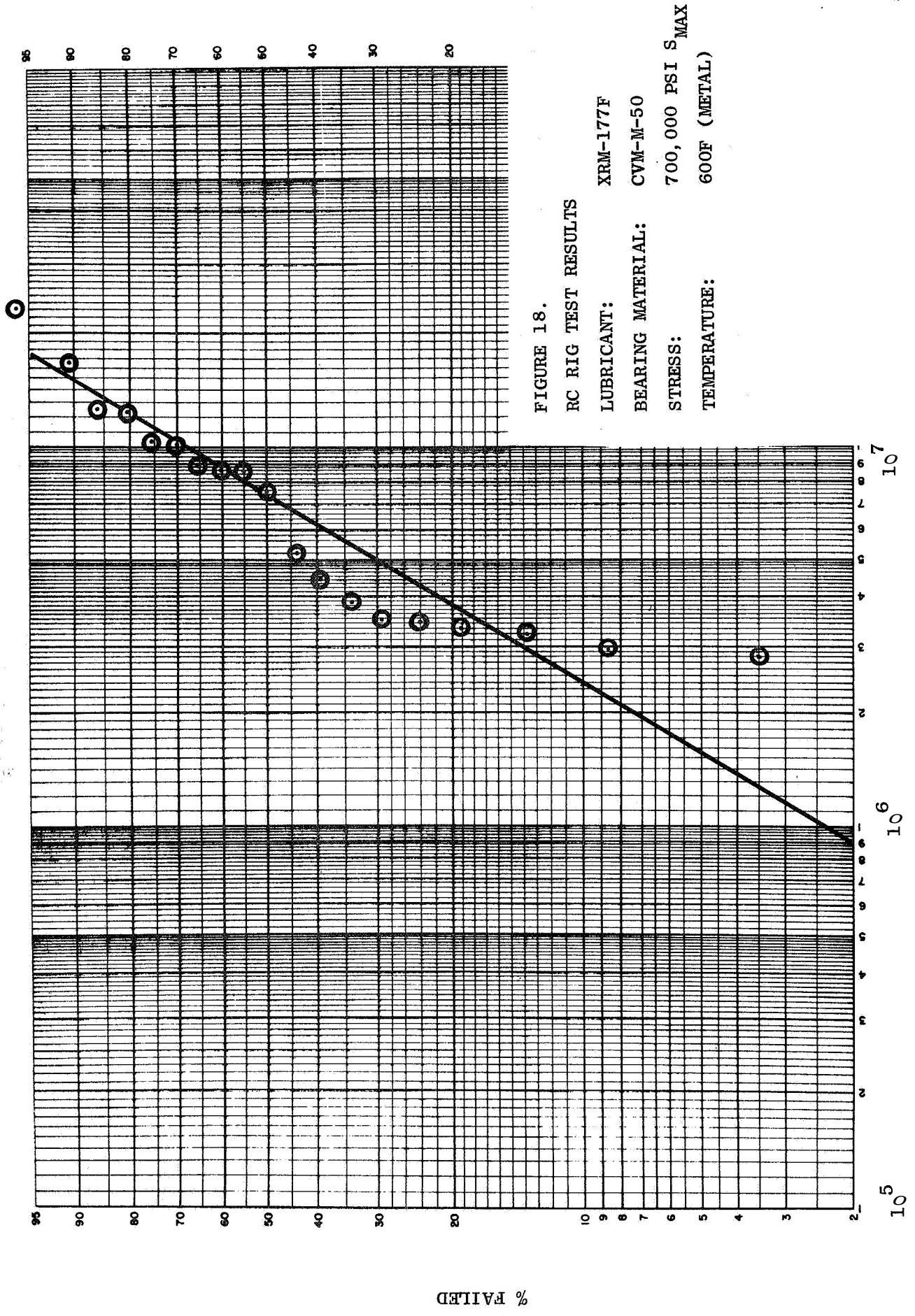


FIGURE 18.  
 RC RIG TEST RESULTS  
 LUBRICANT: XRM-177F  
 BEARING MATERIAL: CVM-M-50  
 STRESS: 700,000 PSI  $S_{MAX}$   
 TEMPERATURE: 600F (METAL)

LIFE - STRESS CYCLES

% FAILED

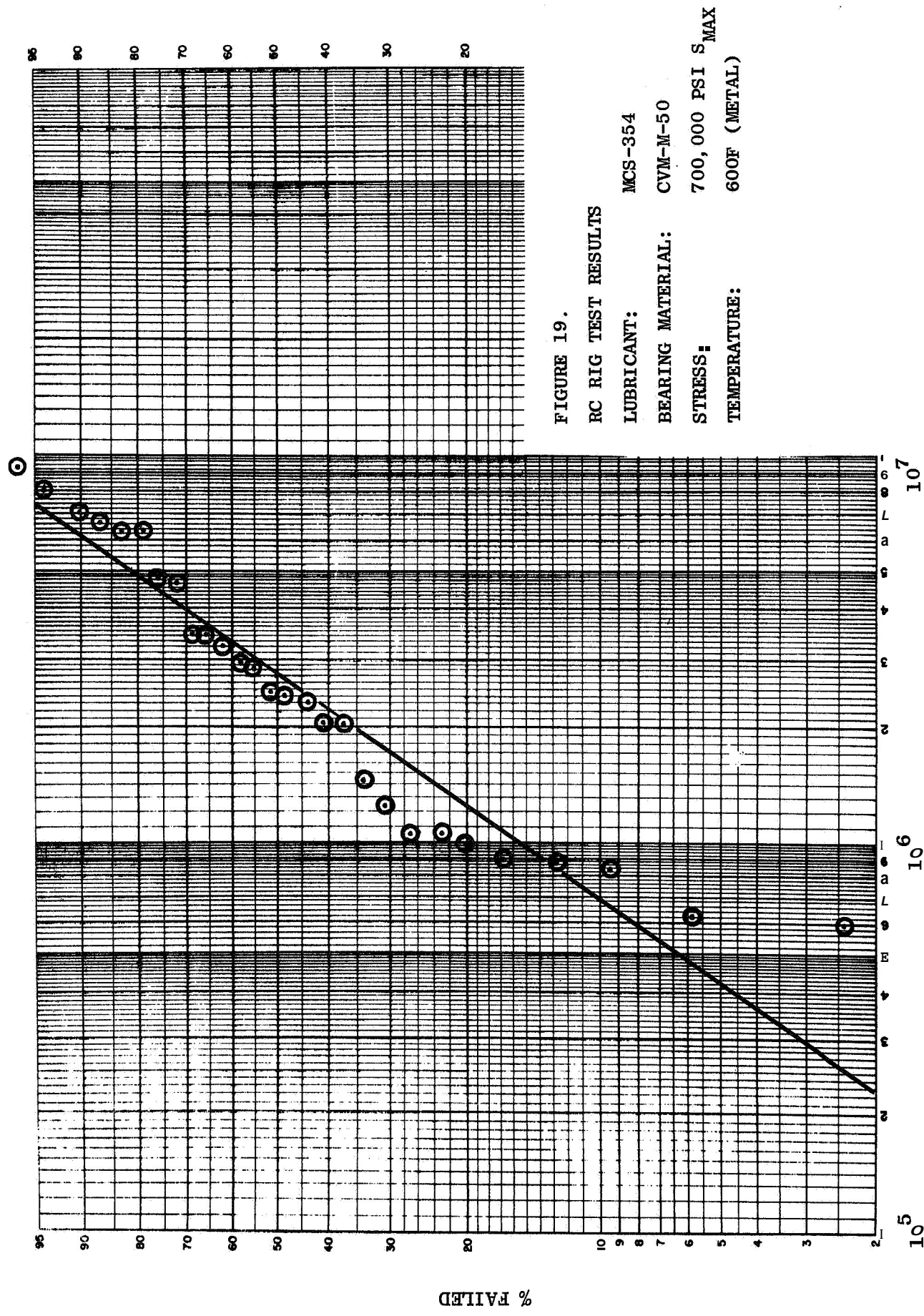


FIGURE 19.

RC RIG TEST RESULTS

LUBRICANT: MCS-354

BEARING MATERIAL: CVM-M-50

STRESS: 700,000 PSI  $S_{MAX}$

TEMPERATURE: 600F (METAL)

LIFE - PRESS CYCLES

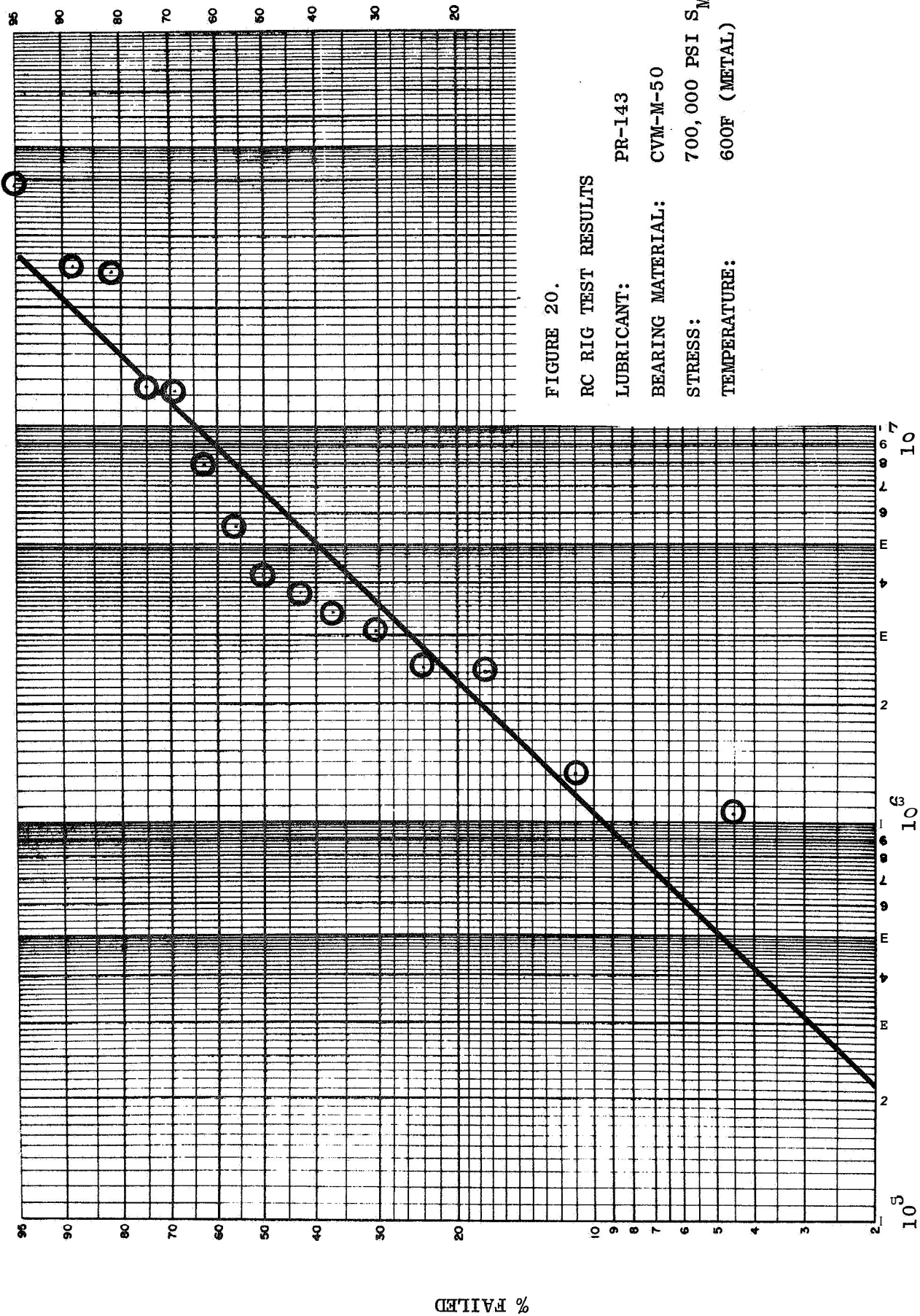


FIGURE 20.

RC RIG TEST RESULTS

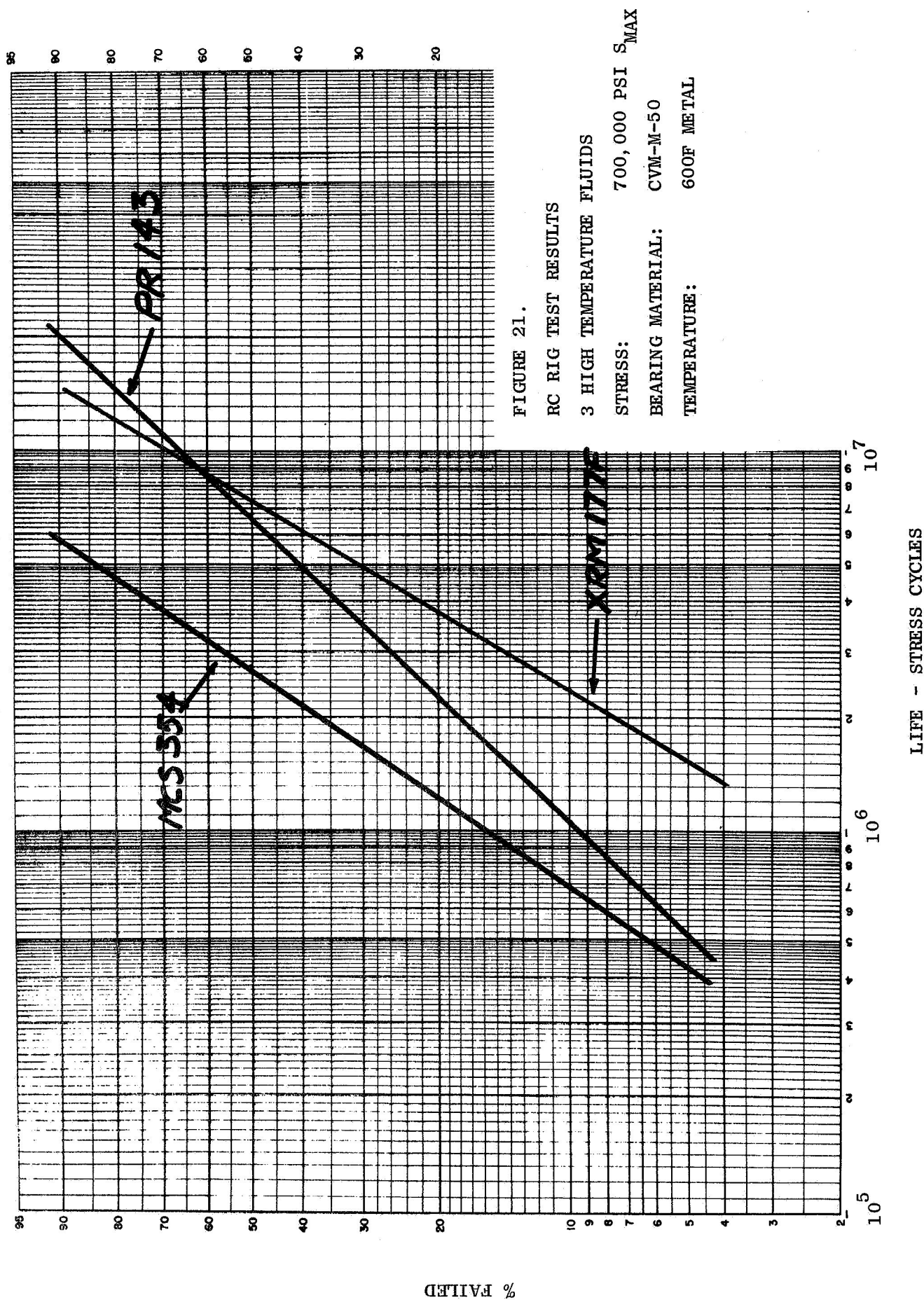
LUBRICANT: PR-143

BEARING MATERIAL: CVM-M-50

STRESS: 700,000 PSI  $S_{MAX}$

TEMPERATURE: 600F (METAL)





The above tabulation shows that the DuPont material will provide approximately AFBMA life, the XRM-177F should better this by about a factor of two, whereas the MCS-354 will show a drastic reduction in fatigue life.

These rankings were verified by the full scale bearing tests as will be shown later.

Secondly, it is interesting to individually examine in the RC Rig the two CVM billet heats of M-50 used for ring and ball manufacture. This is illustrated for XRM-177F in Figure 22 and here it is shown that the ball material is lower in fatigue life versus the ring material ( $B_{10}$  of 2.9 versus  $B_{10}$  of 6.8). The same trend is shown in Figure 23 which compares these two billet heats tested with the Monsanto MCS-354. These observations led to the conclusion that a greater incidence of ball failures should be expected than one would normally expect on a statistical basis. Again, as will be shown later, this was indeed the case. It should be pointed out that this type of prior information is extremely valuable, as armed with this knowledge, the tendency to blame the test or test conditions for the unusual number of ball failures is eliminated and along with it much needless, time consuming and expensive re-examination of test procedures, etc.

The second major test series was conducted with the most promising of the three test fluids (XRM-177F) and the WB-49 bearing material. This data is presented in Weibull distribution in Figure 24. The following life comparison can be made:

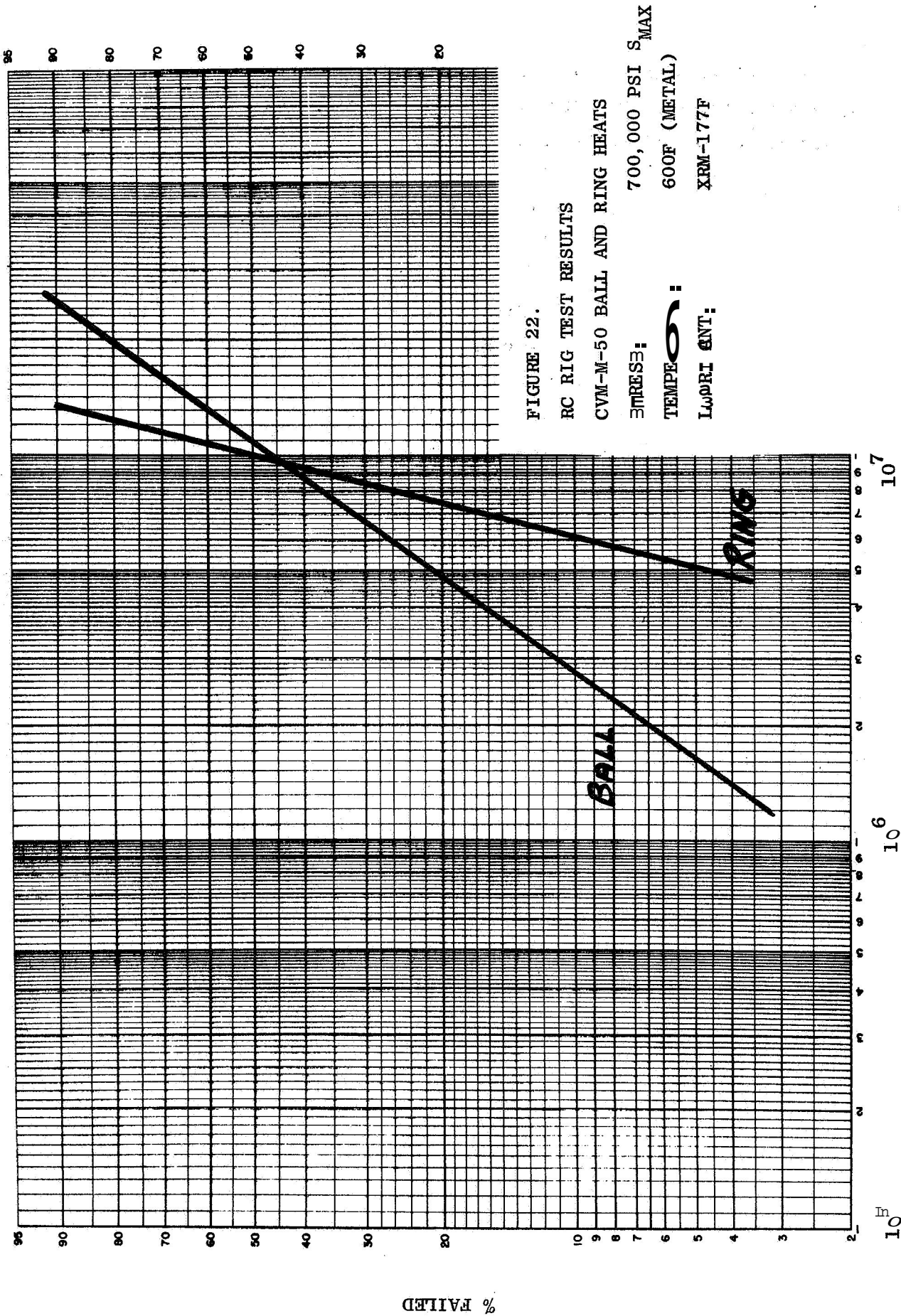


FIGURE 22.

RC RIG TEST RESULTS

CVM-M-50 BALL AND RING HEATS

STRESS: 700,000 PSI  $S_{MAX}$

TEMPERATURE: 600F (METAL)

LOAD: 177F

LIFE - STRESS CYCLES

% FAILED

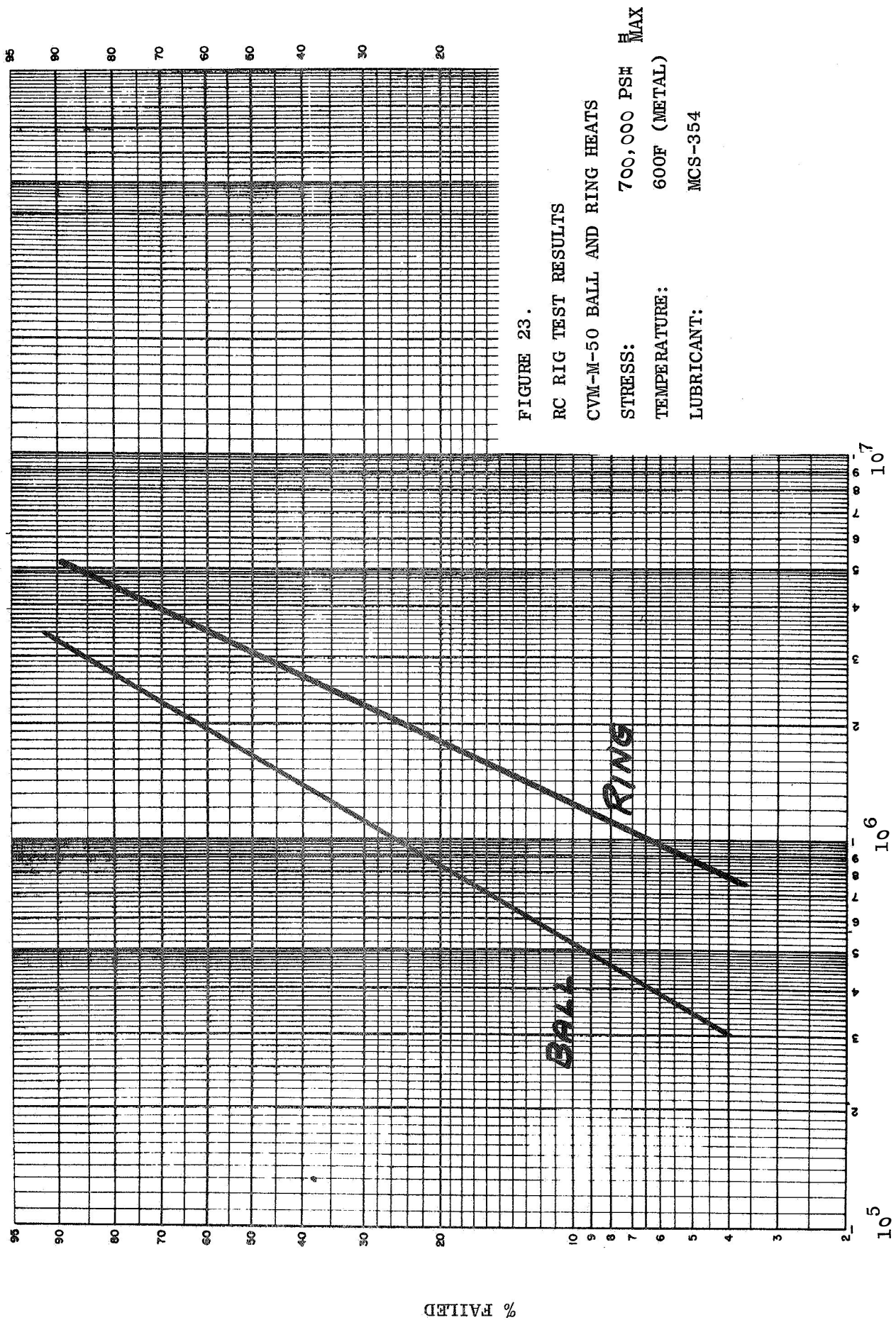


FIGURE 23.

RC RIG TEST RESULTS

CVM-M-50 BALL AND RING HEATS

STRESS: 700,000 PS<sub>H</sub> MAX

TEMPERATURE: 600F (METAL)

LUBRICANT: MCS-354

% FAILED

LIFE - STRESS CYCLES



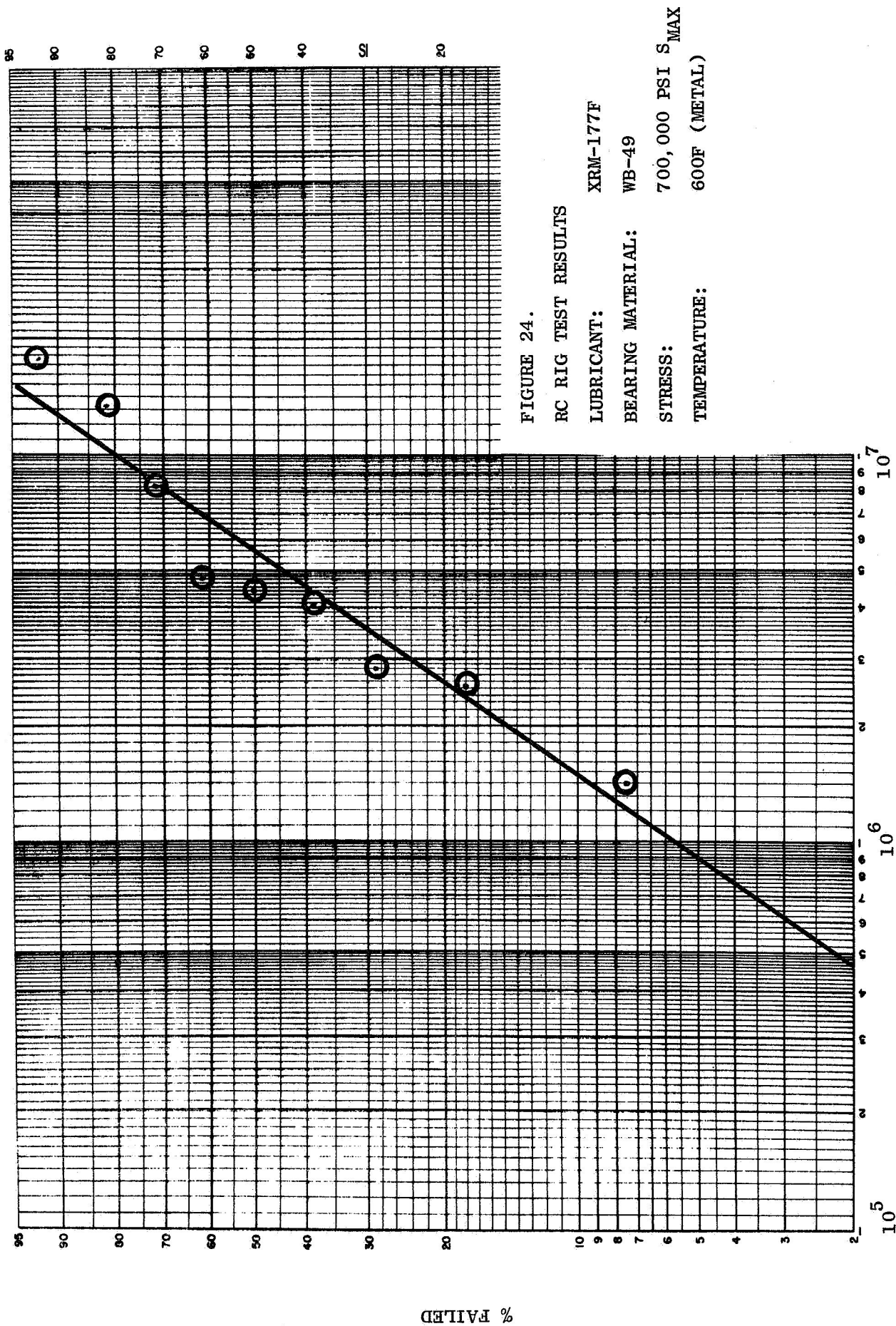


FIGURE 24.

RC RIG TEST RESULTS

LUBRICANT:

XRM-177F

BEARING MATERIAL:

WB-49

STRESS:

700,000 PSI  $S_{MAX}$

TEMPERATURE:

600F (METAL)

LIFE - STRESS CYCLES

% FAILED

<u>Test Material</u>	<u>Fluid</u>	<u>B<sub>10</sub> Life (Stress Cycle)</u>	<u>B<sub>50</sub> Life (Stress Cycle)</u>
M50	XRM-177F	$3.85 \times 10^6$	$9.0 \times 10^6$
WB-49	XRM-177F	$1.45 \times 10^6$	$5.6 \times 10^6$

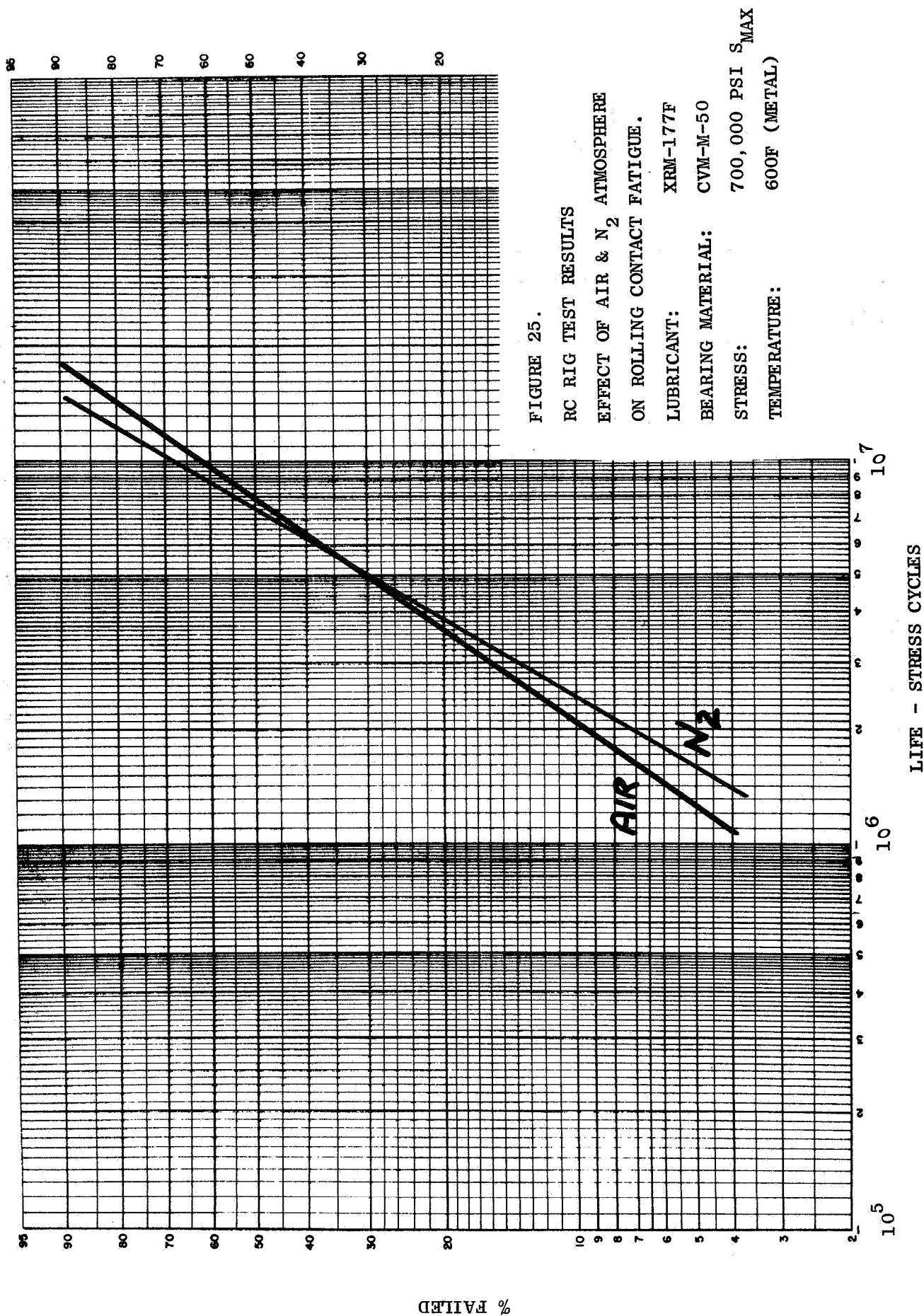
These data indicate the WB-49 to be inferior to the CVM M-50, Again, this observation based on RC Rig testing was verified in subsequent full scale tests.

The last test series which was performed was a determination of the effect of inerting the test fluid, in this case the XRM-177F. As is shown in the curve in Figure 25 essentially no difference in fatigue life is observed when testing the XRM-177F in a nitrogen atmosphere or in air. This is not unexpected as the RC Rig is a once-through system and test times are relatively short, ranging from <1 hour to ~8 hours. Consequently, any oxidation degradation of the oil which could affect the lubricant rheological properties would not have a significant effect on fatigue life. This may not be the case in the actual bearing tests, where the test fluid is recirculated and exposed to high temperatures for time periods as long as 750 hours. Here, inertion at least for two of the experimental fluids is essential to prevent fluid degradation and seizure of the operating components

## 6.2 Full Scale Bearing Tests

The full scale bearing test program as originally proposed consisted of the following schedule:

<u>Test Series</u>	<u>Lubricant</u>	<u>Bearing Material</u>	<u>Test Temp.</u>	<u>B<sub>10</sub>=</u>	<u>B<sub>50</sub> Cut-Off</u>	<u>No. of Tests</u>
I	XRM-177F	CVM M-50	600F	100 hr.	500 hr.	30
II	MCS-354	CVM M-50	600F	100 hr.	500 hr.	30
III	PR-143	CVM M-50	600F	100 hr.	500 hr.	30
IV	(Best of 3 above)	WB-49	600F	100 hr.	500 hr.	30
V	Same as IV	Best of 2 above	600F	50 hr.	250 hr.	30
VI	Same as IV	Same as V	600F	150 hr.	750 hr.	30



The logic behind this test sequence is obvious and has been dealt with in a previous section of this report. However, several events occurred during the course of the program which made it necessary to deviate from the original plan. Early in the program, it was observed that at the 5800 lb. axial load level, the XRM-177F at 600F was still maintaining a hydrodynamic film. In order to decrease the  $B_{10}$  life to 50 hours, or about one-half, the Hertzian load on the bearing would have to be increased by about 10%, assuming that the ninth power relationship between load and life was valid at 600F. It was felt that this would precipitate a mixed or boundary lubrication condition which could seriously affect the validity of the test results. To determine this, four 600F tests were conducted at a 7000 lb. axial load. As suspected, ball wear and some raceway surface distress was observed, indicating a breakdown of the hydrodynamic film with resultant asperity contact. In view of this, the program was re-oriented toward establishing the life-temperature relationship rather than the life-load relationship originally planned.

The second factor influencing the conduct of the program was the late delivery of the WB-49 bearings. The original plan had been to evaluate the best fluid determined in the first three test series with CVM M-50 bearings, with the WB-49 bearings, and then to use the best fluid-bearing material combination for the life-temperature series. The delay in obtaining the WB-49 bearings was so great however, that a decision was made to proceed with the life-temperature series using CVM M-50 bearings. The decision was made based on the relatively poor behavior of the WB-49 in the RC Rig tests, which indicated this material to be inferior to CVM M-50. The subsequent WB-49 bearing tests confirmed the RC Rig data and consequently the decision to proceed with the CVM M-50 was proven technically sound.

In order to maintain a logical sequence in detailing the test results, the WB-49 test series will be reported in their original position in the test schedule. Consequently, the actual test sequence and operating

conditions were as follows and will be discussed in this order.

<u>Test Series</u>	<u>Lubricant</u>	<u>Bearing Material</u>	<u>Test Temp.</u>	<u>B<sub>10</sub>=</u>	<u>B<sub>50</sub> Cut-Off</u>	<u>No. of Tests</u>
I	XRM-177F	CVM M-50	600F	100 hr.	500 hr.	30
II	Mcs-354	CVM M-50	600F	100 hr,	500 hr.	30
III	PR-143	CVM M-50	600F	100 hr.	500 hr.	30
IV	XRM-177F	WB-49	600F	100 hr.	500 hr.	30
V	XRM-177F	CVM M-50	500F	100 hr.	750 hr. (1)	25 (2)
VI	XRM-177F	CVM M-50	400F	100 hr,	750 hr, (1)	25 (2)

(1) In view of the decrease in temperature with the subsequent increase in lubricant viscosity, it was decided to increase the cut-off point to 750 hr. in order to obtain a sufficient number of failures to produce a statistically valid population.

(2) The total number of tests were reduced because of the fact that several bearings had been used for exploratory tests earlier in the program and consequently a 30 bearing complement was not available.

One of the measures taken to insure test repeatability was the use of a new batch of oil with each new set of bearings, with the exception of Test Series VI, where oil which had been previously used was recycled. In the latter case the oil (XRM-177F) was filtered through a series of aircraft and Purolator filters. Oil analysis after these filtering operations showed essentially the same properties as the fresh oil. The recycled oil was used for all of Test Series VI.

A summary of test hours in each test series shows the following:

<u>Test Series</u>	<u>Total No. of Test Hours</u>
I	11,628
II	6,544
III	7,582
IV	1,324
V	11,574
VI	<u>15,450</u>
Total	54,102

Since the entire system was  $N_2$  inerted, there was a question whether it would be necessary to de-aerate the oil prior to its being changed into the bearing tester. Consequently, it was decided that if this became necessary, a relatively large capacity tank would be required which could be used to remove any adsorbed  $O_2$  from the test fluids. The apparatus for accomplishing this is shown schematically in Figure 26 and a photograph of the equipment is shown in Figure 27. Basically, the apparatus consisted of an electrically heated 30-gallon pressure vessel which could be evacuated to a pressure of  $10^{-3}$  torr. The deaeration procedure was as follows:

1. Fill vessel with 25 gallons of test fluid.
2. Heat to 200F.
3. Reduce pressure to  $10^{-3}$  torr.
4. Hold for 72 hours, agitating slowly during this period.
5. Back-fill tank with high purity  $N_2$ .
6. Transfer required quantity to tester oil tank under a nitrogen blanket.

This procedure was used on tests No. 2 through 6 in Test Series I. During this period of time, measurements were made on oil deaerated using the previously described apparatus as well as oil charged directly into the testers without exposure to the deaeration procedure. It was found that within a very short time (approximately 60-90 minutes) the oil placed directly into the testers had been purged of  $O_2$  as efficiently as the oil held for 72 hours at  $10^{-3}$  torr. This assumption was verified by  $O_2$  measurements of the exhaust gas stream as well as the visual appearance of the bearing components and particularly the Monel retainers which would be extremely susceptible to oxidation at the 600F test temperature. The results are not surprising as the oil is: a.) at a very high temperature, b.) vigorously agitated and c.) continually exposed to high purity nitrogen.

In view of the above results, it was decided that it would not be necessary to deaerate the oil prior to placing it into the test units.

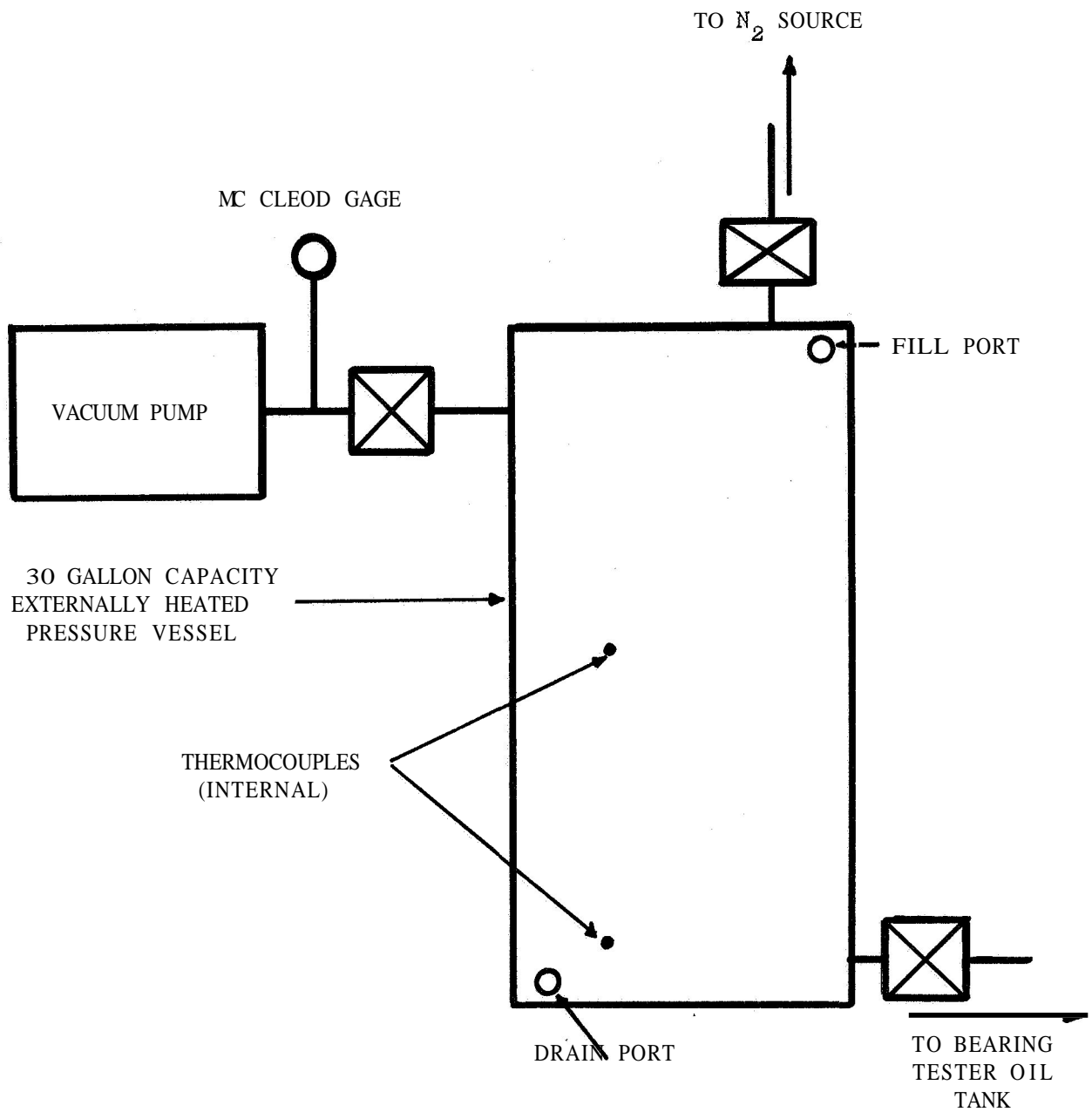


FIGURE 26. SCHEMATIC OF LUBRICANT DEAERATION APPARATUS



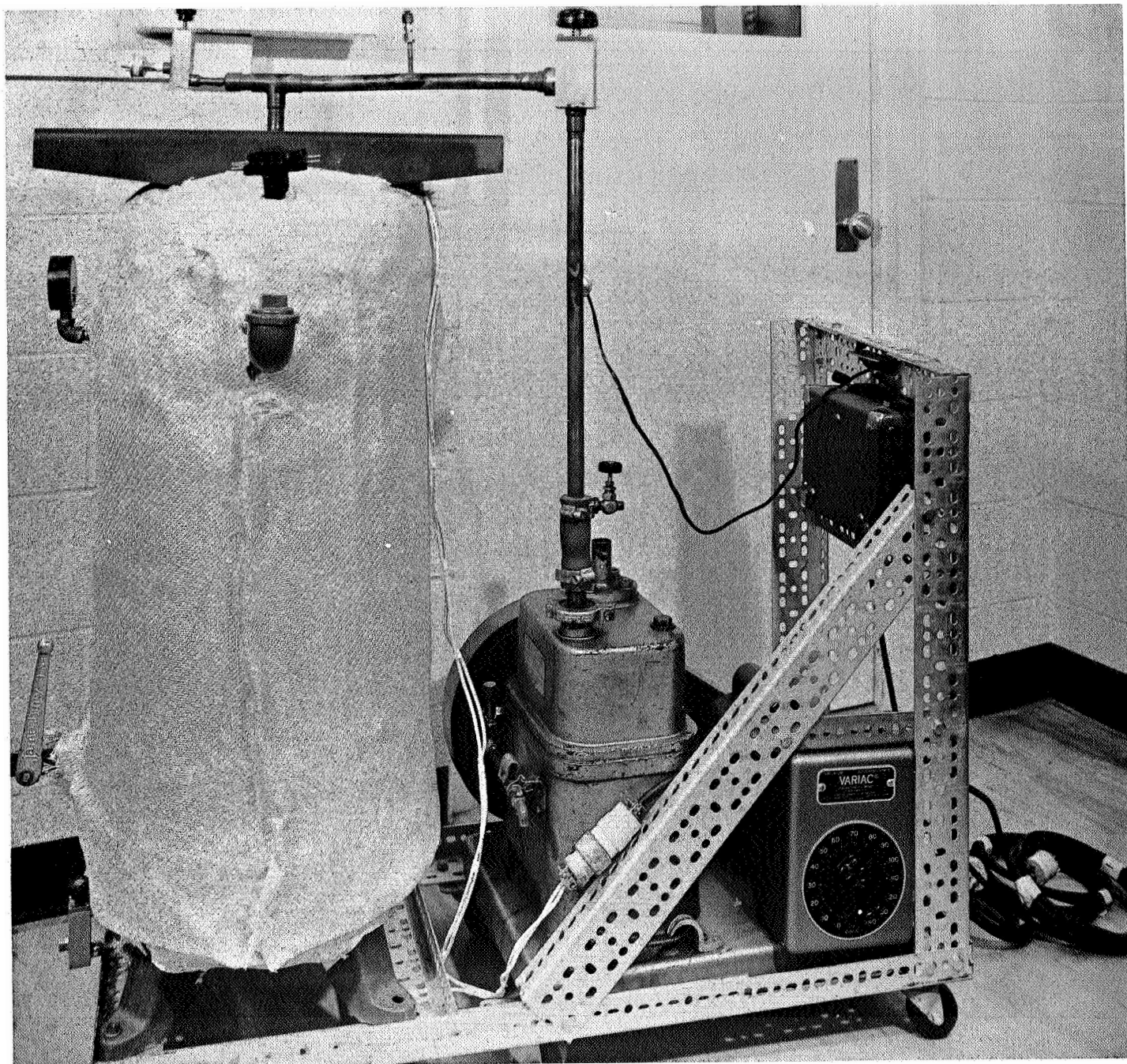


FIGURE 27. APPARATUS FOR DEAERATING **TEST** FLUIDS



### 6.2.1 Test Series I

The first test series was performed with the materials and test conditions given below:

Bearing Material:	Rings :	CMM5 0
	Balls:	CVM-M-50
	Retainer:	S-Mone 1
Lubricant:	Mobil XRM-177F	
Operating Conditions:		
	Temp:	Outer Ring 585F - 5F Inner Ring 600F - 610F Oil In - 545F-565F Oil Out - 585F-600F
	Speed:	12,000 rpm
	Load:	5800 lbs, axial (28 tests) 7000 lbs. axial (4 tests)
	Atmosphere:	N <sub>2</sub> <5 ppm O <sub>2</sub>

The results of these tests are tabulated in Table 12 and the resultant Weibull plot is presented in Figure 28. The Weibull Analysis considers 26 out of the 32 tests, thus carrying a failure index of 6 of 26. Not considered in the analysis are tests #I-2 and I-2a (Bearing #21 and 22) which were damaged during disassembly and tests #I-8, I-8a, I-9, I-9a which were performed at the 7000 lb, load level. The Weibull Analysis is performed using the methods of L. G. Johnson, (8) i.e. the suspensions are included in the calculations. This method was also used for all subsequent analysis.

The failures in Table 12 marked with a rectangle are considered to be normal sub-surface initiated failures. Serial number 20 was an inner ring failure detected just at the point of initiation by an audible noise change. Consequently, the failures were in a very early stage, and mainly because of this, it was decided to allow subsequent failures

Table 12

Results of 120 mm Bearing Tests with XRM-177F Lubricant, CVM M-50 Bearings, at 600F in N<sub>2</sub>

Test No.	Bearing S/N	Load (lb.)	Time (Hr.)	Inner Ring	Outer Ring	Wall
I - 1	19	5800 (1)	144	OK	OK	OK
I - 1a	20	5800	144	Fatigue	OK	OK
I - 2	21	5800	30	OK	OK	( 0005 Wear )
I - 2a	22	5800	30	OK	OK	( 0003 Wear )
I - 3	15	5800	309 (3)	OK	Fatigue	Fatigue
I - 3a	16	5800	309 (3)	OK	OK	OK
I - 4	17	5800	290	OK	OK	OK
I - 4a	18	5800	290	OK	OK	Fatigue
I - 5	9	5800	500	OK	OK	OK
I - 5a	10	5800	500	OK	OK	OK
I - 6	11	5800	500	OK	OK	OK
I - 6a	12	5800	500	OK	OK	OK
I - 7	13	5800	500	OK	OK	OK
I - 7a	14	5800	500	OK	OK	OK
I - 8	27	7000 (2)	117	OK	OK	( 002 Wear )
I - 8a	28	7000	117 (Cage Failure)	OK	OK	( 003 Wear )
I - 9	25	7000	165	OK	OK	( 0005 Wear )
I - 9a	26	7000	165	OK	OK	( 002 Wear )
I - 10	17	5800	375	OK	OK	Fatigue
I - 10a	16	5800	434	OK	OK	OK
I - 11	33	5800	189	Fatigue	OK	OK
I - 11a	34	5800	189	OK	OK	OK

Table 12, Contd.

Test No.	Bearing S/N	Load $\leq 10^6$ lb.	Time (Hr.)	Inner Ring	Outer Ring	Spall
I -12	23	5800	519	OK	OK	OK
I -12a	24	5800	519	OK	OK	OK
I -13	29	5800	500	OK	OK	OK
I -13a	30	5800	500	OK	OK	OK
I -14	31	5800	525	OK	OK	OK
I -14a	32	5800	525	OK	OK	OK
I -15	37 (4)	5800	396	OK	OK	OK
I -15a	38 (4)	5800	396	OK	OK	OK
I -16	35	5800	518	OK	OK	OK
I -16a	36	5800	518	OK	OK	OK
I -17	42	5800	465	OK	OK	OK
I -17a	41	5800	<span style="border: 1px solid black;">465</span>	Fatigue	OK	OK
I -18	16	5800	630	OK	OK	OK
I -18a	34	5800	385	Track Damage	Track Damage	OK

(1) 5800 lb. axial load = 321,000 psi max. hertz on inner.

(2) 7000 lb. axial load = 342,000 psi max. hertz on inner.

(3) Time to initiation of outer ring spall. Bearing run an additional 40 hours after spall initiation.

(4) Severe misalignment.

  Indicates Time to Fatigue Failure

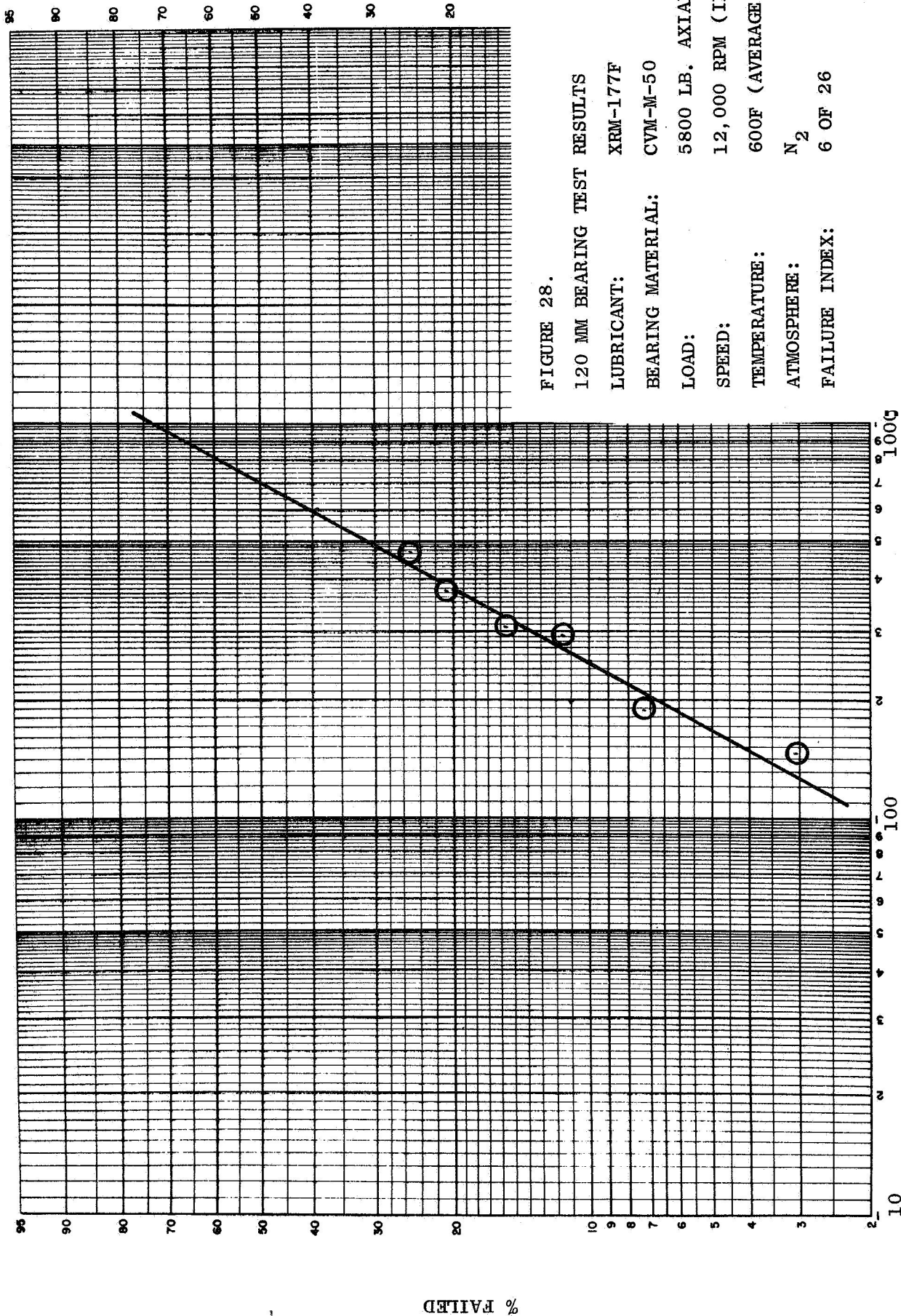


FIGURE 28.

120 MM BEARING TEST RESULTS

LUBRICANT: XRM-177F

BEARING MATERIAL: CVM-M-50

LOAD: 5800 LB. AXIAL

SPEED: 12,000 RPM (INNER)

TEMPERATURE: 600F (AVERAGE METAL)

ATMOSPHERE: N<sub>2</sub>

FAILURE INDEX: 6 OF 26

LIFE - HOURS

% FAILED

to progress to a somewhat larger spall before terminating the test. The running mate of this bearing, serial number 19, showed evidence of some inner ring damage, although it did not appear to be due to fatigue. It is thought that the damage observed may be due to foreign objects in the oil.

Bearing 15 was believed to have had its failure origin in an outer ring spall. Since this was the first positively identifiable fatigue failure, the bearing was run for an additional 40 hours over the 309 hours required to initiate the outer ring spall in order to investigate vibration level change as a function of time. As a result of this, ball failures, evidenced by severe spalling, were encountered and finally a cage web break caused an uncontrollable temperature rise which forced the shutdown of the test. An overall view of this bearing is shown in Figure 29 and a close-up of the cage failure in Figure 30. The initiating spall in the outer ring is shown in Figure 31, whereas Figure 32 shows the severely damaged balls. The assumption of an outer ring spall being the initiating failure is based on the texture of the spalls. It will be noted that the surface of the outer race failure is relatively smooth compared to the rather jagged appearance of most of the failed areas on the balls. The inference here is that the earlier failure, due to continual ball passage, has a surface smoother than the newer failures. In this particular failure, the vibration level did not increase sufficiently to cause automatic shutdown of the equipment, although had the over temperature controls not been bypassed, the machine would have been shutdown shortly after the appearance of the initial spall on the outer ring.

Bearing 18 exhibited a ball failure after 290 hours of operation. This ball failure is shown in Figure 33 along with several other balls from the bearing showing the generally good appearance of these components. Figure 34 shows the inner ring of this bearing, the arrow indicating the dimensions of the ball path. Figure 35 is a view of the cage pockets of this bearing showing the minimal amount of cage wear which has occurred in this period.

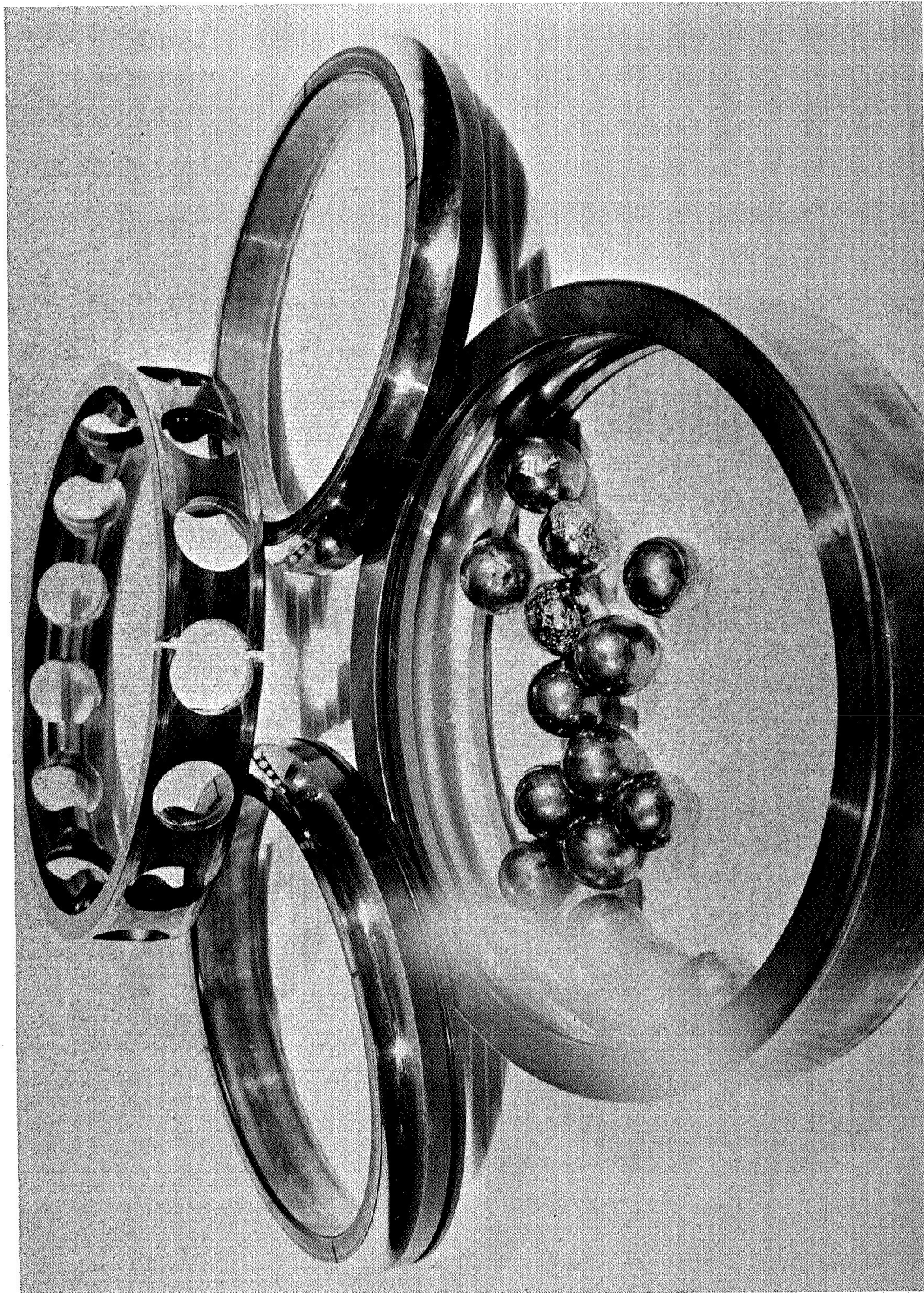


FIGURE 29. OVERALL VIEW OF BEARING S/N 17 AFTER 349 HOURS

RUNNING TIME:	349 HOURS
LUBRICANT:	XRM-177F
TEMPERATURE:	600F
LOAD:	5800 LB. AXIAL
SPEED:	12,000 RPM (INNER)



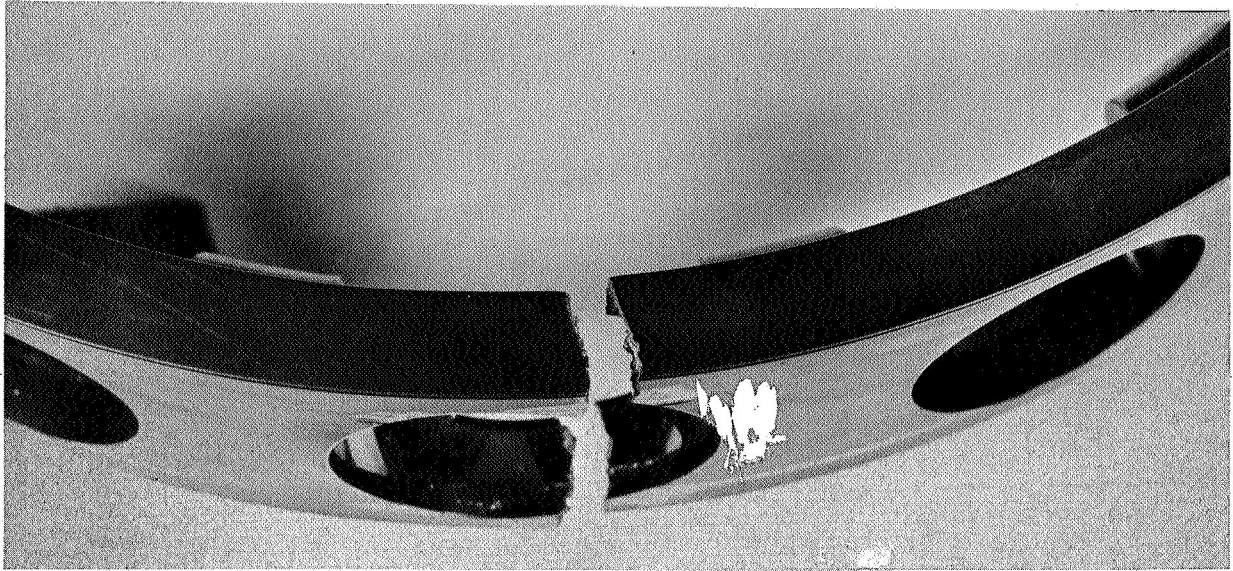


FIGURE 30. CAGE FAILURE - BEARING S/N 15

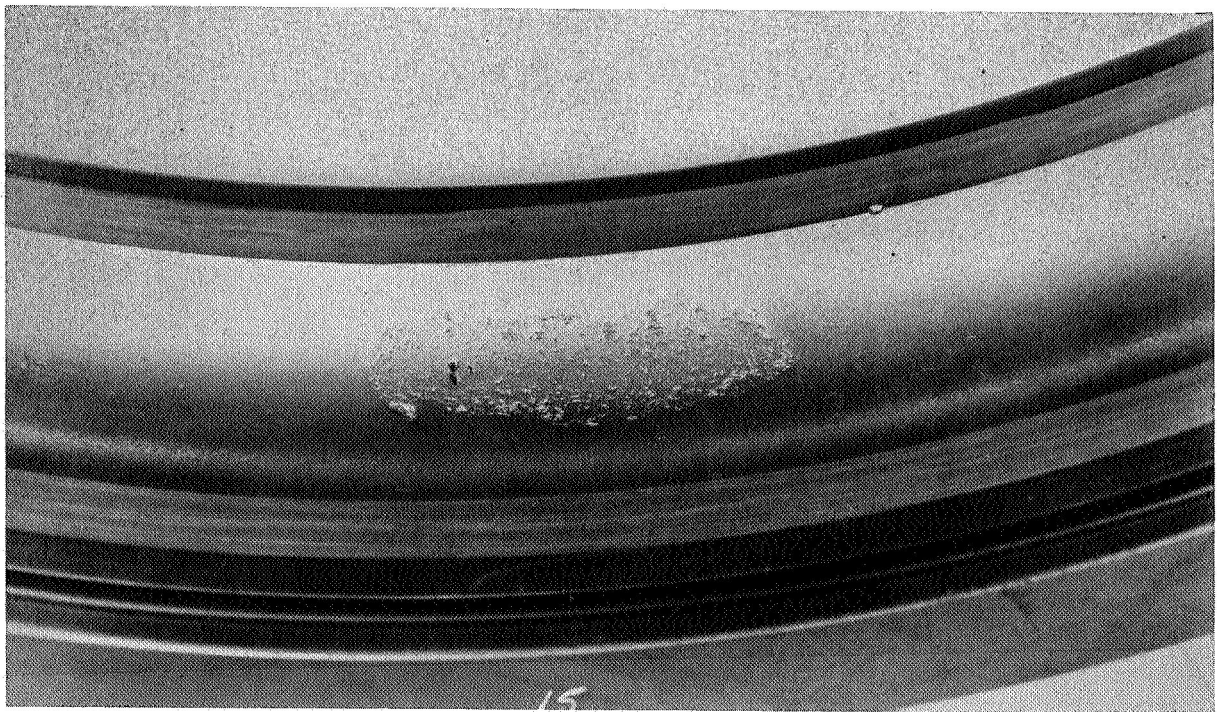


FIGURE 31. FATIGUE FAILURE - OUTER RING - BEARING S/N 15



FIGURE 32. BALL FAILURES - BEARING S/N 15

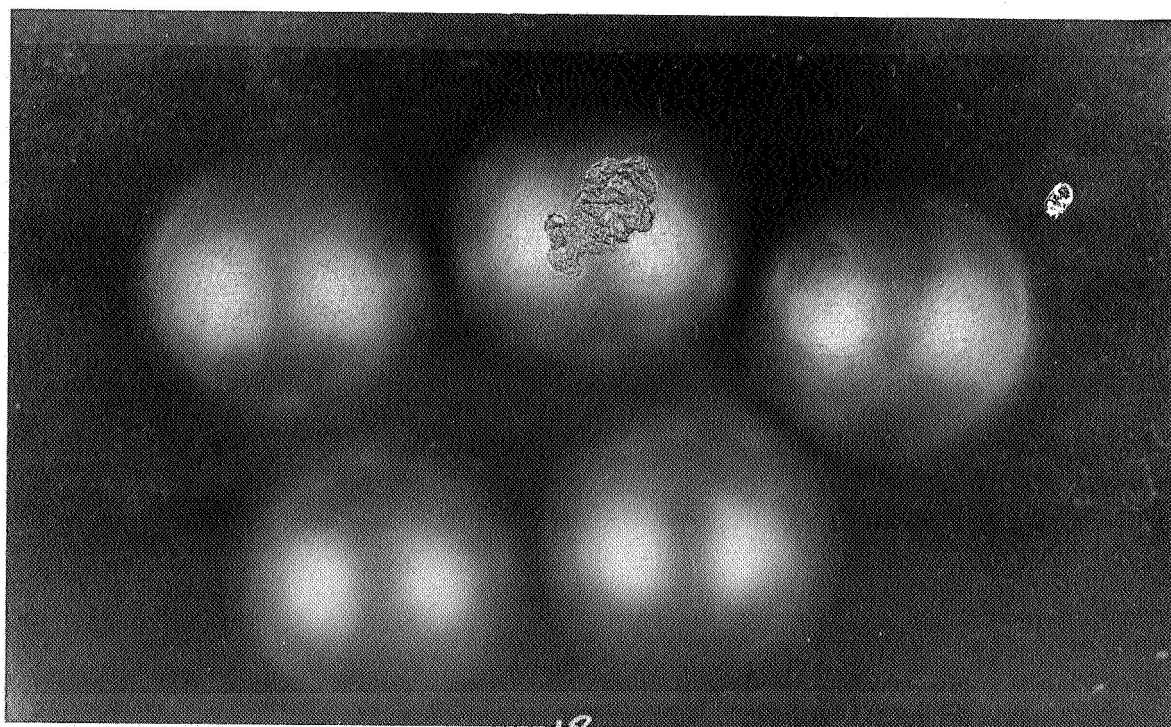


FIGURE 33. BALL FATIGUE FAILURE - BEARING S/N 18

RUNNING TIME:	290 HOURS
LUBRICANT:	XRM-177F
TEMPERATURE:	600F
LOAD:	5800 LB. AXIAL
SPEED:	12,000 RPM (INNER)



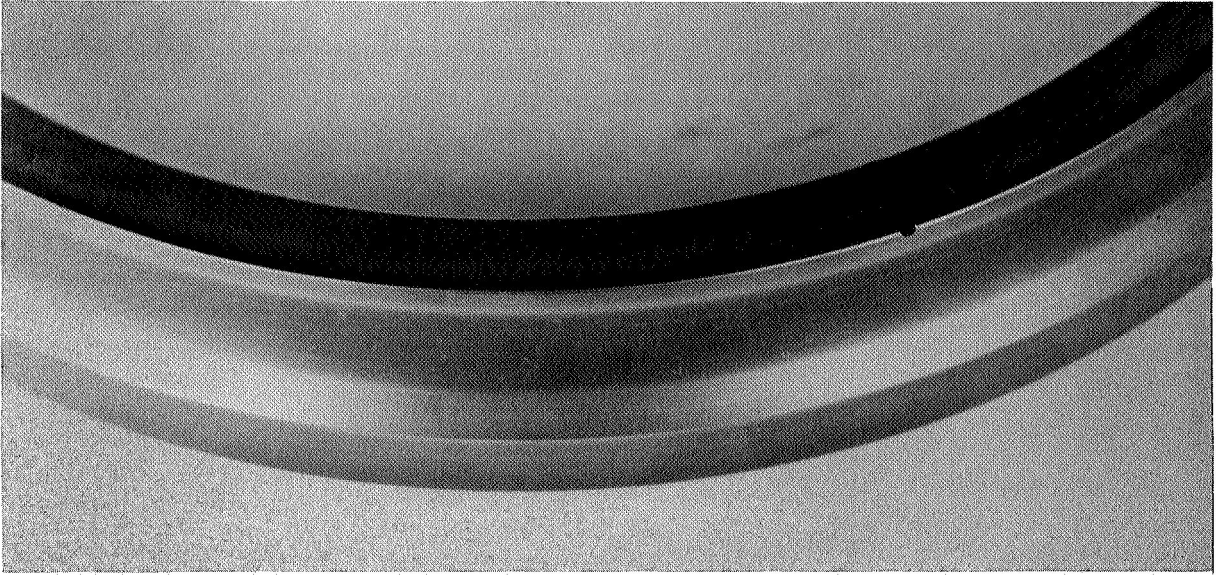


FIGURE 34. INNER RING BALL PATH - BEARING S/N 18

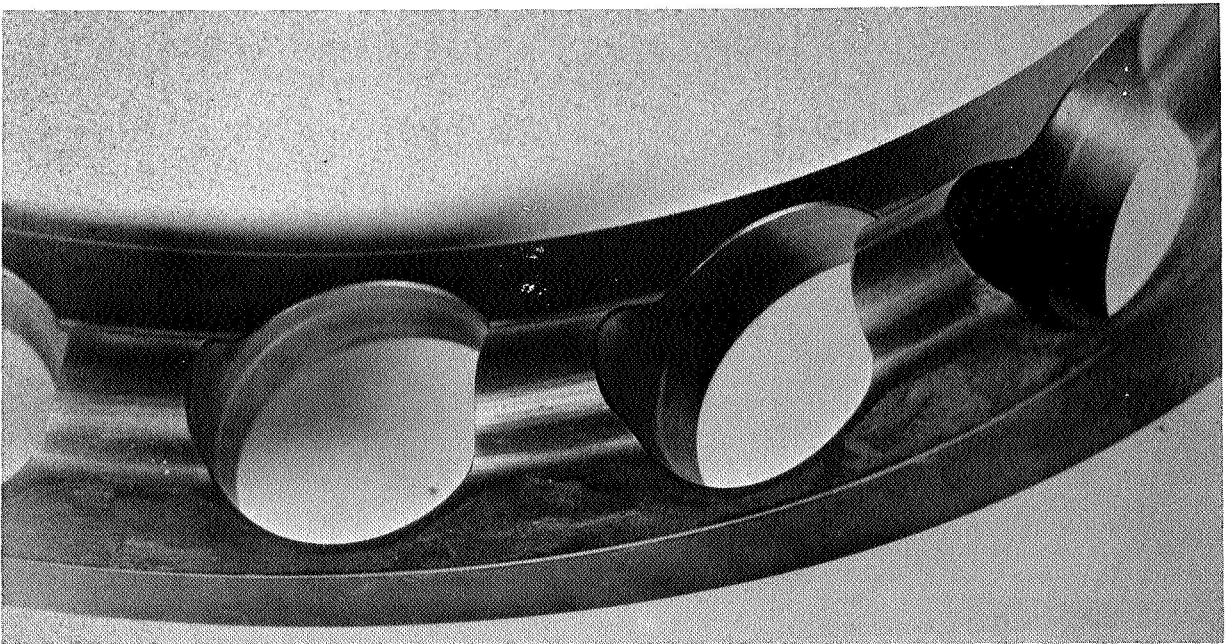


FIGURE: 35. CAGE BALL POCKETS - BEARING S/N 38

An interesting observation can be made regarding the occurrence of the ball failures. In normal bearing fatigue testing, the probability of ball failures is relatively low. In the present case, however, it had been noted in the RC Rig tests that the rolling contact fatigue life of the M-50 CVM billet used for the balls was lower than the ring material. In view of this, a greater incidence of ball failures had been expected, and this expectation appears to have been correct.

Bearing 17 failed after 375 hours. The failure was characterized by a fatigue failure on the outer ring, as well as three ball failures. The failed balls are shown in Figure 36, and the failed outer ring in Figure 37. Bearing 33 had a massive inner ring fatigue failure after 189 hours. The failed ring is shown in Figure 38.

A number of bearings achieved 500 hours. One of these was Bearing #10 and Figure 39 shows several balls from this bearing,. The outer ring ball track of the same bearing is shown in Figure 40.

An overall view of another 500 hour bearing, serial number 13, is shown in Figure 41 with the next several photographs showing the appearance of the balls (Figure 42), retainer (Figure 43) and inner and outer ball paths (Figures 44 and 45). Considering the extremely severe conditions to which these bearings have been exposed, it is highly encouraging to note the almost undamaged appearance of these various components.

At the 5800 lb. load level, the semi-major axis of the pressure ellipse on the inner race is calculated to be .085 inches. The measured wear track is .100 inches, somewhat greater than calculated. This is, however, not unexpected based on the rolling contact fatigue testing and other bearing testing experience.

The only cases of ball wear at the 5800 lb. load level with the XRM-177F occurred with bearings 21 and 22. The balls in both of these

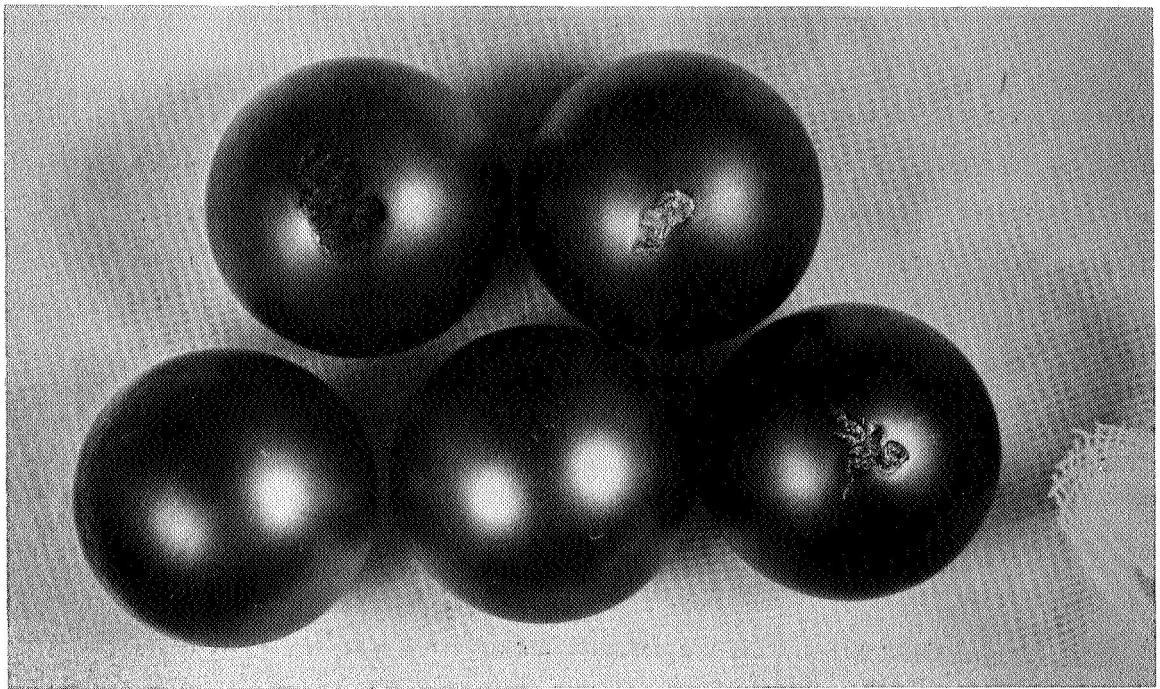


FIGURE 36. BALL FAILURES - BEARING S/N 17

RUNNING TIME:	375 HOURS
LUBRICANT:	XRM-177F
TEMPERATURE:	600F
LOAD:	5800 LB. AXIAL
SPEED:	12,000 RPM (INNER)

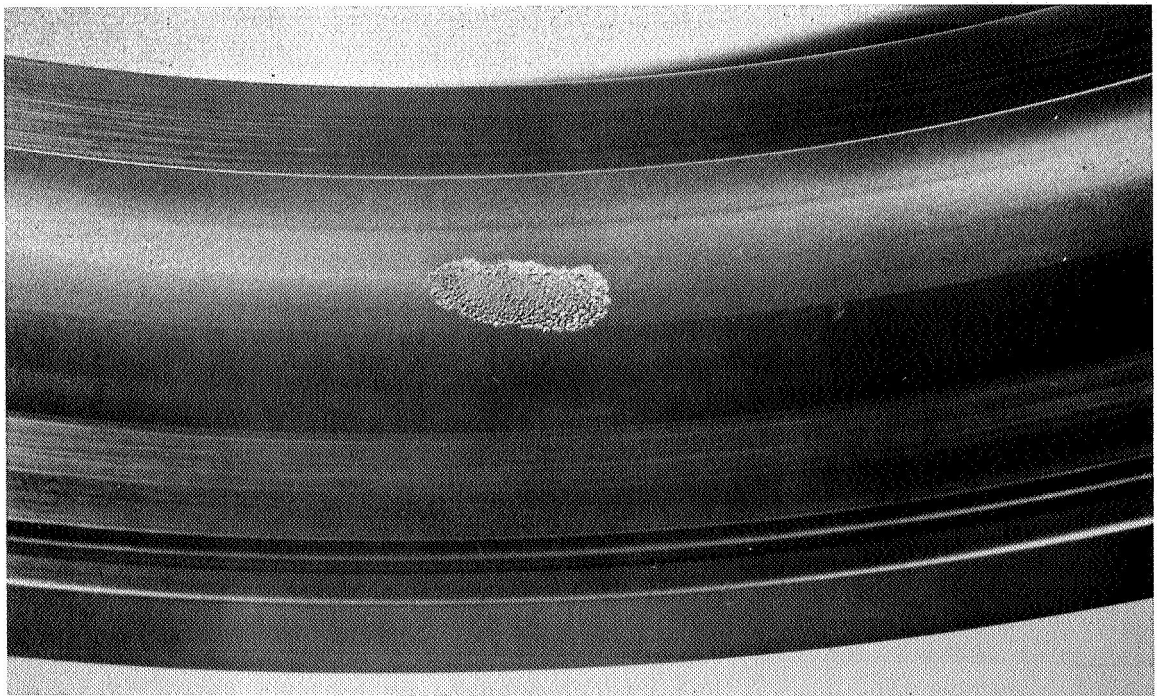


FIGURE 37. FATIGUE SPALL ON OUTER RING OF BEARING S/N 17

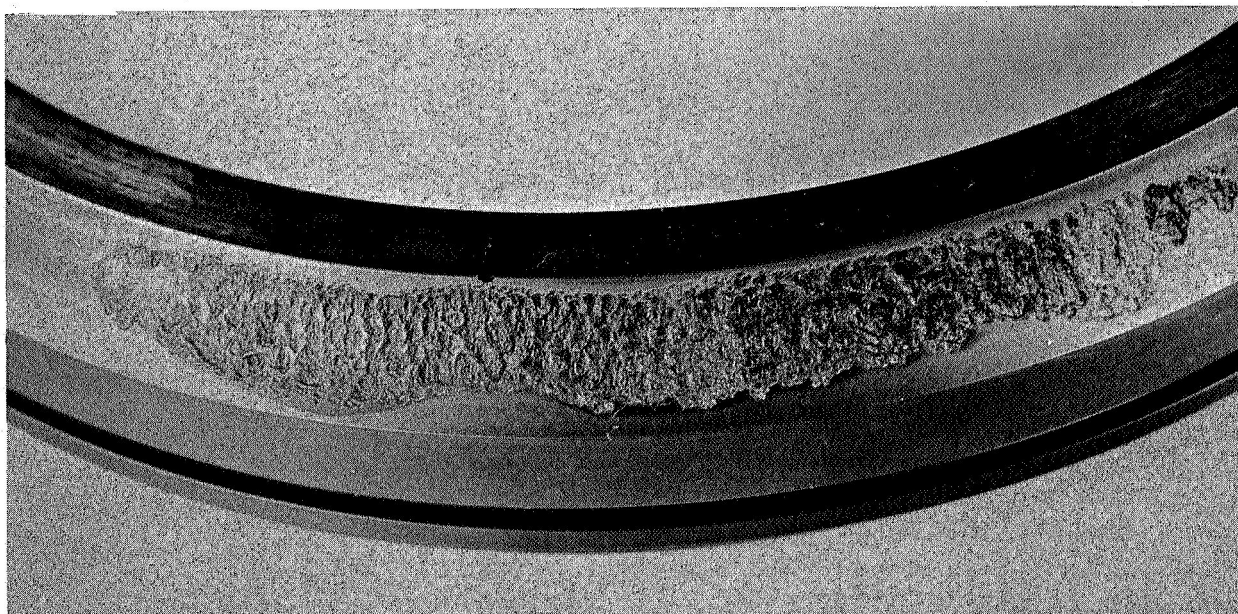


FIGURE 38. FATIGUE SPALL ON INNER RING - BEARING S/N 33

RUNNING TIME:	189 HOURS
LUBRICANT:	XRM-177F
TEMPERATURE:	600F
LOAD:	5800 LB. AXIAL
SPEED:	12,000 RPM (INNER)





FIGURE 39. BALLS FROM BEARING S/N 10

RUNNING TIME:	500 HOURS
LUBRICANT:	XRM-177F
TEMPERATURE:	600F
LOAD:	5800 LB. AXIAL
SPEED:	12,000 RPM (INNER)

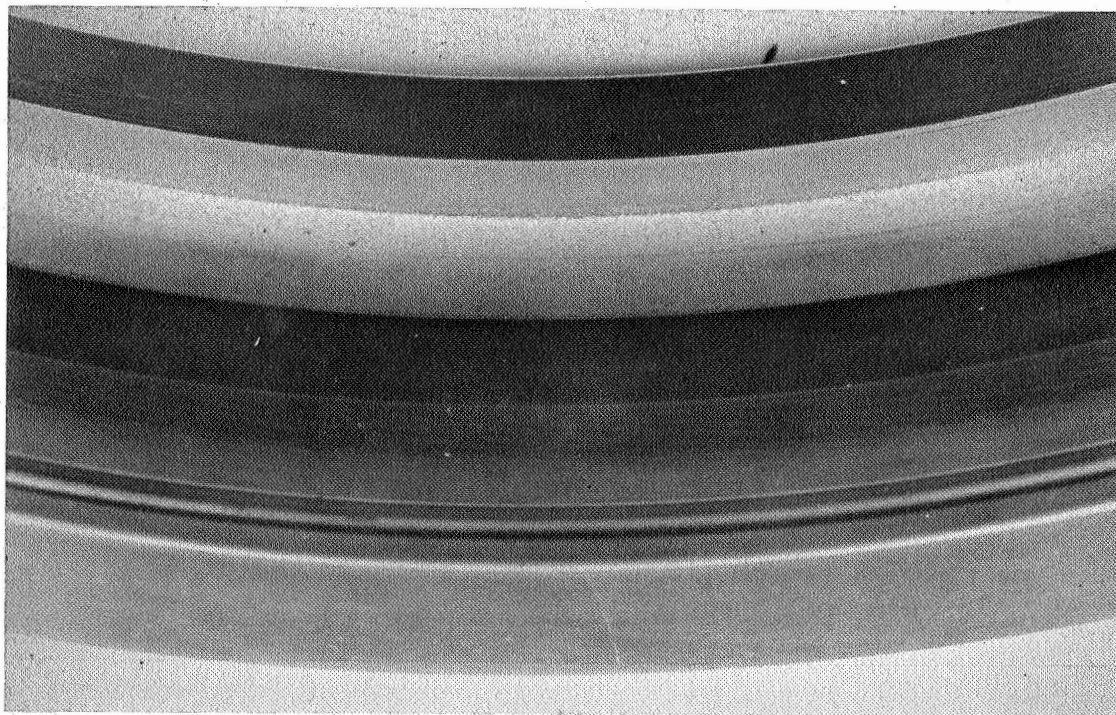


FIGURE 40. OUTER RING - BALL PATH BEARING S/N 10

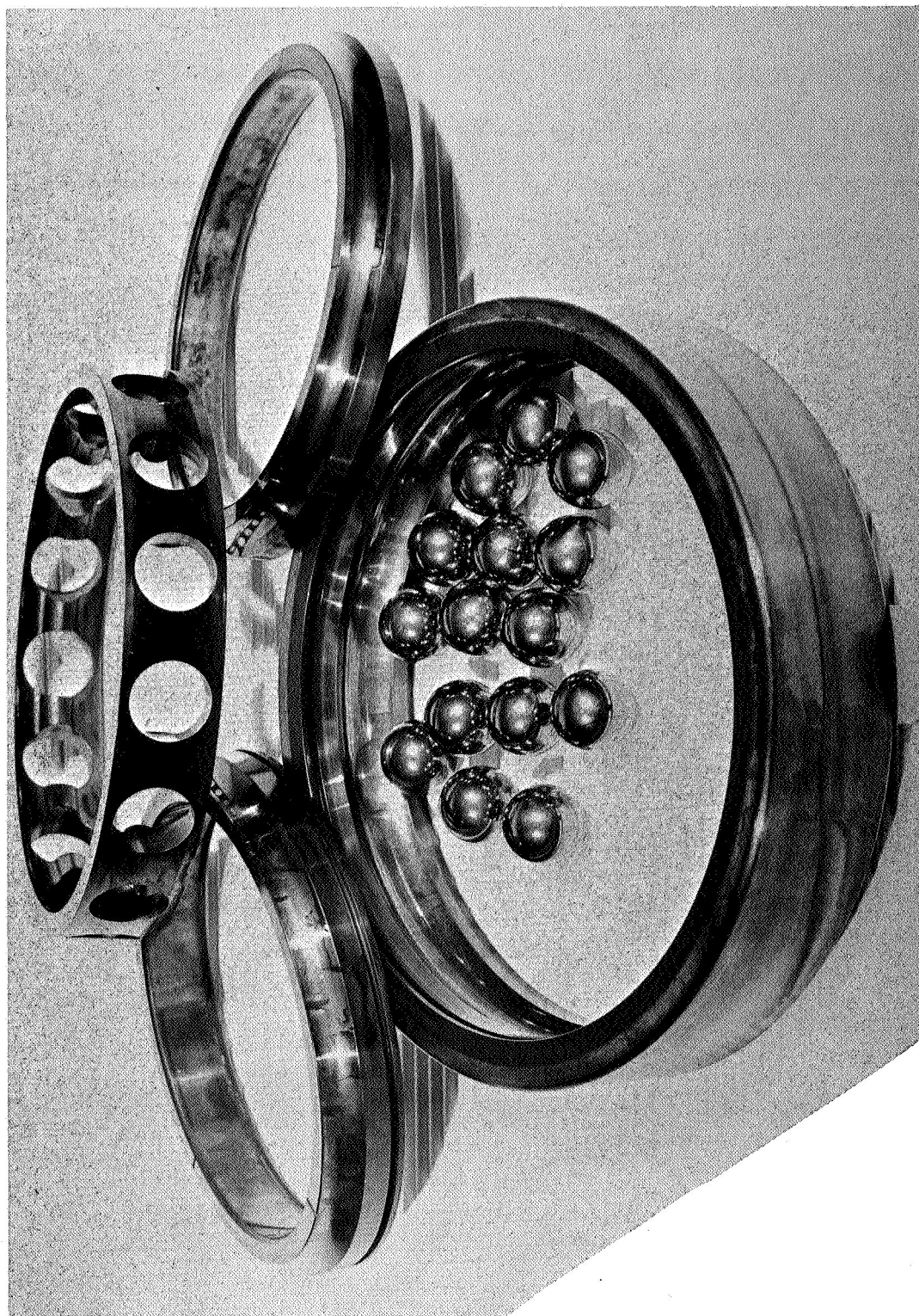


FIGURE 41. OVERALL VIEW OF BEARING S/N 13 AFTER 500 HOURS

RUNNING TIME:	500 HOURS
LUBRICANT:	XRM-177F
TEMPERATURE:	600F
LOAD:	5800 LB. AXIAL
SPEED:	12,000 RPM (INNER)



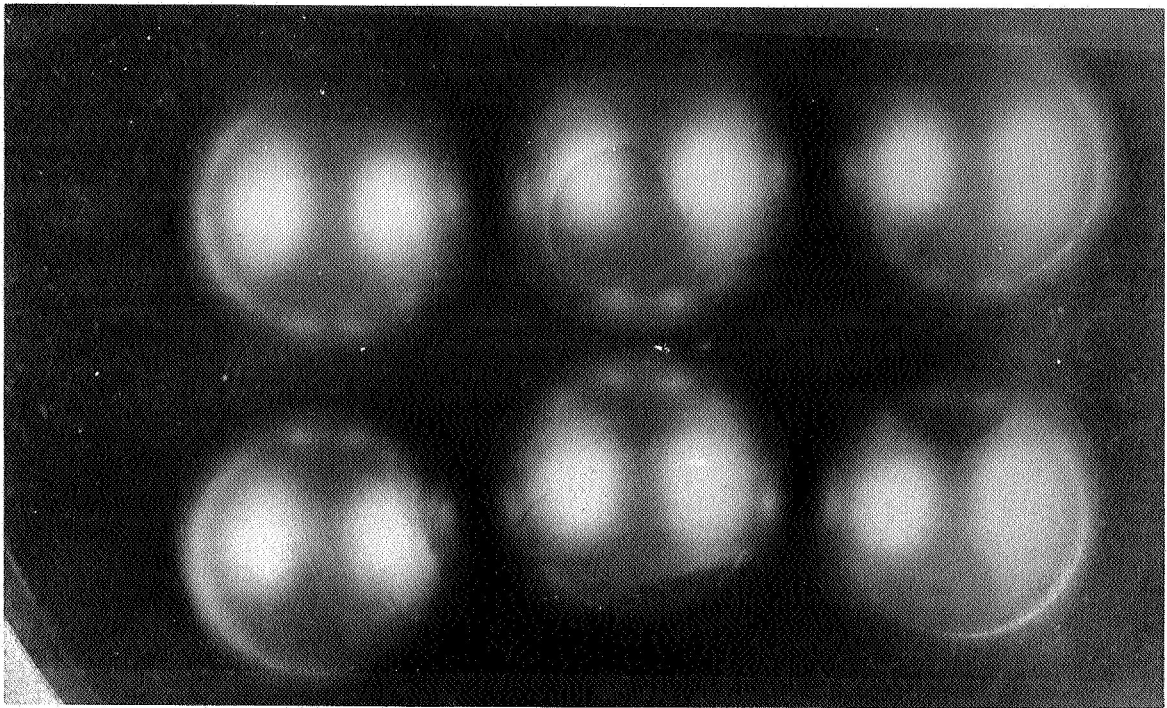


FIGURE 42. BALLS FROM BEARING S/N 13

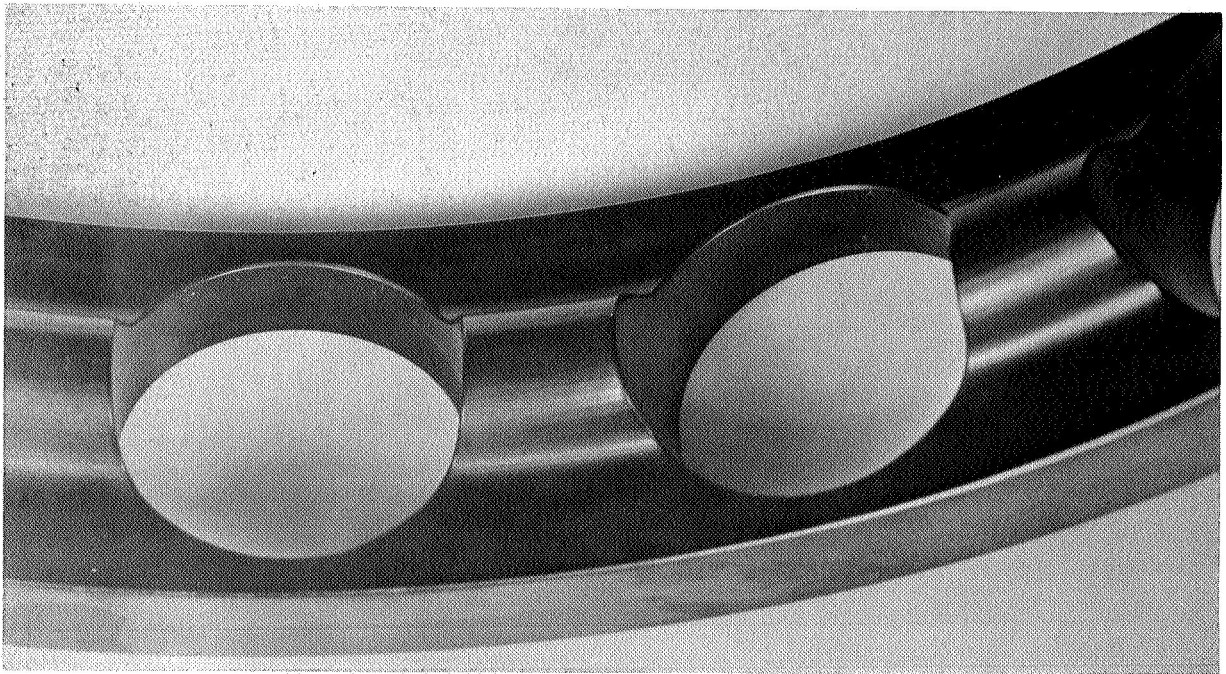


FIGURE 43. CAGE BALL POCKETS - BEARING S/N 13

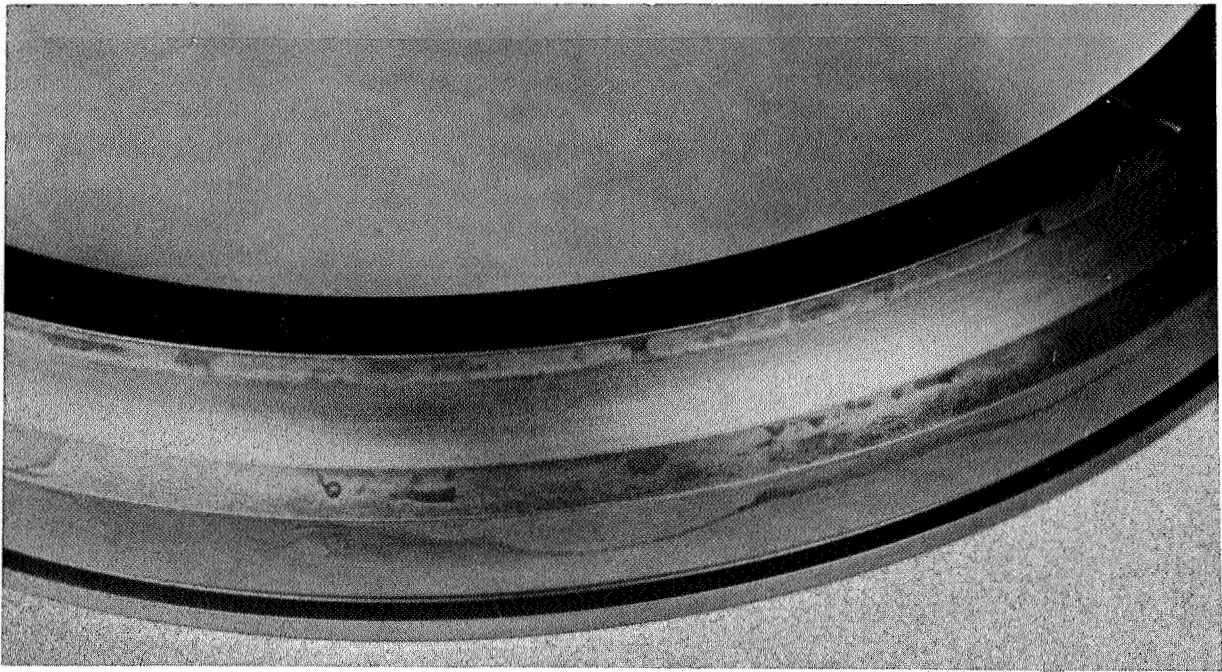


FIGURE 44. INNER RING BALL PATH - BEARING S/N 13

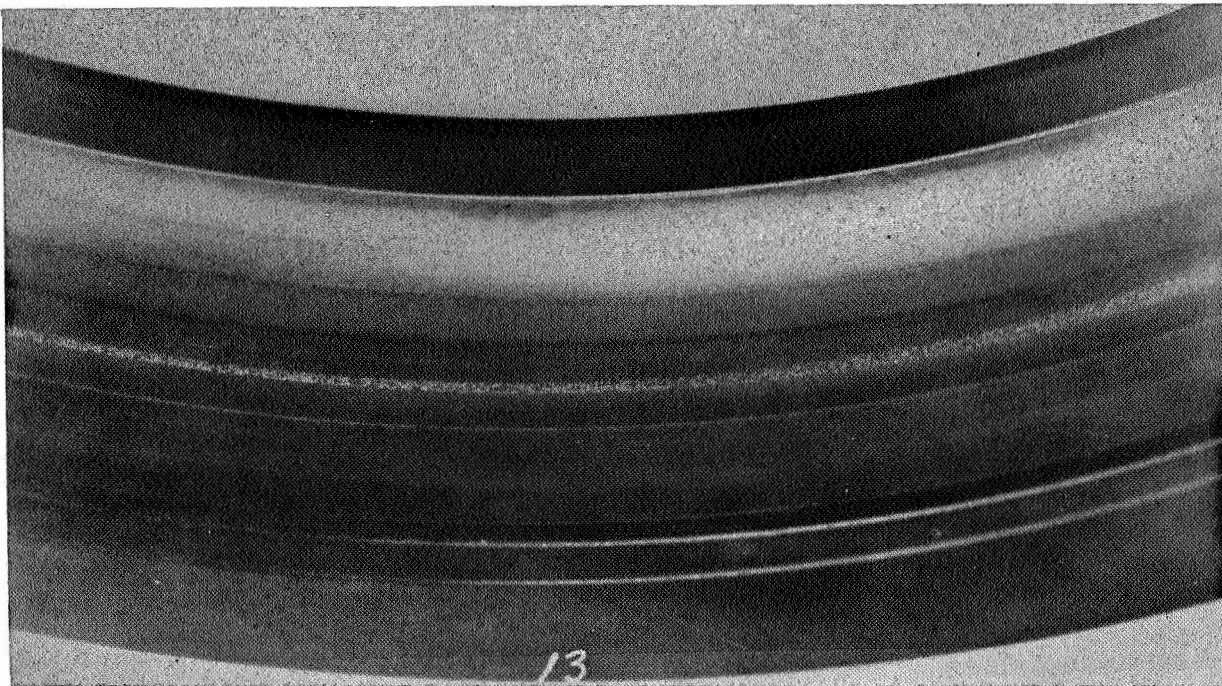


FIGURE 45, OUTER RING BALL PATH - BEARING S/N 13



bearings, unlike all other runs, showed micro pitting similar to that observed on the bearings run subsequently with the polyphenylether fluid. The ball pitting is shown in the photograph in Figure 46 for bearing 21. The remaining bearing components were essentially undamaged. For both of these bearings, it was determined that no misalignment had existed, and the lubricant was in good condition after test. No explanation could be found for the short (30.3 hours) running time and the rapid ball wear which ranged from .0003" - .0005".

Four bearings, serial numbers 25 through 28 inclusive, were run at an axial load of 7000 lb. in order to investigate the effects of higher loading. Bearings 27 and 28 were inspected after 100 hours of operation and found to be in good condition. No component wear was observed at this time. These two bearings were reassembled and ran for an additional 17 hours. At this point, the bearings were shut-down due to over-temperature indications. Subsequent examination of the bearings showed a cage failure and a high degree of ball wear on the order of .0005". The cage was severely deformed, and cracks were observed in all of the side rails on one side. Bearings 25 and 26 ran for 165 hours before they were shut-down by over-temperature indications. Measurements showed ball wear to be on the same order as in the first test. The cage, however, appeared to be in excellent condition with no evidence of plastic deformation or cracking.

The next five photographs, Figures 47 through 51, show views of bearing #28 run at 7000 lb. axial load, which is equivalent to a maximum Hertzian stress of 342,000 psi on the inner ring. The primary failure in this bearing was the severe cage rupture shown in Figure 47, with a number of secondary failures in the cage web as illustrated in Figure 48. In addition to this, severe wear was encountered on the balls. Typical balls from this bearing are shown in Figure 49. Figures 50 and 51 illustrate the condition of the inner and outer raceways.

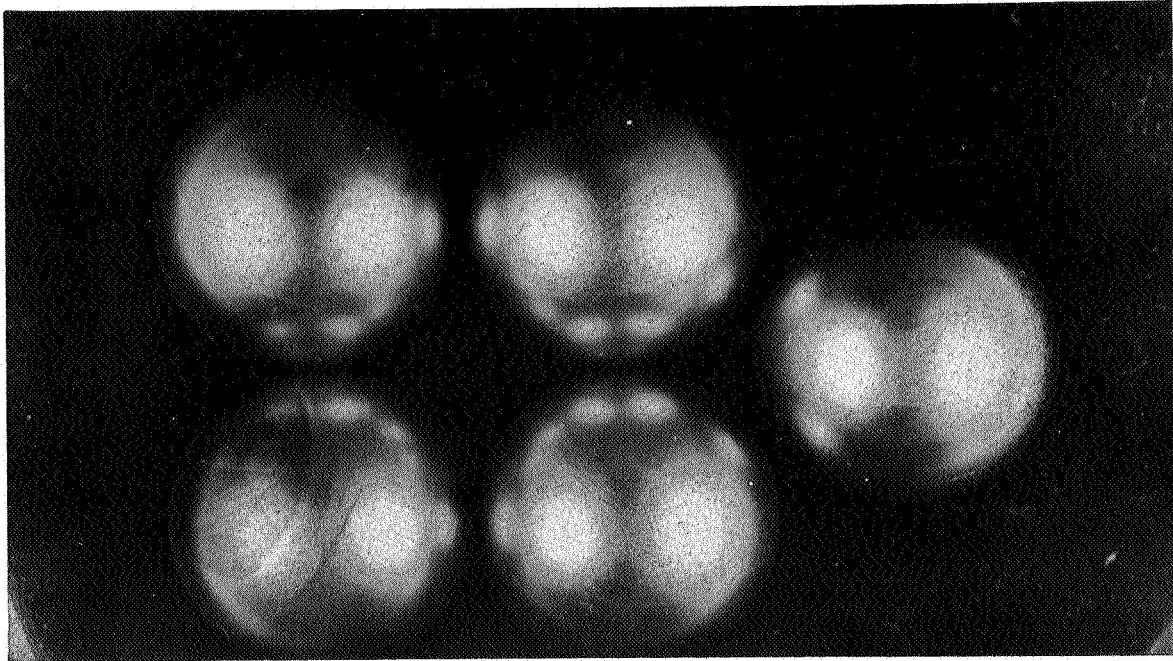


FIGURE 46. WEAR AND MICRO PITTING ON BALLS - BEARING S/N 21

RUNNING TIME:	30.3 HOURS
LUBRICANT:	XRM-177F
TEMPERATURE:	600F
LOAD:	5800 LB. AXIAL
SPEED :	12,000 RPM (INNER)

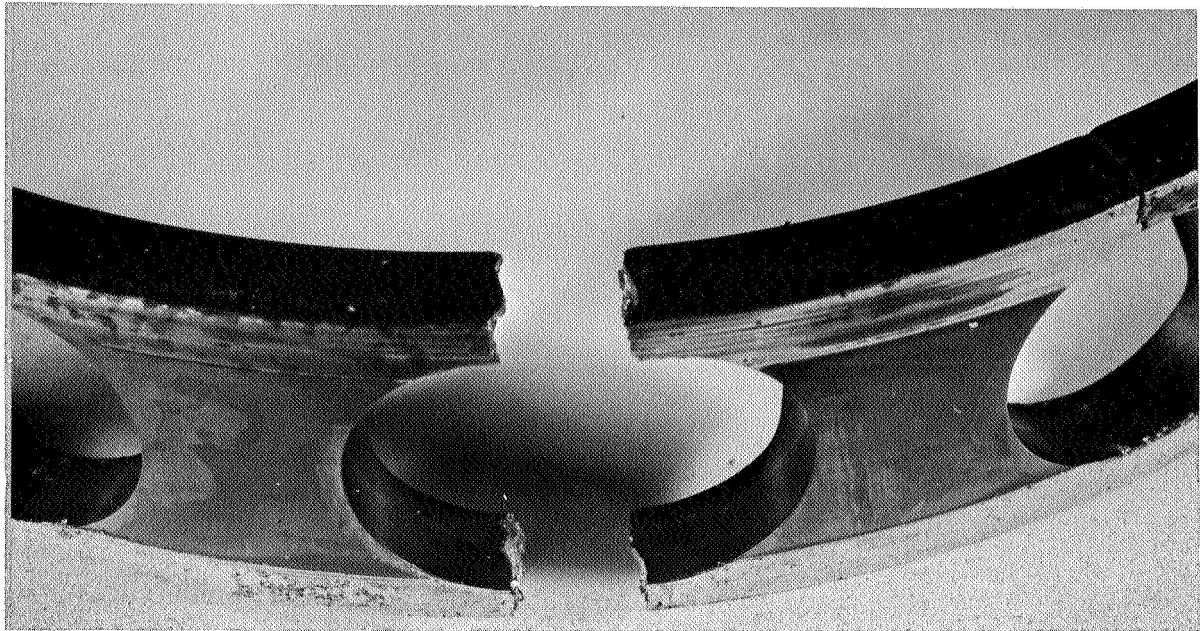


FIGURE 47. PRIMARY CAGE FAILURE - BEARING S/N 28

RUNNING TIME:	117.5 HOURS
LUBRICANT:	XRM-177F
TEMPERATURE:	600F
LOAD:	7000 LB. AXIAL
SPEED:	12,000 RPM (INNER)

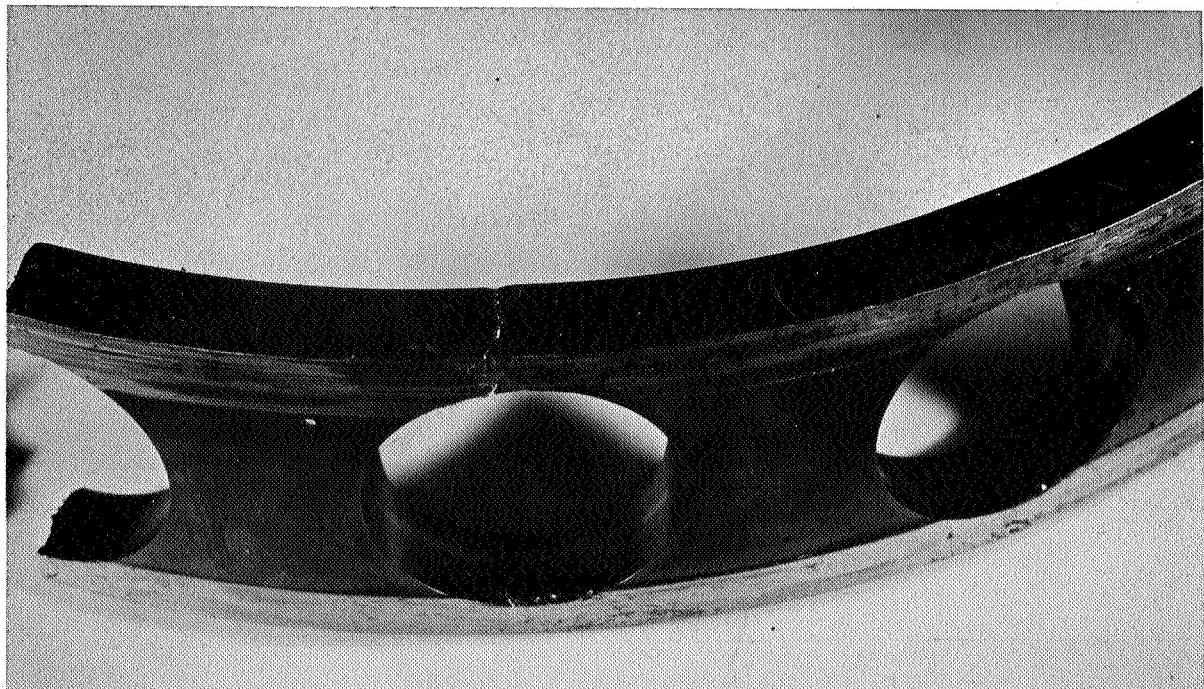


FIGURE: 48. SECONDARY RETAINER FAILURE - BEARING S/N 28

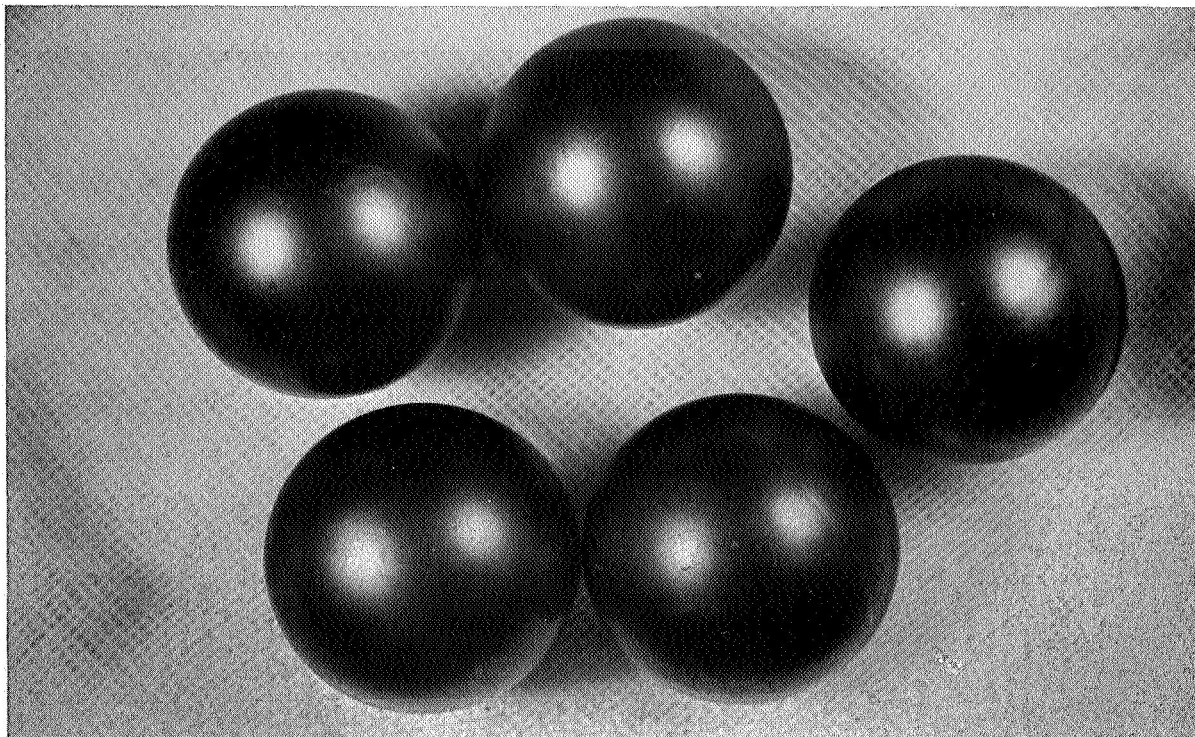


FIGURE: 49. TYPICAL APPEARANCE OF BALLS FROM BEARING S/N 28

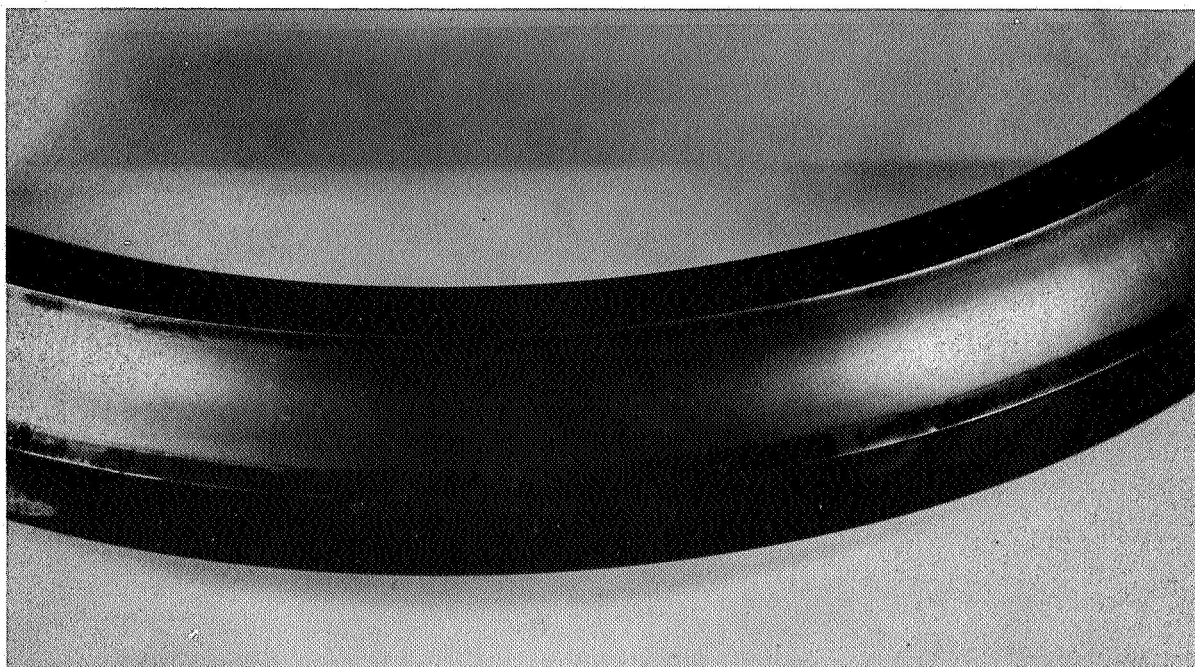


FIGURE 50. INNER RING - BEARING S/N 28



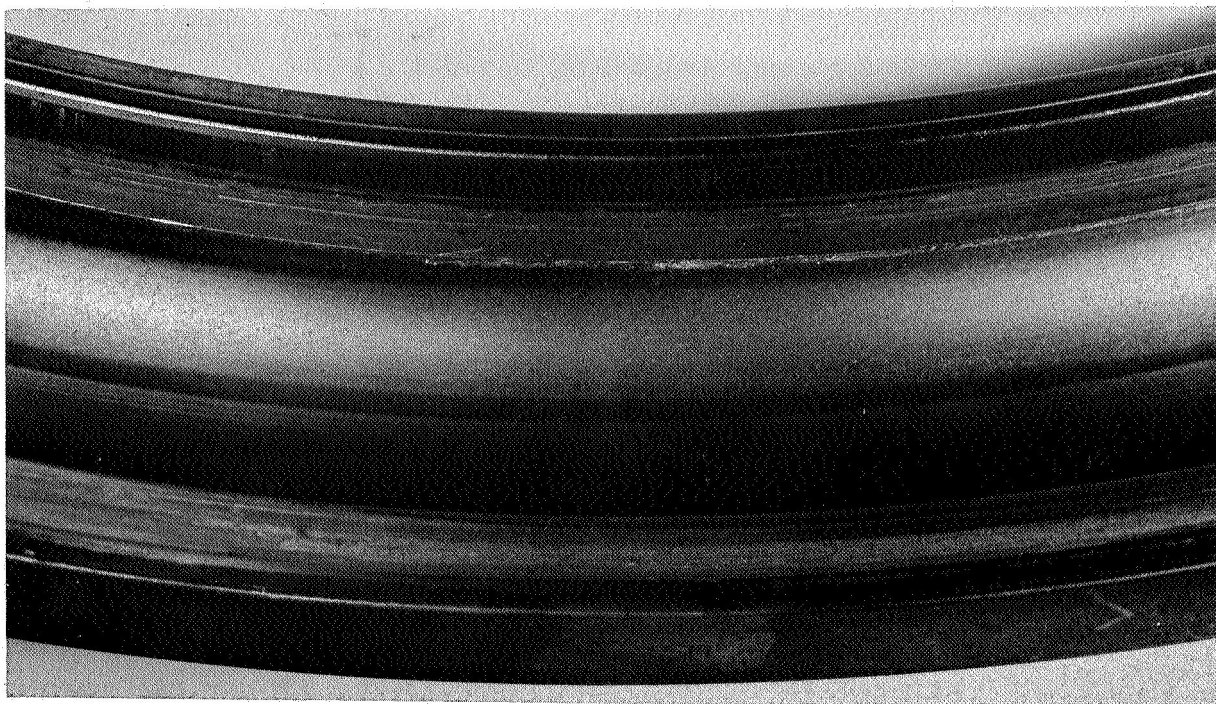


FIGURE 51. OUTER RING - BEARING S/N 28

NOTE: DAMAGE TO SHOULDER **ABOVE** BALL TRACK.

The implication of these results on the conduct of the test program has previously been reviewed.

The next three photographs, Figures 52, 53, and 54 are views of the inner and outer rings and balls respectively, from bearing 24 after 519 hours of running.

Lastly, Figures 55 and 56 illustrate the "Track Damage" observed on the inner and outer rings of bearing 34. The damage, as such, appears to be due to contamination of the lubricant, although an analysis of the fluid failed to reveal any significant evidence of foreign material in the oil.

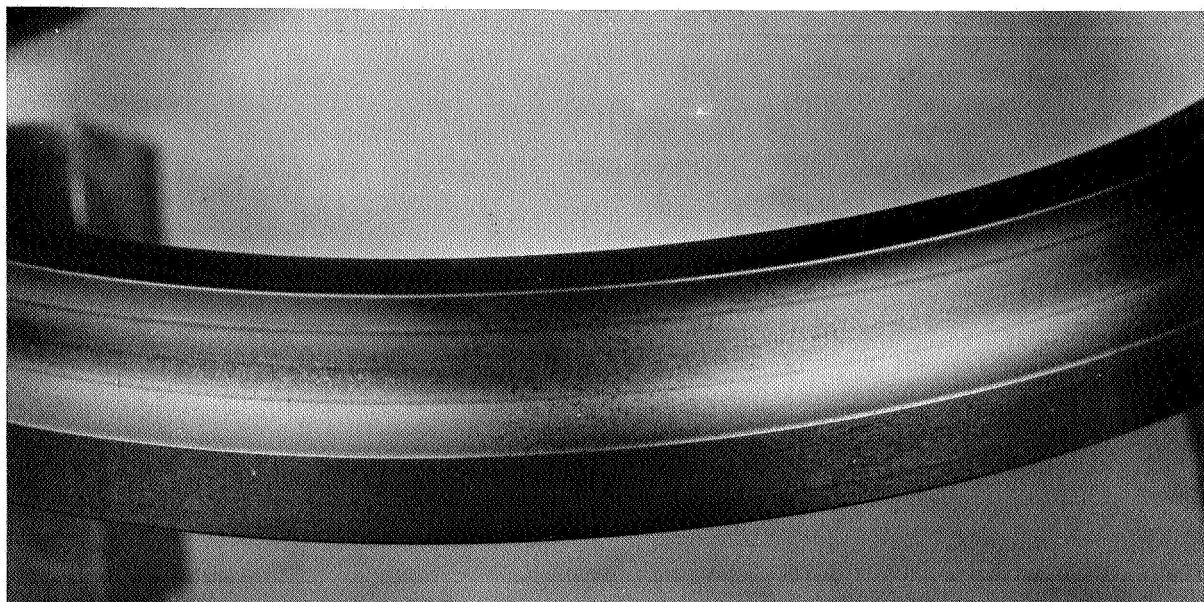


FIGURE 52. BALL PATH OF INNER RING - BEARING S/N 24

RUNNING TIME:	519 HOURS
LUBRICANT :	XRM-177F
TEMPERATURE :	600F
LOAD :	5800 LB. AXIAL
SPEED :	12,000 <b>RPM</b> (INNER)

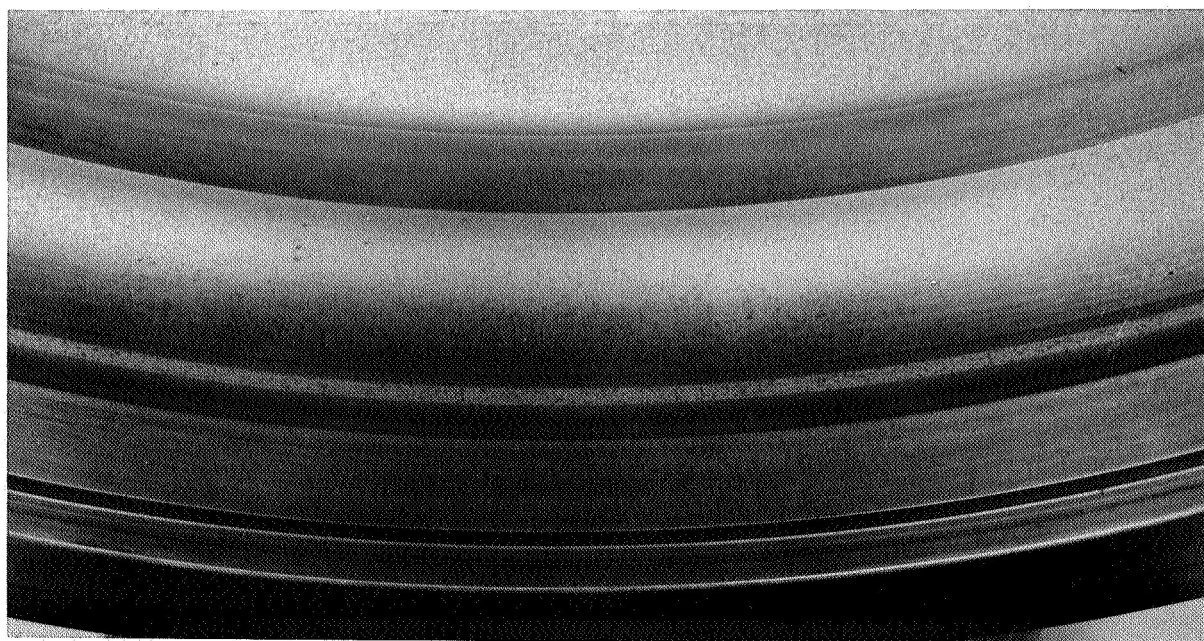


FIGURE 53. BALL PATH ON OUTER RING - BEARING S/N 24

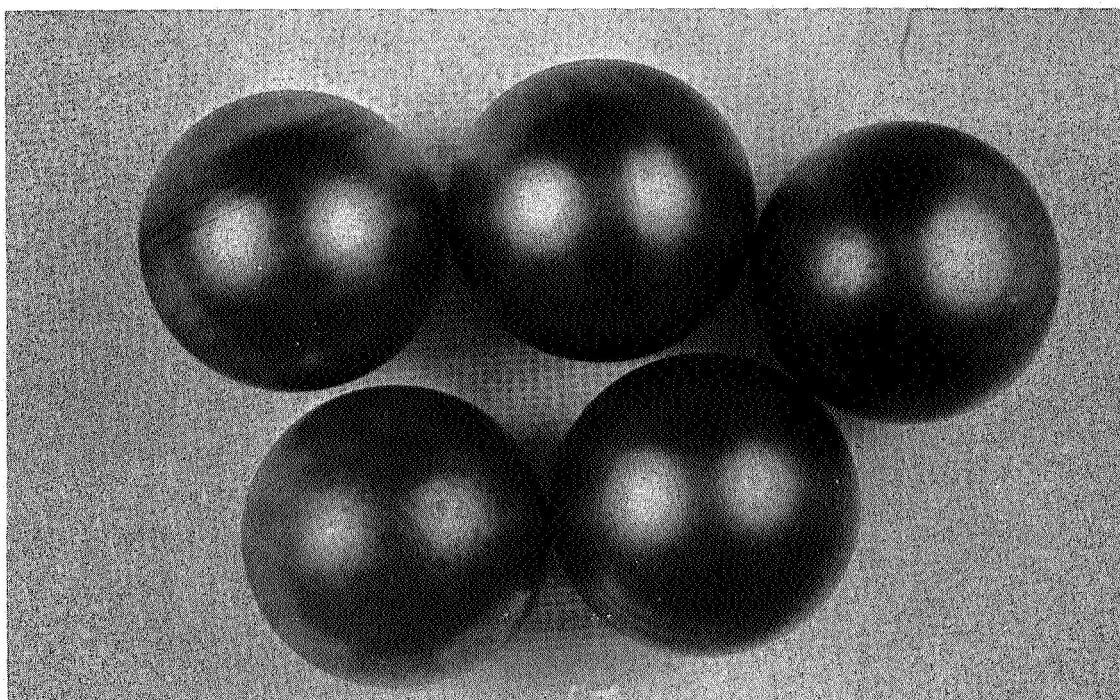
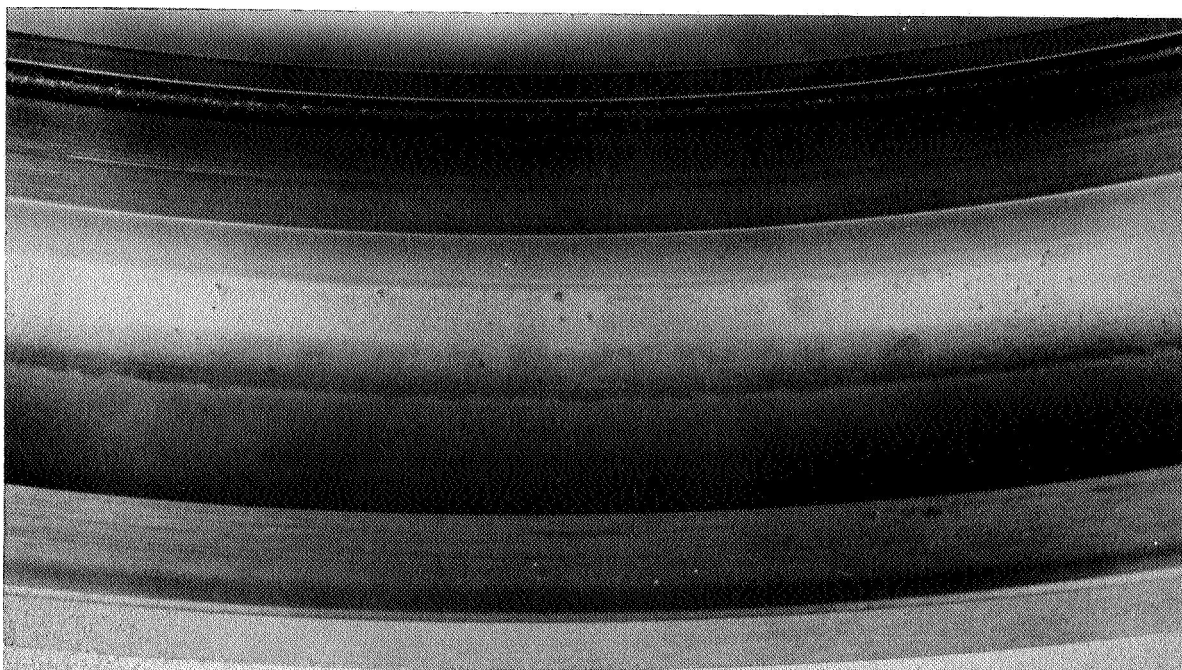


FIGURE 54. BALLS FROM BEARING S/N 24





**FIGURE 55. OUTER RING TRACK DAMAGE - BEARING S/N 34**

<b>RUNNING TIME:</b>	<b>385 HOURS</b>
<b>LUBRICANT:</b>	<b>XRM-177F (N<sub>2</sub> ATMOSPHERE)</b>
<b>TEMPERATURE:</b>	<b>600F</b>
<b>LOAD:</b>	<b>5800 LB. AXIAL</b>
<b>SPEED:</b>	<b>12,000 RPM (INNER)</b>

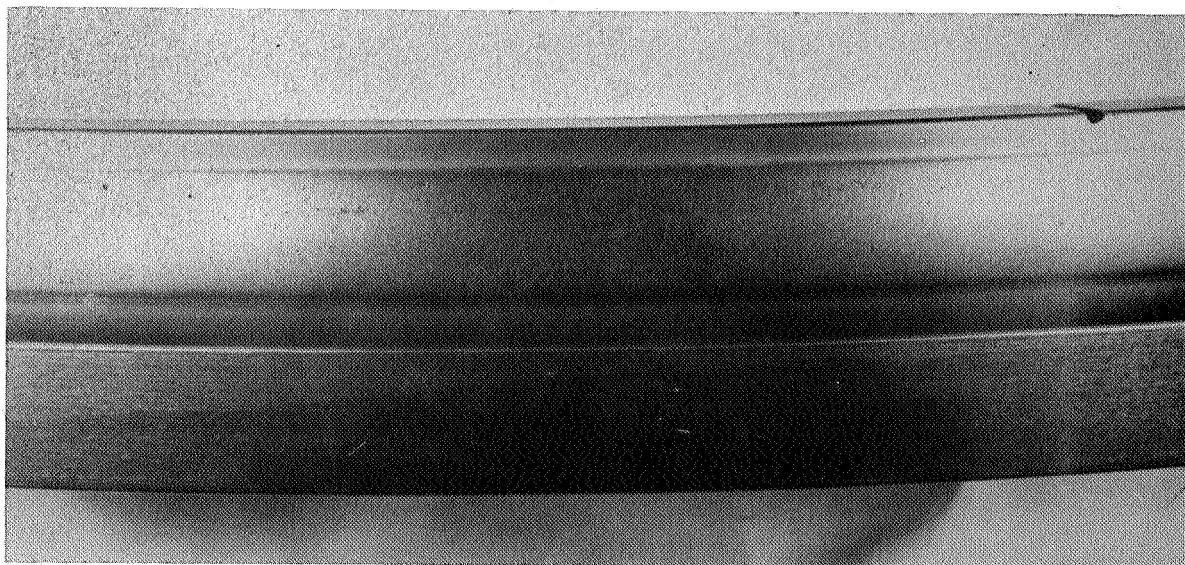


**FIGURE 56. INNER RING TRACK DAMAGE - BEARING S/N 34**

### 6.2.2 Test Series II

The initial plan for Test Series II was to perform 30 tests, using CVM-M-80 bearings, MCS-354 fluid at 600F in a  $N_2$  atmosphere. The applied load was to be the same as for the mineral oil tests or 5800 lb. axial which is equivalent to a maximum Hertzian load of 325,000 psi.

Earlier RC Rig testing indicated that the MCS-354 would have a lower fatigue life than the XRM-177F. In addition, some evidence of surface distress was noted on the RC Rig bars. The first attempt to operate the bearings with the MCS-354 in a  $N_2$  atmosphere at a 5800 lb. axial load resulted in a shut-down after two hours due to the inability to stabilize the temperature accompanied by a very high noise level. The high noise level, incidentally, was always a signal of wear and/or fatigue failures. Disassembly of the bearing showed considerable ball wear, track damage and catastrophic cage failure in bearing S/N 54. These items are illustrated in Figures 57 through 60. In view of this, a halt was called to the testing and the situation reviewed with NASA personnel. It was decided to reduce the load on the bearings, and using the RC Rig data, a number of RECAP analyses were made, the results of which indicated the bearings should be able to attain a  $B_{10}$  life of 100 hours at an axial load of 4365 lbs. or 295,000 psi  $S_{max}$ .

A test was initiated and during the 45 minutes of operation, it was not possible to maintain the temperature at 600F. The outer ring temperature continued to climb above 600F. After 45 minutes of operation, the tester was again shut down due to activation of the over-temperature sensor.

Disassembly of the bearing showed fatigue failures around the entire circumference of the inner raceway of bearing 39 and the inner and outer raceway of bearing 40. Examples of these failures are shown in Figures 61 and 62. In addition, the balls from both of these bearings exhibited severe wear; typical balls from bearing 40 are shown in Figure 63. The cages from both bearings were relatively undamaged as shown in Figure 64.

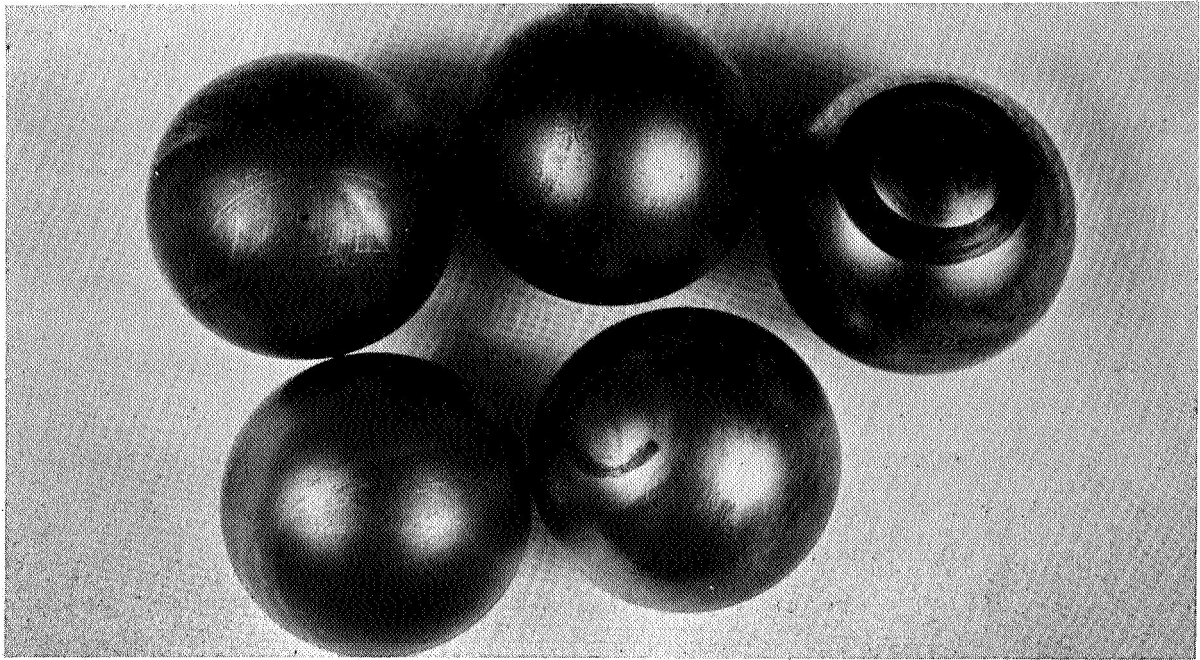


FIGURE 57. TYPICAL APPEARANCE OF BALLS - BEARING S/N 54

RUNNING TIME:	2 HOURS
LUBRICANT:	MCS-354 (AIR ATMOSPHERE)
TEMPERATURE:	600F +
LOAD:	5800 LB. AXIAL
SPEED:	12,000 RPM (INNER)

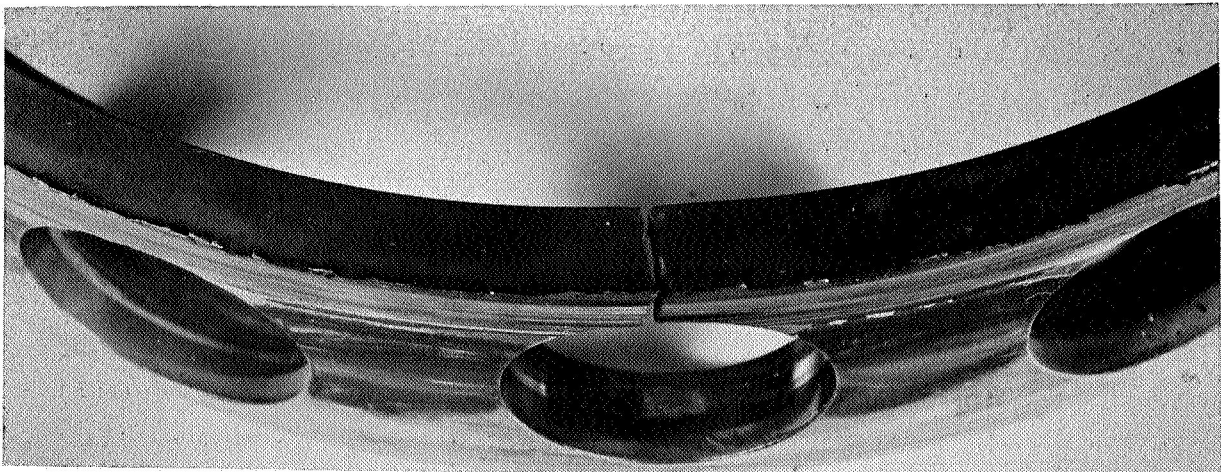
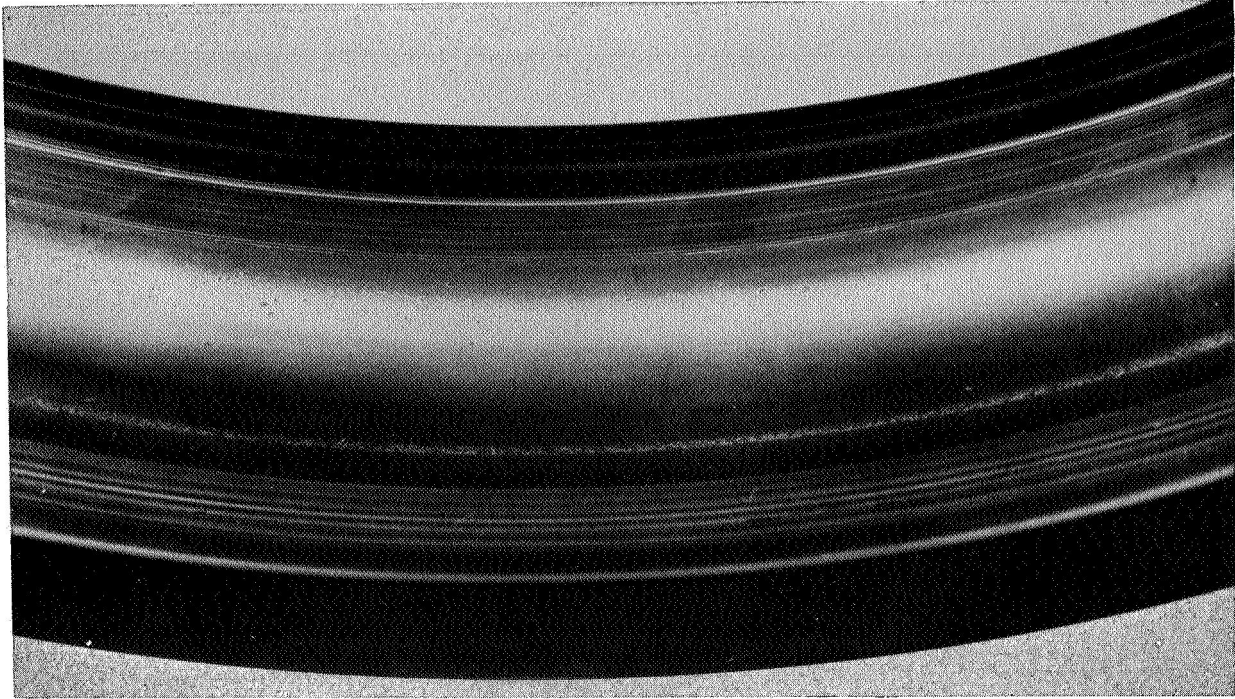
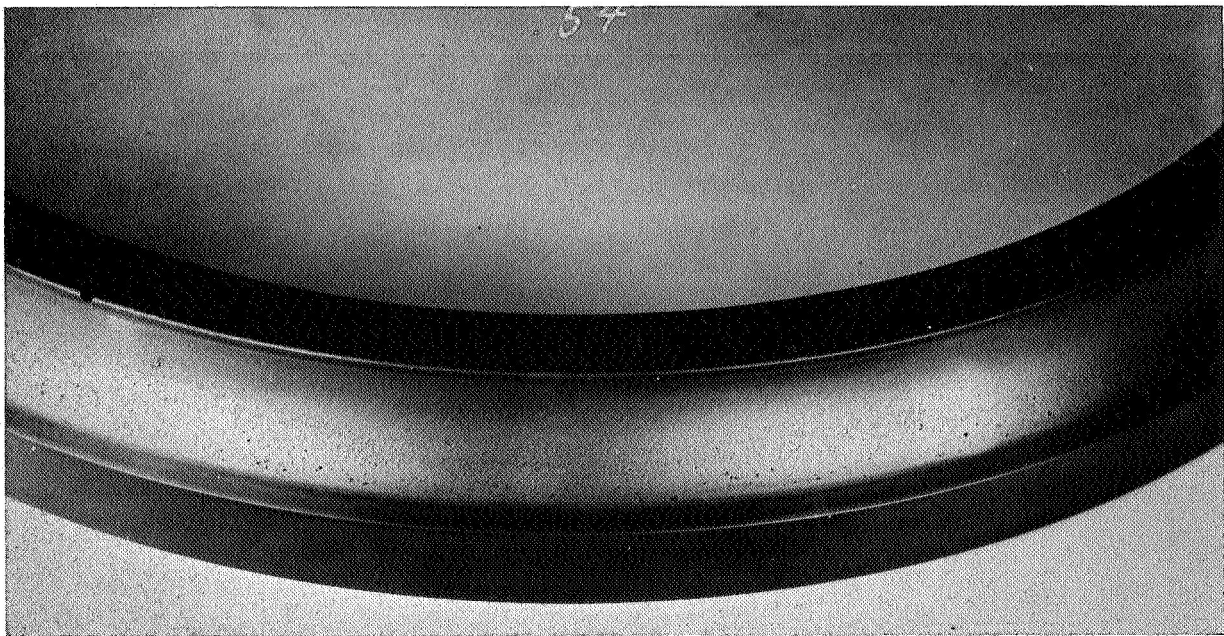


FIGURE 58. CAGE FAILURE AND BALL POCKET WEAR - BEARING S/N 54





FIGURE, 59. OUTER RING - BEARING S/N 54



FIGURE, 60. INNER RING - BEARING S/N 54

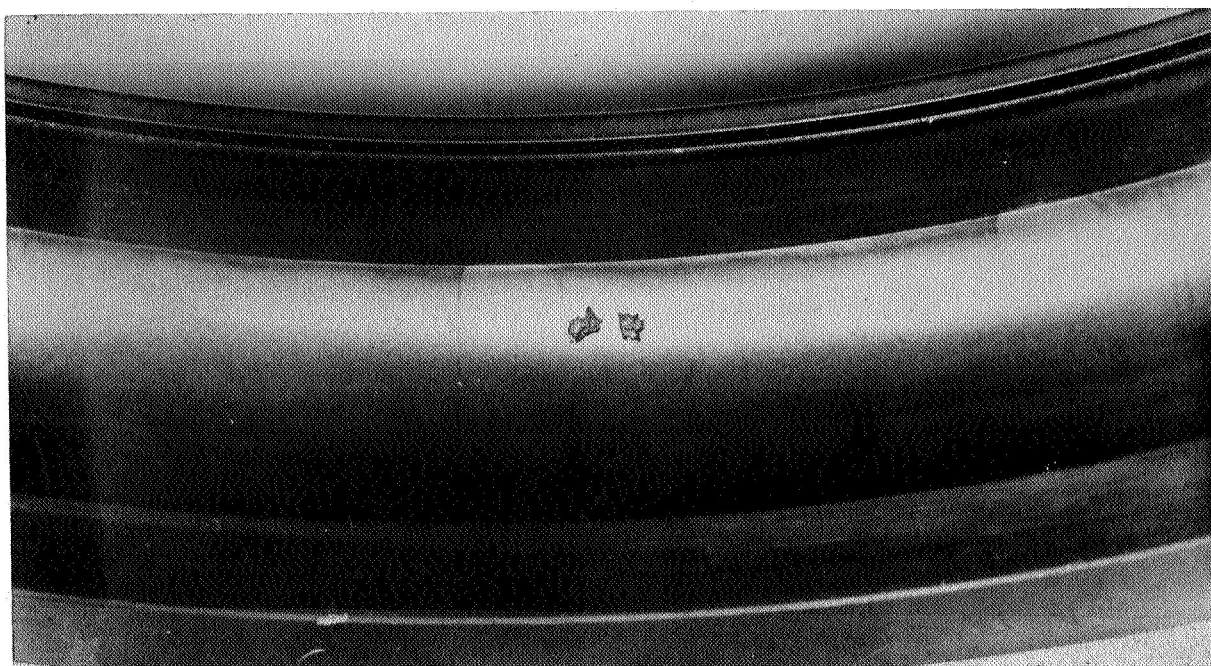


FIGURE 61. TYPICAL FAILURE IN BALL PATH IN OUTER RING - BEARING S/N 40

RUNNING TIME:	'45 MINUTES
LUBRICANT:	MCS-354 N <sub>2</sub> INERTED
TEMPERATURE:	APPROXIMATELY 600F
LOAD:	4365 LB. AXIAL
SPEED:	12,000 RPM (INNER)

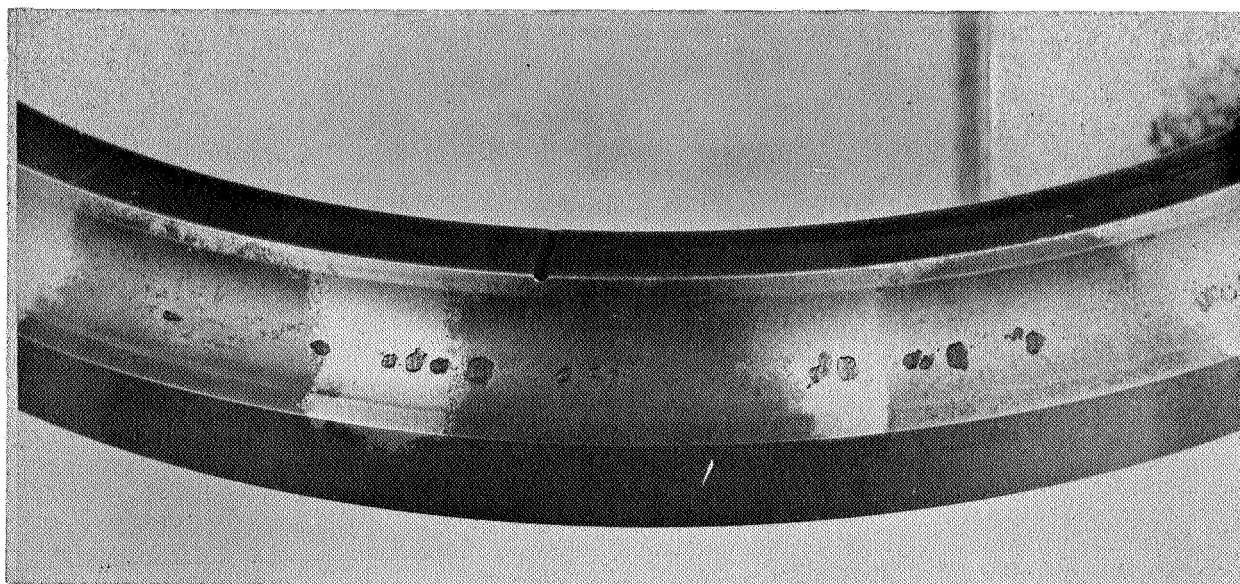


FIGURE 62. TYPICAL FAILURES ON BALL PATH OF INNER RING - BEARING S/N 40

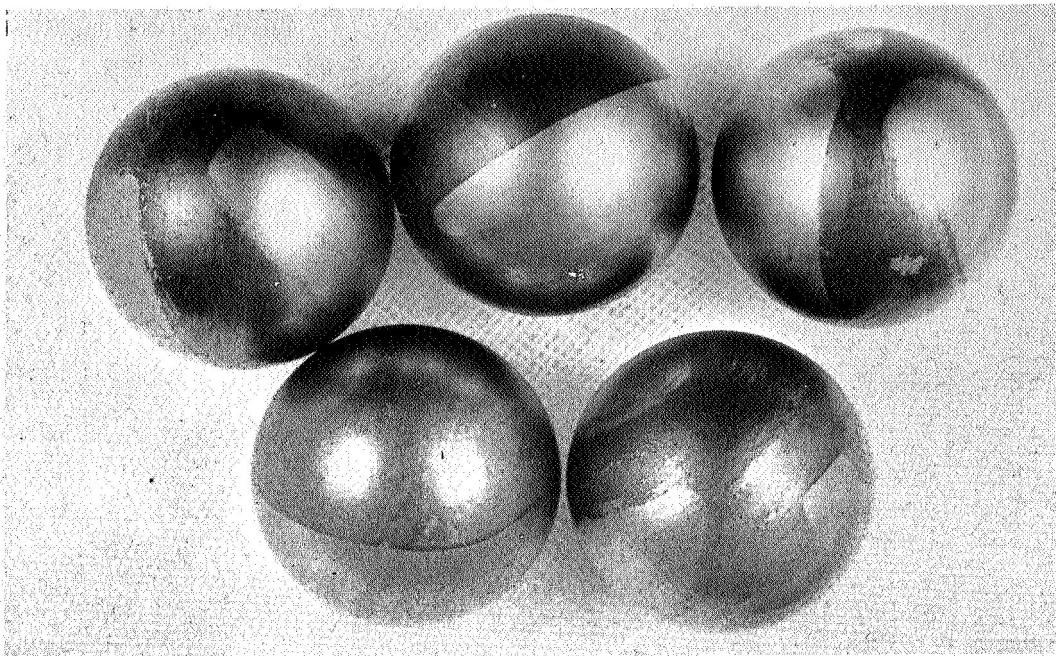


FIGURE 63. BALLS FROM BEARING S/N 40

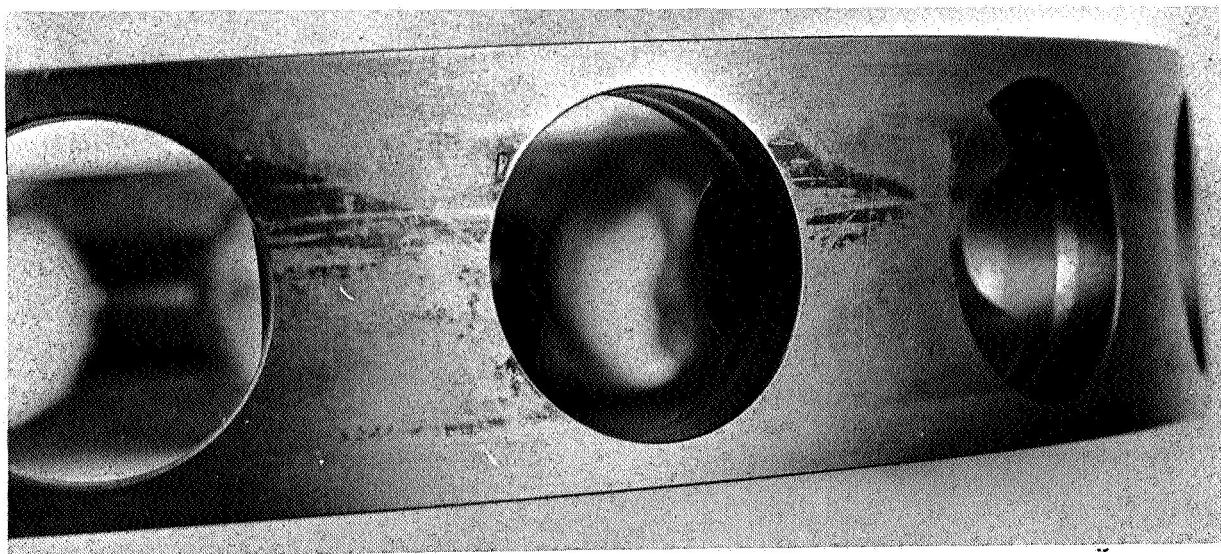


FIGURE 64. CAGE FROM BEARING S/N 40



Based on these results, the situation was again reviewed with NASA Project Management, and an agreement was reached to attempt to operate one set of bearings without the benefit of the nitrogen inertion. To accomplish this the N<sub>2</sub> line was disconnected and replaced with an air line. This was required, as a positive pressure had to be maintained in the tester in order for the J79 tandem carbon seal to be effective. A test was then conducted, running two M-50 bearings at 600F in an air atmosphere. This test continued successfully to 120 hours, at which point the bearing was disassembled and inspected. The bearing components appeared to be in good condition with no apparent evidence of wear or fatigue damage. These observations were reviewed with NASA Project Management, and the decision was made to conduct the entire second test series of this program in an air atmosphere.

Consequently, Test Series II was conducted under the following conditions:

Bearing Material;	Rings	CVM-M-50
	Balls:	CVM-M-50
	Retainer:	S-Monel
Lubricant:	Monsanto	MCS-354
Operating Conditions:		
	Temp:	Outer Ring 585F ± 5F Inner Ring 600F - 610F Oil In - 525F-545F Oil Out - 585F-595F
	Speed:	12,000 rpm
	Load:	4365 lbs, axial
	Atmosphere:	Air

Despite the reduced load, most of the tests with this fluid had to be aborted because of high ball wear. This is shown in the test results tabulated in Table 13, This data is also plotted in Weibull distribution in Figure 65, although the small number of actual fatigue failures (3 of 20)



Table 13

Results of 120 mm Bearing Tests with MCS-354 Lubricant, CVM M-50 Bearings, at 600F in Air

Test No.	Bearing S/N	Load (lb.)	Time (Hr.)	Inner Ring	Outer Ring	Ball
II - 1	53	5800 (2) (N <sub>2</sub> )	2	OK	OK	OK (.003" Wear)
II - 1a	54	5800 (N <sub>2</sub> )	2	OK	OK	OK (.002" Wear)
II - 2	39	4365 (1) (N <sub>2</sub> )	.75	Fatigue	OK	OK (.001" Wear)
II - 2a	40	4365 (N <sub>2</sub> )	.75	Fatigue	OK	OK (.001" Wear)
II - 3	45	4365	500	OK	OK	OK (.0002" Wear)
II - 3a	46	4365	500	OK	OK	OK (.0003" Wear)
II - 4	52	4365	14	OK	OK	Fatigue (.025" Wear)
II - 4a	51	4365	14	Fatigue	Fatigue	Fatigue
II - 5	47	4365	11	OK	OK	OK (.001" Wear)
II - 5a	48	4365	11	OK	OK	OK (.001" Wear)
II - 6	49	4365	65	OK	OK	OK (.0001" Wear)
II - 6a	50	4365	65	OK	OK	OK (.0002" Wear)
II - 7	61	4365	10	OK	OK	OK (.001" Wear)
II - 7a	62	4365	10	OK	OK	OK (.001" Wear)
II - 8	63	4365	20	OK	OK	OK (.001" Wear)
II - 8a	64	4365	20	Wear	Wear	OK (.025" Wear)
II - 9	67	4365	25	OK	OK	OK (.0005" Wear)
II - 9a	68	4365	25	OK	OK	OK (.001" Wear)
II - 10	43	4365	500	OK	OK	OK (.0003" Wear)
II - 10a	44	4365	500	OK	OK	OK (.0003" Wear)
II - 11	57	4365	500	OK	OK	OK
II - 11a	58	4365	500	OK	OK	OK

Table 13, Contd

Test No.	Bearing S/N	Load (lb.)	Time (HH.)	Inner Ring	Outer Ring	Ball
II -12	59	4365	500	OK	OK	OK (.0002" Wear)
II -12a	60	4365	500	OK	OK	OK (.0002" Wear)
II -13	65	4365	269	OK	OK	OK (.0002" Wear)
II -13a	66	4365	269	OK	OK	OK (.0004" Wear)
II -14	69	4365	393	OK	OK	OK (.0002" Wear)
II -14a	70	4365	393	OK	OK	OK (.0005" Wear)
II -15	56	4365	461	OK	OK	OK (.0002" Wear)
II -15a	55	4365	461	OK	O	OK (.0002" Wear)

(1) 4365 lb. axial load = 295,000 psi max. hertz on inner.

(2) 5800 lb. axial load = 321,000 psi max. hertz on inner.

□ Indicates Time to Fatigue Failure

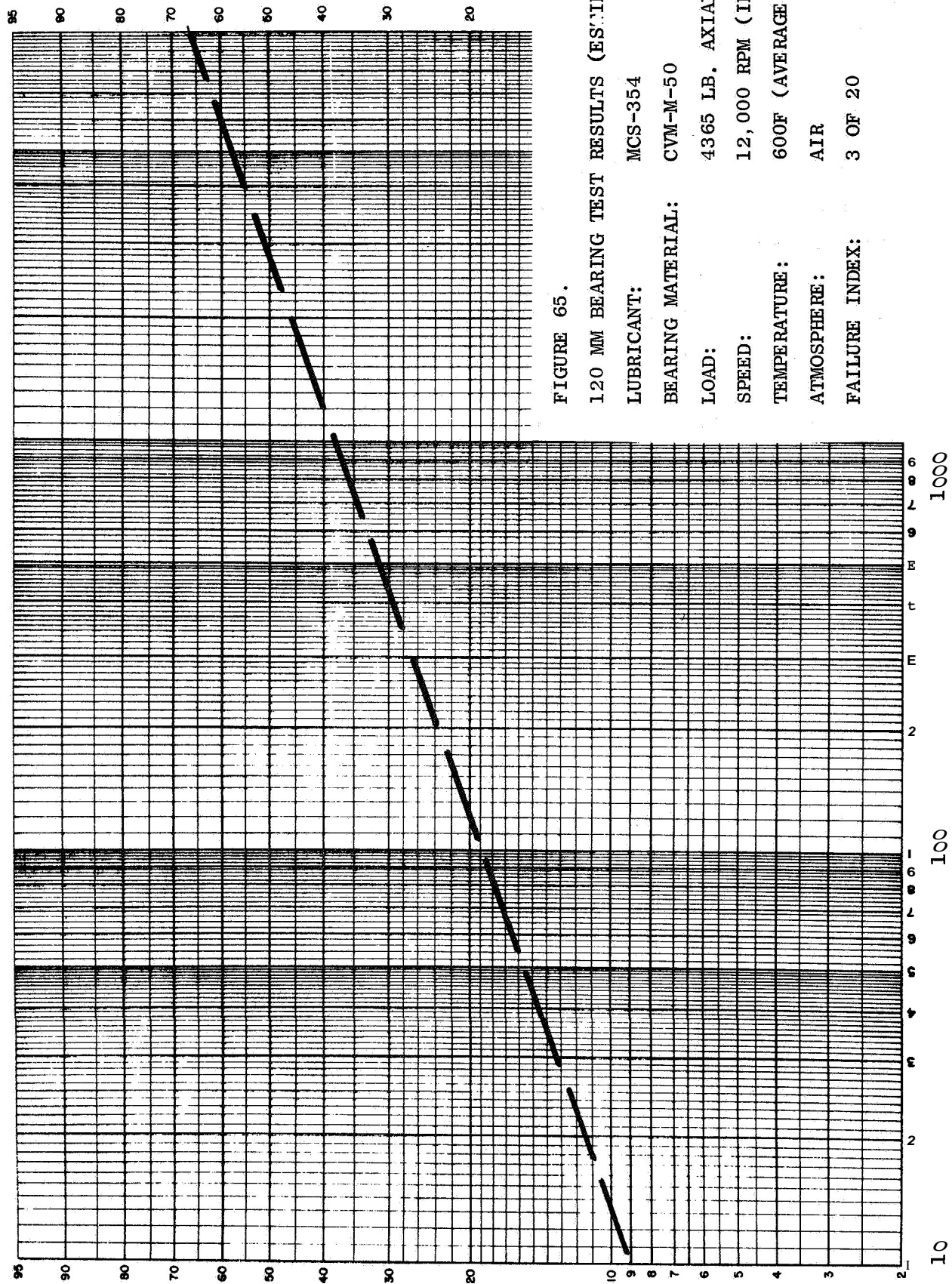


FIGURE 65.

120 MM BEARING TEST RESULTS (ESTIMATE)

LUBRICANT: MCS-354

BEARING MATERIAL: CVM-M-50

LOAD: 4365 LB. AXIAL

SPEED: 12,000 RPM (INNER)

TEMPERATURE: 600F (AVERAGE METAL)

ATMOSPHERE: AIR

FAILURE INDEX: 3 OF 20

carry a very low confidence level and tend to make this curve academic at best.

A significant result of the polyphenyl ether tests was the amount of ball wear observed on all of the bearings, even those which achieved the 500 hour life. In some bearings, ball wear was as high as .025", and the average wear in test times ranging from two to 65 hours was about .001". It was noted that in the case of the 500-hour bearings, ball wear while present, was relatively light, being on the order of .0003" or less. There does not appear to be an apparent relationship between wear and test time, and it can only be assumed that the variations could possibly be due to slight manufacturing tolerances which are not discernable in the allowable tolerance ranges; or it could be due to very small temperature differences such as  $\pm 5$ -IOF from one test to another. There also appears to be no clear-cut relationship between the initiation of wear and the rate at which wear proceeds.

Bearing 45 achieved 500 hours of running with little ball wear. Typical bearing components are illustrated in Figures 66 through 69. Of particular interest here is the surface finish on the balls (Figure 67), which is still quite good and devoid of micro pitting, despite the fact that ball wear ranging up to .0003" was measured. This was generally the case in that despite a considerable amount of wear on some of the balls, the surface finish remained good in contrast to the surface finish observed on the worn, XRM-177F lubricated balls. In the latter case, and in the case of the polyphenyl ether test performed in a nitrogen atmosphere, a considerable amount of micro pitting was present. However, this was not the case with the polyphenyl ether tested in air.

Several photographs are presented which are typical of some of the conditions observed on the bearings tested with the polyphenyl ether. Figures 70 and 71 are the balls and inner raceway of

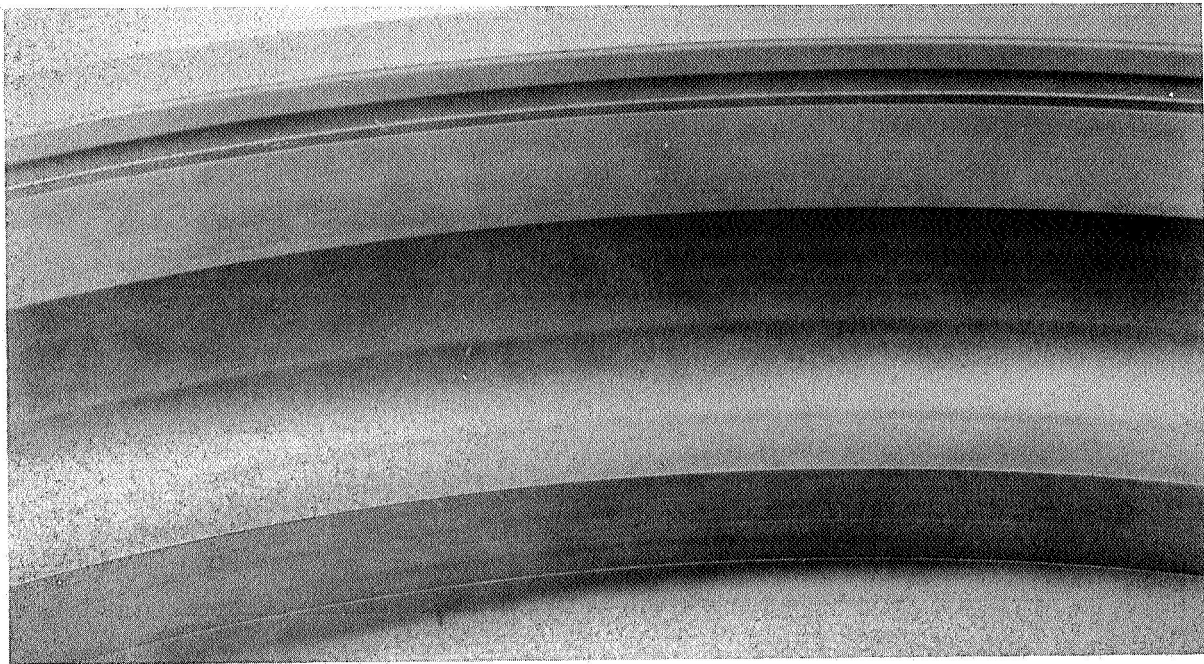


**FIGURE 66. OUTER RING BALL TRACK - BEARING S/N 45**

<b>RUNNING TIME:</b>	<b>500 HOURS</b>
<b>LUBRICANT:</b>	<b>MCS-354 (AIR ATMOSPHERE)</b>
<b>TEMPERATURE:</b>	<b>600F</b>
<b>LOAD:</b>	<b>4365 LB. AXIAL</b>
<b>SPEED:</b>	<b>12,000 RPM (INNER)</b>

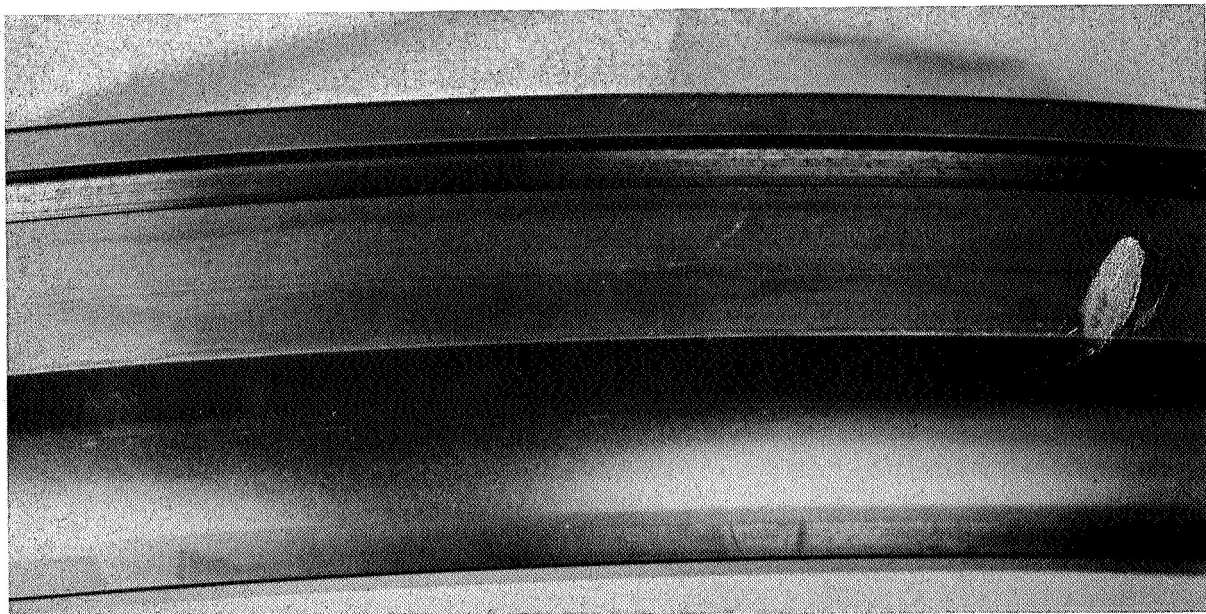


**FIGURE 67. INNER RING BALL PATH - BEARING S/N 45**



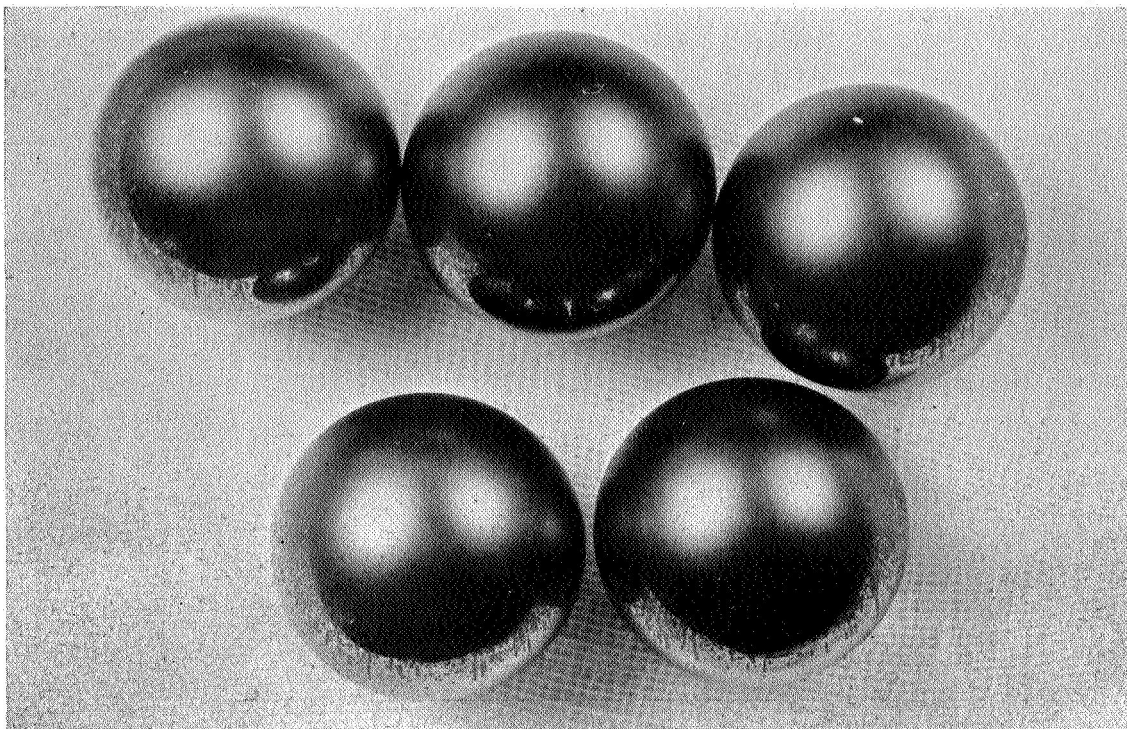


FIGURE 68. CAGE BALL POCKET - BEARING S/N 45

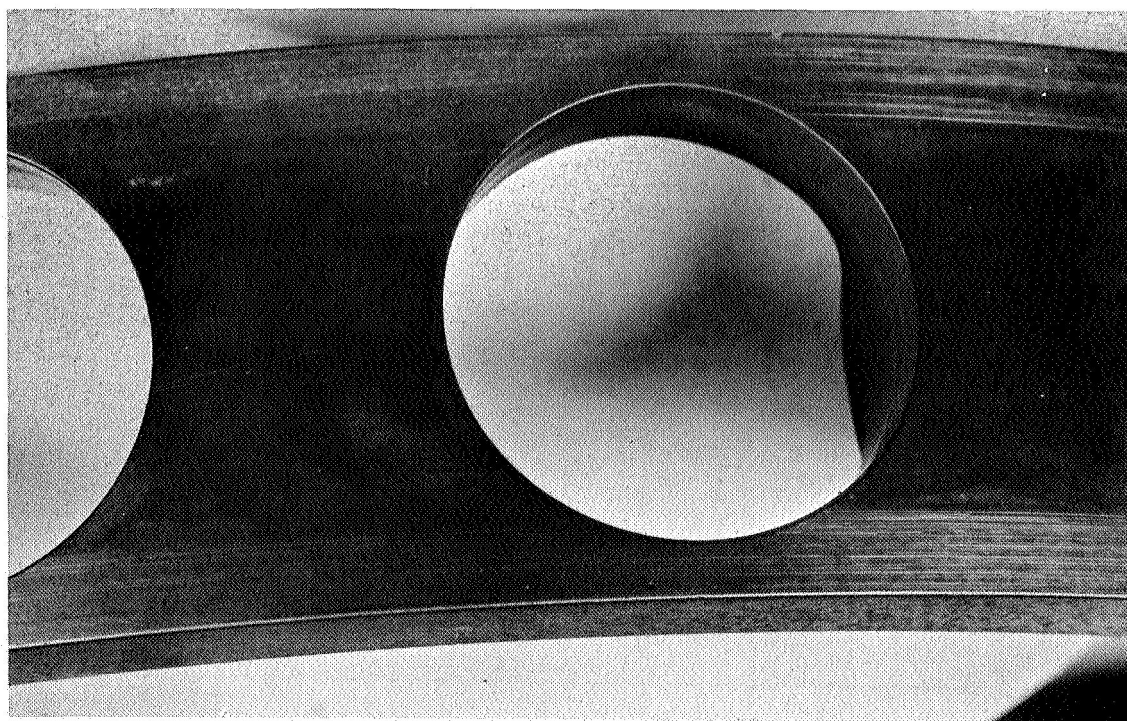
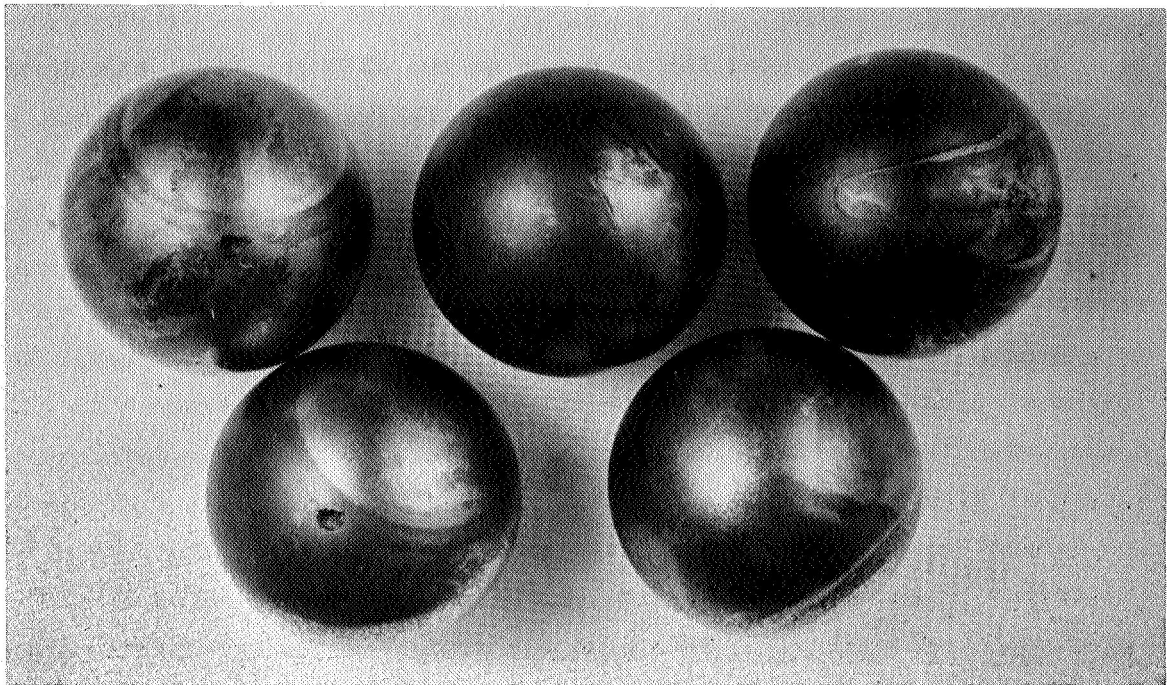


FIGURE 69. BALLS - BEARING S/N 45

bearing 52, which operated for 14 hours at the 4365 lb. level and showed excessive ball wear (.025") as well as ball fatigue. The unusual pattern shown on the balls in Figure 70 is due to staining after shut-down rather than to actual operation. The next four photographs are illustrative of the condition found in bearing 51, which also had accumulated 14 hours. Figure 72 shows the fatigue spalls on several of the balls, and it is interesting to observe the somewhat unusual texture of the failure. The failures appear to be much more brittle than normally observed with compressive fatigue failures (where some evidence of plastic deformation is almost always evident). Figure 73 shows a cage side rail fracture and the damage caused by rubbing against the outer ring after the cage fractured. Figures 74 and 75 are typical fatigue spalls noted on the inner and outer raceways. Note also the damage on the raceway shoulder which occurred when the ball diameter was reduced sufficiently to allow a significant contact angle increase, thereby causing the ball to ride up over the shoulder of the raceway.

With the polyphenyl ether, oil consumption was quite high. Attempts at refluxing were unsuccessful, as very little oil can be reclaimed using this technique. It appears that the basic problem in oil loss is the relatively high evaporation rate of this material. Based on data presented by Monsanto, <sup>(9)</sup> the evaporation loss as measured by ASTM method D-972 is 8 1/2%, in 6 1/2 hours at 500F at 140 millimeters mercury of pressure. This would indicate that in a 24-hour period, approximately 30% of the fluid would be lost due to evaporation at a temperature lower than that to which the fluid was exposed in this program.





**FIGURE 70. BALL FATIGUE FAILURES - BEARING S/N 52**

<b>RUNNING TIME:</b>	<b>14 HOURS</b>
<b>LUBRICANT:</b>	<b>MCS-354 (AIR ATMOSPHERE)</b>
<b>TEMPERATURE:</b>	<b>600F</b>
<b>LOAD :</b>	<b>4365 LB. AXIAL</b>
<b>SPEED :</b>	<b>12,000 RPM (INNER)</b>

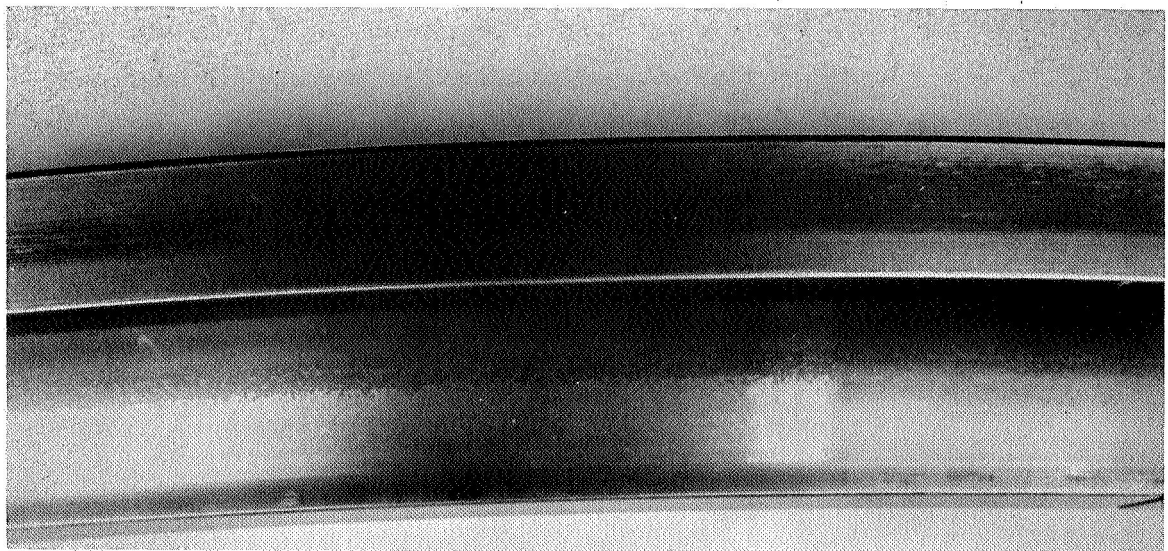


**FIGURE 71. INNER RING BALL PATH - BEARING S/N 52**

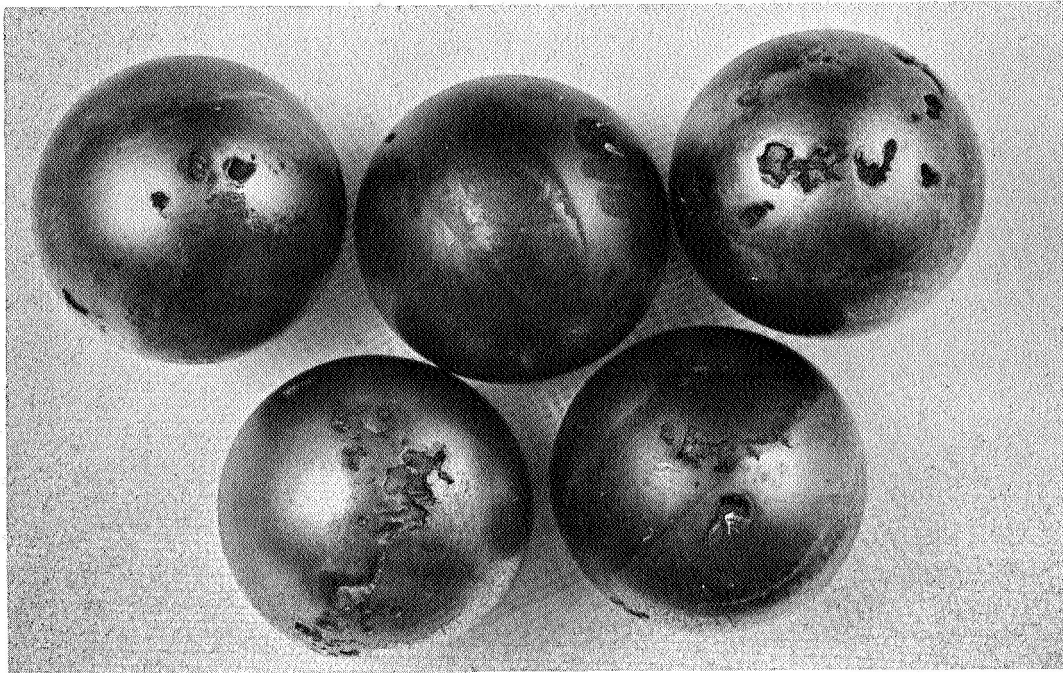


**FIGURE 72. BALL FATIGUE FAILURES - BEARING S/N 51**

<b>RUNNING TIME:</b>	<b>14 HOURS</b>
<b>LUBRICANT:</b>	<b>MCS-354 (AIR ATMOSPHERE)</b>
<b>TEMPERATURE :</b>	<b>600F</b>
<b>LOAD :</b>	<b>4365 LB. AXIAL</b>
<b>SPEED:</b>	<b>12,000 RPM (INNER)</b>

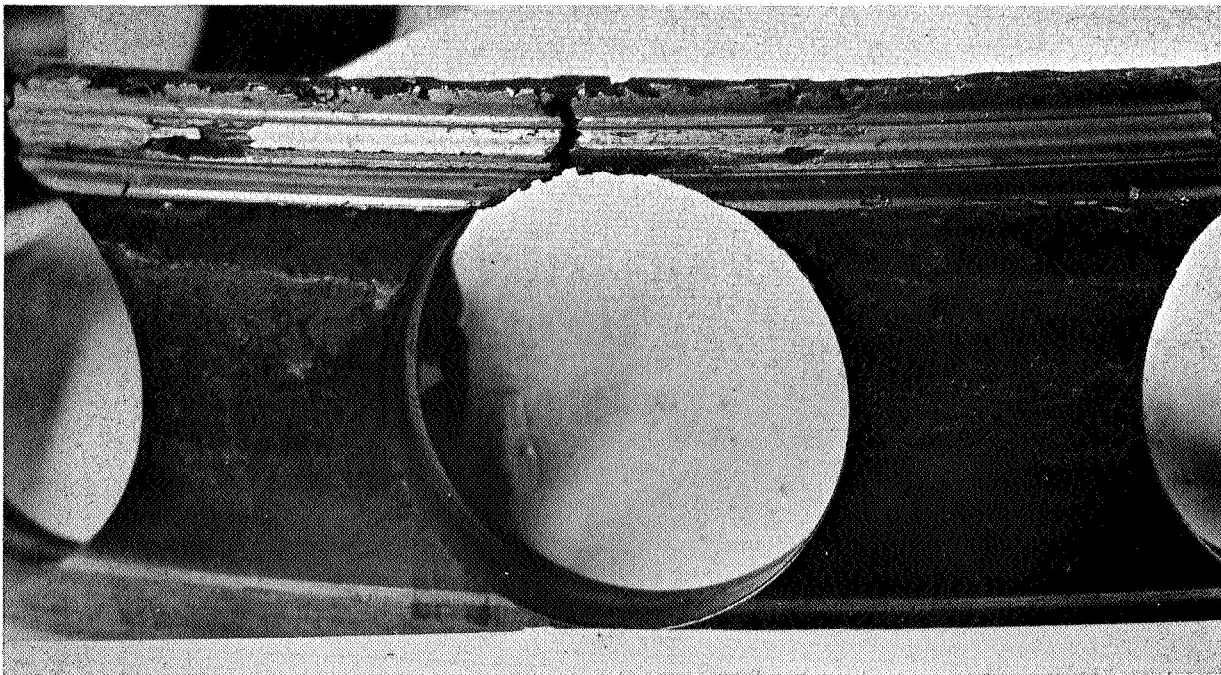
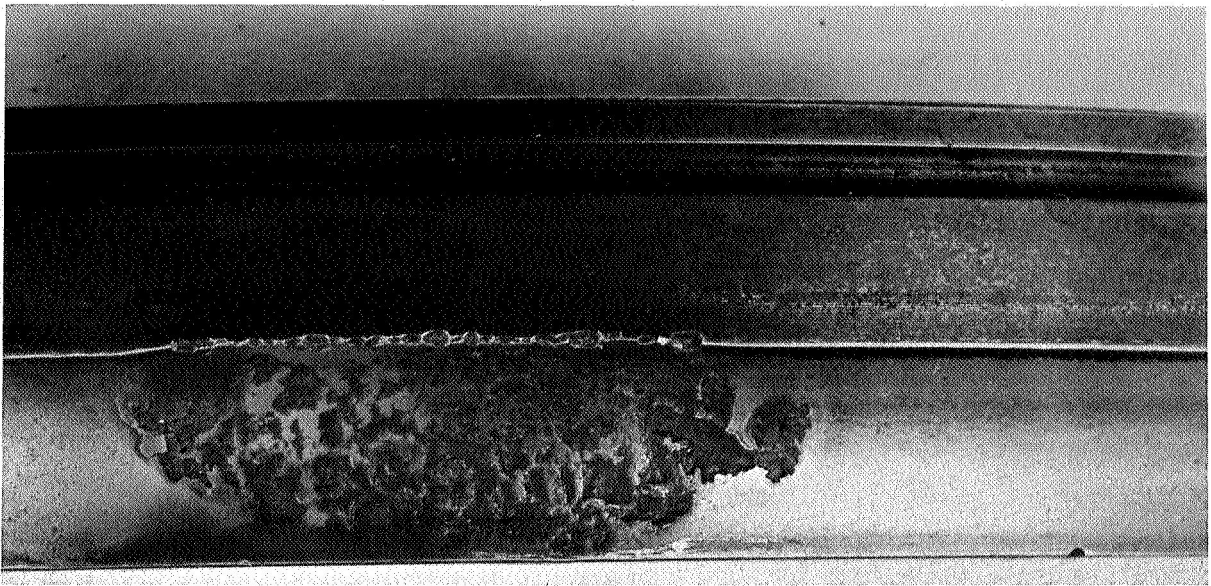
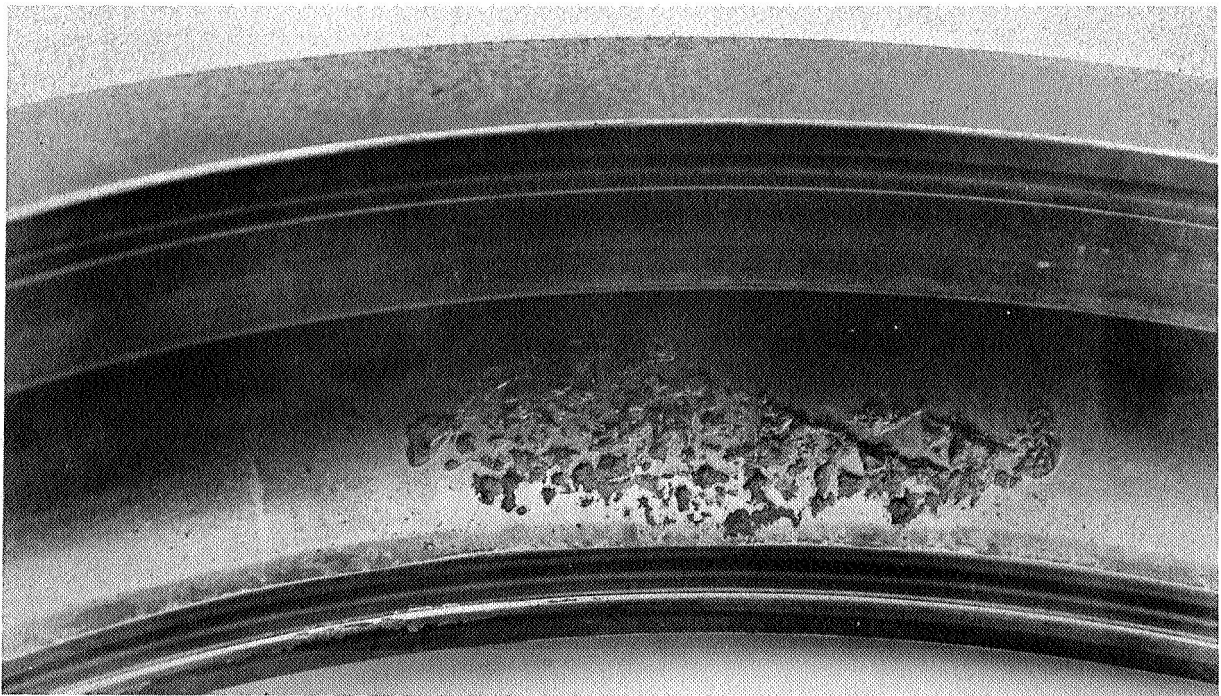


**FIGURE 73. CAGE FAILURE - BEARING S/N 51**





FIGURJI 74. INNER RING FATIGUE FAILURE - BEARING S/N 51



FIGURJI 75. OUTER RING FATIGUE FAILURE - BEARING S/N 51

### 6.2.3 Test Series III

Prior to the initiation of this test series, all tester components were inspected for the quality of nickel plating and those components showing evidence of plating damage were replated.

Again, as with the two earlier test series it had been planned to operate at 5800 lbs. axial load and in a  $N_2$  atmosphere. However, a number of problems were encountered which required a deviation in the program plan,

In the initial check-out test with the PR-143, it was found that the oil-water heat exchanger used to cool the oil, in the previous tests did not have sufficient capacity to maintain the desired temperature range of 585P to 610F. This is primarily due to the higher density of this fluid as well as its low specific heat and low thermal conductivity as compared to the other two test fluids. It was found that the temperature tended to approach stabilization at approximately 100° above the temperature at which the two previous fluids had stabilized. This is in agreement with data presented by other sources who have also performed Pull scale bearing testing with the DuPont PR-143 fluid,

To overcome this problem, a new heat exchanger was designed and checked out. In order to accomplish this in the least amount of time, it was necessary to deviate from the all Monel and nickel plated metallic components which had been judged necessary to provide protection against corrosive effects. Consequently, in the first series of tests using the new heat exchanger, stainless steel (316) fittings and Bundyweld tubing were utilized. The Bundyweld tubing is a low carbon steel tubing encased in a thin layer of copper. Using two M-50 bearings, specifically released by NASA for this study, a 100-hour test was conducted at an axial load of 5800 lbs., a speed of 12,000 RPM, and a bearing temperature of 600F. Samples of the oil were inspected at frequent periods during this run. Initially, the oil assumed a milky color, although after about 50 hours of running, the coloration of the oil became a very light brown, remaining

this color for the 100 hour period, Spectrographic analysis of the oil after 100 hours showed only very minor traces of metallic elements. After 100 hours the tester was disassembled and samples of the stainless steel fittings as well as the Bundyweld tubing were examined metallographically. The stainless steel showed no evidence of corrosion, there was, however, some indication of copper depletion on the ID of the Bundyweld tubing indicating this material to be marginal for this particular application. Based on these results, it was decided that the new heat exchanger system would be constructed entirely of 316 stainless steel components. The lack of corrosion on stainless steel is understandable, in that the maximum oil temperature to which this material is exposed to is in the range of 500F to 525F. The surfaces of the tester per se appeared to be unaffected, although all surfaces which had been in contact with the oil were noticeably darkened. This, of course, included the test bearings.

The test bearings appeared to be in good condition except for some ball wear. Figures 76 through 78 illustrate typical components after the 100 hour test. It was decided however, that in view of the possible contaminant effect of the Bundyweld tubing and copper that these bearings would be shelved.

In all other respects the behavior of the oil was normal and showed evidence of performance consistent with its high density and low specific heat. The viscosity at 600F is similar to the other two fluids in the program. Because of the high density, an increased pressure was developed in the centrifugal pump since pressure varies as:

$$\Delta P = r^2 W^2 P$$

$\Delta P$  = pressure in psia

where  $P$  = fluid mass density per in<sup>3</sup>

$r$  = radius in inches

$W$  = rotational speed in rad. per sec.

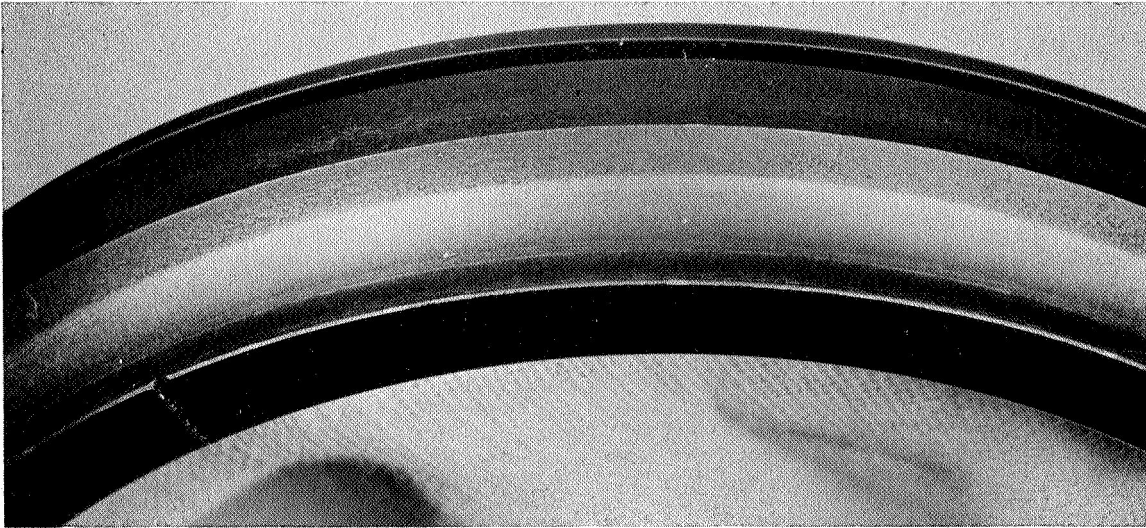
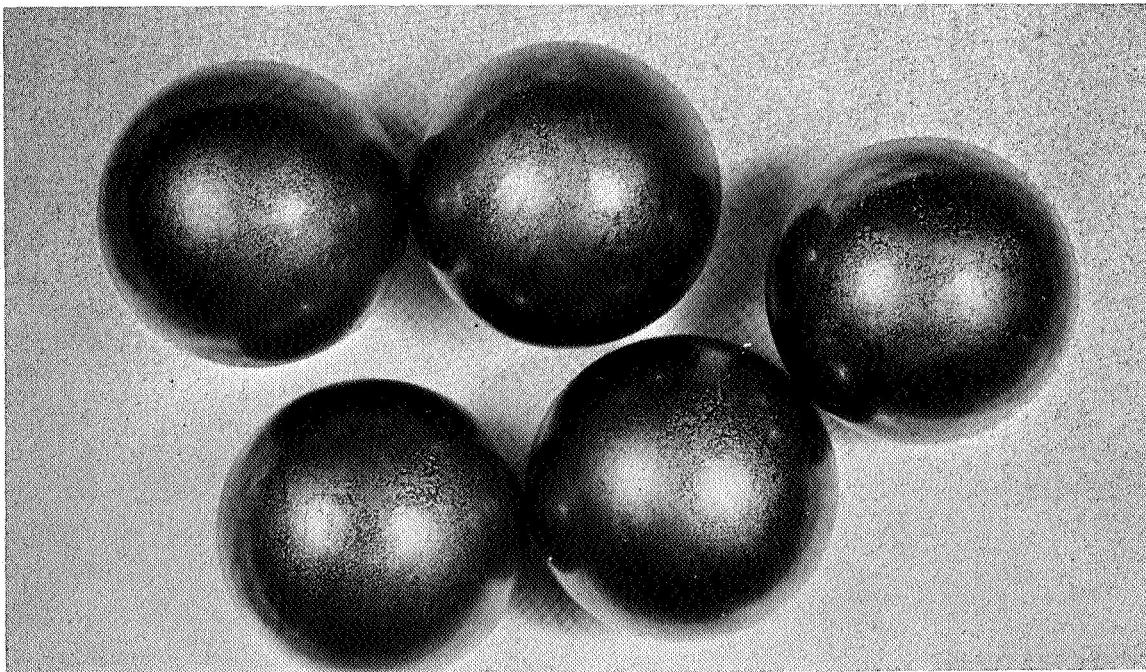


FIGURE 76. BALL TRACK ON INNER RING OF BEARING S/N 71 AFTER 100 HOURS

TEST CONDITIONS:

FLUID:	PR-143
LOAD:	5800 LB. AXIAL
SPEED:	12,000 RPM
TEMPERATURE:	600F



TYPICAL APPEARANCE OF BALLS FROM BEARING S/N 71 AFTER 100 HOURS

NOTE: THE MOTTLED APPEARANCE OF THE BALLS IS AN ARTIFACT, CAUSED BY THE DULLING SPRAY PUT ON THE PARTS PRIOR TO PHOTOGRAPHY.



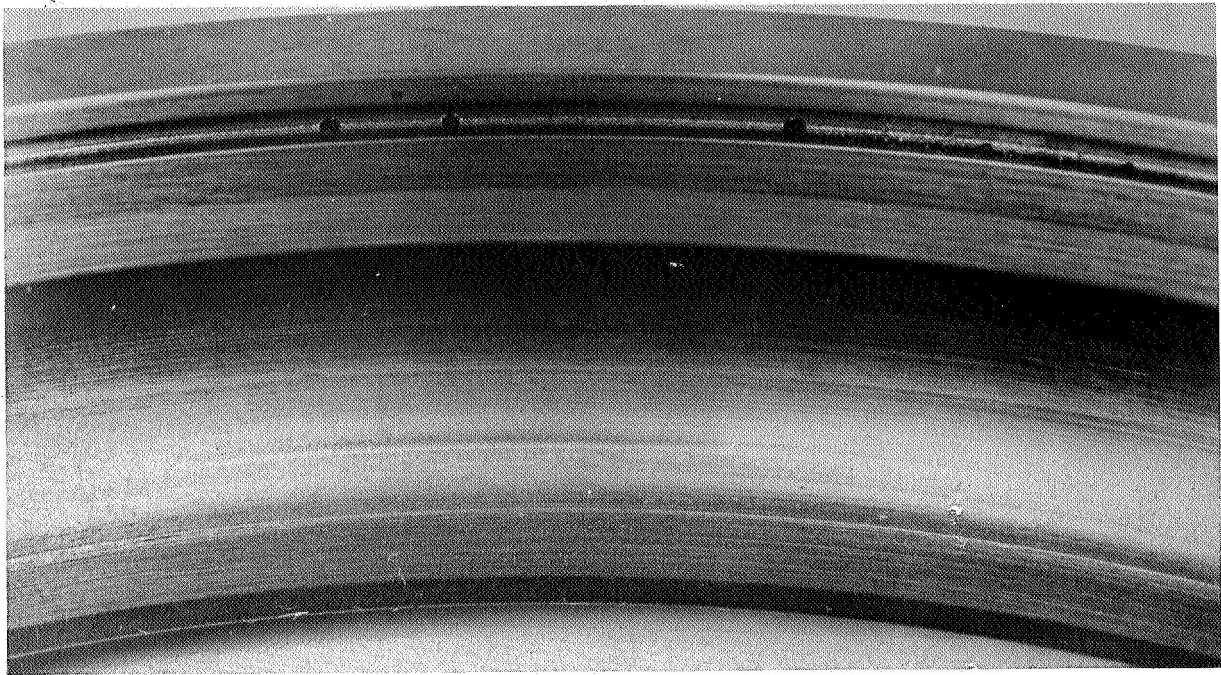


FIGURE 77. BALL TRACK ON OUTER RING OF BEARING S/N 71 AFTER 100 HOURS.

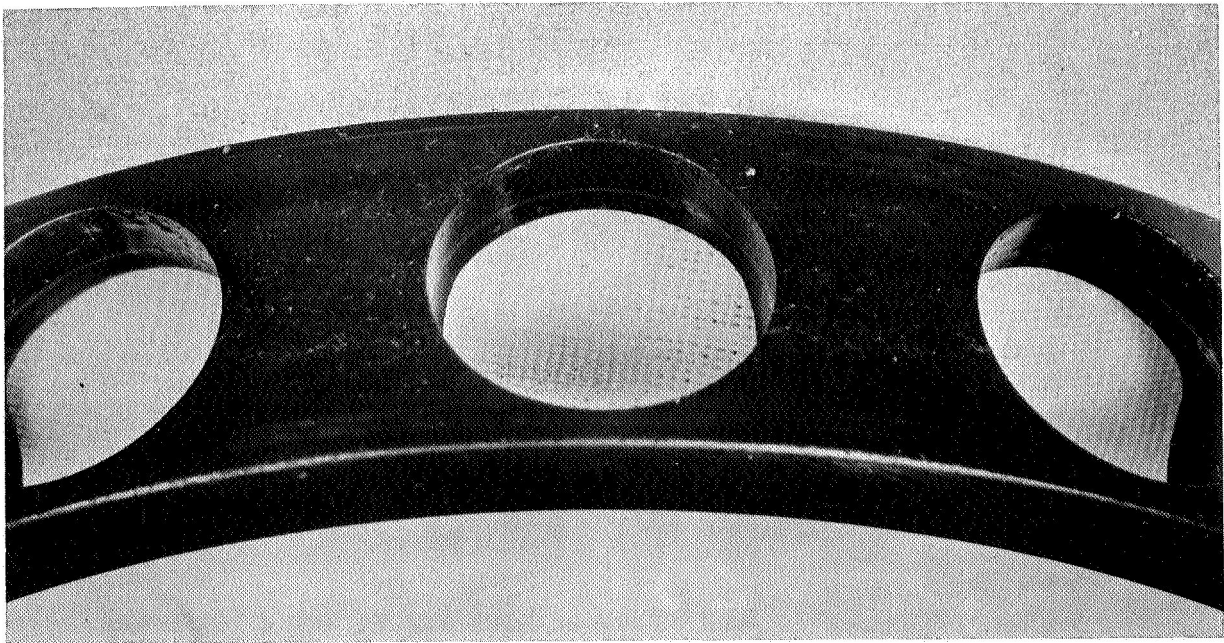


FIGURE 78. RETAINER FROM BEARING S/N 71 AFTER 100 HOURS.



In addition, an increased power loss was observed in the bearing due to the same inertial energy effects.

The foaming problems encountered previously with the other two fluids were not present. However, the high volatility of the fluid necessitated the addition of about 1 1/2 gallons of make up fluid during the 100 hours of tests. This is approximately 50% of the initial charge of oil,

Testing was resumed at the 5800 lb. level, although considerable ball wear and/or surface distress was observed. Consequently, after 8 tests at this load, the testing was halted and the situation reviewed with NASA Project Personnel.

As a result of these discussions, it was again decided to reduce the load to that used for the MCS-354 (4365 lb. axial). The remaining tests in Series III were therefore performed at this reduced load level.

Test Series III therefore was conducted under the following conditions:

Bearing Material :	Rings :	CVM-M-50
	Balls:	CVM-M-50
	Retainer:	S-Mone 1
Eubricant:	DuPont PR-143	
Operating Conditions :		
	Temp :	Outer Ring 585F $\pm$ 5F Inner Ring 600F - 610F Oil In - 525F-560F Oil Out - 590F-615F
	Speed:	12,000 rpm
	Load:	5800 lbs. axial (8 tests) 4365 lbs. axial (22 tests)

The data from these tests is tabulated in Table 14.

Table 14

Results of 120 mm Bearing Tests with PR-143 Lubricant, CVM M-50 Bearings, @ 500F in N<sub>2</sub>

Tire No.	Bearing S/N	Load (lb.)	Time (Hr.)	Inner Ring	Outer Ring	Ball
IIII-1	77	5800 (1)	103	OK	OK	OK (.0003" Wear)
IIII-1a	78	5800	103	amaged (2)	Damaged	Damaged
IIII-2	75	5800	243	OK	OK	OK (.0004" Wear)
IIII-2a	76	5800	243	OK	OK	OK (.0004" Wear)
IIII-3	79	5800	201	OK	OK	OK (.0015" Wear)
IIII-3a	80	5800	201	Damaged	Damaged	Damaged
IIII-4	83	5800	202	OK	OK	OK (.0005" Wear)
IIII-4a	84	5800	202	Damaged	Damaged	OK (.0005" Wear)
IIII-5	85	4365 (3)	171	OK	OK	OK (.0005" Wear)
IIII-5a	86	4365	171	Fatigue	OK	Fatigue
IIII-6	81	5800	506	OK	Fatigue	OK (.0020" Wear)
IIII-6a	82	5800	502	OK	OK	OK (.0020" Wear)
IIII-7	73	5800	436	Fatigue	Fatigue	OK (.0025" Wear)
IIII-7a	74	5800	436	Fatigue	Fatigue	OK (.0025" Wear)
IIII-8	93	4365	159	Damaged	Damaged	Fatigue
IIII-8a	94	4365	159	OK	OK	OK
IIII-9	87	4365	500	OK	OK	OK (.0002" Wear)
IIII-9a	88	4365	500	OK	OK	OK
IIII-10	89	4365	134	Damaged	Damaged	OK (.0005" Wear)
IIII-10a	90	4365	134	OK	OK	OK (.0005" Wear)
IIII-11	99	4365	.01	OK	OK	OK
IIII-11a	100	4365	.01			

Table 14 Contd

Test No.	Bearing S/N	Load (lb.)	Time (Hr.)	Inner Ring	Outer Ring	Ball
III -12	95	4365	91	OK	OK	OK (.0005" Wear)
III -12a	96	4365	91	Damaged	Damaged	OK (.0005" Wear)
III -13	97	4365	142	OK	Fatigue	OK (.0005" Wear)
III -13a	98	4365	142	OK	OK	OK (.0005" Wear)
III -14	91	4365	500	OK	OK	OK (.0004" Wear)
III -14a	92	4365	500	OK	OK	OK (.0005" Wear)
III -15	99	4365	403	OK	Fatigue	OK (.0015" Wear)
III -15a	101	4365	403	OK	OK	OK (.0015" Wear)

- (1) 5800 lb. axial load = 321,000 psi max. hertz on inner.  
(2) Damage refers to surface distress as a result of seizure  
(3) 4365 lb. axial load = 295,000 psi max. hertz on inner.  
□ Indicates Time to Fatigue Failure

The fatigue failures at the lower load are presented in a Weibull distribution in Figure 79.

During these tests, continued problems with high power loss due to high oil density and marginal boundary film conditions were encountered. Belt life, normally in excess of 500 hours, was reduced severely. Damage to shafts and pumps was also a problem and as a result, a number of the major tester components required repair and/or overhaul during and after this test series. Of the three oils tested, the PR-143 precipitated the most severe and recurrent operational problems. From an engine application standpoint, the most serious of these problems was the significantly greater difficulty in rejecting heat which required re-sizing the heat exchanger.

The photographs shown in Figures 80 through 97 are presented as typical examples of the appearance of the M-50 bearings tested with the PR-143. Figures 80 to 83 are views of Bearing S/N 78 which suffered a catastrophic failure after 103 hours. More normal fatigue failures are shown in Figures 84 and 85, whereas Figures 86 through 88 illustrate the appearance of a bearing (S/N 81) which successfully completed 500 hours of test. Figures 89 and 90 are examples of fatigue failure encountered after 436 hours of operation at the 5800 lb. axial load. Figure 89 shows a normal fatigue failure on the inner ring of bearing S/N 74, whereas Figure 90 shows a second type of failure encountered. This one being on the outer ring of the same bearing. The failures here are more similar to those experienced with the polyphenylether (MCS-354). Figure 91 is a close-up of a surface of the inner ring of bearing S/N 74 showing the type of chemical corrosion observed on the long life bearings. Figure 92 shows an example of surface damage encountered at the lower load level (4365 lbs.). The S-Monel retainer of this bearing (Figure 93) appears to be in excellent condition, as was the case with most of these components during this and the previous test series. Figures 94 through 96 are additional examples of bearing components having successfully survived 500 hours of testing. The last photograph (Figure 97) shows the cage rub experienced after .01 hours of operation on bearing S/N 100,

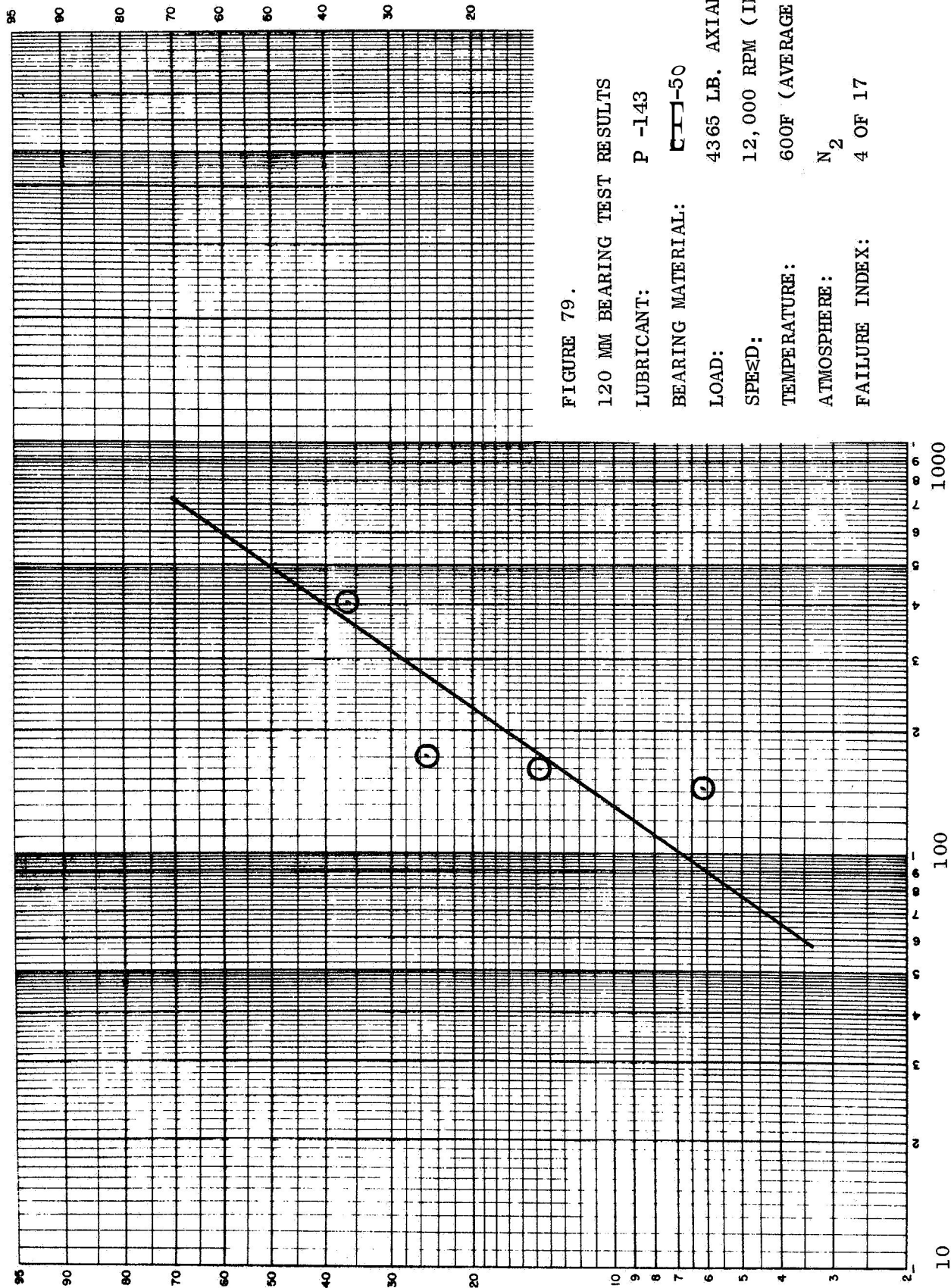


FIGURE 79.

120 MM BEARING TEST RESULTS

LUBRICANT: P -143

BEARING MATERIAL: C-10-50

LOAD: 4365 LB. AXIAL

SPEED: 12,000 RPM (INNER)

TEMPERATURE: 600F (AVERAGE METAL)

ATMOSPHERE: N<sub>2</sub>

FAILURE INDEX: 4 OF 17

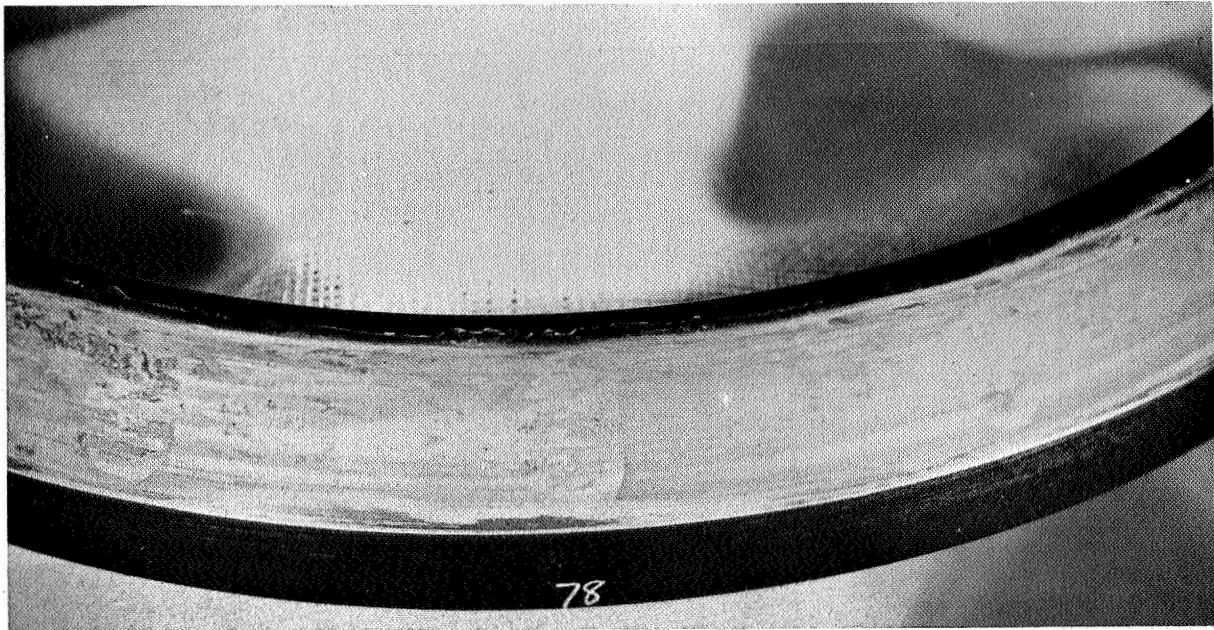


FIGURE 80. BEARING S/N 78. DAMAGED INNER RING.

TEST CONDITIONS:

LOAD :	5800 LB, AXIAL
SPEED:	12,000 RPM
TEMPERATURE :	600F
LUBRICANT:	PR-143
TIME TO FAILURE:	103 HOURS

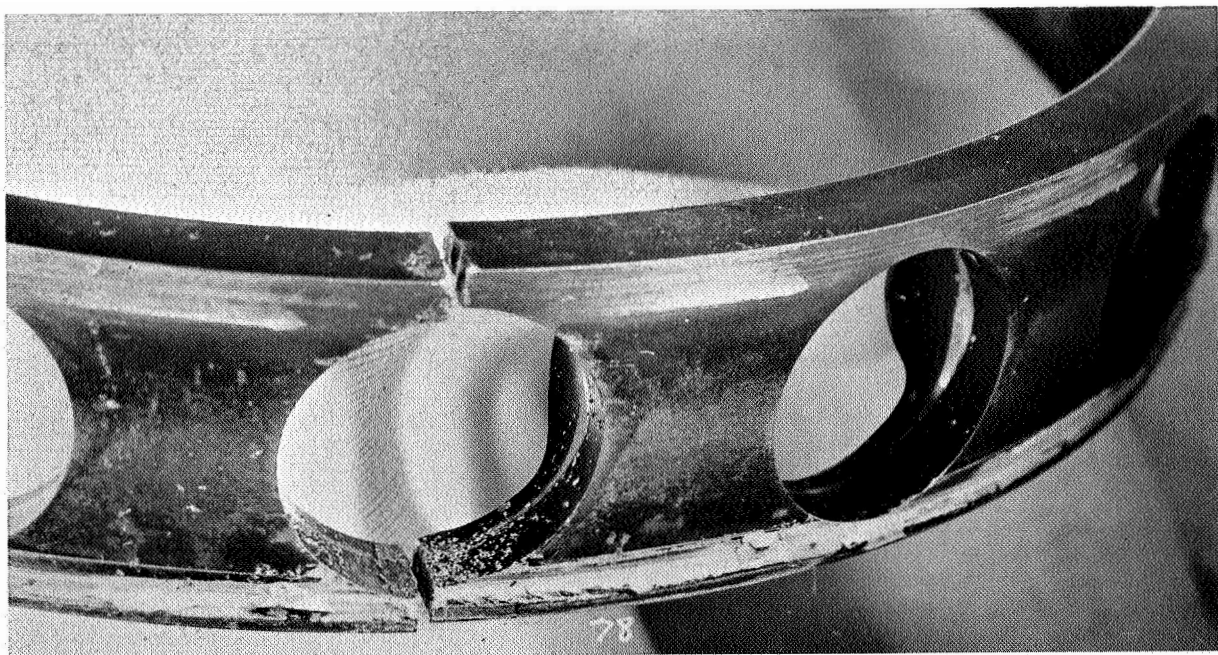
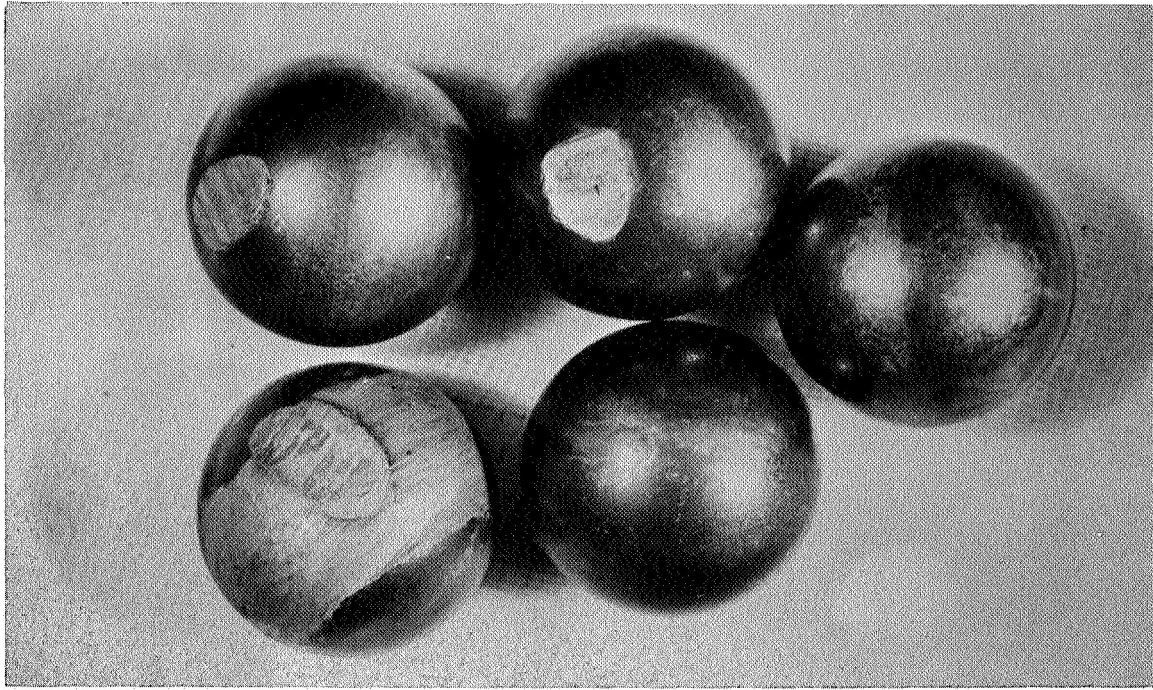


FIGURE 81. BEARING S/N 78. FRACTURED CAGE, NOTE EVIDENCE OF CAGE RUB.





FIGURF: 82. BEARING S/N 78. DAMAGED BALLS.

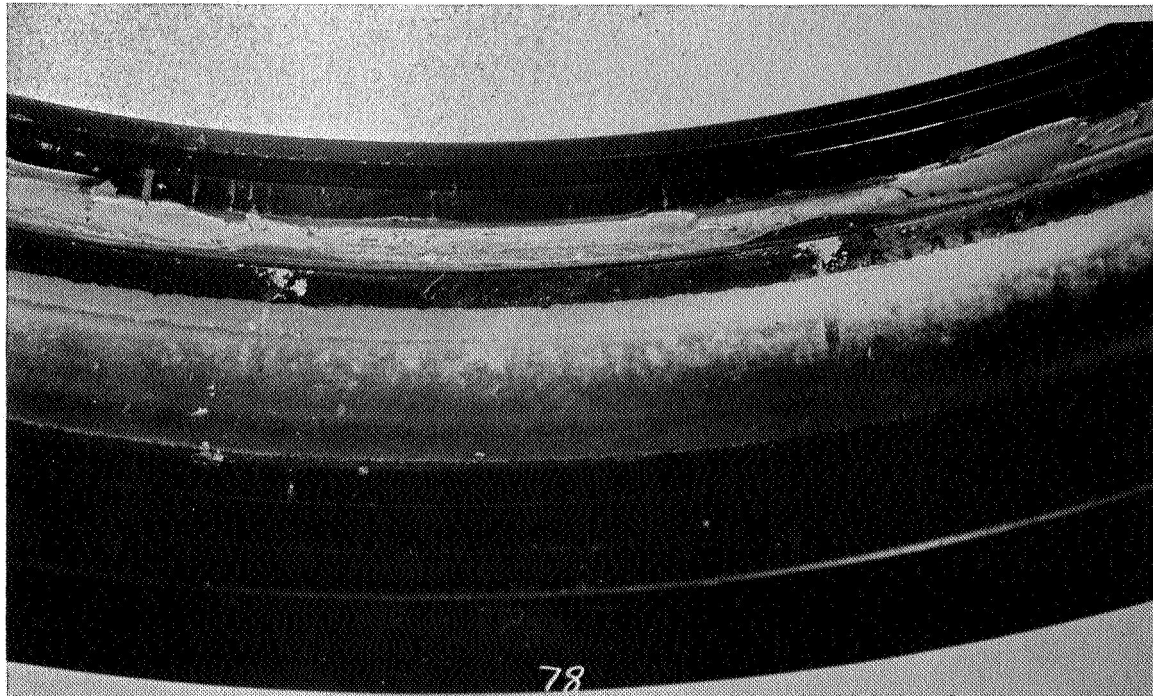


FIGURE 83. BEARING S/N 78. DAMACED OUTER RING.



FIGURE 84. BEARING S/N 73. FATIGUE FAILURE ON INNER RING.

TEST CONDITIONS:

LOAD :	5800 LBS.
SPEED:	12,000 RPM
TEMPERATURE:	600F
LUBRICANT:	PR-143
TIME TO FAILURE:	436 HOURS

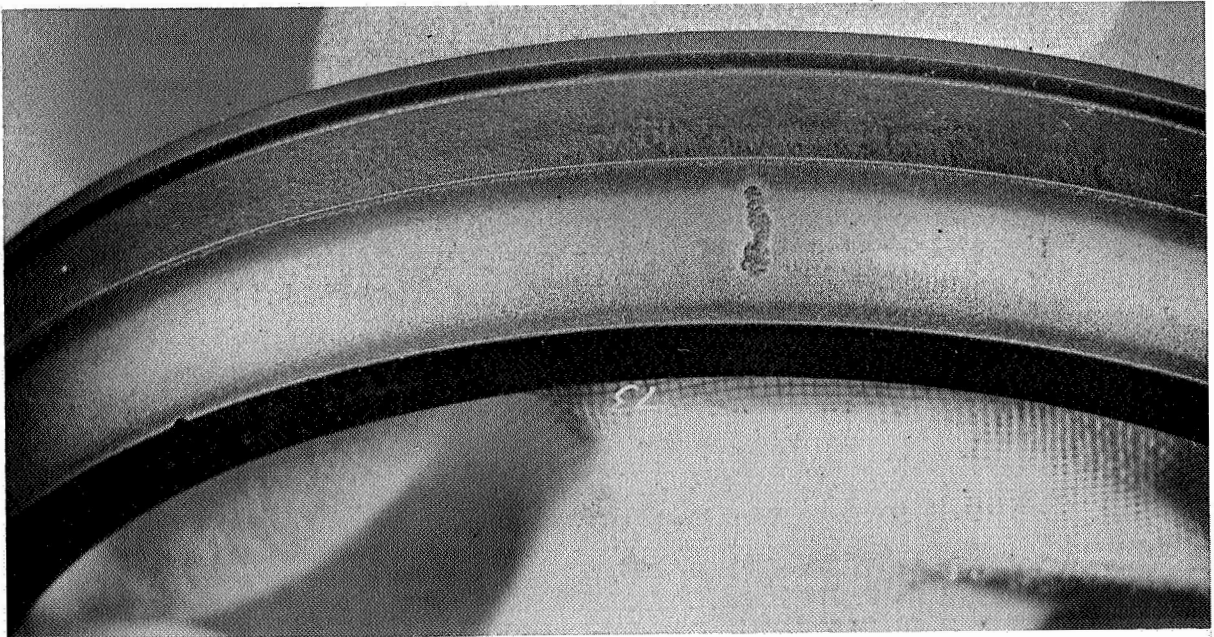


FIGURE 85. BEARING S/N 73. FATIGUE FAILURE ON OUTER RING.

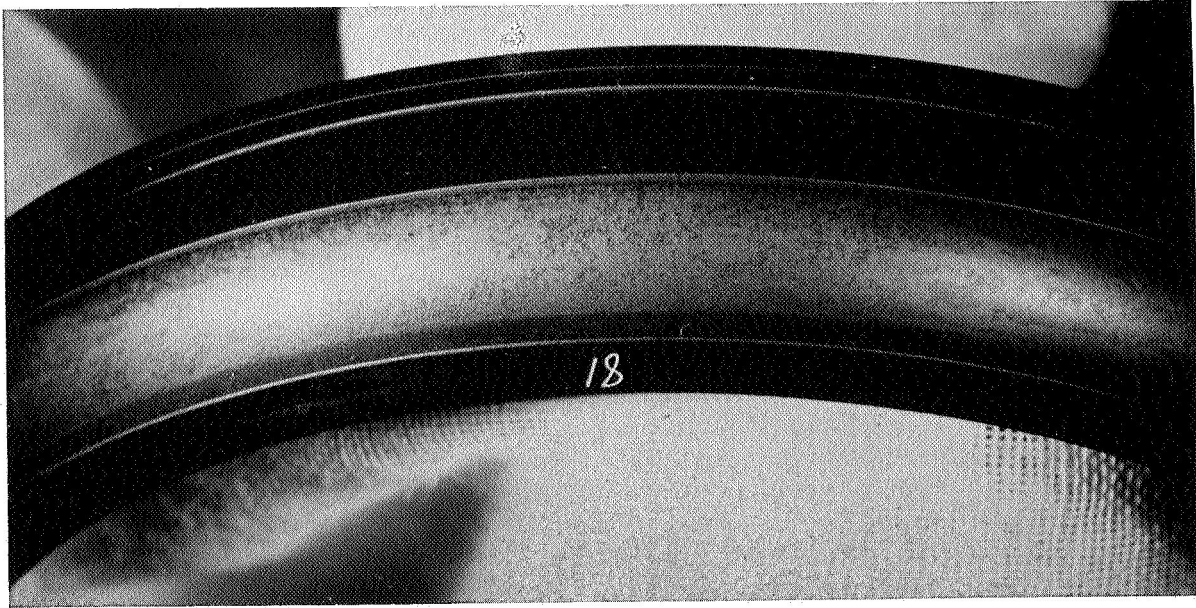


FIGURE 86. BEARING S/N 81. INNER RING.

TEST CONDITIONS:

LOAD :	5800 LB. AXIAL
SPEED:	12,000 RPM
TEMPERATURE:	600F
LUBRICANT:	PR-143
TIME TO FAILURE:	506 HOURS

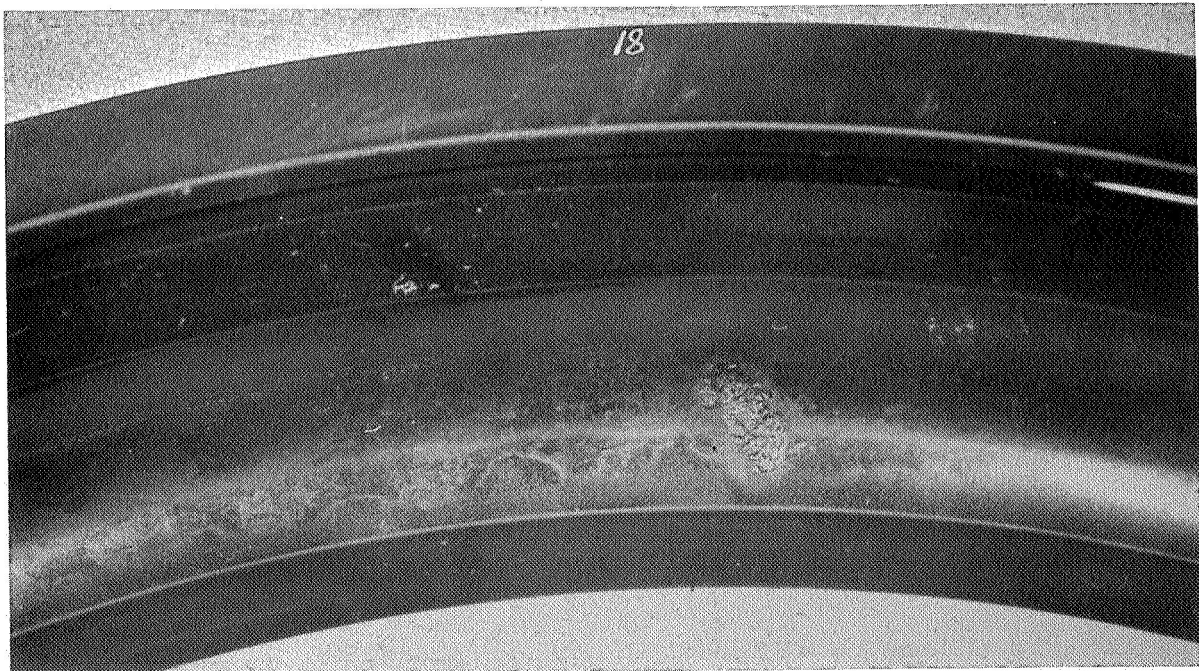
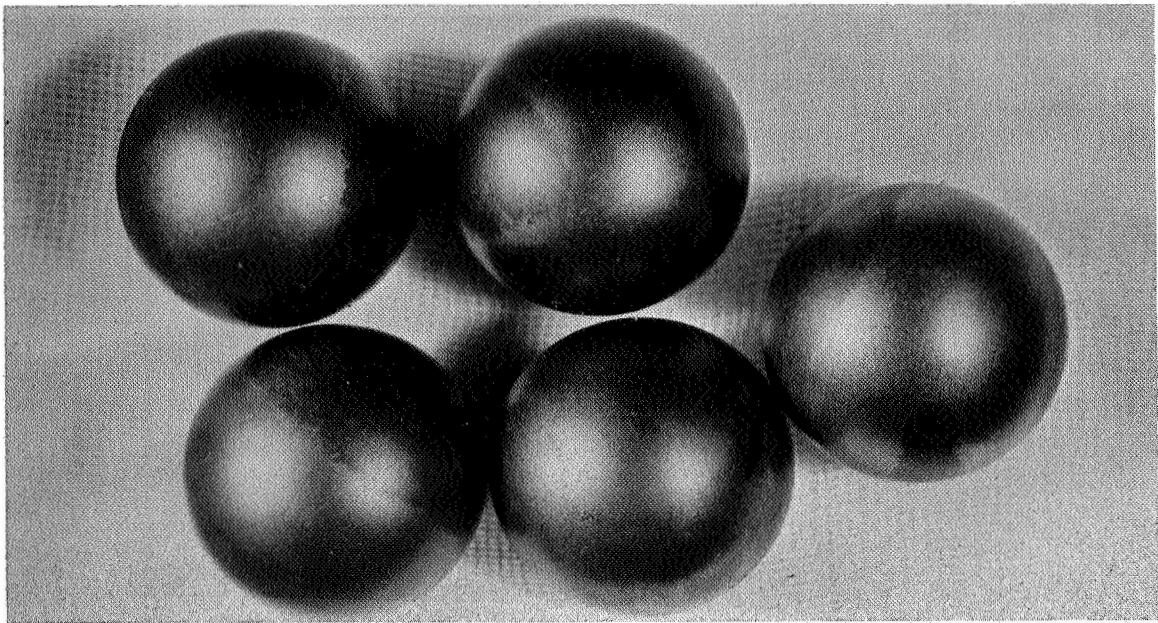
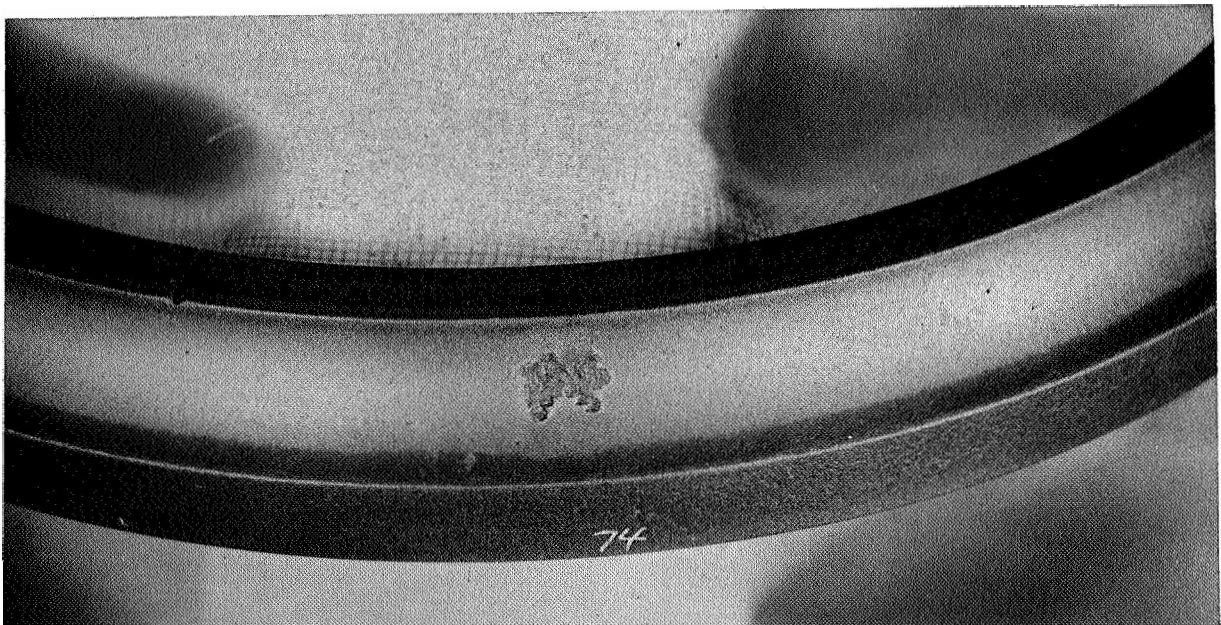


FIGURE 87. BEARING S/N 81. FATIGUE FAILURE ON OUTER RING





**FIGURE 88. BEARING S/N 81. BALLS**



**FIGURE 89. BEARING S/N 74. .FATIGUE FAILURE ON INNER RING.**

**TEST CONDITIONS:**

<b>LOAD :</b>	<b>5800 LB.</b>
<b>SPEED:</b>	<b>12,000 RPM</b>
<b>TEMPERATURE:</b>	<b>600F</b>
<b>LUBRICANT:</b>	<b>PR-143</b>
<b>TIME TO FAILURE:</b>	<b>436 HOURS</b>

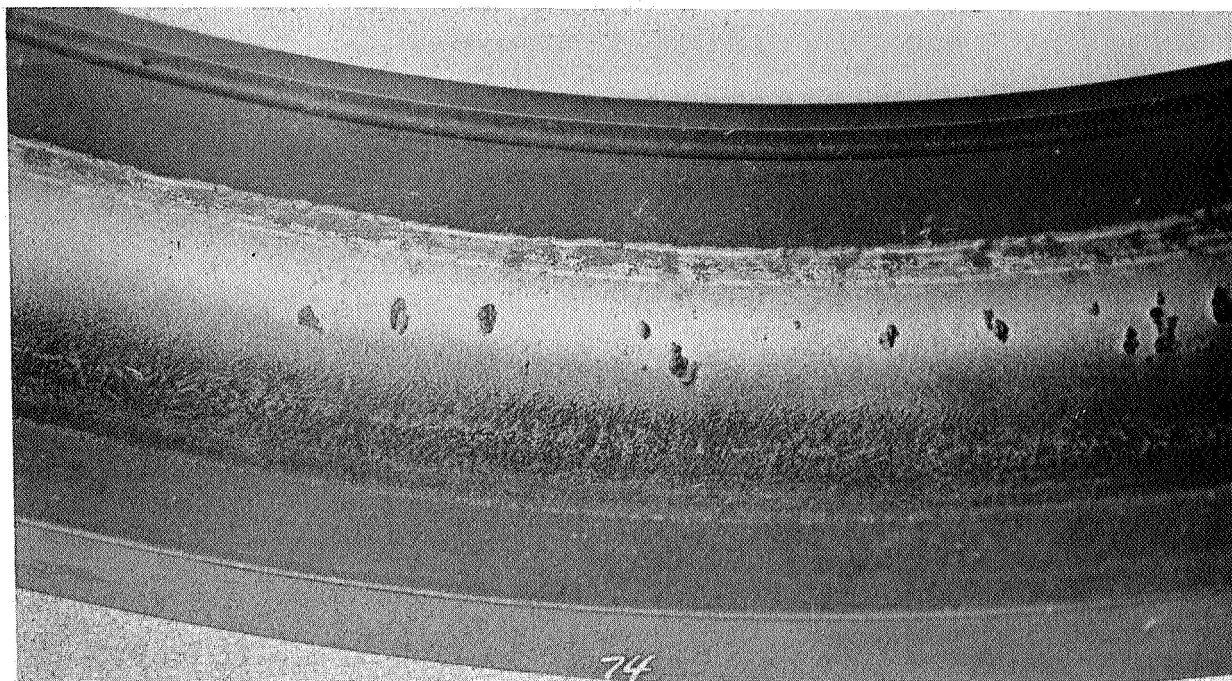


FIGURE 90. BEARING S/N 74. FATIGUE FAILURE ON OUTER RACE, NOTE EVIDENCE OF CHEMICAL CORROSION.

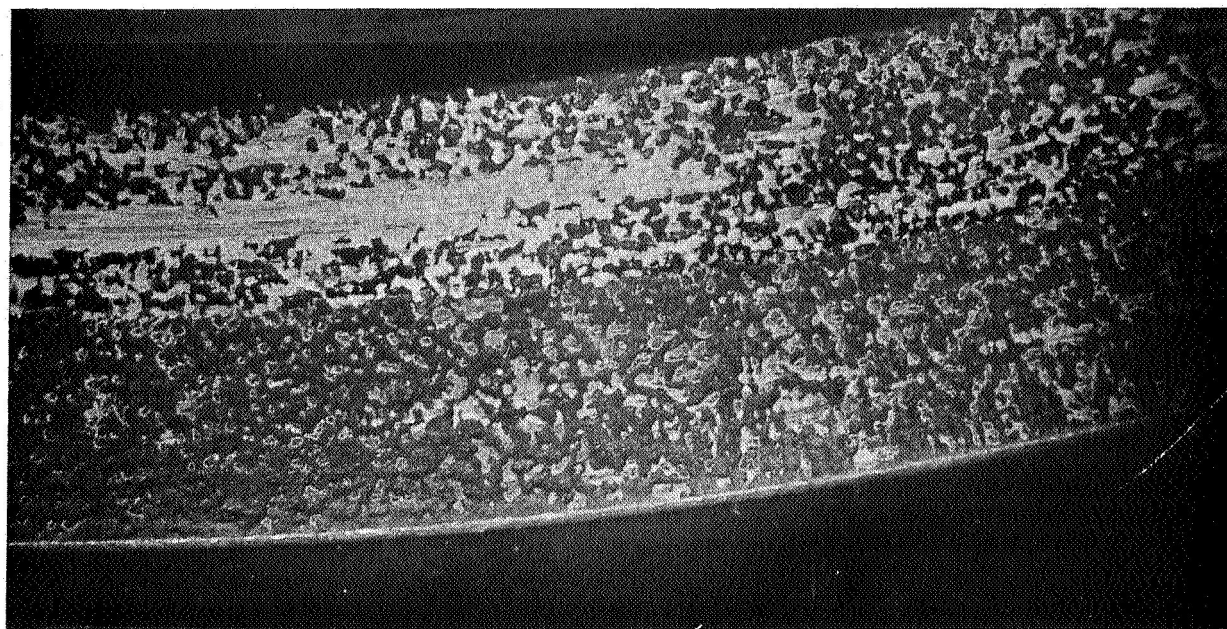


FIGURE 91. BEARING S/N 74. 10X MAGNIFICATION OF INNER RACE SHOULDER SHOWING EXTENT OF CHEMICAL CORROSION.





**FIGURE 92. BEARING S/N 93. DAMAGED INNER RING**

**TEST CONDITIONS:**

<b>LOAD:</b>	<b>4365 LB.</b>
<b>SPEED:</b>	<b>12,000 RPM</b>
<b>TEMPERATURE:</b>	<b>600F</b>
<b>LUBRICANT:</b>	<b>PR-143</b>
<b>TIME TO FAILURE:</b>	<b>159 HOURS</b>

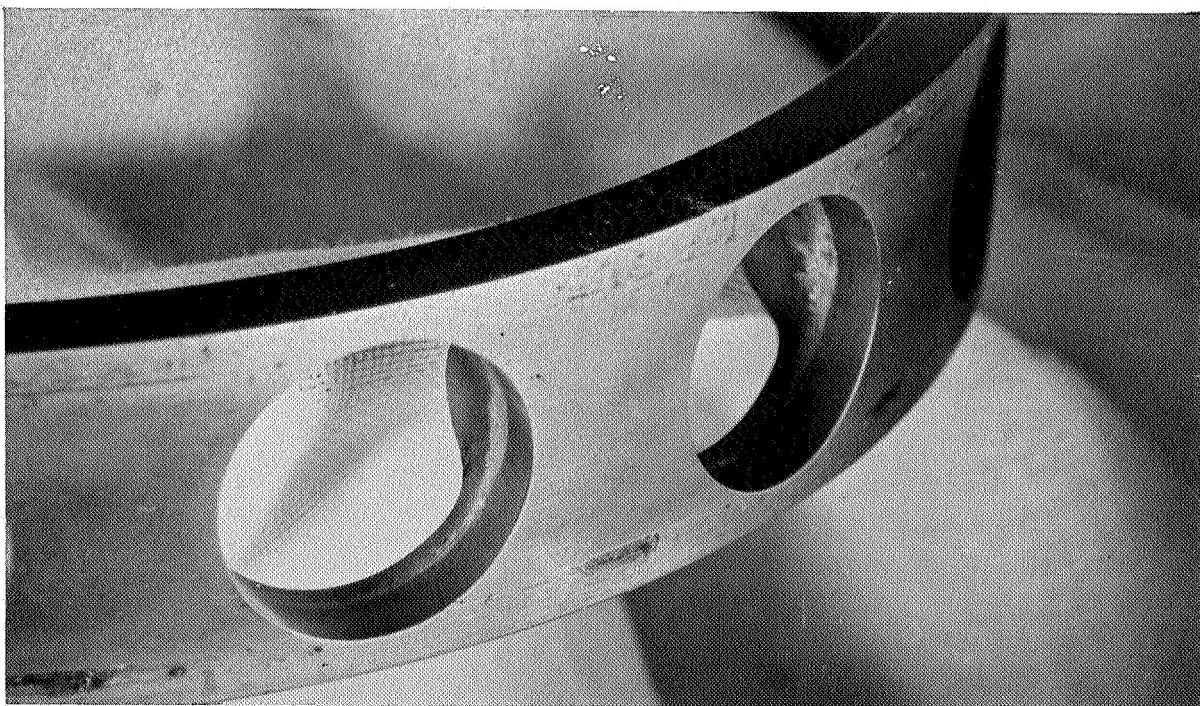


**FIGURE 93. RETAINER, BEARING S/N 93**



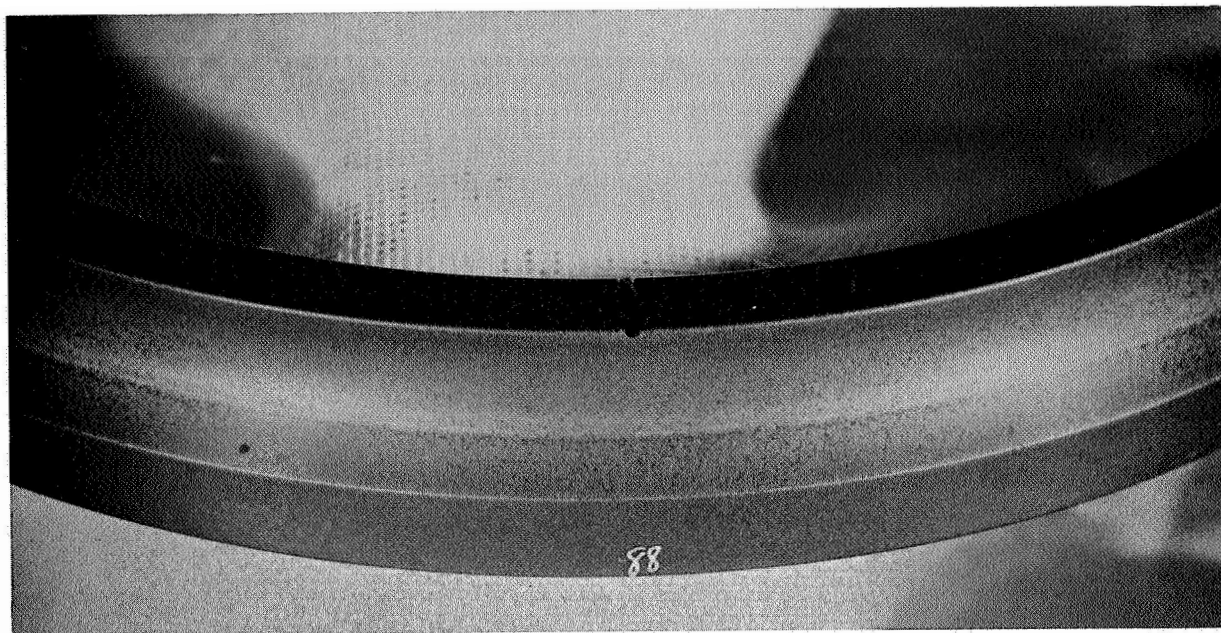


FIGURE 94. BEARING S/N 88. INNER RING.

TEST CONDITIONS:

LOAD :	4365 LB. AXIAL
SPEED:	12,000 RPM
TEMPERATURE ;	600F
LUBRICANT:	PR-143
TEST TERMINATED AT 500 HOURS.	
NO FAILURE.	

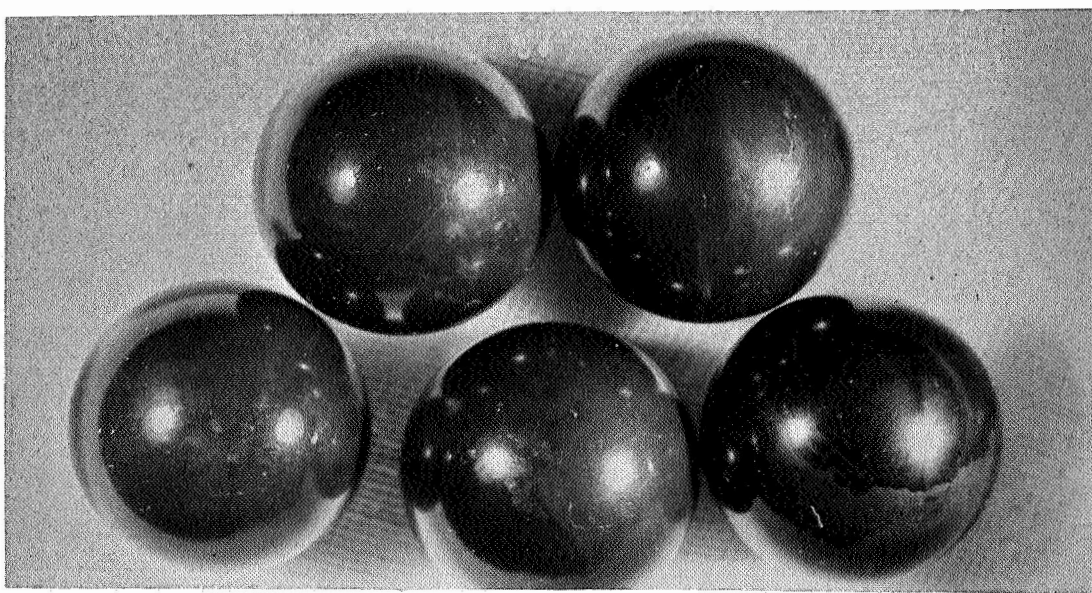
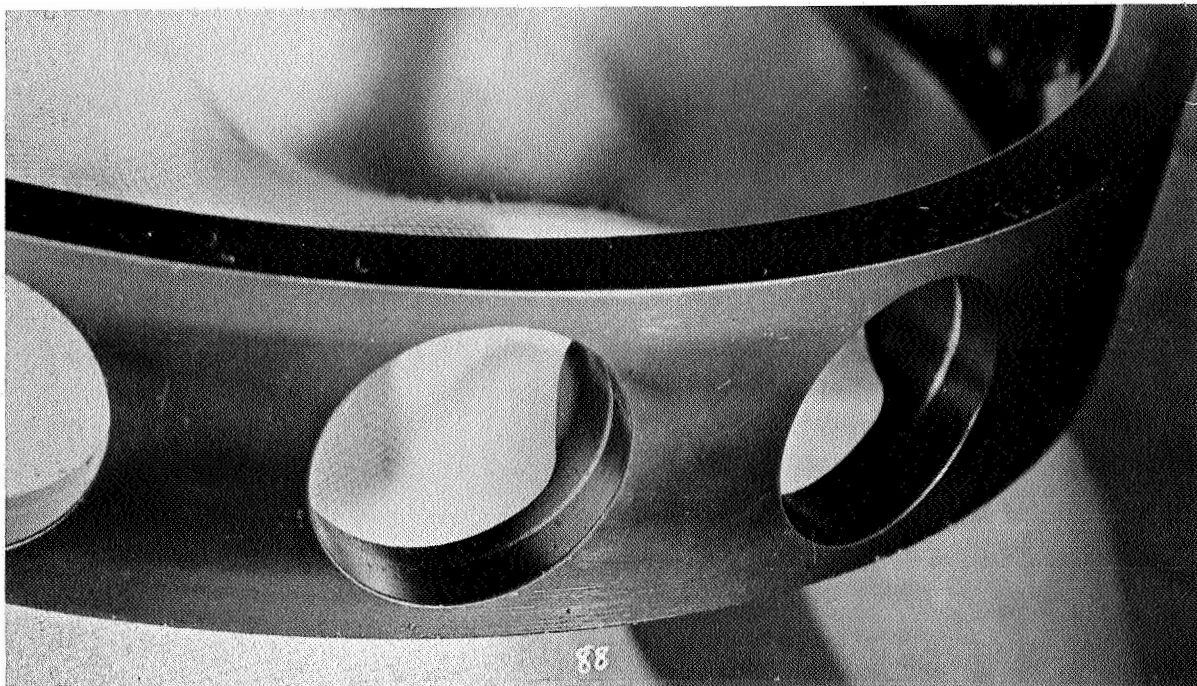
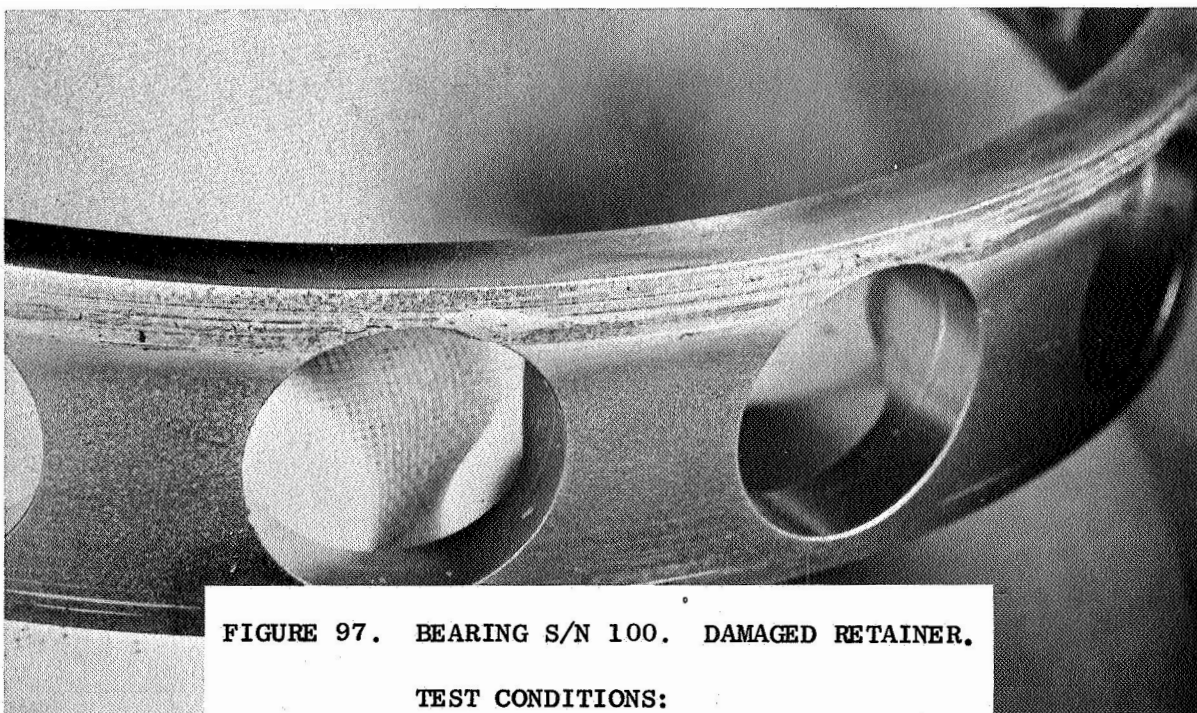


FIGURE 95. BEARING S/N 88. BALLS



**FIGURE 96. BEARING S/N 88. CONDITION OF RETAINER AFTER 500 HOURS.**



**FIGURE 97. BEARING S/N 100. DAMAGED RETAINER.**

**TEST CONDITIONS:**

<b>LOAD :</b>	<b>4365 LB.</b>
<b>SPEED:</b>	<b>12,000 RPM</b>
<b>TEMPERATURE:</b>	<b>600F</b>
<b>LUBRICANT :</b>	<b>PR-143</b>
<b>TIME TO FAILURE:</b>	<b>.01 HOURS</b>

While the expected corrosion problems did not materialize in the magnitude initially feared, there was evidence that the PR-E43 was chemically attacking the bearing material. This attack is associated with long time tests such as bearings S/N 73 and 74, where chemical attack of all of the bearing surfaces was noticeable. In the case of these two bearings, fatigue spalling, wear and chemical attack is noted. The Monel cages, however, appear to resist quite well the corrosive effects of the PR-143.

It should be pointed out, however, that the overall corrosiveness of the PR-143 at 600F was less than had been expected based on previous data. ( 3 ) The tester components which include Ni-plated steel, Monel and 300 series SS showed essentially no deterioration after exposures in excess of 1,000 hours to the fluid. This can, of course, be attributed to a large extent to the excellent inertion system of the testers which consistently maintained the O<sub>2</sub> level at less than 5 ppm.

One additional difficulty with the PR-143 was the evidence of poor cage lubrication. Bearing S/N 100 seized after one minute of operation due to cage pick-up on the outer land riding surface. This was the only instance of this event in all of the testing and while therefore unique, does perhaps tend to demonstrate the lack of boundary lubrication of the PR-143.

The last bearing tested (S/N 99) is perhaps typical of the type of operation which can be expected with the DuPont Fluid. This bearing showed evidence of chemical attack, ball wear and fatigue. Ball wear was on the order of .0015" and an etching effect was plainly visible in the running track,

#### 6.2.4 Test Series IV

The conditions for this test series were:

Bearing Material:	Rings:	WB-49
	Balls:	M-1
	Cages:	M-1
Lubricant :	Mobil XRM-177F	
Operating Conditions:		
	Temp :	Outer Ring 585F $\pm$ 5F Inner Ring 600F - 610F Oil In - 545F-565F Oil Out - 585F-600F
	Speed:	12,000 rpm
	Load :	5800 lbs. axial
	Atmosphere:	N <sub>2</sub> <5 ppm O <sub>2</sub>

Results of the bearing tests are presented in Table 15 and graphically illustrated in Weibull distribution in Figure 98.

A trend of low fatigue life was established with this material early in the test program. The reason for this appears to be related to the micro-structure of the material as will be discussed later.

The failures encountered were with one exception, normal sub-surface initiated fatigue failures. Figures 99 through 108 are photographs of typical WB-49 bearing components failed in fatigue. The only deviation from these failures was in bearing S/N 272, where a circumferential outer ring fracture was observed. Generally, the balls made out of M-1 material appear to be relatively undamaged despite the rather severe fatigue failures observed on other components. This is illustrated in the bottom of Figure 99. While there have been a number of ball fatigue failures, it is difficult to establish whether these failures are unique **or** are caused by a prior failure of the inner **or** outer ring. As may be noted in Table 15 the ball

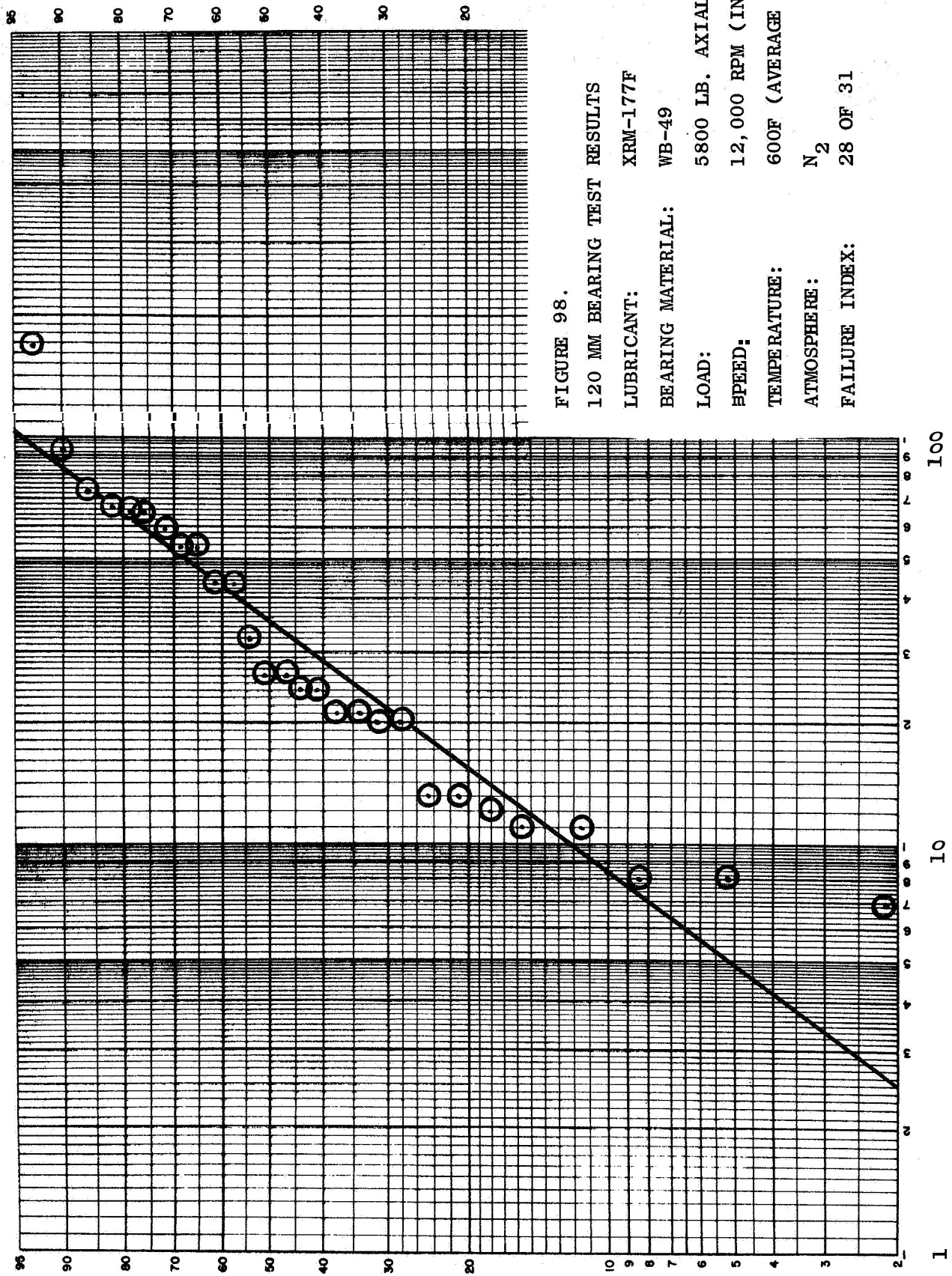


FIGURE 98.

120 MM BEARING TEST RESULTS

LUBRICANT: XRM-177F

BEARING MATERIAL: WB-49

LOAD: 5800 LB. AXIAL

SPEED: 12,000 RPM (INNER)

TEMPERATURE: 600F (AVERAGE METAL)

ATMOSPHERE: N<sub>2</sub>

FAILURE INDEX: 28 OF 31



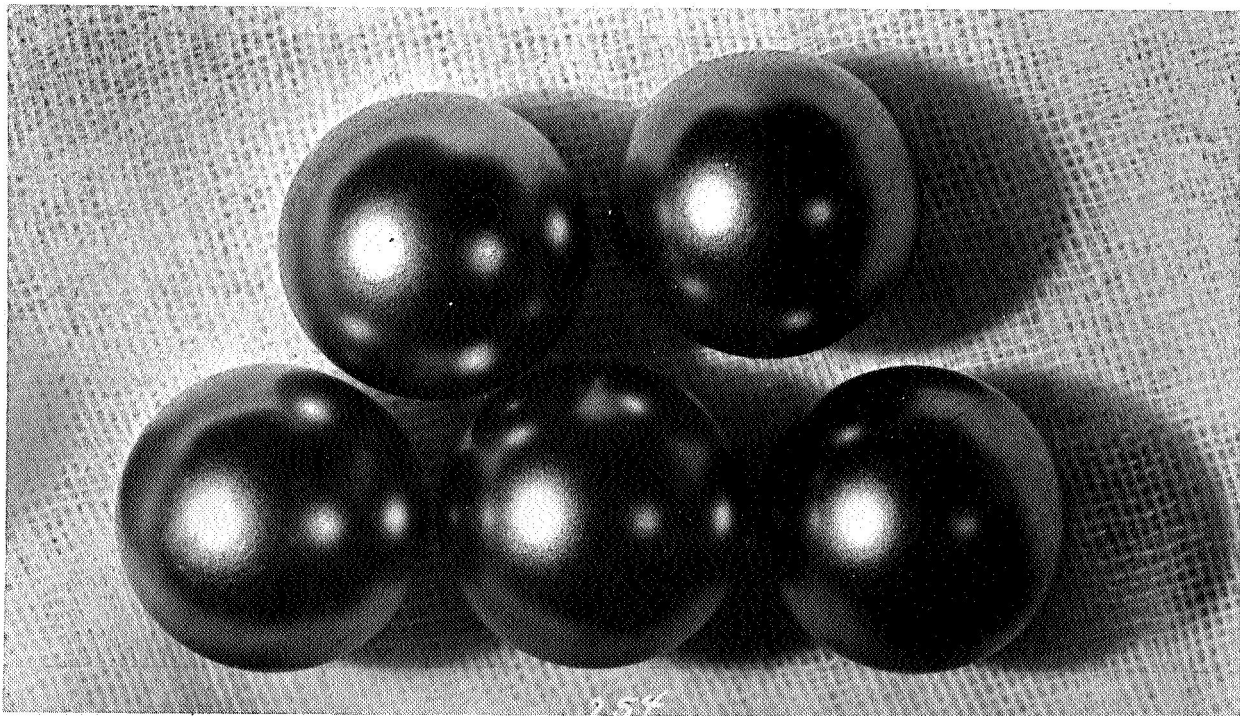


FIGURE 99. TOP: INNER RING FATIGUE FAILURE, S/N 254  
 BOTTOM: BALLS FROM S/N 254

BEARING MATERIAL:	WB-49 RINGS
	M-1 BALLS
LUBRICANT:	XRM-177F
LOAD:	5800 LB. AXIAL
<b>SPEED:</b>	12,000 RPM
TEMPERATURE:	600F (METAL)
TIME TO FAILURE:	26 HOURS



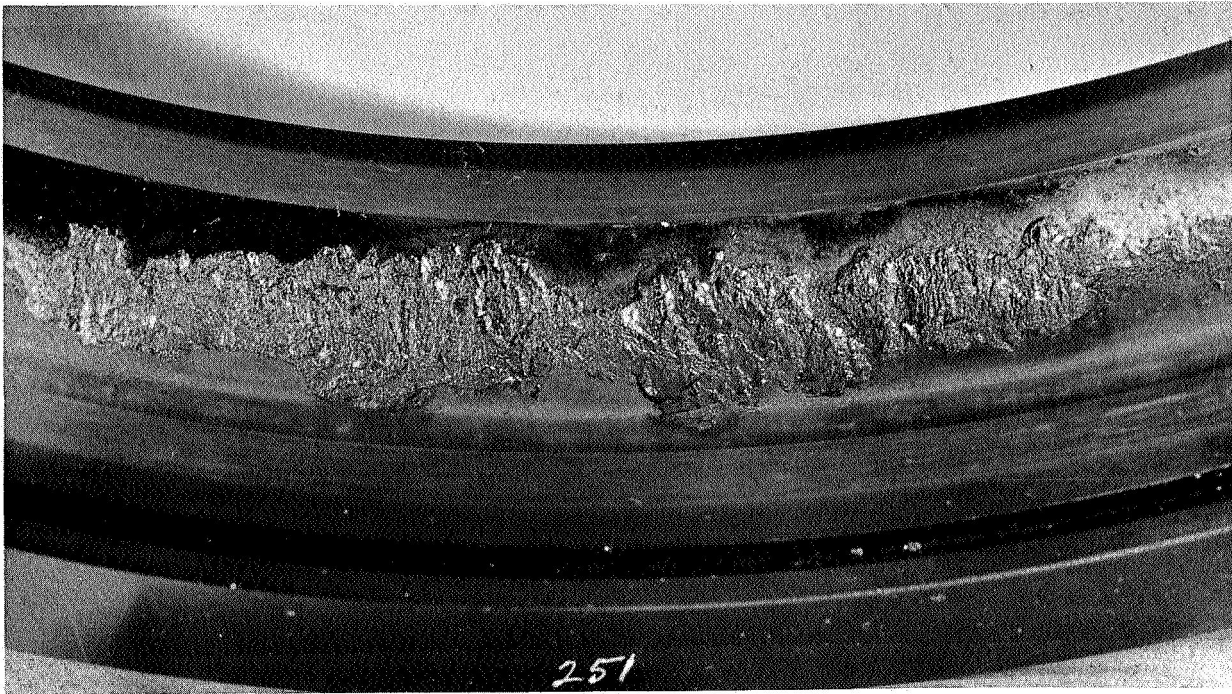


FIGURE: 100. OUTER RING FAILURE, S/N 251

BEARING MATERIAL:	WB-49 RINGS
	M-1 BALLS
LUBRICANT:	XRM-177F
LOAD :	5800 LB. AXIAL
SPEED:	12,000 RPM
TEMPERATURE::	600F (METAL)
TIME TO FAILURE:	8 HOURS



FIGURE 101. INNER RING FATIGUE FAILURE, S/N 256

BEARING MATERIAL:	WB-49 RINGS
	M-1 BALLS
LUBRICANT:	<b>XRM-177F</b>
LOAD :	5800 LB. AXIAL
SPEED:	<b>12,000 RPM</b>
TEMPERATURE:	600F (METAL)
TIME TO FAILURE:	26 HOURS

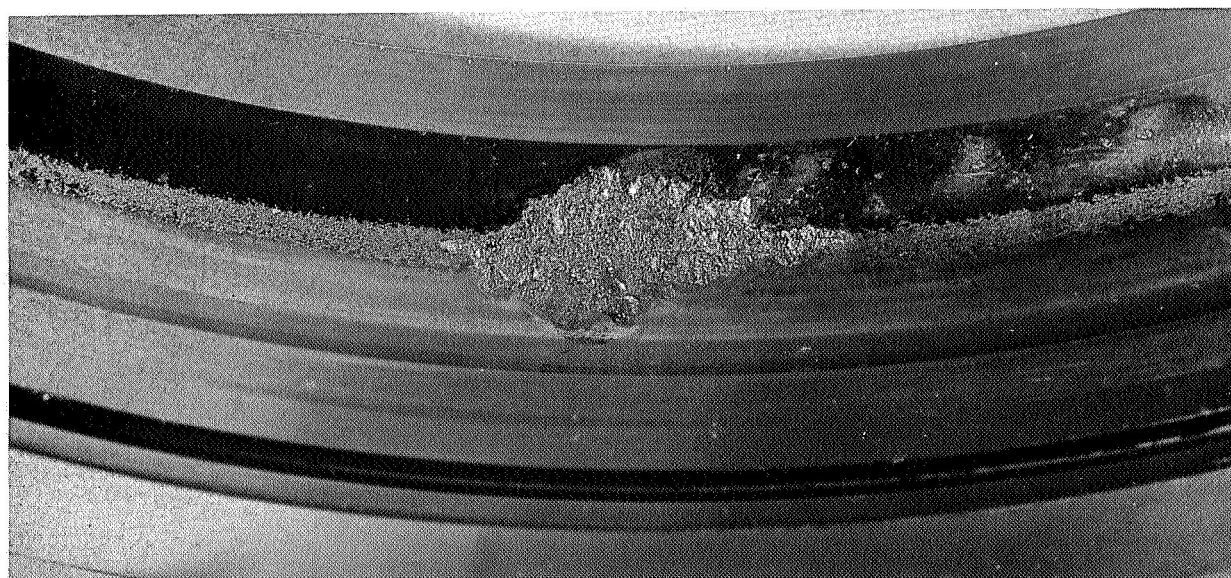


FIGURE 102. INNER AND OUTER RING FATIGUE FAILURES, S/N 257

BEARING MATERIAL:	WB-49 RINGS M-1 BALLS
LUBRICANT:	XRM-177F
LOAD:	5800 LB. AXIAL
SPEED:	12,000 RPM
TEMPERATURE:	600F (METAL)
TIME TO FAILURE:	24 HOURS

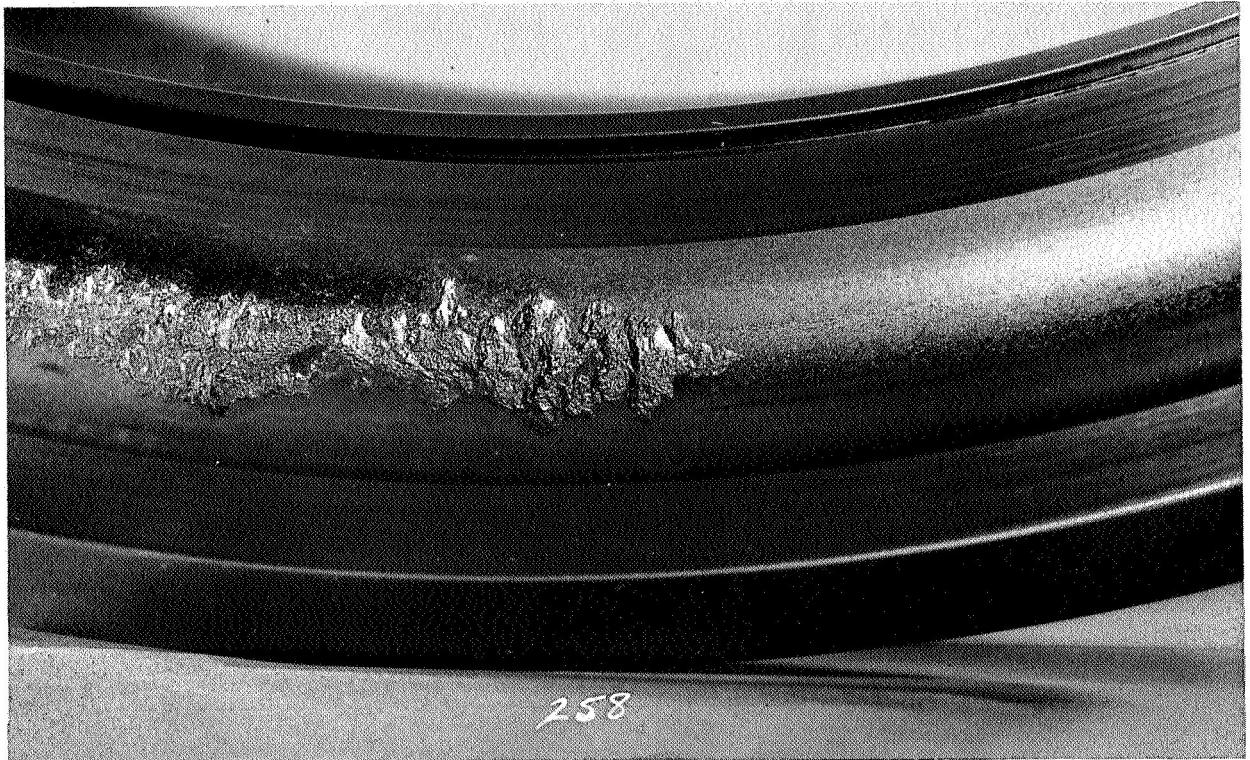


FIGURE 103. OUTER RING FATIGUE FAILURE, S/N 258

BEARING MATERIAL:	WB-49
	M-1 BALLS
LUBRICANT:	XRM-177F
LOAD :	5800 LB. AXIAL
<b>SPEED:</b>	12,000 RPM
TEMPERATURE :	600F (METAL)
TIME TO FAILURE:	24 HOURS



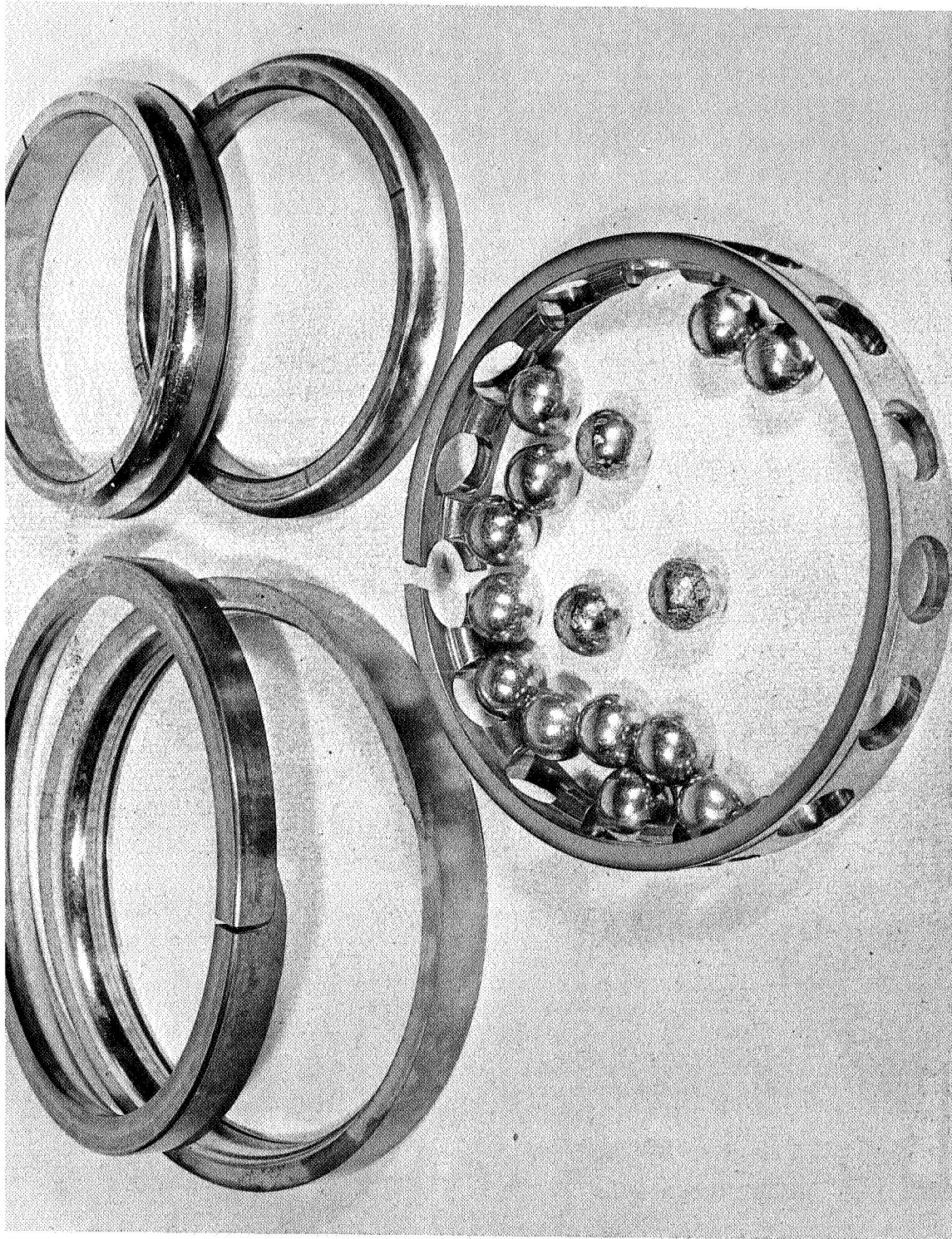


FIGURE 104. BEARING CON 272

MATERIAL:	WB-49 RINGS
	M-1 BALLS
LUBRICANT:	XRM-177F (N <sub>2</sub> ATMOSPHERE)
TEMPERATURE:	600F
LOAD:	5800 LB. AXIAL
SPEED:	12,000 RPM
TIME TO FAILURE:	13 HOURS



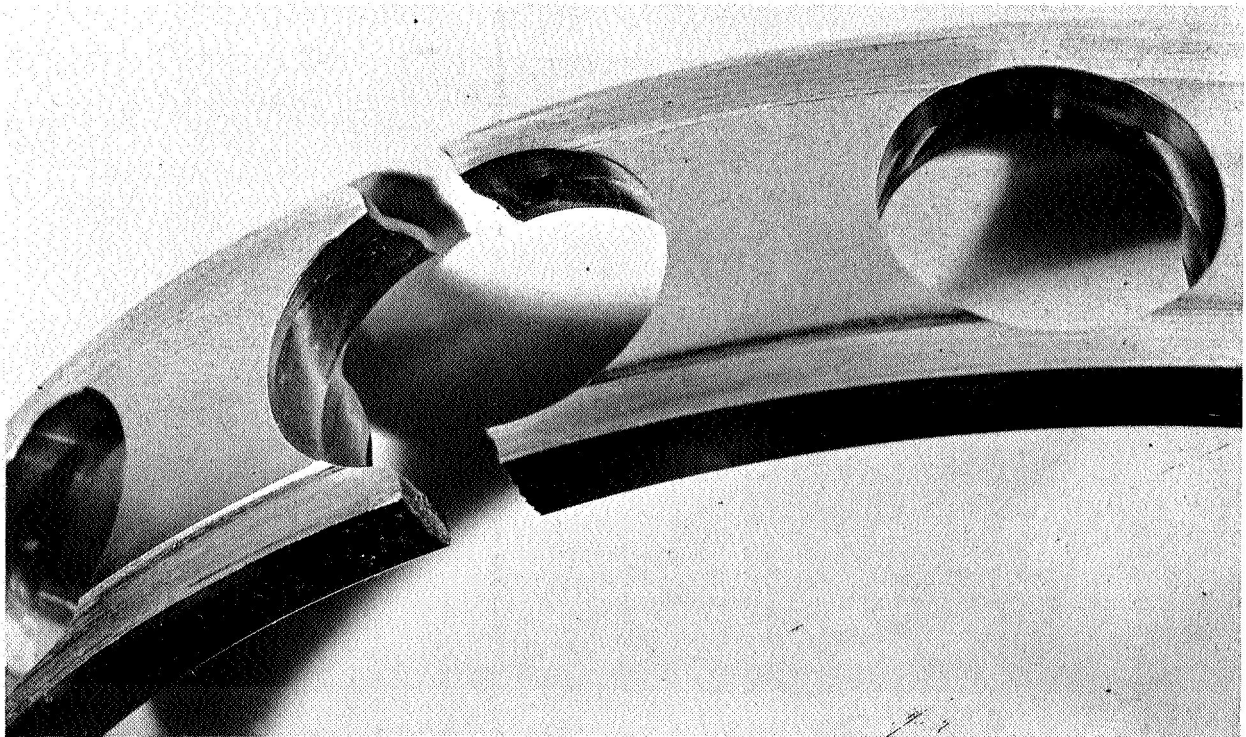
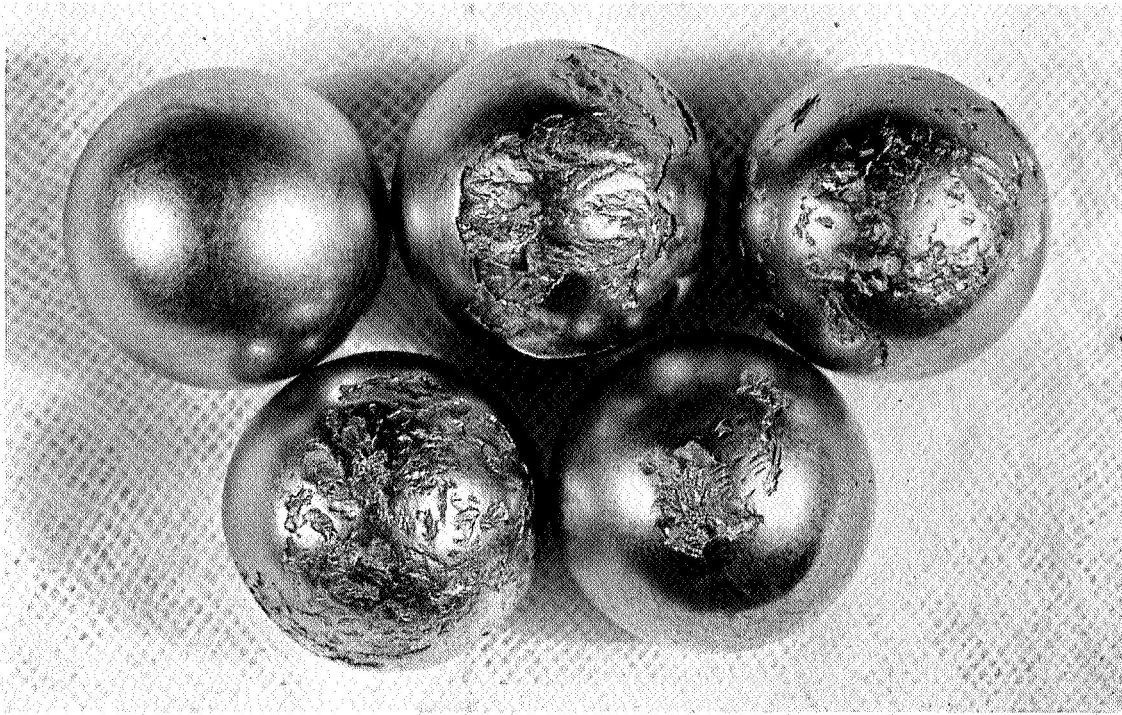


FIGURE 105. BEARING S/N 272.

BALL FATIGUE AND CAGE FRACTURE AFTER 13 HOURS.  
NOTE EXTENSIVE DEFORMATION IN CAGE BALL POCKET.

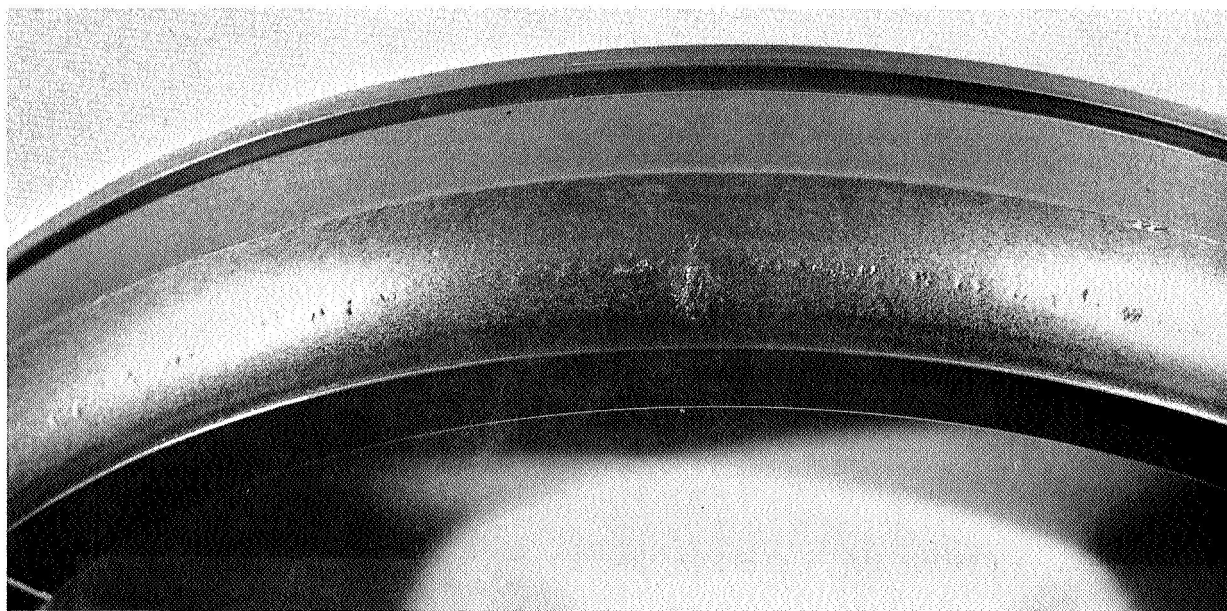
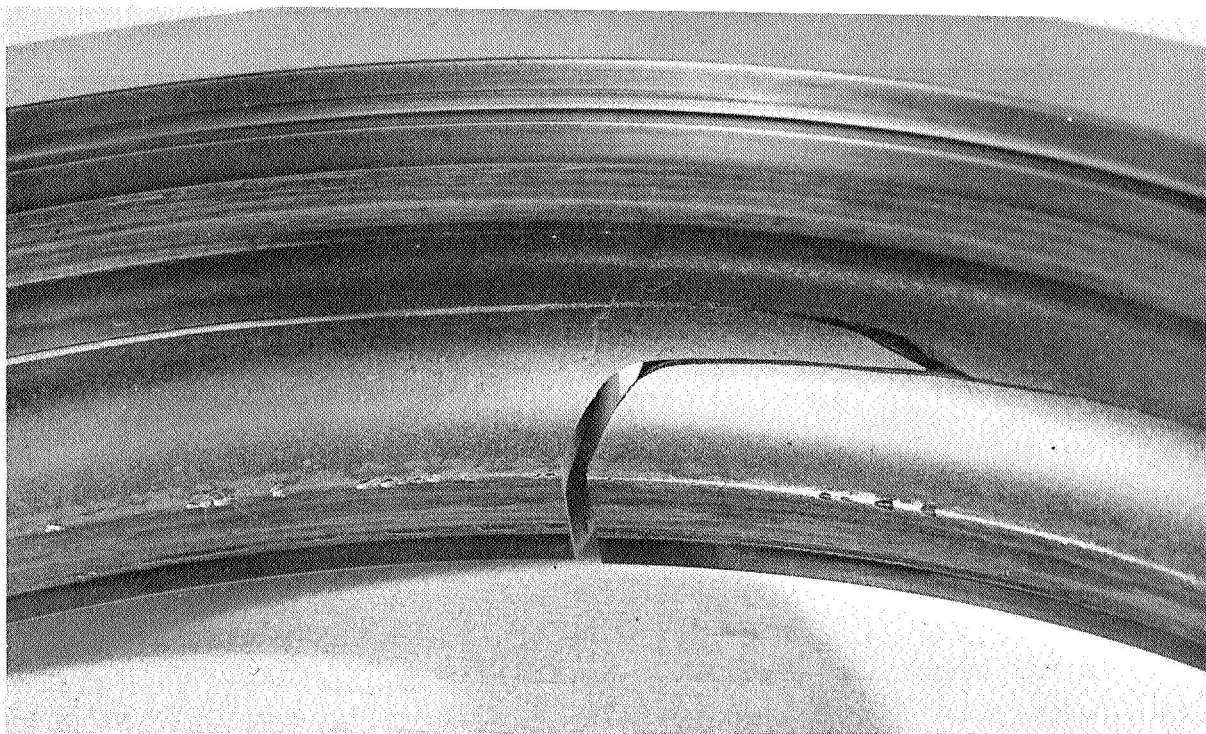


FIGURE 106. BEARING S/N 272.

CLOSE-UP OF FRACTURE ON OUTER RING AND  
FATIGUE FAILURES ON INNER RING.





FIGURE 107. BEARING S/N 272.

CLOSE-UP OF CIRCUMFERENTIAL OUTER  
RING FRACTURE AFTER 13 HOURS.

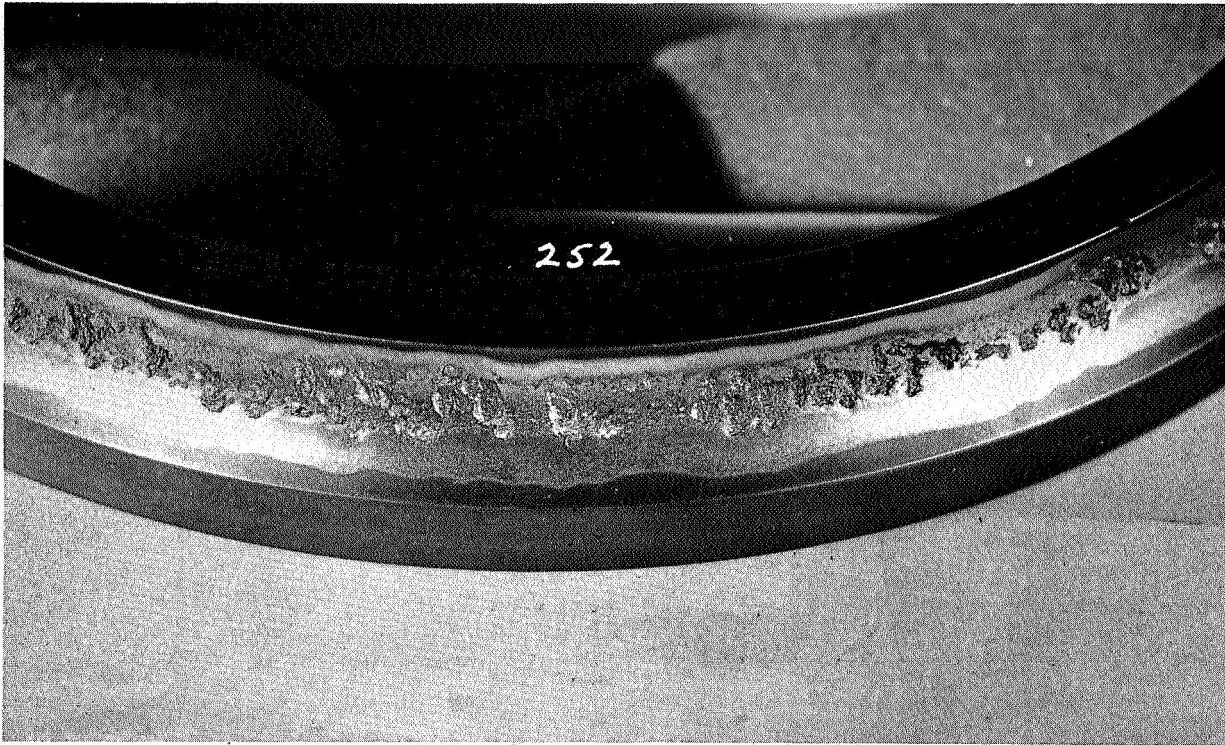


FIGURE 108. . INNER RING FATIGUE FAILURE, S/N 252

BEARING MATERIAL:	WB-49 RINGS
	M-1 BALLS
LUBRICANT:	XRM-177F
LOAD:	5800 LB. AXIAL
SPEED:	12,000 RPM
TEMPERATURE:	600F (METAL)
TIME TO FAILURE:	8 HOURS

failures have always occurred in conjunction with another component failure or in a bearing having received excessive foreign object damage,

Of particular interest in this test series were the M-1 steel cages which were used instead of the S-Monel in order to evaluate their behavior at 600F. While most of the cages performed satisfactorily, it was found that eight of the cages fractured similar to the one shown in Figure 105. This is a far greater incidence of cage fractures than had been observed in the previous test where S-Monel was used as the structural material for these parts. It was also observed that the M-1 cages had a greater amount of ball pocket wear than had been observed on the S-Monel cages, The data would tend to indicate that at least for the higher temperature applications, S-Monel may be superior to M-1 steel for use as a cage material .

The overall low fatigue life exhibited by the WB-49 bearings had been predicted by RC rig testing.



### 6.2.5 Test Series V

The following conditions were observed in this test series:

Bearing Material:	Rings:	CVM M-50
	Balls:	CVM M-50
	Retainer:	S-Mone 1
Lubricant :	Mobil XRM-177F	
Operating Conditions:		
	Temp:	Outer Ring 490F - 500F Inner Ring 505F - 515F Oil In - ~482F Oil Out - ~518F
	Speed:	12,000 rpm
	Load:	5800 lbs. axial
	Atmosphere:	N <sub>2</sub> <5 ppm O <sub>2</sub>

Test results are presented in Table 16 and a Weibull plot of the data is shown in Figure 109.

The Weibull plot is based on a failure index of 11 out of 26. Several of the extremely short time failures have been eliminated in the analysis as there was sufficient evidence in each case of foreign object damage. The foreign object damage and the small amount of ball wear which was observed were traced to debris from pump damage due to the PR-143,

In this test series, the cut-off point was raised to 750 hours rather than the 500-hour limit observed in the previous tests, as it was reasoned that the increased viscosity at the lower testing temperature would provide a better elastohydrodynamic lubrication.

Table 16

Results of 120 mm Bearing Tests with XRM-177F Lubricant, CVM M-50 Bearings, at 500F in N<sub>2</sub>

Test No.	Bearing S/N	Load (lb.)	Time (Hr.)	Inner Ring	Outer Ring	Ball
V - 1	107	5800 (1)	48	OK	OK	OK ( 0005" Wear )
V - 1a	108	5800	48	OK	OK	OK ( 0005" Wear )
V - 2	105	5800	256	OK	OK	OK ( 0002" Wear )
V - 2a	106	5800	<u>256</u>	Fatigue	OK	OK ( 0002" Wear )
V - 3	109	5800	226	OK	OK	OK ( 0004" Wear )
V - 3a	110	5800	226	OK	OK	OK ( 0004" Wear )
V - 4	119	5800	20	OK	OK	OK
V - 4a	120	5800	<u>20</u>	OK (FOD)	OK	Fatigue
V - 5	103	5800	536	OK	OK	OK
V - 5a	104	5800	536	OK	OK	OK
V - 6	111	5800	573	OK	OK	OK
V - 6a	112	5800	<u>573</u>	OK	OK	OK
V - 7	121	5800	373	OK	OK	OK
V - 7a	122	5800	373	Cage Break	OK	Seized
V - 8	115	5800	508	OK	OK	OK
V - 8a	116	5800	<u>508</u>	Fatigue	OK	Fatigue
V - 9	127	5800	<u>8</u>	Fatigue (FOD)	OK	OK
V - 9a	128	5800	8	OK	OK	OK
V - 10	103	5800	558	OK	OK	OK ( 0005" Wear )
V - 10a	104	5800	558	OK	OK	OK ( 0005" Wear )
V - 11	117	5800	661	OK	OK	OK ( 0005" Wear )
V - 11a	118	5800	<u>661</u>	Fatigue	OK	OK

Test No.	Bearing S/N	Load (lb.)	Time (Hr.)	Inner Ring	Outer Ring	Ball
V -12	113	5800	758	OK	OK	Fatigue
V -12a	114	5800	758	OK	OK	Fatigue
V -13	115	5800	529	Fatigue	OK	Multiple Fatigue
V -13a	128	5800	9	OK	OK	OK
V -14	117	5800	663	OK	OK	OK
V -14a	128	5800	12	Fatigue (FOD)	OK	Multiple Fatigue
V -15	121	5800	677	OK	Multiple Fatigue	Multiple Fatigue
V -15a	111	5800	877	Fatigue	OK	OK
V -16	123	5800	751	OK	OK	OK (.0002" Wear)
V -16a	124	5800	751	OK	Fatigue	OK (.0003' Wear)
V -17	125	5800	729	OK	OK	Fatigue
V -17a	126	5800	729		Plugged Jet	

(1) 5800 lb. axial load = 321,000 psi max. hertz on inner.

□ Indicates Time to Fatigue Failure

FOD = Foreign Object Damage

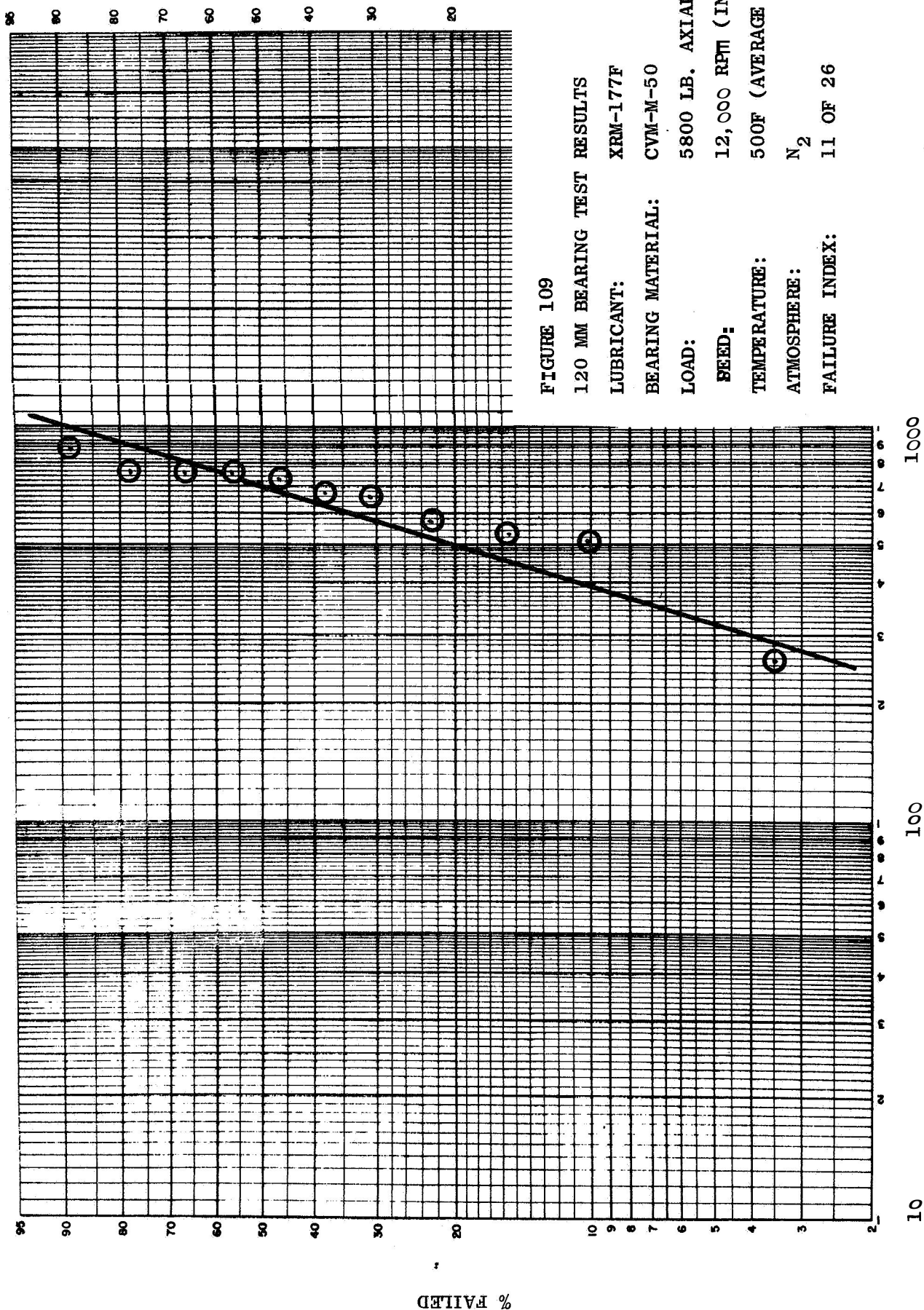


FIGURE 109

120 MM BEARING TEST RESULTS

LUBRICANT: XRM-177F

BEARING MATERIAL: CVM-M-50

LOAD: 5800 LB. AXIAL

SEED: 12,000 RPM (INNER)

TEMPERATURE: 500F (AVERAGE METAL)

ATMOSPHERE: N<sub>2</sub>

FAILURE INDEX: 11 OF 26

% FAILED

LIFE - HOURS

#### 6.2.6 Test Series VI

Test conditions for this series were as follows:

Bearing Material:	Rings:	CVM-M-50
	Balls :	CVM-M-50
	Retainer:	S-Mone 1
Lubricant,:	Mobil XRM-177F	
Operating Conditions:		
	Temp:	Outer Ring 395F - 410F Inner Ring 405F - 415F Oil In - 370F Oil Out - 400F
	Speed:	12,000 rpm
	Load:	5800 lb. axial
	Atmosphere:	N <sub>2</sub> 5 ppm O <sub>2</sub>

The results of the tests are presented in Table 17 and shown in Weibull distribution in Figure 110. Three tests (#2, 2a, 6) were eliminated from the analysis. The first two because the test was aborted due to a plugged lube jet and the third one because the bearing had superficial foreign object damage because of the plugged jet,

The photographs in Figures 111 through 113 illustrate the typical condition of the M-50 bearings after prolonged operation at 400F in nitrogen inerted XRM-177F. As can be seen from the photographs, the bearing components are in excellent condition. Of particular interest is the fact that several of the bearings in this test series including the one shown in the referenced photographs had been given a black oxide coating (Dulitizing) in order to more sharply define the ball track and thus the operating contact angle. The oxide coating apparently had no effect on the bearing life, although it did serve to accurately delineate the ball path as is illustrated in Figure 113,

Again, as in Test Series V, cut-off was at 750 hours rather than 500 hours.



Table 17

Results of 120 mm Bearing Tests with XRM-177F Lubricant, CVM M-50 Bearings, at 400F in N<sub>2</sub>

Test No.	Bearing S/N	Load (lb.)	Time (Hr.)	Inner Ring	Outer Ring	Ball
VI - 1	131	5800	<u>278</u>	Fatigue		Fatigue
VI - 1a	132	5800	278	OK	OK	OK
VI - 2	145	5800	.1	OK	OK	OK
VI - 2a	146	5800	.1	Plugged Jet	Pickup	
VI - 3	133	5800	<u>163</u>	Fatigue	OK	Fatigue
VI - 3a	134	5800	163	OK	OK	OK
VI - 4	129	5800	755	OK	OK	OK
VI - 4a	130	5800	755	OK	OK	OK
VI - 5	149	5800	31	OK	OK	OK
VI - 5a	134	5800	<u>194</u>	Fatigue	POD	Fatigue
VI - 6	145	5800	<u>1</u>	Fatigue	POD	Fatigue
VI - 6a	132	5800	280	OK	OK (.0003" Wear)	
VI - 7	135	5800	778	OK	OK	OK
VI - 7a	136	5800	778	OK	OK	OK
VI - 8	137	5800	752	OK	OK	OK
VI - 8a	138	5800	752	OK	OK	OK
VI - 9	141	5800	<u>683</u>	Fatigue	OK	OK
VI - 9a	142	5800	683	POD	OK	OK
VI - 10	139	5800	768	OK	OK	OK
VI - 10a	140	5800	768	OK	OK	OK
VI - 11	147	5800	<u>775</u>	OK	atig	OK
VI - 11a	148	5800	775	OK	OK	OK

Table 17, Contd.

Test No.	Bearing S/N	Load (lb.)	Time (Hr.)	Inner Ring	Outer Ring	Ball
VI -12	143	580 <sub>0</sub>	<u>788</u>	Fatigue	OK	OK
VI -12a	144	580 <sub>0</sub>	788	OK	OK	OK
VI -13	132	580 <sub>0</sub>	<u>828</u>	OK	Fatigue	OK (.0003" Wear)
VI -13a	149	580 <sub>0</sub>	<u>744</u>	FOD	OK	Fatigue
VI -14	170	580 <sub>0</sub>	<u>554</u>	Fatigue	FOD	Fatigue
VI -14a	171	580 <sub>0</sub>	<u>554</u>	OK	Fatigue	OK
VI -15	172	580 <sub>0</sub>	767	OK	OK	OK
VI -15a	173	580 <sub>0</sub>	767	OK	OK	OK

(1) 5800 lb. axial load = 321,000 psi max. hertz on inner

(2) FOD = Foreign Object Damage

       Indicates Time to Fatigue Failure

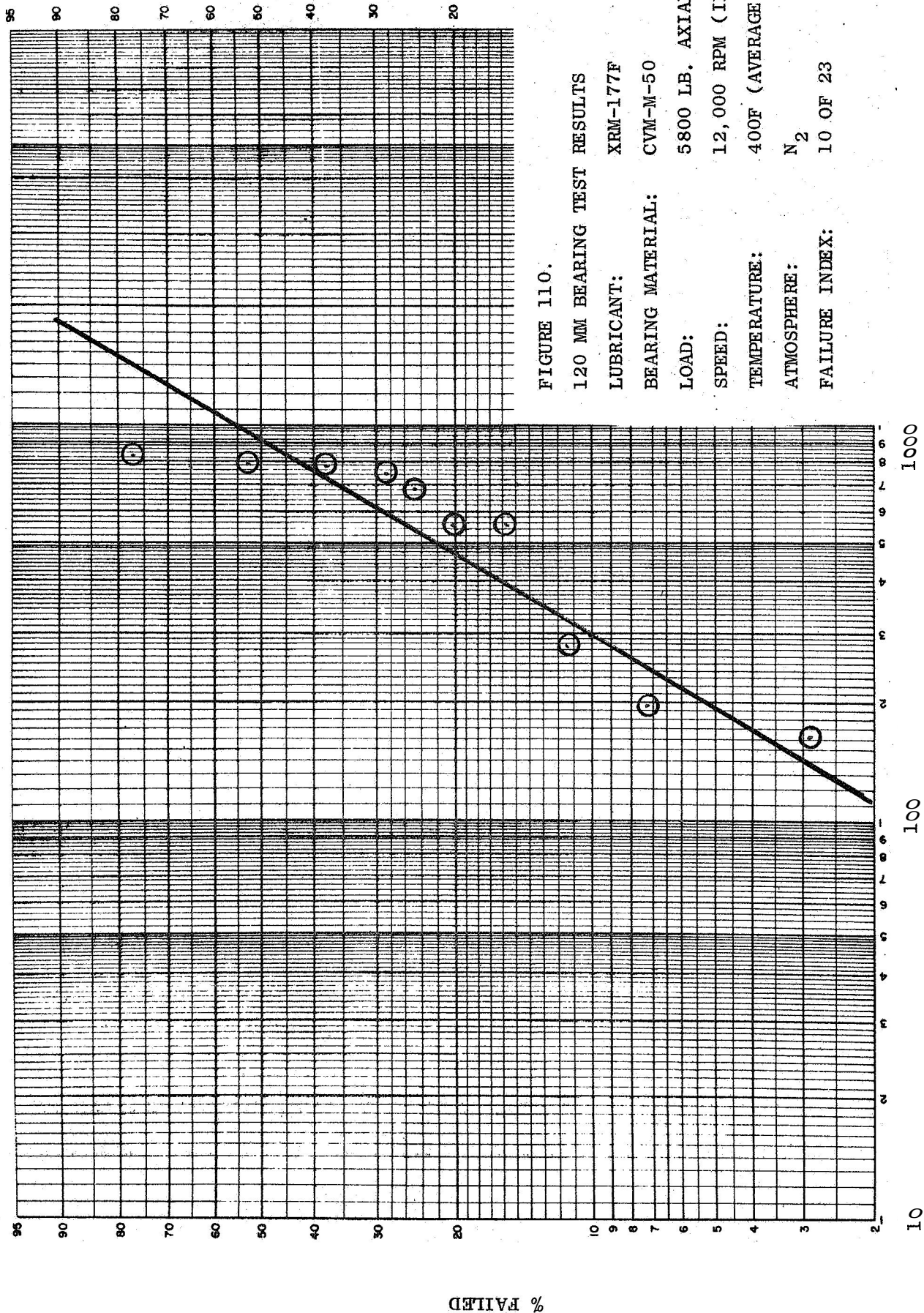


FIGURE 110.

120 MM BEARING TEST RESULTS

LUBRICANT: XRM-177F

BEARING MATERIAL: CVM-M-50

LOAD: 5800 LB. AXIAL

SPEED: 12,000 RPM (INNER)

TEMPERATURE: 400F (AVERAGE METAL)

ATMOSPHERE: N<sub>2</sub>

FAILURE INDEX: 10 OF 23

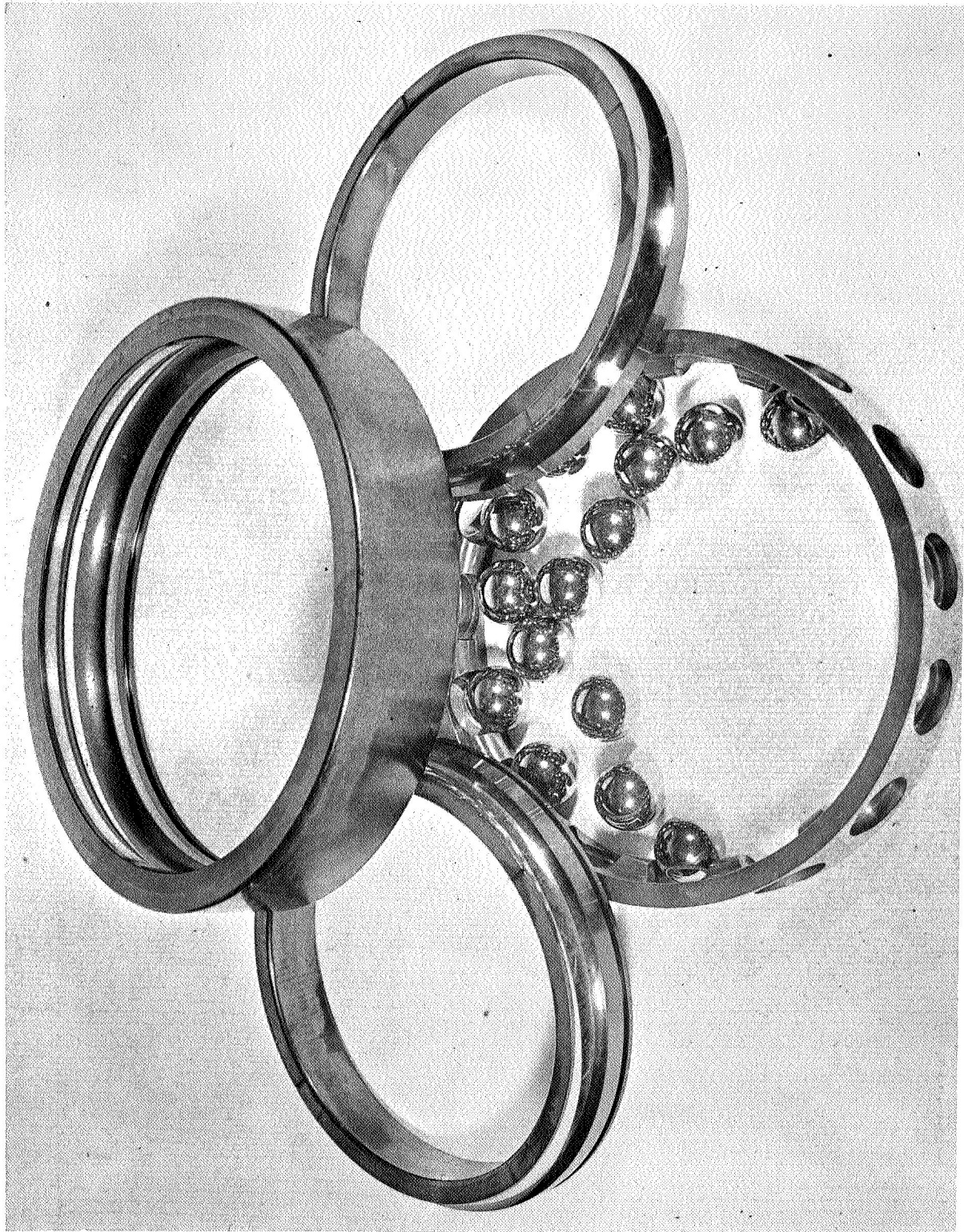


FIGURE 111. BEARING S/N 172

LUBRICANT:	XRM-177F (N <sub>2</sub> ATMOSPHERE)
TEST TEMPERATURE:	400F
LOAD:	5800 LB. AXIAL
SPEED:	12,000 RPM
MATERIAL:	M-50 BALLS AND RINGS S-MONEL CAGE
TEST SUSPENDED AT 767 HOURS	



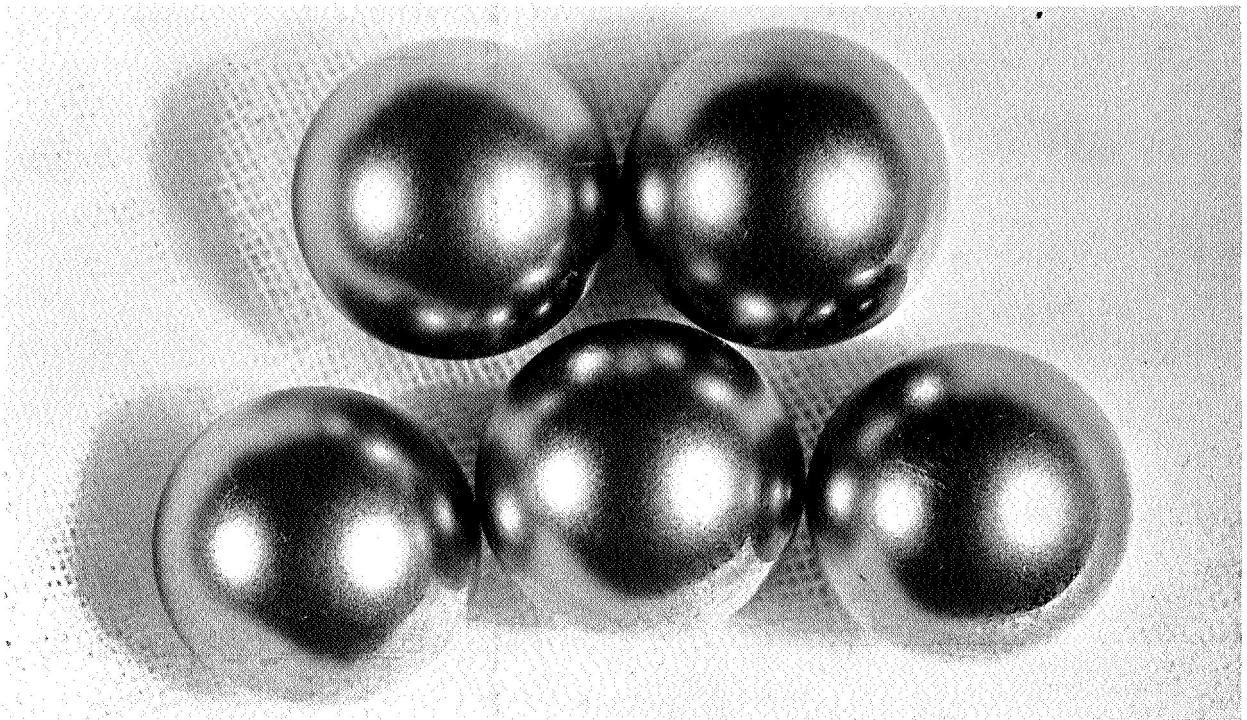


FIGURE 112. BEARING S/N 172.

APPEARANCE OF BALLS **AND** RETAINER  
AFTER 767 HOURS AT 400F WITH XRM-177F.



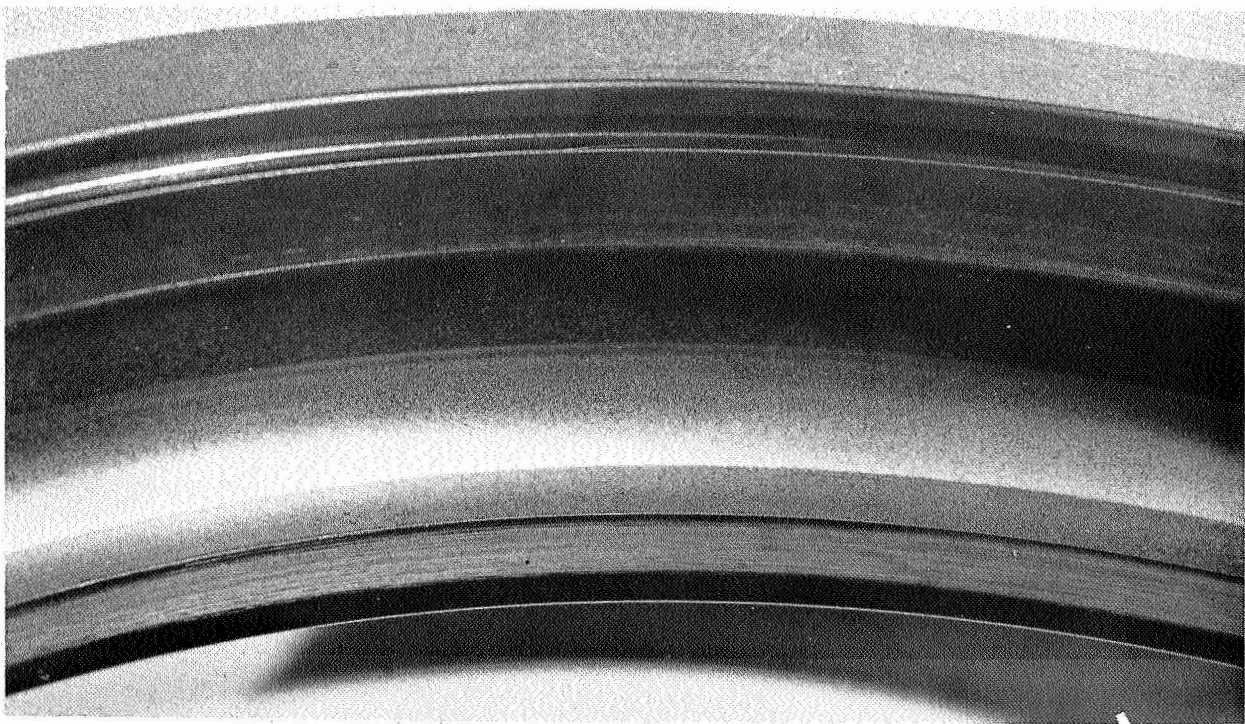
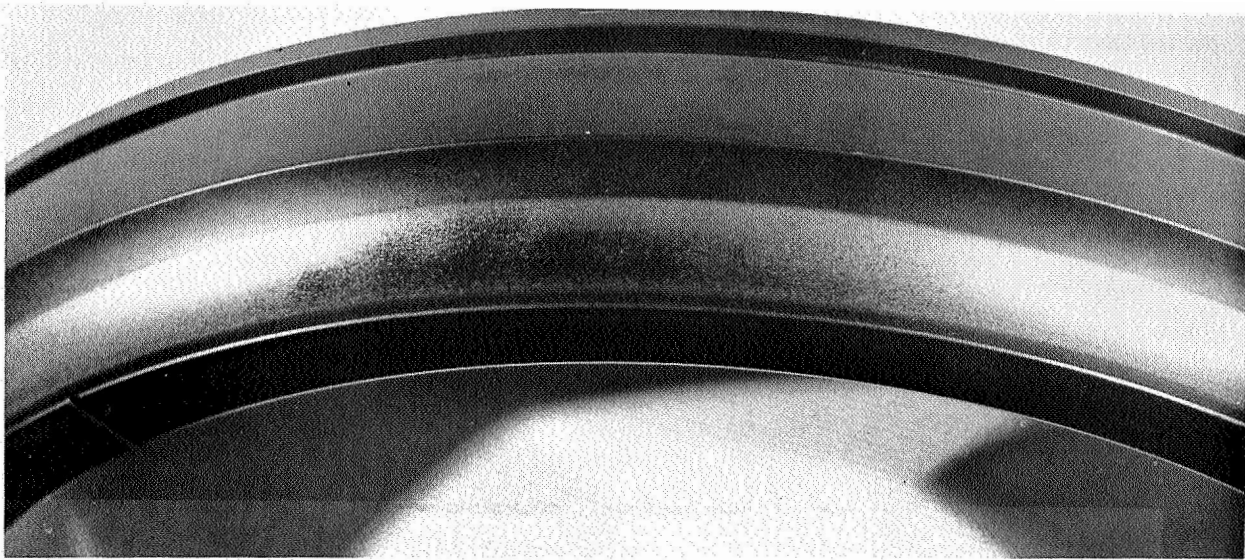


FIGURE 113. BEARING S/N 172.

APPEARANCE OF INNER RING (TOP) AND OUTER RING (BOTTOM)  
BALL PATH AFTER 767 HOURS AT 400F WITH XRM-177F.

## 7.0 Metallurgical Investigation

Metallurgical analysis of the bearing failures did not reveal any unusual or unexpected conditions with the exception of the WB-49. The failures obtained at 600F with the three test fluids were generally typical sub-surface initiated spalling fatigue, very similar to the failures obtained under more moderate temperature conditions. The photographs in Figures 114 through 124 are presented as representative of the micro-structures observed.

In general, the photographs in the subject figures are self-explanatory, although there are a few specific comments which can be made relative to some of the photomicrographs. For example, the ball fatigue failure shown in Figure 116 is somewhat unique in regard to the multiplicity of the cracks observed. Based on the RECAP analysis which indicates that the depth of maximum sub-surface shear stress should be approximately .010" below the surface, the indications are that the primary failure is the crack farthest below the surface with the remaining cracks being secondary and possibly being more of a brittle shattering nature, rather than fatigue.

Figure 117 is a cross-section through an area of ball wear, the wear being evident by the relative unevenness of the ball surface.

Figure 118 is presented as a record of the micro-structure of the M-50 material being tested and shows this material to be the normal fine grained martensitic structure judged optimum for bearing applications. The primary purpose for exhibiting Figure 119 is to show the relative lack of surface deformation or micro-structural damage in a ball which had been shown to have a slight amount of wear. Again, note the unevenness of the surface. Despite this, however, there appears to be no micro-structural damage at or near the surface.

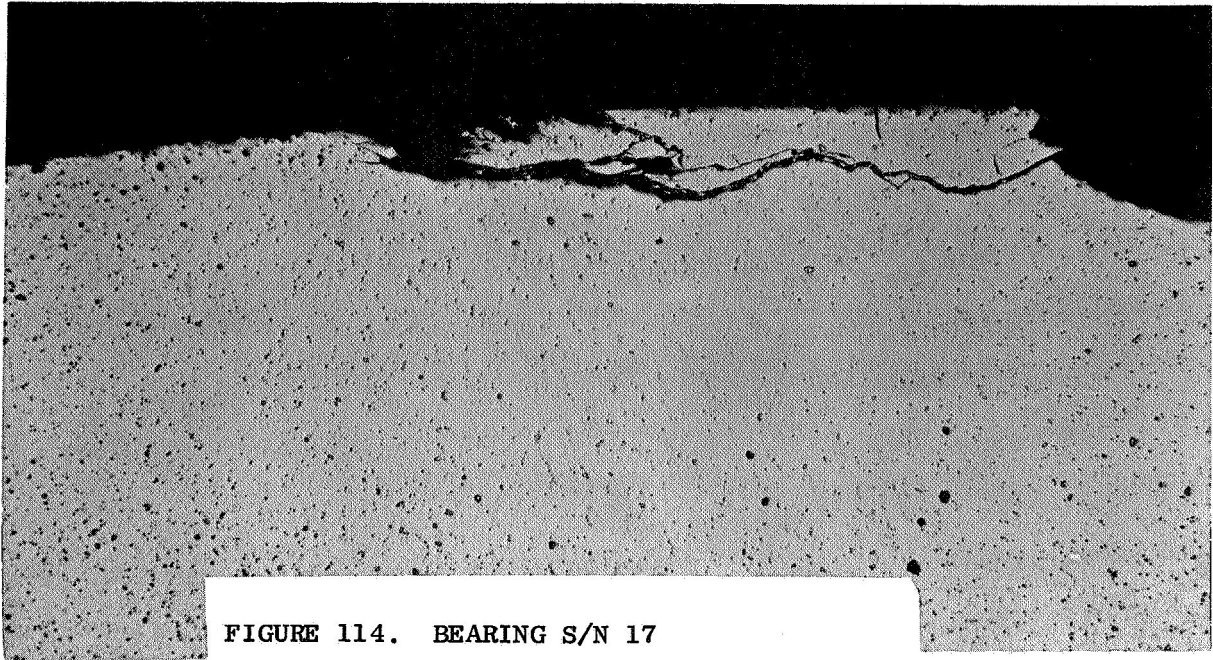


FIGURE 114. BEARING S/N 17

375 HOURS @ 5800 LB. @ 600F  
LUBRICANT: XRM-177F  
BALL FATIGUE FAILURE  
MATERIAL: CVM-M-50  
MAG: 100X UNETCHED

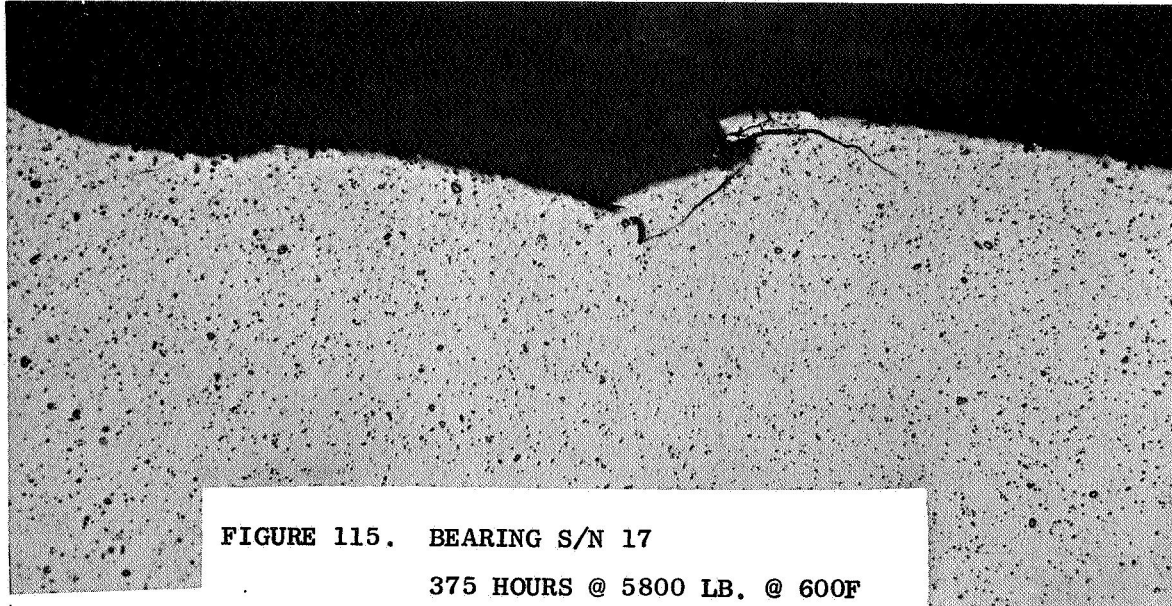


FIGURE 115. BEARING S/N 17

375 HOURS @ 5800 LB. @ 600F  
LUBRICANT: XRM-177F  
BALL FATIGUE FAILURE  
MATERIAL: CVM-M-50  
MAG: 100X UNETCHED

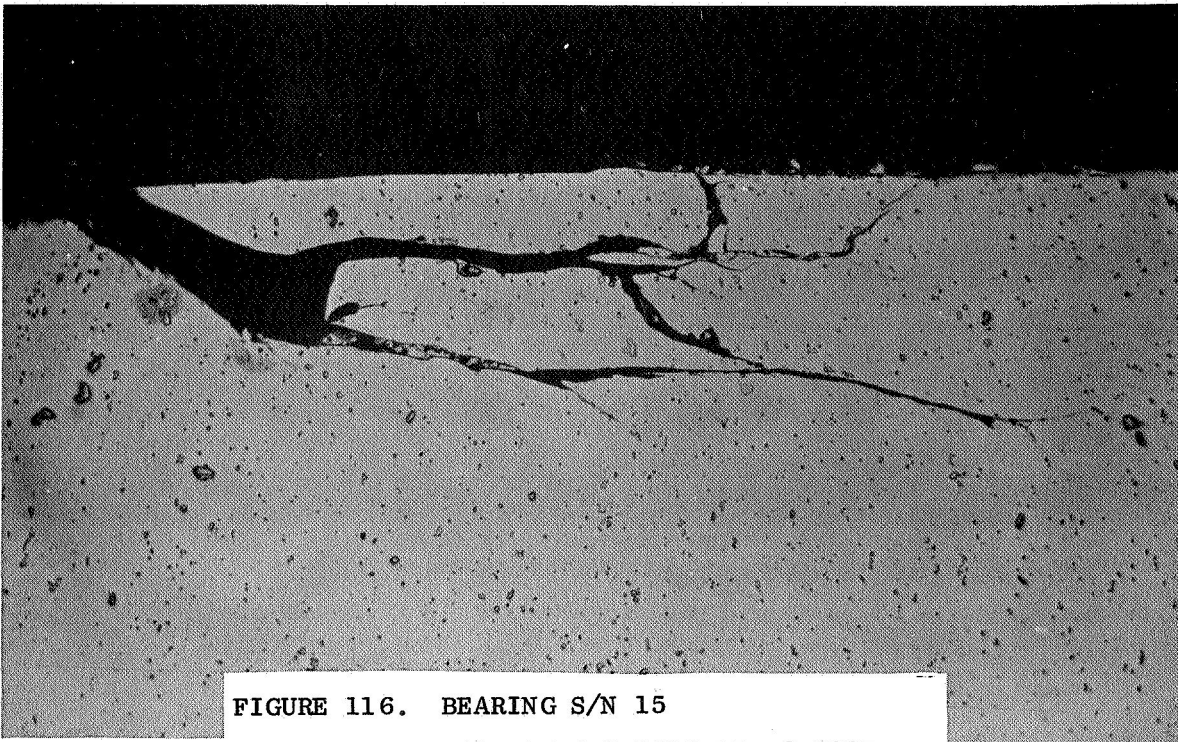


FIGURE 116. BEARING S/N 15

309 HOURS @ 5800 LB. @ 600F  
LUBRICANT: XRM-177F  
BALL FATIGUE FAILURE  
MATERIAL: CVM-M-50  
MAG: 250X UNETCHED

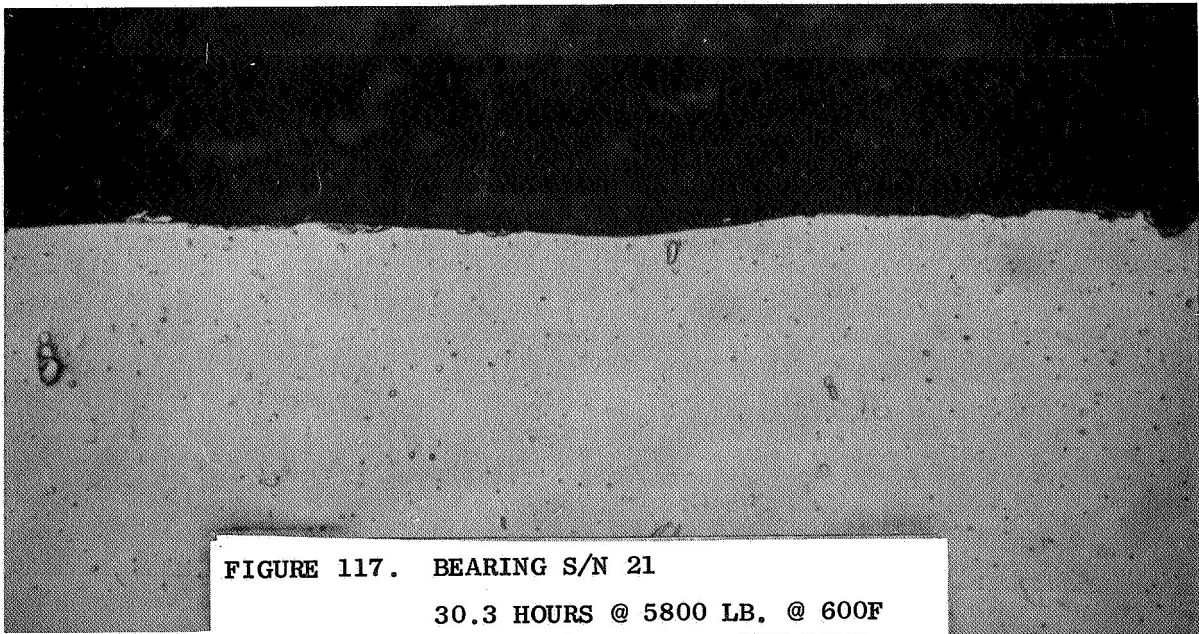


FIGURE 117. BEARING S/N 21

30.3 HOURS @ 5800 LB. @ 600F  
LUBRICANT: XRM-177F  
BALL WEAR  
MATERIAL: CVM-M-50  
MAG: 500X UNETCHED





FIGURE 118. BEARING S/N 21

**30.3 HOURS @ 5800 LB. @ 600F**

LUBRICANT: XRM-177F

TYPICAL STRUCTURE: INNER RING

MATERIAL: CVM-M-50

MAG: 500X

**ETCHANT: 3%NITAL**



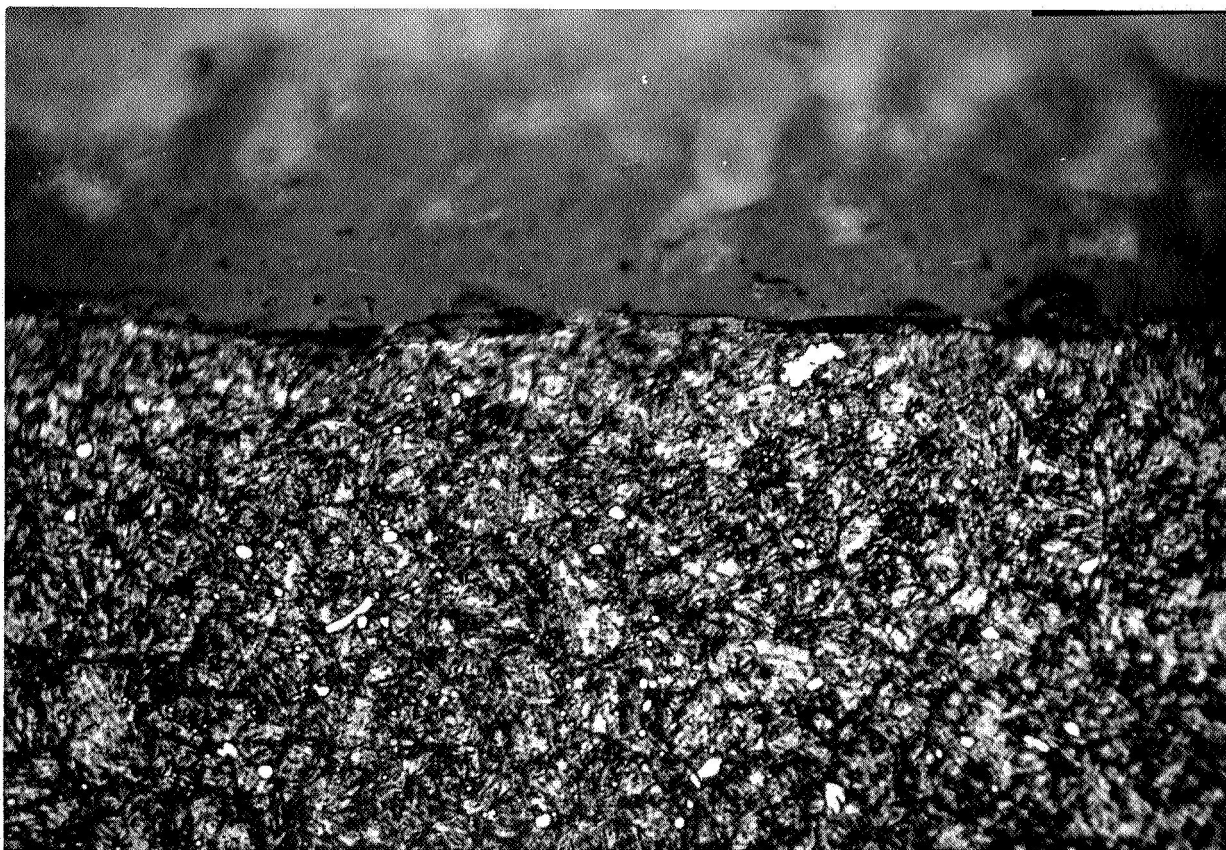


FIGURE 119. BEARING S/N 21

**30.3 HOURS @ 5800 LB. @ 600F**

LUBRICANT: XRM-177F

SURFACE OF BALL, SHOWING WEAR

MATERIAL: **CVM-M-50**

MAG: 1000X

ETCHANT: **3% NITAL**

In visual examination of the fatigue failures encountered with the MCS-354 it was noted that the failures were somewhat different than those obtained with either of the other two fluids. Despite this, however, the appearance of the failures on a micro basis is very close to what might be called classical fatigue except that the nucleus of the failure is closer to the surface than would be expected based on calculations of the depth of maximum sub-surface shear stress. This is illustrated in Figures 120 and 121.

The WB-49 material which exhibited a relatively poor fatigue life, showed a micro-structure which is not considered conducive to long rolling element fatigue life. A metallographic examination was conducted on the failed WB-49 bearings and typical photomicrographs are shown in Figures 122 through 124. Of primary interest is the massive carbide banding noted in the structure of this material. This is illustrated specifically in Figure 123 which shows the extremes of carbide banding noted in the structure. There is no question that this banding is one of the primary reasons for the short lives being encountered by these bearings. This type of structural deficiency does however, raise the question whether the material being tested is typical of the particular material. There is always the possibility that the specific material being evaluated was not produced with optimum forging practices.

However, in examining the structure of the RC Rig test bars, as well as the structures illustrated in a NASA report,<sup>(10)</sup> it appears that the massive carbide banding is common in this material. This is not too surprising in view of the high percentage of carbide forming elements present in this material. In view of this, it appears then that in order to derive the maximum usefulness from this material, improved techniques will be required in the reduction of the billet to the final shape. Obviously, as a first step, the severe carbide banding will need to be broken up and homogenized.

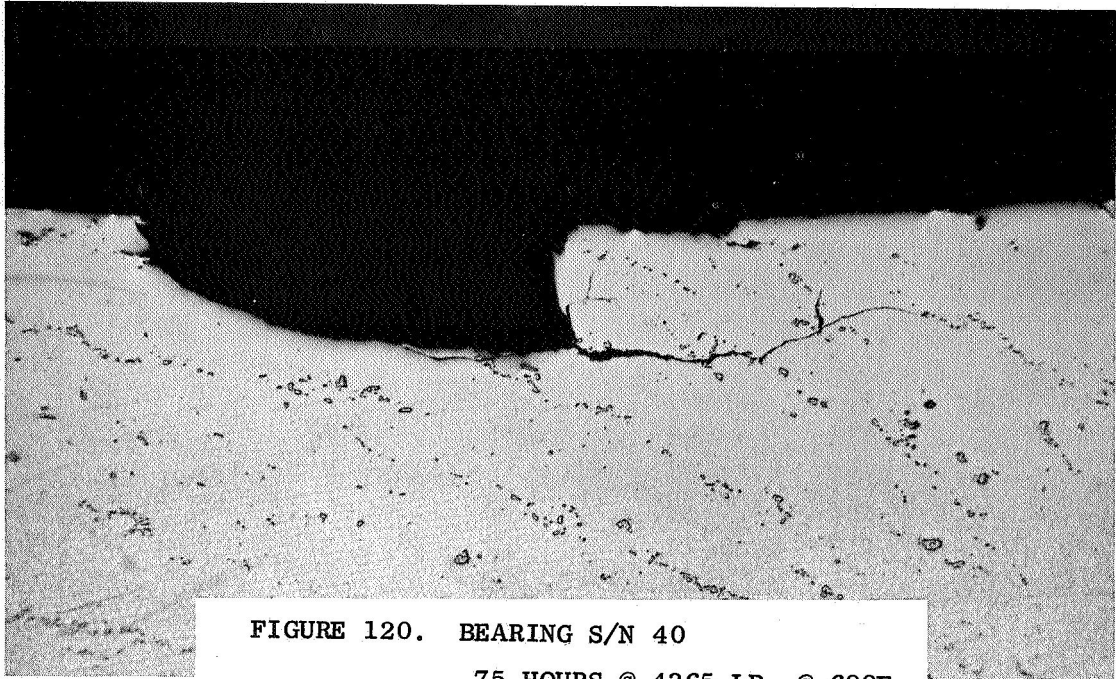


FIGURE 120. BEARING S/N 40

.75 HOURS @ 4365 LB. @ 600F  
LUBRICANT: MCS-354  
INNER RING FATIGUE FAILURE  
MATERIAL: CVM-M-50  
MAG: 200X UNETCHED

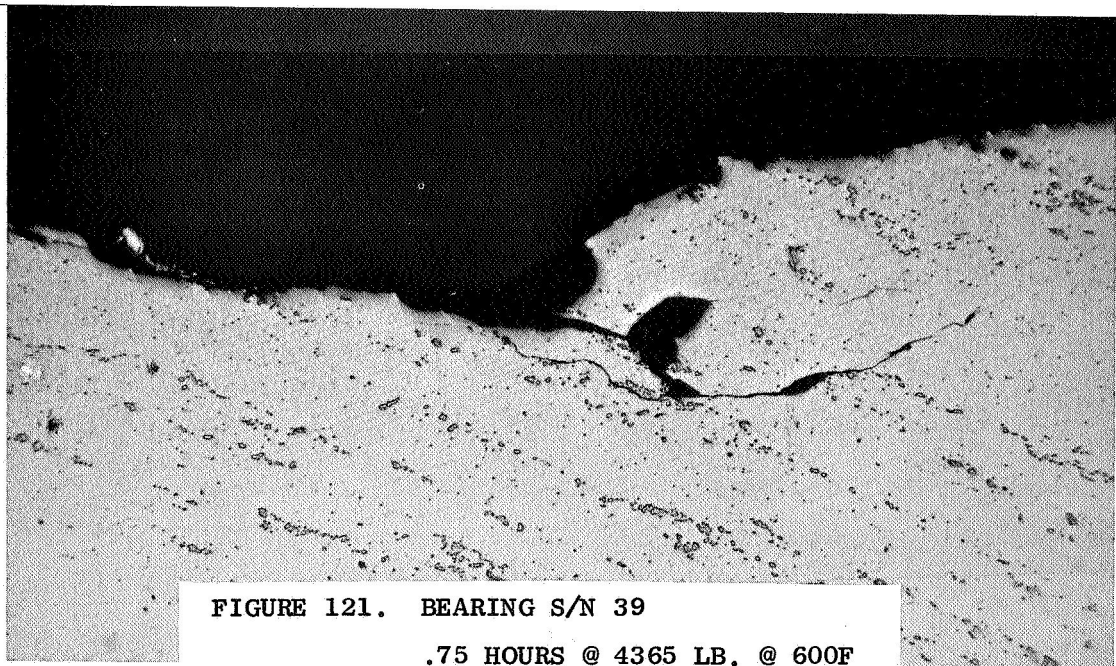


FIGURE 121. BEARING S/N 39

.75 HOURS @ 4365 LB. @ 600F  
LUBRICANT: MCS-354  
INNER RING FATIGUE FAILURE  
MATERIAL: CVM-M-50  
MAG: 200X UNETCHED



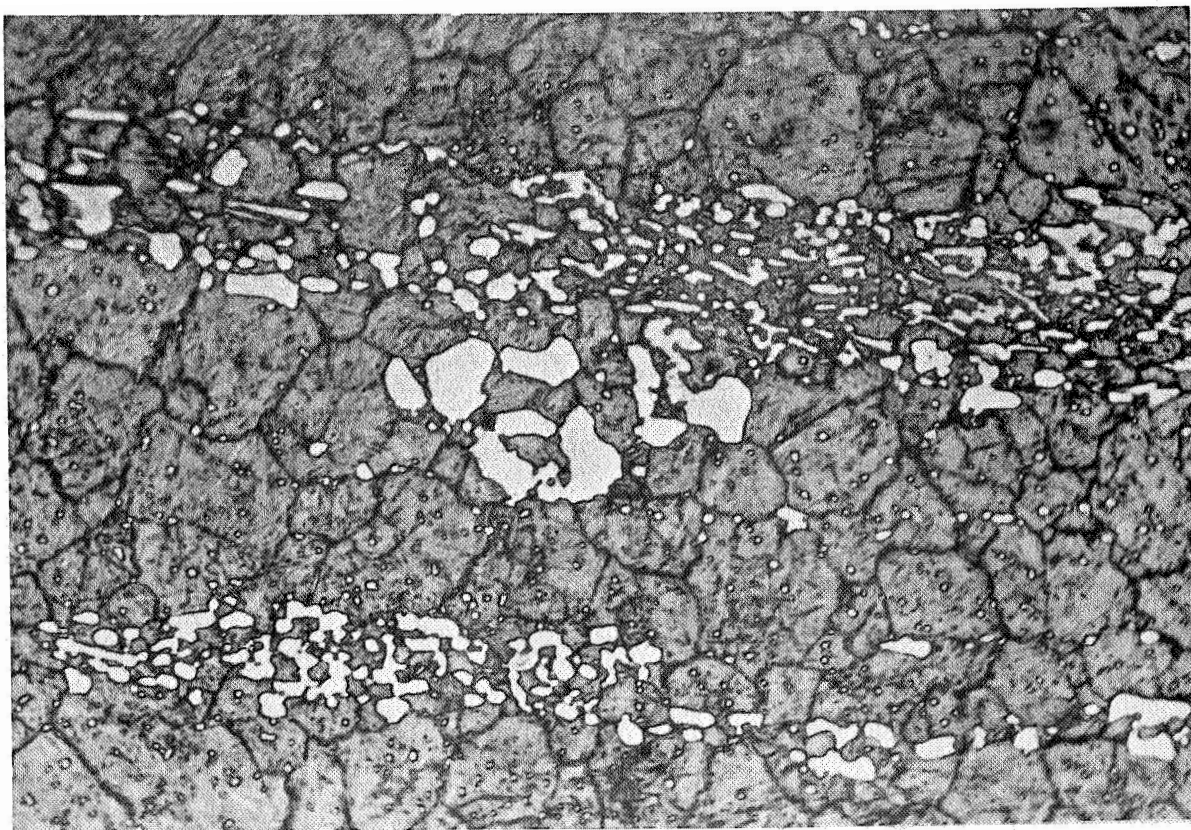
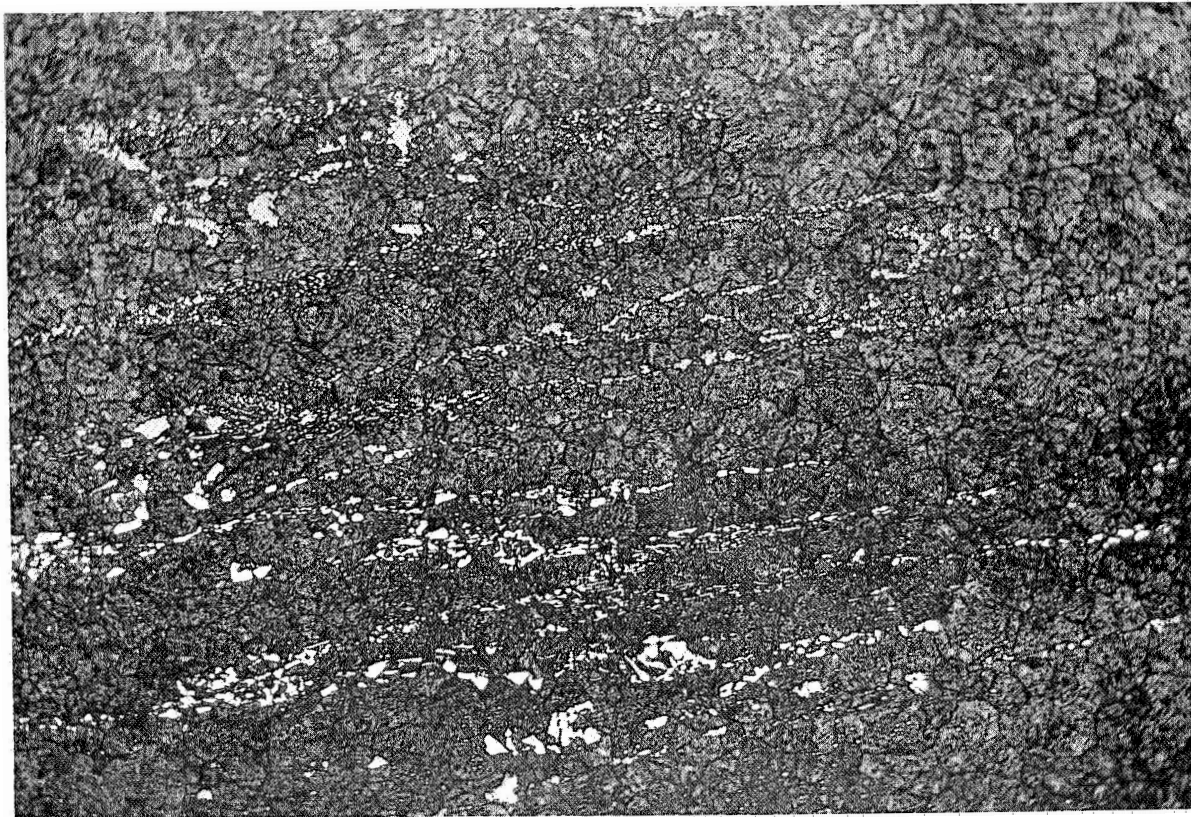


FIGURE 122. TYPICAL MICROSTRUCTURES OF WB-49.

BEARING S/N 256. NOTE MASSIVE CARBIDE BANDING.

MAG.	TOP:	250X	ETCHANT:	3% NITAL
	BOTTOM:	1000X		

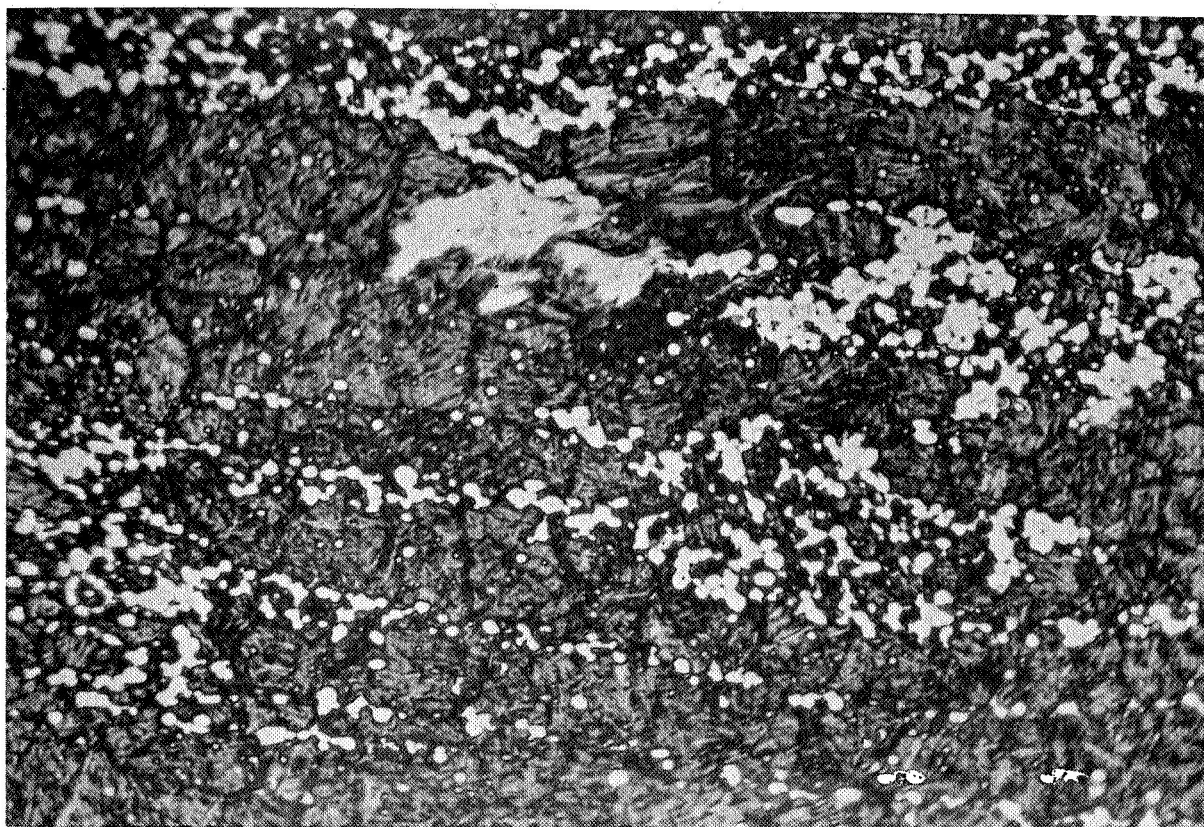
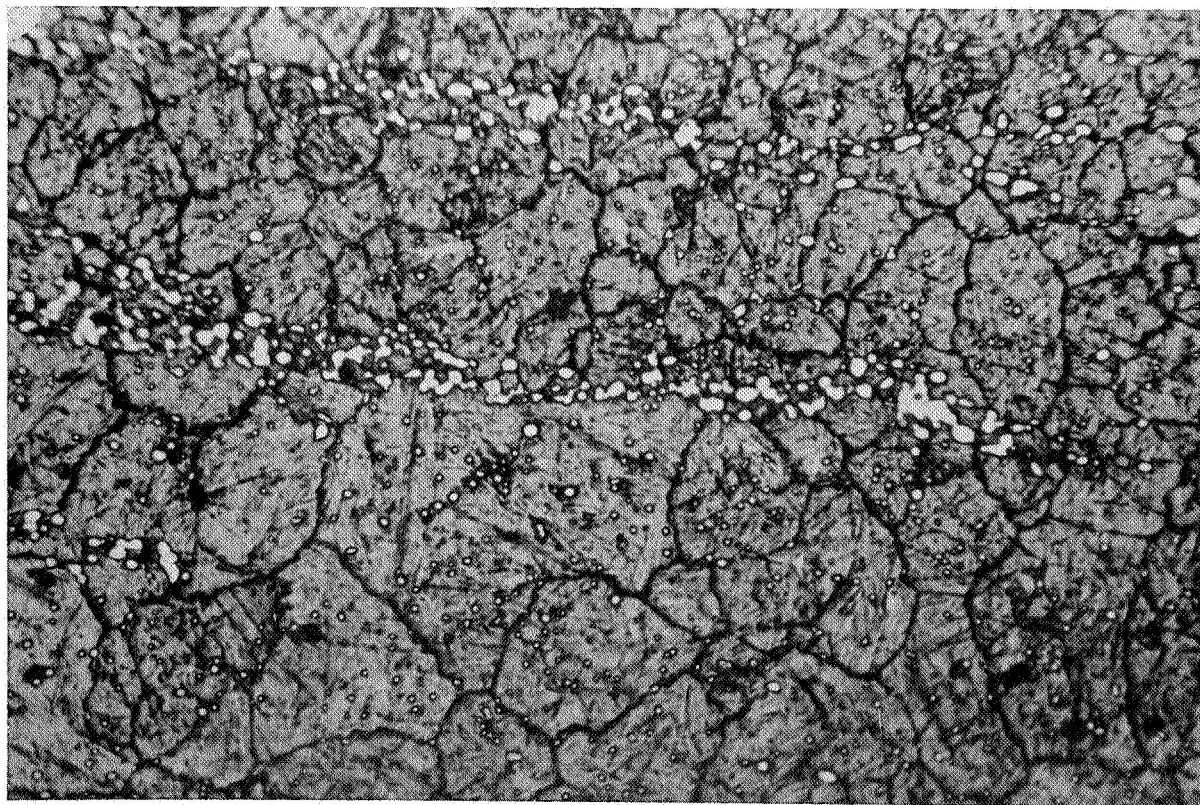


FIGURE 123. TYPICAL EXAMPLES OF MASSIVE CARBIDE BANDING IN WB-49

TOP SHOWS MINIMUM BANDING, WHEREAS BOTTOM  
PHOTOGRAPH SHOWS AREA OF MAXIMUM BANDING.

MAG: 1000X

ETCHANT: 3%NITAL



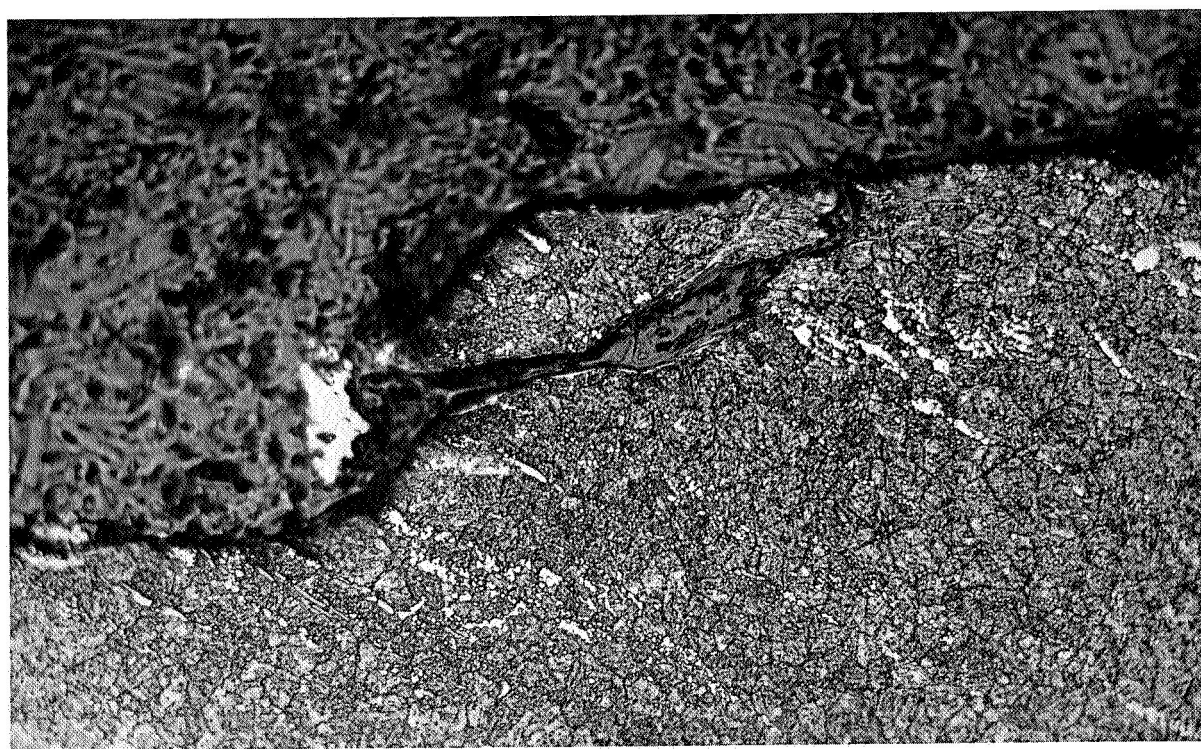
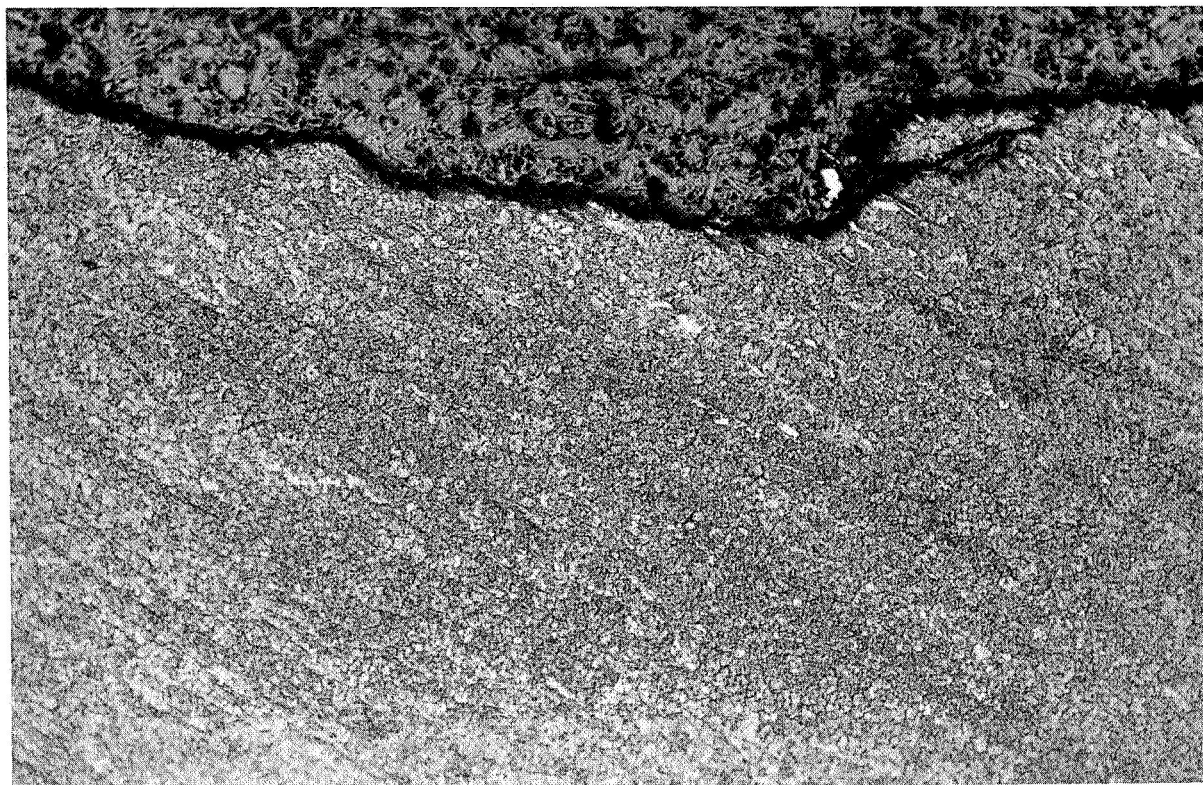


FIGURE 124. INNER RING FATIGUE FAILURE

BEARING S/N 256

TIME TO FAILURE:	26 HOURS	
MAG.	TOP: 100X	ETCHANT: 3%NITAL
	BOTTOM: 250X	

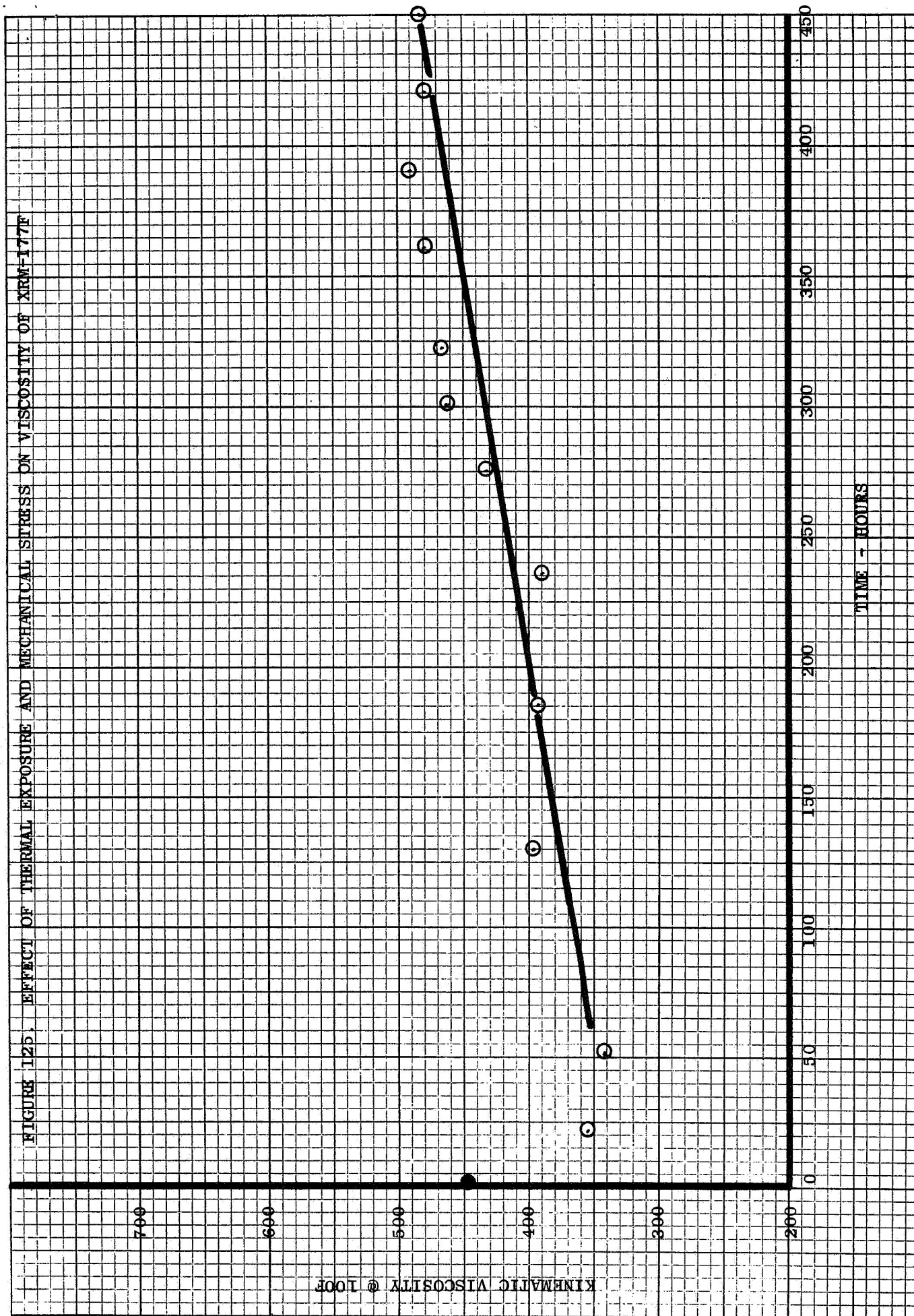
## 8.0 Lubricant Analysis

A continuous check was maintained on the test lubricants during the time the lubricant was in the bearing testers. Samples of oil were taken at approximately 24 hour intervals from the individual testers and analyzed for viscosity, acid number and contamination.

Viscosity measurements were performed at 100F and per ASTM specification D445. Neutralization number measurements were made per ASTM specification D974-58T. KOH is used as the titrant, with para-naphtholbenzein used for the indicator. Contamination was checked using infra-red spectrophotometric methods. This test was established primarily to assure that the test fluid had not been contaminated with another fluid. In the tester set-up, this could occur if seal leakage allowed the MIL-E-7808 slave bearing lubricant into the tester cavity. No evidence of this was ever noted indicating the efficiency of the seals being used,

The viscosity measurements made on the XRM-177F generally indicated an initial decrease in viscosity with time. This was expected as at the 600F temperature, some cracking of the oil must be expected. The slight decrease in neutralization number observed was not considered significant in view of the initial low value of the as-received fluid. Actually, the deviations of the samples, during and after test, from the initial ones are within the accuracy range of the test method. These measurements are additional evidence that this oil is capable of operating under the severe environmental conditions of this test,

While there was some discoloration observed in the oil after test, these visual observations also tend to indicate that no significant thermal breakdown of the oil is occurring at the test temperature and under total N<sub>2</sub> inertion. Figure 125 is a typical viscosity-time curve for the XRM-177F. This curve is representative of the measurements made on the 600F test series.



With the MCS-354, a definitive trend is somewhat more difficult to determine, mainly because the high volatility of the fluid required relatively large quantities of "make-up" oil. Consequently, the periodic diluent effect of these oil additions made it difficult to establish the true viscosity changes. However, it does appear that the MCS-354 shows a slight overall, increase in viscosity with time. A representative viscosity-time curve: is presented in Figure 126.

Lastly, the PR-143 shows a significant increase in viscosity after a relatively short period of time followed by a more gradual but constant increase as time progresses. This behavior is as expected with a polymeric fluid, where the light ends are volatilized leaving the heavier, high viscosity ends. This is illustrated in Figure 127 which shows representative viscosity-time relationships for the PR-143.



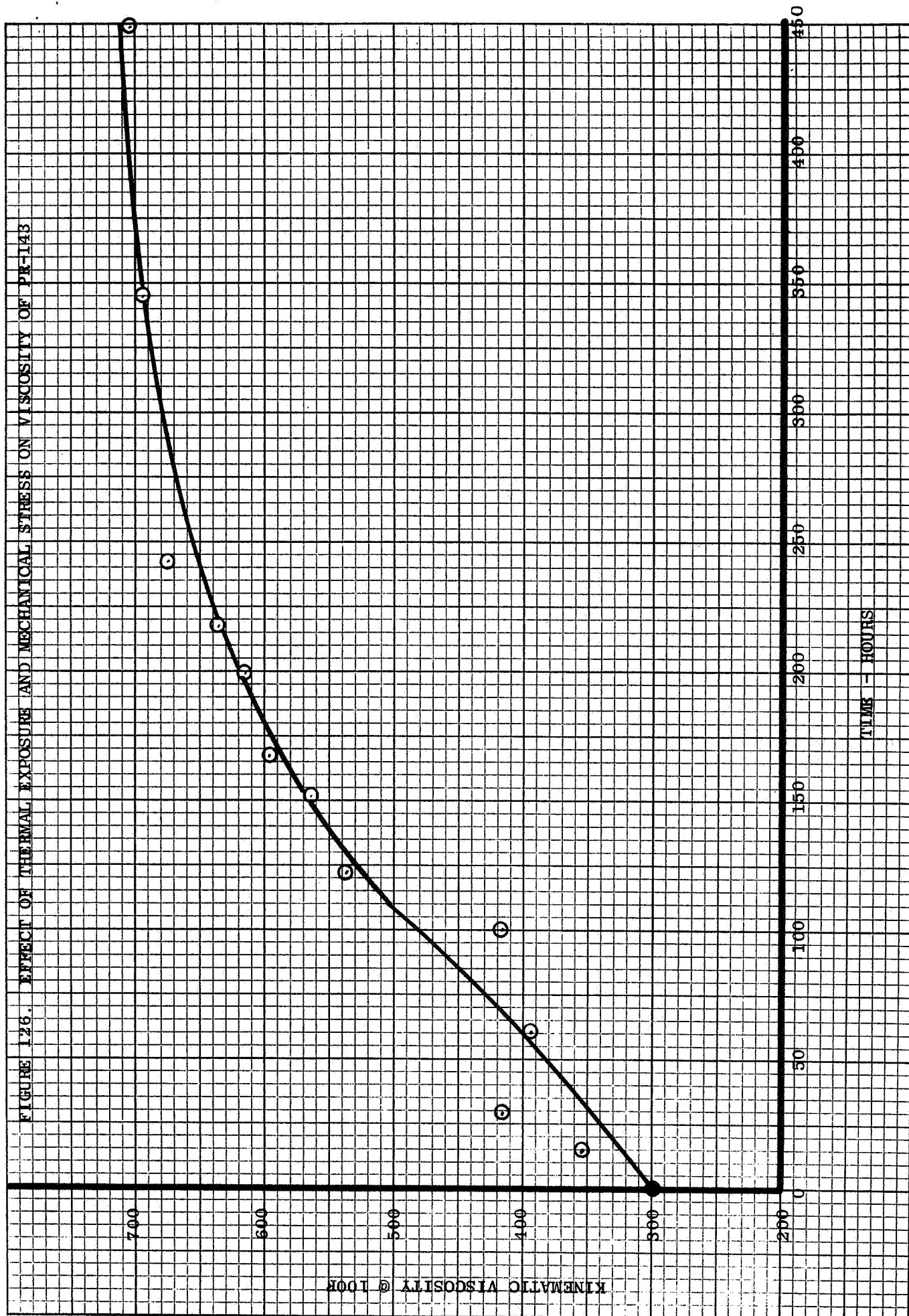
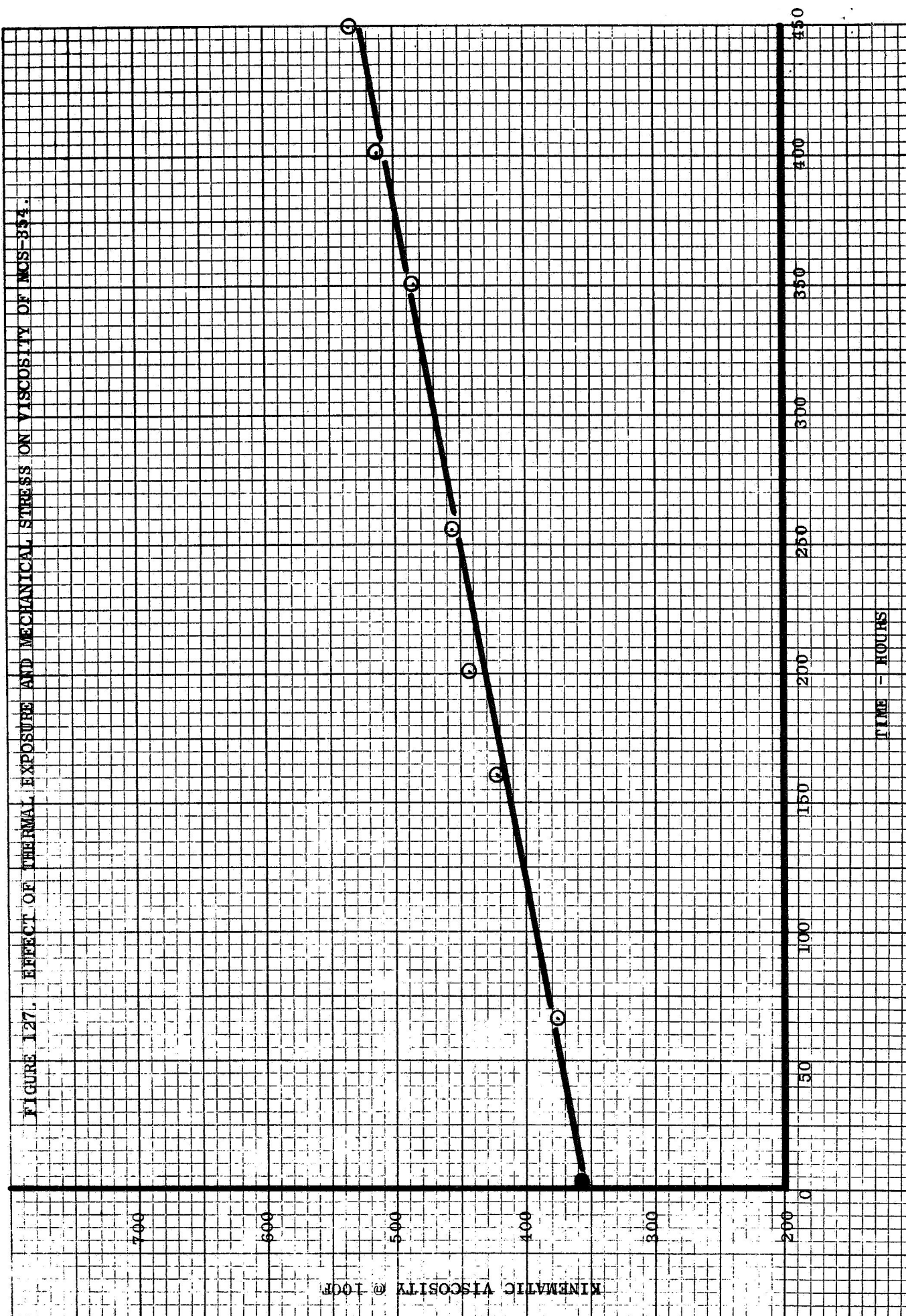




FIGURE 127. EFFECT OF THERMAL EXPOSURE AND MECHANICAL STRESS ON VISCOSITY OF MOS-354.



## 9.0 Bearing Measurements

To assist in the evaluation of the bearing data, a complete record was kept on all bearing and bearing component dimensions, and weights, both prior to and after testing. Additionally, surface profile measurements were made on the inner and outer bearing raceways prior to and after testing,

The individual bearing components which were weighed were the outer ring, the two segments of the split inner and the balls. These measurements were made on a scale calibrated into one-hundredths of a gram. Surface profile measurements were made on the outer and inner raceways using a Proficorder with measurements made at three locations around the tracks.

An analysis of all of these data does not add too much to the general body of knowledge regarding these bearings. The weight measurements indicate that, in the XRM-177F fluid there is essentially no measurable weight change in the bearing components. This, of course, is totally expected as no visual evidence of wear was observed in the bearings tested with this fluid. In the case of the MCS-354 there are some rather drastic weight losses, particularly in the ball components, although even here, there is considerable variation from one bearing to the other. In the bearing components tested with the PR-143, there is also a relatively random change in the weight measurements.

The surface profile measurements also indicate basically the same type of information. On those bearings tested with the XRM-177F, the surface profiles indicate essentially no deformation or wear, indicating that a total elastohydrodynamic film was maintained throughout the course of testing. With the MCS-354 there is evidence of wear as well as some plastic deformation taking place, although there is no discernible pattern to these effects. The surface profile traces are extremely difficult to interpret due to the poor condition of the raceway surfaces. The surfaces of the bearings lubricated with the fluorinated polymer, PR-143, indicate

generally very little wear and essentially no plastic deformation, again lending support to the theory that this lubricant does provide a mixed, if not total, elastohydrodynamic film at the 600F temperature. However, as was the case with the weight measurements taken on these bearings, there was some disagreement in the data in that some of the surface profile measurements indicated a total lack of wear, whereas others did indicate some evidence of abrasive metal removal due to asperity contacts. Some of this is also most likely due to the corrosion observed on the bearing components.

The major conclusion which can be drawn from these attempts at measurements are that either the large size and/or weight of the bearing per se, or the relatively heavy load placed on the bearing, put it beyond the realm of extremely precise measurement such as can be made on smaller, perhaps less lightly loaded bearings or on bench rig test specimens. This is particularly true in the case of the weight measurements where the total weight of the components is such that a small amount of wear resulting in a slight weight change would be extremely difficult to detect and pinpoint. Visual observations such as the condition of the ball track surfaces, or actual physical measurements such as were used to determine the changes in ball dimensions are perhaps a much better and certainly more economical means of determining what type of lubrication regime existed at the test conditions.

## 10.0 Discussion

The work reviewed in this report has provided a good insight into the feasibility of operating bearings at temperatures that exceed today's conditions by at least 150° to 200°F. The demonstration that conventionally designed bearings can operate successfully at 600F is an important milestone in the state-of-the-art of bearing technology, and should serve as the basis for additional high temperature bearing and lubricant development and evaluation. It will also serve as a guideline for the future when it is expected that the test temperatures employed in this program will be commonly seen in high performance turbo-jet engines.

Before proceeding into a discussion of the results, it might be well to briefly review the rationale of conducting a test program such as the one discussed in this report under conditions which are not at the present time contemplated for actual engine operation. Specifically, this refers to the use of the nitrogen atmosphere used in the current series of tests. The total inertion of a propulsion system is an extremely difficult endeavor and would be considered only when all other means to accomplish the same purpose had been exhausted. Consequently, it might be asked why a test program was conducted under such currently unrealistic conditions. The reason is actually quite simple, insofar the prime purpose of the program was to establish the capability of three advanced fluids to sustain elastohydrodynamic bearing operation under extreme temperature conditions. Therefore, as is the case with many basic engineering studies, a test environment had to be selected so that the primary purpose of the test program could be achieved. The data obtained is valid whether it be conducted in a nitrogen system or in a more normal air environment. It is the basic data which is of interest and the generation of which justifies the use of a controlled environment.

A parallel to this can be drawn in much of the high temperature metallurgical testing which is conducted. Much of this testing is conducted in either an inerted atmosphere or in a vacuum. Obviously, the materials

being evaluated will generally not operate in these environments. In order to obtain the data, however, it is necessary to control the atmosphere so that proper, reliable, and repeatable engineering information can be obtained. It is expected that under the impetus of the increasing performance requirements made on jet engines, the lubricant manufacturers will develop fluids which will be viable at temperatures approaching 600F and which will at the same time, be thermally stable to the point that they can operate in an air atmosphere. When these fluids are available, the information obtained in this study will be directly applicable and will serve as a guideline to judging the efficacy of the lubricants.

The three fluids evaluated in this program are representative of the most advanced high temperature materials available today. They also represent three distinctly separate families of fluids, and as such, it is logical to assume that the data obtained will be representative of other fluids of the same generic base stock. Based on the test results, the synthetic paraffinic oil, XRM-177F, is presently the most promising candidate for high temperature bearing lubrication. The appearance of the bearing components and particularly, the rolling elements and raceways, gave full evidence that elastohydrodynamic lubrication was maintained in the 600F temperature range with this fluid. Obviously, the same comment applies to the 500F and 400F temperature range. The best evidence of this was the appearance of the balls and raceways which, when observed at high magnification, still showed the original grinding marks, indicating that no asperity contact had taken place. Secondly, the surface profile measurements made after testing also indicated that essentially no changes had occurred in the stressed areas of these bearings. As discussed previously, the surface profile measurements were in general not highly conclusive, except in the case of the XRM-177F where no indication of wear and/or plastic deformation was observed. Lastly, the weight measurements made on the bearings prior to and after the test which, while, also not conclusive, did indicate that with the XRM-177F, no weight changes had taken place, :



further indicating the absence of wear. Highly encouraging also were the relatively small changes in lubricant viscosity and acid number observed after exposure of the fluid to a prolonged period of time at high temperature, This is quite significant, as it tends to indicate a long time thermal stability for this fluid. The data obtained by General Electric on this fluid also agrees well with that obtained by other organizations engaged in performing similar testing.<sup>(1)</sup>

Lastly, the data on the XRM-177F clearly indicates that this fluid is useful in the total temperature range of interest, i.e., 400F to 600F. This is not unexpected considering the good viscosity index of this fluid.

Compared to the XRM-177F, performance of the modified polyphenyl ether, MCS-354 was not satisfactory. The inability of this fluid to operate in an inerted atmosphere was not too surprising, as there are a number of fluids which require oxygen to form reactive boundary lubricants. However, the subsequent continued poor performance in an air atmosphere was disappointing. The operation of the bearings at 600F with the MCS-354 was characterized by extreme wear which necessitated a shut-down of many tests prior to the initiation of any normal fatigue failures. There was definite visual evidence of the lack of elastohydrodynamic conditions. The rolling elements as well as the races exhibited evidence of burnishing and polishing with most of the original grinding marks being completely obliterated, indicative of mixed or boundary lubrication. In most instances, surface distress was severe enough so as not to allow a meaningful surface profile analysis. Also, the weight measurements, while not consistent, did indicate significant weight losses, particularly on the balls and to a lesser extent, on the inner and outer rings. In the few instances where the bearings failed in fatigue, visual examination showed these failures to be more apparently surface initiated rather than the more classic sub-surface originating spalling. This was a deceptive observation, however, as metallographic examination indicated that the failures did initiate sub-surface at about the depth of the calculated maximum shear stress region.

The most interesting fluid of the three investigated was the fluorinated polymer, PR-143. Based on the chemical make-up of the three fluids, the polymeric material has the greatest potential as an extremely high temperature lubricant. It exhibits a number of properties which make it extremely attractive to engine designers, chief among which is its inherent fire safe operation. Conversely, the corrosive aspect would tend to make it difficult to apply in existing lubricating systems, although this should not be a major problem in advanced engines, where the lubricating system can be designed with materials which will accommodate the potential corrosive effects of this material. On this subject it should be pointed out that the fluid did not exhibit the severe corrosive effects which had been anticipated and in fact, the overall damage to either the test facilities or the test bearings themselves was within tolerable limits.

While the PR-143 gave fatigue lives close to those predicted by RECAP analysis, the performance of the fluid in the test series was not consistent. Unlike the XRM-177F where obvious elastohydrodynamic lubrication conditions existed at 600F and unlike the polyphenyl ethers, where just as obviously boundary conditions existed, there appears to be evidence of both conditions in the PR-143 between various tests. As can be seen from Table 14, there were tests which resulted in fatigue failures with none or a minimal amount of wear. There were also tests which were aborted because of rather extensive wear, and there were some tests which were terminated at 500 hours, which exhibited extremely good surfaces with no evidence of incipient fatigue failures or significant amounts of wear. One can only assume that this fluid is perhaps more sensitive to minute variations in bearing geometry or very minor changes in the test conditions.

The most serious drawback of the fluorinated polymer appears to be its tendency to increase the difficulty of bearing heat rejection, most likely due to its high density as well as its low thermal conductivity. It was

observed that the PR-143 test bearings when operated under identical conditions as the other two fluids, tended to stabilize out at a temperature approximately 100F to 125F above that observed on the other bearings. Coincidentally, it was noted that the horsepower requirements required to drive the testers was increased significantly and in fact resulted in a rash of drive belt failures. It could be assumed that the primary cause of this, is that in such a situation the retainer will act as a water brake generating considerable heat in the process. This increased bearing stabilization temperature with the PR-143 has also been noted by other organizations evaluating this fluid in high temperature bearing operations. At the present time, this factor becomes an extremely serious one in terms of applying this fluid into an engine. There is no question that, if this material is to be used, it will be necessary to re-evaluate the entire cooling system of the engine, or to make drastic changes in the basic bearing design to accommodate the fluid. Despite this, however, it is believed that this fluid has considerable promise, especially in view of its performance demonstrated in this program. This performance was achieved without the benefit of any type of additive packages such as EP or wear improvers.

In the analysis of the data there are a number of interesting observations which can be made, although the most intriguing and perhaps the most significant from a standpoint of further design of high-temperature lubricants, is the apparent viscosity/life relationship which can be demonstrated at the 600F level. Figure 128 shows the viscosity temperature relationships of the three test fluids. It can be seen that the XRM-177F and the fluorinated polymer are relatively close and have essentially the same viscosity index. The polyphenyl ether on the other hand, has a less attractive viscosity index and deviates somewhat from the other two fluids. If one now establishes a simple relationship such as plotting the log of the  $B_{10}$  life versus the kinematic viscosity, the curve shown in Figure 129 can be constructed. While it is conceded that

ASTM STANDARD VISCOSITY-TEMPERATURE CHARTS  
FOR LIQUID PETROLEUM PRODUCTS (D 341)  
CHART G: KINEMATIC VISCOSITY, EXTENDED RANGE

FIGURE 128.

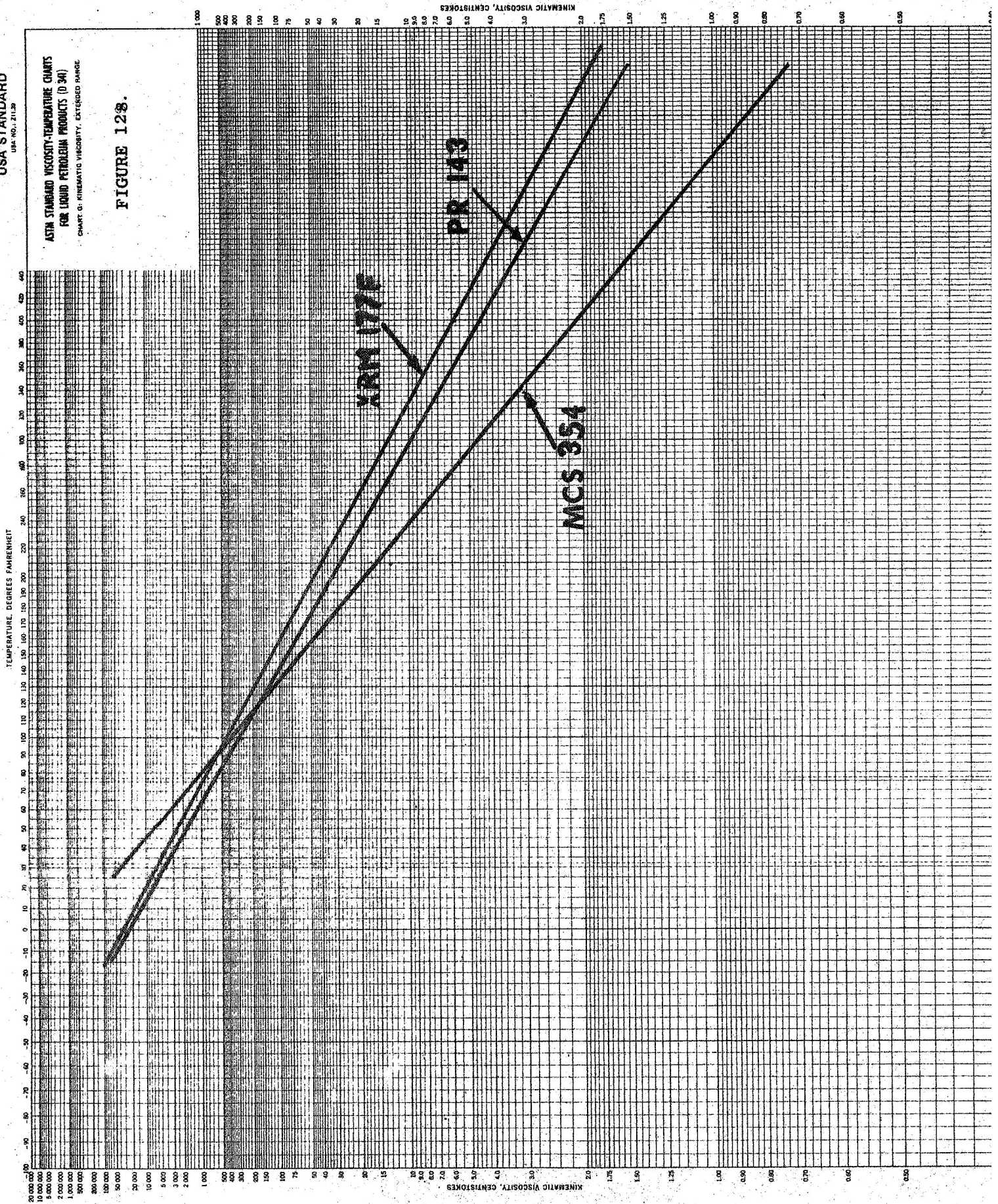
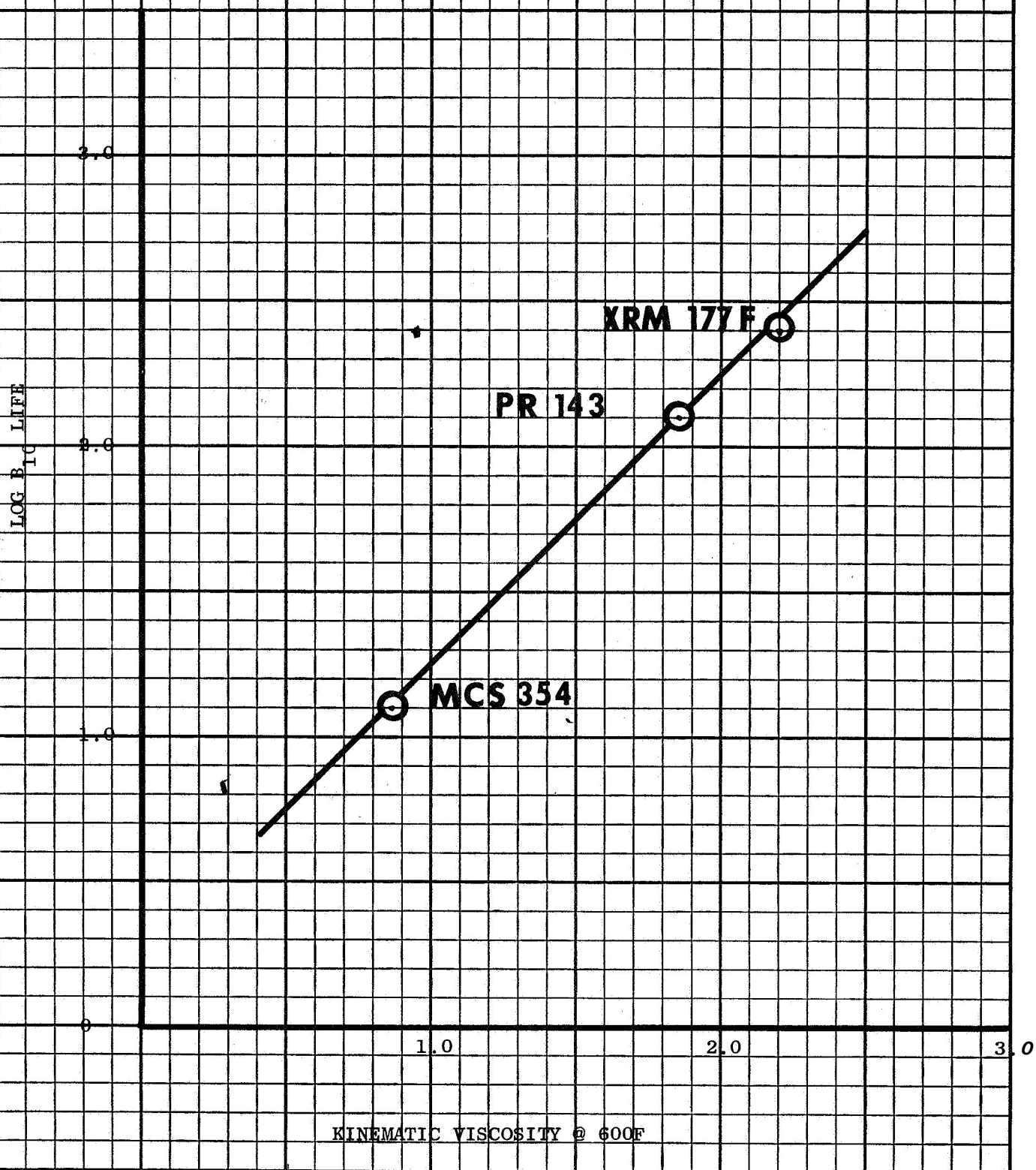


FIGURE 129  
RELATIONSHIP BETWEEN ROLLING  
CONTACT FATIGUE LIFE  
AND LUBRICANT VISCOSITY AT 600F





in view of the scarcity of data for the polyphenyl ether, the  $B_{10}$  life is at best a poor estimate, the straight line relationship which is achieved is quite remarkable. Pursuing this argument somewhat further, if one assumes that the  $B_{10}$  lives indicated on the subject curve are indicative of bearing tests where true elastohydrodynamic lubrication existed, even in the case of the polyphenyl ether, then one might speculate that, in order to achieve bearing life on the order of AFBMA or better, the lubricant viscosity must exceed 1.5 CS at the operating temperature. If this is indeed the case, then a useful guideline has been established for the development of fluids designed to operate at extreme temperature levels.

The extremely disappointing performance of the **WB-49** bearing material is thought to be a result of the basic difficulty of working this material to achieve a sound, homogenous structure. This has been pointed out previously in that the severe carbide banding which was observed unquestionably, contributed to the very early failures observed with this material. However, since reviewing this condition with other sources which have evaluated this material, it can only be assumed that at the present time, this is the best structure which can be obtained with this material and if this is indeed the case, the material cannot be considered for extended reliable high temperature bearing applications.

While on the subject of bearing materials, two other significant items were identified as a result of this program. The first of these is the excellent performance of the M-50 at the 600F temperature. This certainly provides a high degree of assurance that M-50 as presently constituted will be useful for quite some time to come, and that at the present time the limitation on high temperature bearing operation is still the lubricating fluid. Secondly, the performance of the S-Monel cage material was highly gratifying. While there were a few isolated cases of cage failure, in general, the performance of this part was extremely reliable. In most cases the cage pocket exhibited a very minimal amount of wear and no deformation. This can be seen from the several photographs which have been used

to illustrate the condition of these parts. On the other hand, the performance of the tool steel (M-1) cages used in conjunction with the WB-49 bearings was somewhat less reliable. Approximately 2% of the tool steel cages exhibited fracture failures. Consequently, based on these data it appears that the S-Monel may be a more attractive material for high temperature bearing applications.

Lastly, the results of the RC Rig tests, when viewed against the full-scale bearing test data, again illustrates the usefulness of such bench-type testing in predicting the behavior of large bearing test results. This is illustrated in the tabulation shown below:

RC Rig/120 mm Bearing Test Results @ 600F

<u>Brg .</u> <u>Matl.</u>	<u>Fluid</u>	<u>B<sub>10</sub> Life</u>		<u>Ranking</u>			
		<u>AFBMA</u> <u>RC Rig*</u> <u>(Stress</u> <u>Cycles)</u>	<u>Actual</u> <u>RC Rig</u> <u>(Stress</u> <u>Cycles)</u>	<u>RECAP</u> <u>Bearing *</u> <u>(Hrs.)</u>	<u>Actual</u> <u>Bearing</u> <u>(Hrs.)</u>	<u>RC</u> <u>Rig</u>	<u>Brg.</u>
M-50	XRM-177F	1.4 x 10 <sup>6</sup>	2.35 x 10 <sup>6</sup>	100	252	1	1
M-50	MCS-354	1.4 x 10 <sup>6</sup>	0.69 x 10 <sup>6</sup>	100	12.7	3	3
M-50	PR-143	1.4 x 10 <sup>6</sup>	1.04 x 10 <sup>6</sup>	100	128	2	2
WB-49	XRM-177F	1.4 x 10 <sup>6</sup>	1.7 x 10 <sup>6</sup>	100	84		

\* Corrected for CVM M-50

It can be seen from the above data that the RC Rig ranked the three fluids in exactly the same order as the large scale bearing test and in fact, the percentage of difference between the fluids in relationship to the AFBMA rating is in very good agreement. The RC Rig also predicted a lower fatigue life for WB-49, as compared to M-50, although here the magnitude of failure severity was much greater in the actual bearings than had been predicted with the RC Rig. Again, this is thought to be due to the fact that the RC Rig bars did achieve perhaps a more uniform working and consequently, contained a more homogeneous structure than the large bearing components.

## 11.0 LIST OF REFERENCES

1. C. J. Wachendorfer, L. B. Sibley, "Bearing Lubricant Endurance Characteristics at High Speeds and High Temperature", Final Report, NASA Contract NAS-W-492, 1965.
2. W. H. Gumprecht, "PR-143.- A New Class of High Temperature Fluids", ASME Preprint 65LC-3, 1965.
3. R. E. Dolle, F. J. Harsacky, H. Schwenker, R. L. Adamczak, "Chemical, Physical and Engineering Performance Characteristics of a New Family of Perfluorinated Fluids", ASD Technical Report AFML-TR-65-358, September, 1965.
4. R. L. Adamczak, H. Schwenker, "A Bibliography of Technical Reports and Papers of Research and Development on Polyphenyl Ether Fluids", ASD Technical Documentary Report AFML TDR-66-403, September, 1966.
5. E. V. Zaretsky, W. J. Anderson, "Evaluation of High Temperature Bearing Cage Materials", NASA TN D-3821, January, 1967.
6. A. B. Jones, "A General Theory for Elastically Constrained Ball and Radial Roller Bearings Under Arbitrary Load and Speed Conditions", ASME.
7. R. J. Parker, E. N. Bamberger, E. V. Zaretsky, "Bearing Torque and Fatigue Life Studies with Several Lubricants for Use in the Range 500 to 700F", NASA TN D-3948, May, 1967.
8. L. G. Johnson, "The Statistical Treatment of Fatigue Experiments", Report #GMR 202, General Motors Corp., April, 1959.
9. Anon, "Developmental Synthetic Fluids", Technical Bulletin, Monsanto Company.

LIST OF REFERENCES, Cont.

10. T. L. Carter, E. V. Zaretsky, W. J. Anderson, "Effect of Hardness and Other Mechanical Properties on Rolling-Contact Fatigue Life of Four High-Temperature Bearing Steels", NASA TN D-270, 1960.

REPORT DISTRIBUTION LIST FOR

CONTRACT NAS3-7261

	<u>No. of Copies</u>
NASA-Lewis Research Center Air-Breathing Engine Procurement Section 21000 Brookpark Road Cleveland, Ohio 44135 Attention: Mr. E. L. Wiskemann	(1)
NASA-Lewis Research Center Air-Breathing Engine Division 21000 Brookpark Road Cleveland, Ohio 44135 Attention: J. Howard Childs Dennis Townsend W. Roudebush L. Macioce	(2) (4) (1) (1)
NASA-Lewis Research Center Technical Utilization Office 21000 Brookpark Road Cleveland, Ohio 44135 Attention: Mr. Paul Foster	(1)
NASA-Lewis Research Center Office of Reliability and Quality Assurance 21000 Brookpark Road Cleveland, Ohio 44135 Attention: James Pelouch Vincent Lalli	(1) (1)
NASA-Lewis Research Center Fluid System Components Division 21000 Brookpark Road Cleveland, Ohio 44135 Attention: I. I. Pinkel E. E. Bisson R. L. Johnson W. R. Loomis W. J. Anderson M. A. Swikert E. V. Zaretsky	(1) (1) (1) (1) (1) (1) (12)
Air Force Materials Laboratory Wright-Patterson AFB, Ohio 45433 Attention: MANL R. Adamczak & F. Harsacky MAMD Walter Strapp	(1) (1)



Air Force Aero Propulsion Lab. Wright Patterson AFB, Ohio 45433	
Attention: APFL, K. L. Berkey	(1)
APFL, G. A. Beane IV	(1)
APTL, I. J. Gershon	(1)
Supersonic Transport Office Wright-Patterson AFB, Ohio 45433	
Attention: SESH, J. L. Wilkins	(1)
NASA-Lewis Research Center 21000 Brookpark Road Cleveland, Ohio 44135	
Attention: P.T. Hacker, MS 5-3	(1)
FAA Headquarters 800 Independence Avenue, S.W. Washington, D.C. 20546	
Attention: M. Lott, J. Chavkin	(1)
NASA-Headquarters 600 Independence Avenue, S.W. Washington, D.C. 20546	
Attention: Nelson Rekos (RAP)	(1)
M. Comberiate	(1)
A. J. Evans (RAD)	(1)
NASA-Langley Research Center Langley Station Hampton, Virginia 23365	
Attention: Mark R. Nichols	(1)
United Aircraft Corporation Pratt & Whitney Aircraft Division East Hartford, Connecticut 06108	
Attention: R. P. Schevchenko	(1)
P. Brown	(1)
Curtiss-Wright Corporation Wright Aeronautical Division Wood-Ridge, New Jersey 07075	
Attention: S. Lombardo	(1)
Cleveland Graphite Bronze Clevite Corporation 540 East 105th Street Cleveland, Ohio 44108	
Attention: Library	(1)

Celanese Chemical Company  
 Celanese Corporation of America  
 New York, New York 10001  
 Attention: Thomas G. Smith (1)

Shell development Company  
 Emeryville, California 94608  
 Attention: Dr. C. L. Mahoney (1)

Gulf Research and Development Company  
 P.O. Drawer 2038  
 Pittsburgh, Pennsylvania 15230  
 Attention: Dr. H. A. Ambrose (1)

California Research Corporation  
 Richmond, California 94802  
 Attention: Neil Furby (1)  
                   Douglas Godfrey (1)

Dow Chemical Company  
 Abbott Road Buildings  
 Midland, Michigan 48640  
 Attention: Dr. R. Gunderson (1)

Kendall Refining Company  
 Bradford, Pennsylvania 16701  
 Attention: F. I. I. Lawrence (1)

Aerojet-General Corporation (1)  
 20545 Center Ridge Road  
 Cleveland, Ohio 44126

Texaco, Incorporated  
 P.O. Box 509  
 Beacon, New York 12508  
 Attention: Dr. G. B. Arnold (1)

Olin Mathieson Chemical Corporation  
 Organics Division  
 275 Winchester Avenue  
 New Haven, Connecticut 06474  
 Attention: Dr. C. W. McMullen (1)

Heyden Newport Chemical Corporation  
 Heyden Chemical Division  
 290 River Drive  
 Garfield, New Jersey 07026  
 Attention: D. X. Klein (1)

Crucible Steel Company of America (1)  
The Oliver Building  
Mellon Square  
Pittsburgh, Pennsylvania 15222

Dow Corning Corporation  
Midland, Michigan 48640  
Attention: Re We Awe & H. M. Schiefer (1)

Allegheny Ludlum Steel Corporation (1)  
Oliver Building  
Pittsburgh, Pennsylvania 15222

U. S. Naval Air Material Center  
Aeronautical Engine Laboratory  
Philadelphia, Pennsylvania 19112  
Attention: A. L. Lockwood (1)  
Sup. Engine Lubri. Branch

U. S. Naval Research Laboratory  
Washington, D.C. 20546  
Attention: Mr. Charles Murphy (1)

Department of the Navy  
Bureau of Naval Weapons  
Washington, D.C. 20546  
Attention: A. B. Nehman, RAAE-3 (1)  
C. C. Singleterry, RAPP-4 (1)

U. S. Army Ordnance  
Rock Island Arsenal Lab.  
Rock Island, Illinois 61201  
Attention: Re LeMar (1)

Mechanical Technology, Incorporated  
Latham, New York 14603  
Attention: B. Sternlicht (1)

Government Research Laboratory  
Esso Research & Engineering Company  
P.O. Box 8  
Linden, New Jersey 07036  
Attention: Director (1)

Industrial Tectonics, Incorporated  
Research & Development Division  
18301 Santa Fe Avenue  
Compton, California 90220  
Attention: Heinz Hanau (1)

Alcor Incorporated  
2905 Bandera Road  
San Antonio, Texas 78205  
Attention: Mr. L. Hundere (1)

Monsanto Chemical Company  
800 North Lindbergh Boulevard  
St. Louis, Missouri 63166  
Attention: Mr. Ken McHugh (1)

Monsanto Research Corporation  
Everett Station  
Boston, Massachusetts 02109  
Attention: Dr. John O. Smith (1)

The Koppers Company, Incorporated  
Metal Products Division  
Piston Ring and Seal Department  
7709 Scott Street  
Baltimore, Maryland 21203  
Attention: T. C. Kuchler (1)

Sinclair Refining Company  
600 - 5th Avenue  
New York, New York 10020  
Attention: C. W. McAllister, Mgr.  
Aviation Sales & Tech. (1)

Union Carbide Chemicals Company  
Division of Union Carbide Corporation  
Tarrytown, New York 10591  
Attention: W. H. Millett (1)

Sun Oil Company  
Automotive Laboratory  
Marcus Hook, Pennsylvania 19061  
Attention: J. Q. Griffith (1)

Rohm and Haas Company  
Washington Square  
Philadelphia, Pennsylvania 19105  
Attention: V. Ware & P. H. Carstensen (1)

Crane Packing Company  
6400 W. Oakton Street  
Morton Grove, Illinois 60053 (1)

Pennsylvania State University  
Department of Chemical Engineering  
University Park, Pennsylvania 16801  
Attention: Dr. E. E. Klaus (1)

Stein Seal Company 20th and Indiana Avenue Philadelphia, Pennsylvania 19132	(1)
Sealol Company 100 Post Road Providence, Rhode Island 02904	(1)
Fafnir Bearing Company 37 Booth Street New Britain, Connecticut 06051 Attention: <del>He</del> B. Van Dorn	(1)
General Electric Company General Engineering Laboratory Schenectady, New York 12305	(1)
Fairchild Engine and Airplane Corporation Stratos Division Bay Shore, New York	(1)
Rocketdyne Division of North American Aviation Canoga Park, California 90052	(1)
Borg-Warner Corporation Roy C. Ingersoll Research Center Wolf and Algonquin Roads Des Plaines, Illinois 60016	(1)
General Motors Corporation New Departure Division Bristol, Connecticut 06010 Attention: W. O'Rourke	(1)
Franklin Institute Labs 20th and Parkway Philadelphia, Pennsylvania 19133 Attention: Otto Decker	(1)
Avco Corporation Lycoming Division 550 Main Street Stratford, Connecticut 06497 Attention: Me S. Saboe	(1)
NASA-Lewis Research Center Reports Control Office 21000 Brookpark Road Cleveland, Ohio 44135	(1)



Westinghouse Electric Corporation  
Research Laboratories  
Beulah Road, Churchill Borough  
Pittsburgh, , Pennsylvania 15235  
Attention: Mr. John Boyd (1)

Allison Division (1)  
General Motors Corporation  
Plant #8  
Indianapolis, Indiana 46206

Boeing Aircraft Company  
Aerospace Division  
Materials and Processing Section  
Seattle, Washington 98101  
Attention: Mr. J. W. Van Wyk (1)

Battelle Memorial Institute  
505 King Avenue  
Columbus, Ohio 43201  
Attention: C. Allen (1)

Lockheed Aircraft Corporation  
Lockheed Missile and Space Company  
Material Science Laboratory  
3251 Hanover Street  
Palo Alto, California 94301  
Attention: Francis J. Clauss (1)

North American Aviation  
Downey, California 90240  
Attention: W. A. Strsalkmski (1)

EPPI Precision Products Company  
227 Burlington Avenue  
Clarendon Hills, Illinois 60514  
Attention: C. Dean (1)

Midwest Research Institute  
425 Volker Boulevard  
Kansas City , Missouri 64110  
Attention: V. Hopkins & A. D. St. John (1)

Socony Mobil Oil Company  
Research Department  
Paulsboro Laboratory  
Paulsboro, New Jersey 08066  
Attention: Ed. Oberright (1)

Douglas Aircraft Company  
3000 Ocean Park Boulevard  
Santa Monica, California 90406  
Attention: Robert McCord (1)

The Marlin-Rockwell Corporation  
Jamestown, New York 14701  
Attention: Arthur S. Irwin (1)

Chicago Rawhide Manufacturing Company  
1311 Elston Avenue  
Chicago, Illinois 60607  
Attention: Richard Blair (1)

Southwest Research Institute  
San Antonio, Texas 78205  
Attention: P. M. Ku (1)

IIT Research Institute  
West 35th Street  
Chicago, Illinois 60616  
Attention: Warren Jamison (1)

E. I. DuPont de Nemours and Company  
Organic Chemicals Department  
Freon Products Division  
Wilmington, Delaware 19899  
Attention: John J. Daly, Jr. (1)

E. I. DuPont de Nemours and Company  
1007 Market Street  
Wilmington, Delaware 19899  
Attention: George Finn (1)

NASA-Lewis Research Center  
21000 Brookpark Road  
Cleveland, Ohio 44135  
Attention: Library (1)

Department of the Navy  
Bureau of Ships  
Washington, DC. 20025  
Attention: Harry King, Code 634A (1)

Sinclair Research, Incorporated  
400 E. Sibley Boulevard  
Harvey, Illinois 60426  
Attention: M. R. Fairlie  
Director of Products Division

Republic Aviation Corporation Space Systems and Research Farmingdale, Long Island, New York 11735 Attention: R. Schroeder	(1)
NASA-Scientific & Technical Information Facility Box 5700 College Park, Maryland 20740 Attention: NASA Representative	(6)
Hercules Powder Co., Inc. 900 Market St. Wilmington, Delaware 19899	(1)
Airesearch Manufacturing Company Department 93-3 9851 Sepulveda Boulevard Los Angeles, California 90009 Attention: Hans J. Poulsen	(1)
General Electric Company Silicone Products Department Waterford, New York 12188 Attention: J. C. Frewin	(1)
Stewart-Warner Corporation 1826 Diversey Parkway Chicago, Illinois 60614 Attention: R. F. Wharton	(1)
Department of the Army U.S. Army Aviation Material Labs, Fort Eustis, Virginia 23604 Attention: J. W. White, Propulsion Division	(1)
SKF Industries, Inc. Engineering & Research Center 1100 First Avenue King of Prussia, Pennsylvania 19104 Attention: L. B. Sibley T. Tallian	(1) (1)
Nyatt Division New Departure Bearing Company Sandusky, Ohio 44870 Attention: D. Ruley	(1)
Timkin Roller Bearing Company Canton, Ohio 44701 Attention: Dr. W. Littmann	(1)

Caterpillar Tractor  
Peoria, Illinois 61601  
Attention: B. Kelley (1)

General Motors Research Lab.  
Warren, Michigan  
Attention: Nils L. Muench (1)

Department of the Navy  
**Naval Ship** Research  
Development Center  
Anapolis, Maryland 21402  
Attention: **Paul** Schatzberg (1)